Biology of murine CD84 in the context of autoimmunity

Olga Zharkova

2017

http://hdl.handle.net/10356/71172

https://doi.org/10.32657/10356/71172

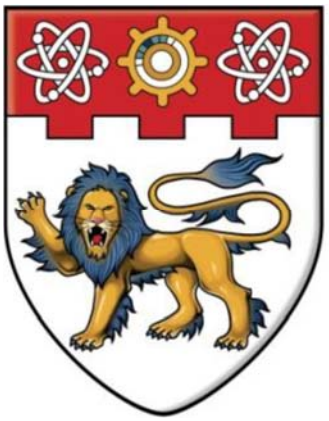

NANYANG TECHNOLOGICAL UNIVERSITY

Biology of murine CD84 in the context of autoimmunity

OLGA ZHARKOVA

SCHOOL OF BIOLOGICAL SCIENCES

A thesis submitted to the Nanyang Technological University

in partial fulfillment of the requirement for the degree of

Doctor of Philosophy

2016

ACKNOWLEDGMENTS

First and foremost I would like to express my deepest gratitude to my supervisor, Dr. Anna-Marie Fairhurst, for giving me this opportunity to undertake the project. I am extremely grateful for her support, patience and guidance throughout over the past 4 years. Thank you for creating a working environment where learning and constant challenges of science was a pleasure and motivation for continually self-improvement. Thank you for been a great teacher, adviser and an example of a professional scientist.

Thanks to the thesis advisor committee members: Dr. Peter Cheung, Dr Maria Curotto de Lafaille, and Dr. Alex Low for advice, discussions and critical feedback throughout my project.I wish to express my most heartfelt gratitude to my colleagues to whom I am indebted for the knowledge and skills I received through their patient training and support: Dr.Susannah Thornhill, Dr. Teja Celhar, Lee Hui Yin and Pang Ann Giat for their thorough guidance and mentoring at every step of the way throughout this project.

In addition, I would like to extend my sincere thanks to Hiroko, students and the former members of the AMF lab of SIgN for their kind assistance and support during my time there.

I also thank all my blood donors, the mouse core and SIgN flow cytometry facility staff, it would be almost impossible to finish my project without you.

I also thank our collaborators in IMCB: to Dr. John Connolly and JEC lab members, as well as collaborators in NUS, to Dr. Lina Lim and lab members, especially to Dr. Leonardo Moraes for his advice and suggestions in platelets work.I would like gratefully acknowledge Prof Gerhard Gruber and NTU professors and lecturers for the excellent courses in science and methodology of teaching.

Thanks to SINGA for the scholarship and to A*STAR for the financial support of this research.

I would like to say a very big thank you to the people who helped me to polish my English, especially Dr. Richard Betts, Dr. David Skibinski, Zdenek, Daniel, Catherine, Irina and Prabha.

Special gratitude is devoted to Anastasia Fadieieva, Dr.Marina Yurieva and Dr. Igor Khalin for pushing me far beyond I think I could go and supporting with great advice and providing constant feedback, even when it was not always positive.

Thanks to my friends in Singapore from all over the world, it would be much more difficult without your sincere support and constant encouragement to work harder in order to cure lupus.

Lastly, I would like to thank my family and friends in Ukraine, whose constant support during these years away from home helped me to keep moving forward during difficult times. My father's immune illness is what inspired to me study immunology with the goal of helping

others, and I hope that my small contribution to immunology knowledge forms part of something bigger that ultimately helps those in need.

TABLE OF CONTENT

LIST OF FIGURES

LIST OF TABLES

ABBREVIATIONS

ANA	anti-nuclear antibodies
APC	antigen presenting cells
BCR	B cells receptor
CVDs	cardiovascular diseases
EAT-2	Ewing's sarcoma associated transcript 2
EBV	Epstein-Barr Virus
ERT	EAT-2 related transducer
HKIR	VH knock-in transgenic mouse line encoding dual spesific
HAP	haplotypes
ITSMs	immunoreceptor tyrosine-based switch motifs
INF-α	interferon - alpha
MF	macrophage
Min	minute
MS	multiple sclerosis
NK-cells	natural killer cells
NETs	neutrophil extracellular traps
PCR	polymerase chain reaction
pDCs	plasmacytoid dendritic cells
PI	propidium iodide
PIE	polyethylenimine
PMNs	neutrophils -
RA	rheumotoid artritis
RT	room temperature
Sec	second
SAP	SLAM associated proteins
SLAMF	signaling lymphocytic activation molecules family
SLE	systemic lupus erethrematosys
Tfh	follicular helper T cells
TLR	toll-like receptors
Treg	regulatory T cells

ABSTRACT

Systemic lupus erythematosus (SLE) is characterized by the production of autoantibodies (ANAs), these form self-reactive immune complexes with self-antigens which results in tissue inflammation. The SLAM family (SLAMF) receptors are regulators of the innate and adaptive immune response. In mice, SLAMF are located within the *sle1* lupus-susceptibility locus. When present on a B6 background, *sle1* drives B and T cell hyper-reactivity and ANAs production.

We investigate differences between B6 and B6.*Sle1* CD84, one of the SLAMF. We find increased CD84 expression across multiple leukocytes in B6.*Sle1* mice; however no functional role of CD84 was determined. A preliminary investigation into the influence of CD84 on TLR7 signaling also revealed an increased response to TLR7-ligand in the presence of the autoimmune haplotype of CD84. To investigate the role of CD84 in NETosis a novel flow cytometry based assay has been developed. Taken together, this research highlights the importance of CD84 in murine SLE pathology.

1 INTRODUCTION

1.1 Autoimmunity

The human body is constantly challenged by invading pathogens (viruses, bacteria, and protozoa) however is able to guard itself with the help of immune system. The immune system can be divided into innate mechanisms, which provide a non-specific yet rapid response to potential pathogens, and the adaptive immune system which generates a specific long-term immune response, over a much longer period of time (Charles A Janeway, 2001).

It is essential for the immune system to maintain a balance between strong protection against invaders and tolerance to self (Van Parijs and Abbas, 1998). The phenomena of tolerance means a sophisticated differentiation between self-arising antigens and invading pathogens, which evolve to evade the immune system by trying to resemble body own cells. The mechanisms leading to tolerance occur can be “central”, occurring in the thymus and bone marrow, or “peripheral”, occurring in lymph nodes or tissues. Central tolerance facilitates the ability to distinguish self from non-self, whilst peripheral tolerance is a key factor preventing an overreaction to environmental substances (Kenneth Murphy, 2016).

Control of innate immunity occurs at multiple levels, starting from the short life-span of innate immune cells, such as neutrophils (PMNs), and negative feedback loops within innate signaling pathways (Kendrick and Jones, 2008). The regulation of the adaptive immune system is more advanced, including various stages of B and T cell maturation, multiple check points for B and T cell receptors and the formation and eventual elimination of almost 90% of the cells during tolerance tests (Charles A Janeway, 2001).

However, when the intrinsic balance is disturbed, pathologies arise. A hyper-activated, poorly controlled immune system, which is unable to tolerate self-antigens, becomes a dangerous enemy to its own body enabling the development of autoimmune disorders. Autoimmunity is estimated to affect approximately 8% of the USA population or approximately 25 million people (Cooper, Bynum et al. 2009). This translates to 1 person out of 31 being affected in one way or another by autoimmune pathology. The incidence is increasing due to a number of factors, including growing awareness and improved clinical diagnoses (Ines, Silva et al. 2015).

More than 100 autoimmune diseases are currently known, with the number increasing; around 40 other conditions are also suspected to be of autoimmune origin (Mackay 2000). Autoimmunity in general affects more females than males, moreover there is evidence that it is a leading cause of death in young females within the USA (Schmidt 2011). Typically autoimmune disorders are classified as either organ specific,

such as diabetes mellitus (pancreas), myastenia gravis (muscles) (McGrogan, Sneddon et al. 2010), Hashimoto's thyroiditis (thyroid) etc., or systemic, which affect the whole body. The most prevalent examples of systemic disorders include rheumatoid arthritis (RA), systemic lupus erythematosus (SLE), scleroderma, Sjogren's syndrome and multiple sclerosis (MS).

While a person of any racial, ethnic or social economic group at any age may be affected by autoimmunity, some races are more prone (Gonzalez, Toloza et al. 2014). For example, the SLE incidence is greater amongst African-American and Hispanic populations than amongst Caucasians (Jacobson et al., 1997; Sinha et al., 1990). Autoimmune diseases are a tough burden for public healthcare, with an estimated cost of the therapy for a disease like RA reaching up to 9 billion USD per year. On top of the high economic cost, autoimmunity also causes high day-to-day suffering due to the decreased quality of life, loss of productivity and inability to work, chronic afflictions and mental illnesses. Since autoimmunity predominantly affects females in child-bearing age, family structures are usually affected. For unidentified reasons, the incidence of autoimmune disorders is increasing every year (Zerhouni 2002) and so scientific investigation in this field has become a necessity.

Over the past decade, with the development of new scientific methods and animal models of disease, research has given many insights into the mechanisms of disease. Diagnosis at earlier stages and development of new medicines allow maintenance of a better and longer life for patients affected with autoimmunity. An advancement in kidney dialysis improves life quality for SLE patients with glomerulonephritis, however major questions regarding the causes of the disease pathologies remain to be answered.

1.2 Lupus

Every disease of autoimmune origin breaches immune tolerance in some way. An example of a resulting harmful pathology with an unclear etiology is systemic lupus. Lupus is a potentially fatal disease and mostly affecting inflammation of the skin, joints, kidney, lungs, blood vessels, brain and heart (Tan, Cohen et al. 1982) Historically, kidney failure was the main reason for mortality in lupus patients (Fei, Shi et al. 2014). However, with the improvement of kidney dialysis and better monitoring of disease status, life expectancy has increased and infections or cardiovascular diseases (CVDs) are now the most common reasons for mortality in patients (Abu-Shakra and Novack 2012, Elfving, Puolakka et al. 2014).

While using the term lupus, people most commonly refer to systemic lupus erythematosus or SLE, however there are more pathologies that possibly could be

involved. Neonatal lupus affects 40% of newborns from mothers with lupus or babies from healthy women with auto-antibodies. It is a disease that usually affects only the skin of a newborn or sometimes the cardiovascular system and subsides on its own. There are three more types of lupus affecting only the skin, and in 5% of cases that could progress to systemic lupus. Among them are discoid lupus erythematosus and subacute lupus erythematosus; they vary dependent upon the type of lesions and are diagnosed by biopsies (J. 1995).

Drugs are known to induce lupus; however this form of lupus is temporal and usually clears by itself several months after the medication is stopped. More and more doctors are trying to avoid these types of medications (J. 1995).

1.3 Systemic lupus erythematosus (SLE)

1.3.1 INCIDENCE

As the name suggests, Systemic Lupus Erythematosus (SLE) is a disease that affects the whole body (systemic) and most patients display redness of the skin caused by dilatation and congestion of capillaries (erythematosus). These abnormalities lead to the resemblance of a patient's face to the face of a wolf (lupus). SLE is a complex autoimmune disease, with an incidence rate from approximately 1 – 10 per 100,000 people (Pons-Estel, Alarcon et al. 2010). Millions are affected with SLE disease worldwide; in the USA, where the monitoring of autoimmune diseases is at the highest level, up to 24,000 new cases of SLE are registered every year with an incidence of 5 - 45 per 100,000 people (Lim, Bayakly et al. 2014, Somers, Marder et al. 2014). In Europe the incidence of SLE is less and 1 to 5 cases are reported per year per 100,000 (Laustrup, Voss et al. 2010, Rees, Doherty et al. 2016).

SLE affects predominantly women, with a ratio to men of 9 to 1 (Pons-Estel, Alarcon et al. 2010). Although this bias is higher in SLE, the majority of other autoimmune diseases also have a female bias (Brunelleschi 2016). However, incidence of male to female ratio in spondyloarthritis is 1 to 1 (Stolwijk, Boonen et al. 2012), and idiopathic pulmonary fibrosis developed mostly in males with ratio 11 to 1 (Brunelleschi 2016). SLE also has a racial bias, affecting more commonly people of Afro-Caribbean origin (Flower, Hennis et al. 2012), Asians (Yeh, Yu et al. 2013) (there is less incidence of lupus in Korea as compared to China) (Ju, Yoon et al. 2014) and native Americans (Ferucci, Johnston et al. 2014) followed by Caucasians (Gonzalez, Toloza et al. 2014).

1.3.2 CAUSE OF THE DISEASE

The specific mechanisms leading to autoimmunity and specifically, the onset of SLE are largely unclear, due to the multiple factors involved and their complex interactions. They include genetic predisposition and the influence of environmental factors with the addition of the influence of gender. SLE is characterized by the development of ANAs to nuclear containing material (Kaul, Gordon et al. 2016) however almost 5% of the population has ANAs but will never develop full disease as discussed in (Celhar, Magalhaes et al. 2012).

1.3.2.1 GENETIC FACTORS THAT INFLUENCE DISEASE PATHOLOGY

Genetic predisposition is the strongest risk factor associated with the development of SLE. There is approximately 25-50% disease concordance in identical twins and close relatives of SLE patients are at a higher risk of developing the disease (Mok and Lau 2003, Tsokos 2011, Kaul, Gordon et al. 2016).

With the advances in genetic research and the possibility of genome-wide association study studies, lupus research has shed light on a number of genes either directly involved or linked to the development of pathology. Polymorphisms in more than 100 genes have been shown to increase the risk of autoimmunity (Kaul, Gordon et al. 2016). To understand complex genetic interactions more clearly, it is convenient to divide the pool of available genes into pathways, subsequently analyzing genes involved in each particular pathway (Kaul, Gordon et al. 2016).

Genes involved in pathology could be grouped in several pathways with particular functions: apoptotic debris clearance, phagocyte function, complement system and immune complex deposition, antigen presentation, signaling and TLR function, T and B cell activation, energy metabolism and epigenetic modification for example (Concetta Ferretti 2012). The alterations in one or several genes within either single or multiple pathways may ultimately lead to the development of pathology.

Whilst a single genetic polymorphism alone is not significant enough to cause SLE, epistatic interactions between several polymorphisms result in full blown pathology.

1.3.2.2 ENVIRONMENTAL FACTORS THAT INFLUENCE DISEASE PROGRESSION

Environmental factors like viral infections, UV light and also certain types of drugs are well described triggers for SLE development. Over 100 currently used drugs can induce lupus, including blood pressure drugs like hydralazine and methyldopa, which affect DNA methylation (Du, Johnson et al. 2015). Likewise anti-acne drugs, anti-TNFα drugs and medicine used against metal poisoning may trigger lupus, however the usage of these types of drugs are decreasing (J. 1995)

Chemicals widely used in food and cosmetic production, like pristane, are known to provoke lupus development in non-autoimmune mice (Reeves, Lee et al. 2009). There are references demonstrating that individuals exposed to industrial substances such as silica dust or mineral oils, solvents, pesticides and hair dye are more likely to develop SLE (Cooper and Parks 2004, Cooper, Parks et al. 2004).

Tobacco smokers and cocaine users are also known to be more predisposed to autoimmunity symptoms (Rivera, Belmont et al. 2009). There is an association between the number of cigarettes smoked per year and the risk of SLE development due to smoking causing excessive necrosis (Costenbader, Kim et al. 2004, Arnson, Shoenfeld et al. 2010).

Viral infection, in particular Epstein-Barr Virus (EBV) infection, is one of the possible triggers of SLE. EBV can activate innate immune cells, followed by B cell secretion of auto-antibodies directed against amino-acid sequences similar between host and virus (Yadav, Tran et al. 2011).

Exposure to UV light brings about damage to DNA, such as hypomethylation (Wu, Li et al. 2013) resulting in mutations provoking auto-antibody production and disease complications such as rashes (Kuhn, Ruland et al. 2010).

1.3.2.3 GENDER AND HORMONES AS FACTORS INFLUENCING DISEASE

Knowing the disease bias towards the female gender, with the ratio of 9 female patients to 1 male, it is impossible to ignore the contribution of gender. It is especially hard not to address the influence of estrogen on disease establishment and progression, particularly after the data from murine experiments demonstrating that ovariectomy delays disease onset (Verthelyi and Ahmed 1994).

In addition men with XXY genotype are more prevalent among lupus patients rather than those with XY genotype (Scofield, Bruner et al. 2008). Plausible effects of estrogen might be due to immune cells having estrogen receptors (Liu, Loo et al. 2003),

however multiple studies attempting to block these receptors did not demonstrate successful elimination of pathology.

Other hormones like dopamine and prolactin contribute to disease pathology in some patients (Mok and Lau 2003). The serum level of prolactin is elevated in some cohorts of lupus patients (Costenbader, Feskanich et al. 2007). Lymphocytes are known to secrete prolactin and can use it in either autocrine or paracrine regulation, which make it immunogenic (Mok and Lau 2003).

Within the complicated field of SLE onset usually several factors are required to come together in order for disease pathology to progress.

1.3.3 DIAGNOSIS

The diagnosis of rheumatic diseases, of which SLE is, is always complicated due to heterogeneity of symptoms. Diagnosis of lupus can take years due to the complicated nature of the disease. Clinicians all over the world try to develop specific and precise guidelines to make diagnosis more standard, which will furthermore help to recruit patients for clinical trials (Kaul, Gordon et al. 2016) and Figure 1.1.

Currently diagnosis is based on the clinical manifestations and laboratory tests, including screening for auto-antibodies, functional tests, and imaging data. Usually doctors use the revised American College of Rheumatology (ACR) classification criteria for SLE (Tan, Cohen et al. 1982, Hochberg 1997, Amezcua-Guerra, Higuera-Ortiz et al. 2015) however, since initially these criteria were developed for classification of disease severity and not diagnosis, some significant symptoms, like some types of skin inflammation or neuropsychiatric manifestations are missing.

Currently, SLE is diagnosed upon the completion or presence of at least 4 of 17 criteria recommended by NIH in 2015 (Amezcua-Guerra, Higuera-Ortiz et al. 2015) and summarized in Figure 1.1

Clinical criteria*	Immunological criteria*
1. Acute cutaneous lupus including lupus malar rash (do not count if malar discoid);	1. ANA above laboratory reference range
2. Chronic cutaneous lupus including classical discoid rash;	2. Anti-dsDNA above laboratory reference range, except ELISA: twice above laboratory reference range
3. Oral ulcers;	3. Anti-Sm antibody
4. Nonscarring alopecia (diffuse thinning or hair fragility with visible broken hairs) ;	4. Antiphospholipid antibody: any of the following lupus anticoagulant; false-positive RPR; anticardiolipin; anti-β2 glycoprotein I ;
5. Synovitis involving two or more joints;	5. Low complement level;
6. Serositis;	6. Direct Coombs test in the absence of hemolytic anemia;
7. Renal: Urine protein/creatinine or Red blood cell casts;	
8. Neurologic seizures psychosis and other;	
9. Hemolytic anemia;	
10. Leukopenia;	
11. Thrombocytopenia;	

Criteria are cumulative and need not be present concurrently.

Figure 1.1 Criteria for SLE diagnostic.
Adapted from (Petri, Orbai et al. 2012)

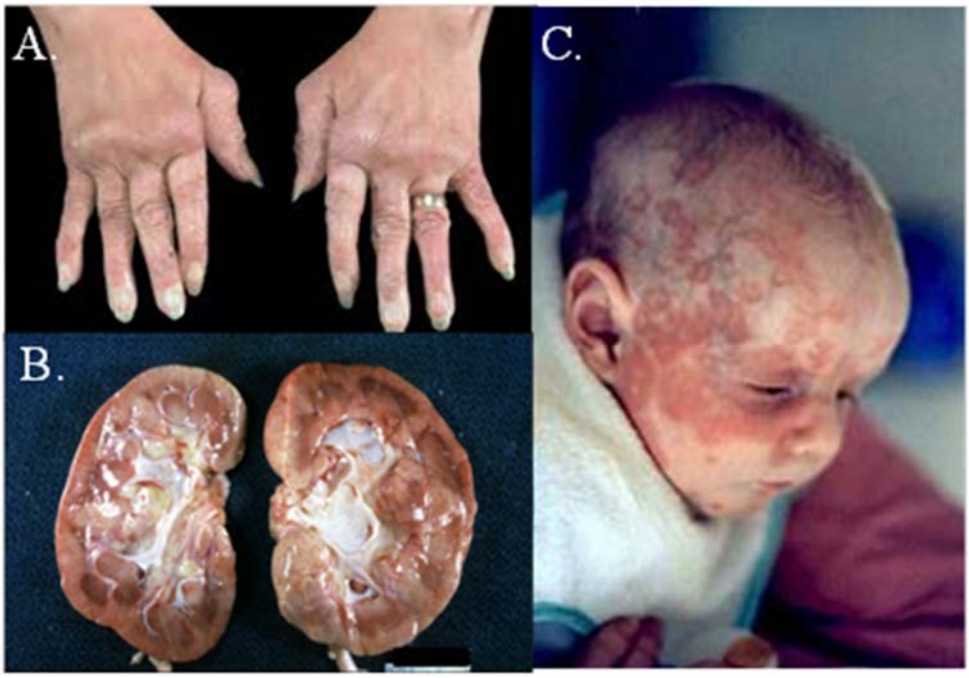

Figure 1.2 Clinical symptoms of SLE:
(A) joint inflammation (B) organ injury and (C) skin rash
Pictures adapted from Medical Pictures Info. 2012 (http://medicalpicturesinfo.com/)

1.3.4 PATHOLOGY

SLE patients may present with a wide diversity of clinical manifestations, ranging from slight symptoms such as fatigue and swelling, all the way to major organ system disorders such as joint inflammation **(Figure 1.2 A),** glomerulonephritis (GN) **(**Figure 1.1 **B)**, pulmonary hypertension and neurological complications (Mosca, Tani et al. 2011, Strand, Galateanu et al. 2013). Thus far, the most common clinical symptoms associated with SLE are the "butterfly rash" **(**Figure 1.1 **C)** and inflammation.

The exact mechanism of SLE development is far from been understood. The main feature is the production of autoantibody, mainly anti-nucleolus autoantibody (ANAs), which then form self-reactive immune complexes. These deposit in the tissues resulting in inflammation. The current hypothesis is that SLE develops in two stages: initially there is a loss of tolerance to self and autoreactive T and B cells development. The second step involves immune complex deposition, inflammatory cell activation and tissue destruction (Celhar, Magalhaes et al. 2012).

1.3.5 INNATE IMMUNE SYSTEM HYPERACTIVATION

Aberrant clearance of apoptotic debris, which is a normal function of the immune system, results in the availability of self antigens to innate immune receptors (Munoz, Lauber et al. 2010) and initiation of SLE pathology. In support of this, defective clearance of apoptotic debris has been demonstrated in some mouse models of lupus (Licht, Dieker et al. 2004). Apoptotic debris has also been detected in germinal centers (GCs), which make it possible for autoreactive B cells to survive checkpoints (Baumann, Kolowos et al. 2002).

Disturbance in cleaning of cellular debris occurs due to several reasons, one of which could be complement or complement receptor (C3b/C4b) deficiency (Gualtierotti, Biggioggero et al. 2010, Munoz, Lauber et al. 2010). C1q component could be considered as a protective component from SLE, if it targets ICs and make it "visible" for macrophages rather than plasmacytoid dendritic cells (pDCs), which would produce interferon - alpha (IFN - α), provoking SLE development (Santer, Hall et al. 2010). Excessive IFN - α production or an "IFN signature" is a common sign of SLE, however not only activated pDCs secrete abnormal amounts of IFN (Crow, Olferiev et al. 2015).

Microarray data demonstrated similar patterns of IFN gene expression in neutrophils upon neutrophils extracellular traps (NETs) release, suggesting its role in the activation of the immune system (Bennett, Palucka et al. 2003). NETs themselves make self DNA complexes available for the activation of toll-like receptors (TLRs) inducing IFN - α production by pDCs (Villanueva, Yalavarthi et al. 2011). High levels of IFN - α expression in SLE patients correlate with increased level of autoantibodies against RNA-binding proteins such as RNP, La, Sm, etc. (Kirou, Lee et al. 2005). This data points to the important role of TLRs, IFN - α and RNA-containing immune complexes in SLE development.

A critical role for the innate immune system has emerged in the initiation and progression of pathology only recently (Pathak and Mohan 2011). Pathological changes in the innate immune system happen much earlier than the development of full disease, making it very difficult to diagnose or prevent SLE in early stages.

1.3.5.1 INNATE IMMUNE RECEPTORS HYPERACTIVATION

The complex mechanism of monitoring extracellular and intracellular environment utilizes several families of receptors, these include toll-like receptors (TLRs), C-type lectin receptors (CLRs), nucleotide-binding oligomerization domain-like receptors, NOD-like receptors (NLRs) and (absent in melanoma 2) AIM2 like receptors (ALRs) (Vance 2016).

Nucleic acid sensing TLRs are located on the endosome and comprise TLR3, 7 and 9 recognizing dsRNA, ssRNA and dsDNA respectively. NLRs are sensors for damage-associated molecular patterns (DAMPs) and pathogens located intracellular in immune cells like macrophages, monocytes, PMNs, dendritic cells, lymphocytes and also epithelial cells (Franchi, Warner et al. 2009). DNA can also be recognized by ALRs, and NLRs located in the cytosol (Iwasaki 2012).

TLRs

TLR7 and TLR9 depend on MyD88-signalling pathways and have been implicated in the development of autoimmunity and the progression of SLE (Celhar, Magalhaes et al. 2012). In addition, multiple research reports have demonstrated an important role of TLR receptors in autoimmunity, especially TLR3, 7 and 9 (Celhar, Magalhaes et al. 2012, Giltiay, Chappell et al. 2013, Celhar, Hopkins et al. 2015). TLR7 is located inside the cells, in the endosome and requires acidification for its activation. It recognises ssRNA viruses and is expressed in B-cells, NK cells, pDCs and PMNs. TLR9 and TLR3 are also endosomal nucleotide sensors involved in the recognition of viruses (Medzhitov and Janeway 2002).

During aberrations in murine immune system function, TLR7 may be activated by self-derived ssRNA**.** Normally, extracellular RNases degrade the ssRNA released from cells that undergo cell death by apoptosis or after tissue injury. However, in mouse models of lupus nephritis TLR7 recognition of self ssRNA was observed to contribute to disease (Celhar, Hopkins et al. 2015). However it is not yet known whether human autoimmunity develops through a similar pathway (Celhar, Magalhaes et al. 2012).

One study demonstrated that level of TLR7 mRNA is increased in adult SLE patients and its level correlates with IFN-α mRNA expression, suggesting this as a possible input for the lupus initiation (Komatsuda, Wakui et al. 2008).

NLRs and ALRs

A stimulation of either ALR or NRL leads to inflammation through caspase activation and results in pro-inflammatory cytokines expression IL-1b and IL-18 (Schroder and Tschopp 2010, Wen, Miao et al. 2013). The role of ALRs and NRLs in SLE pathogenesis is less clear. Necrotic, apoptotic or cells undergoing NETosis are proven sources of DAMPs which can be recognized by TLRs, ALRs and NLRs (O'Reilly 2015).

Misrecognition of cytosolic DNA by ALR leads to psoriasis, dermatitis and autoimmunity (Man, Karki et al. 2016). A recent study demonstrated that unstimulated male macrophages had higher mRNA levels of AIM2, however in unstimulated female

macrophages, AIM2 mRNA was lower (Yang, Huang et al. 2015). This suggests a divergence in the role of SLE according to sex in SLE. In another study, methylation of AIM2 was also lower in SLE patient macrophages compared to their siblings, pointing on the role of epigenetic modifications in SLE onset and progression (Javierre, Fernandez et al. 2010). Limited reports from murine studies from Stacey and colleagues described that defective AIM2 and are almost absent from NLRP3 in NZB autoimmune mice, suggesting that defects in the intracellular sensors lead to prolonged cytokines expression, eventually leading to autoantibody development (Sester, Sagulenko et al. 2015).

Recent data has shown that NLRs contribute to hyperactivation of the immune system, resulting in autoinflammatory diseases. This is where the inflammation is directed towards self-ligands and the adaptive component is minimal or unknown (Kim, Shin et al. 2016). In addition, activation of these receptors has been associated with the development of rheumatoid diseases (Takeuchi and Akira 2010). A report from Shin and colleagues has shown that immune complexes containing dsDNA stimulate the production of IL1b by healthy human monocytes through a NLRP3-dependent mechanism (Shin, Kang et al. 2013). An elevated level of NLRP3 mRNA in unstimulated female macrophages was demonstrated (Man, Karki et al. 2016). In contrary to the report from Shaw and colleagues suggesting no evidence of NLR involvement in SLE pathology (Shaw, McDermott et al. 2011).

1.3.5.2 NEUTROPHILS AS INITIATORS OF SLE

Since the mid-twentieth century, neutrophils were known as important players in SLE. However, after discovering ANAs, attention in SLE research has been mostly devoted to B cells (Baugh, Kirol et al. 1960). More recently, a genomic approach revealed a granulopoesis signature in the blood of SLE patients, implicating a role of neutrophils in the disease progression (Bennett, Palucka et al. 2003). A mechanism by which neutrophils impaired proper B cell development was reported, revealing a new link between the innate and adaptive immune system in SLE (Palanichamy, Bauer et al. 2014).

1.3.5.3 HUMAN NEUTROPHILS AS INITIATORS OF PATHOLOGY

Human neutrophils play an essential role in inflammation by performing a series of distinct functions, which include the phagocytosis of immune complexes, antibody-dependent cell-mediated cytotoxicity (ADCC) and the release of reactive oxygen intermediates together with proteolytic enzymes (Ravetch and Kinet 1991, Pillinger and

Abramson). Defects in neutrophil function result in recurrent bacterial infections such as those characterised in chronic granulomatous disease (Harlan, Schwartz et al. 1985). Excessive or inappropriate activation of neutrophils results in tissue damage from the release pro-inflammatory mediators (Harlan, Schwartz et al. 1985, Marx 1987) as observed in chronic inflammatory disorders such as RA and SLE (Edwards and Hallett 1997, Garcia-Romo, Caielli et al. 2011).

Over a decade ago a novel type of cell death by neutrophils was described, termed NETosis (Brinkmann, Reichard et al. 2004). NETosis differs from the many other recognised mechanisms of cell death, including apoptosis and other regulated necrosis pathways (Vanden Berghe, Linkermann et al. 2014). During apoptosis, the intracellular content of cells is compartmentalised and neatly packaged into apoptotic blebs. This process is actively controlled, minimising the release of pro-inflammatory substances (Geering and Simon 2011). Simultaneously, a researcher from the platelets field, Dr. Wagner, reported presence of NETs in the blood and its pathological influence for thrombosis development (Fuchs, Brill et al. 2010). In this elegant work, authors at first described a link between inflammation and thrombosis via NETs.

Necrotic pathways can however result in the release of intracellular contents, which may provoke an inflammatory response and include necroptosis, parthanoatos, pyronecrosis and NETosis (reviewed in (Vanden Berghe, Linkermann et al. 2014)). During NETosis, decondensed nuclear material and granular content are expelled into the extracellular environment in order to trap pathogens, as schematically described in **(Figure 1.3 A)** (Brinkmann, Reichard et al. 2004) and depicted by confocal microscopy **(**Figure 1.3 **B)** (Zharkova O, in preparation). This process plays an important role in host defence, preventing the spread of infection and keeping it localized in a sticky DNA mesh.

Dysregulation of NETosis has been asssociated with numerous severe pathologies including atherosclerosis, sepsis, preeclampsia and vasculitis of the microvessels (Gupta, Joshi et al. 2010, Warnatsch, Ioannou et al. 2015). More recently, NETosis has been proposed as a primary mechanism by which self-ligand, particularly DNA, is generated in the autoimmune disease SLE (Garcia-Romo, Caielli et al. 2011, Lande, Ganguly et al. 2011). In addition, increased levels of NETosis have been associated with various pathologies and cellular processes including, mammary and lung cancers, inflammatory lung diseases, the prognosis of infections and in wound healing of diabetic mice and

human patients (Demers, Krause et al. 2012, Cheng and Palaniyar 2013, Cedervall and Olsson 2015, Cedervall, Zhang et al. 2015, Fadini, Menegazzo et al. 2016).

1.3.5.4 NETOSIS IN THE ONSET OF SLE

Recent studies have revealed that PMNs are an additional source of autoantigens in the periphery. Aside from apoptosis and necrosis, PMNs may also die releasing neutrophil extracellular traps (NETs) during NETosis. These NETs contain LL37, HMGB1 and nucleic acids which act as the self-antigen. LL37 is an antimicrobial cationic peptide that promotes bacteria entrapment and killing (Brinkmann, Reichard et al. 2004). Moreover, Lande et al. showed that the LL37 peptide released from PMNs stabilizes the negatively charged nucleic acids by aggregating and protecting them from DNase I degradation, thus making them more immunogenic. Most importantly, NETs activate pDCs in a TLR9-dependent manner, leading to the production of IFN-α as mentioned before (Garcia-Romo, Caielli et al. 2011, Lande, Ganguly et al. 2011). IFN-α is also found to be able to prime SLE PMNs to undergo further NETosis, creating a feed forward loop. IFN- α may also be induced upon TLR7 ligation (Niewold, Kelly et al. 2008).

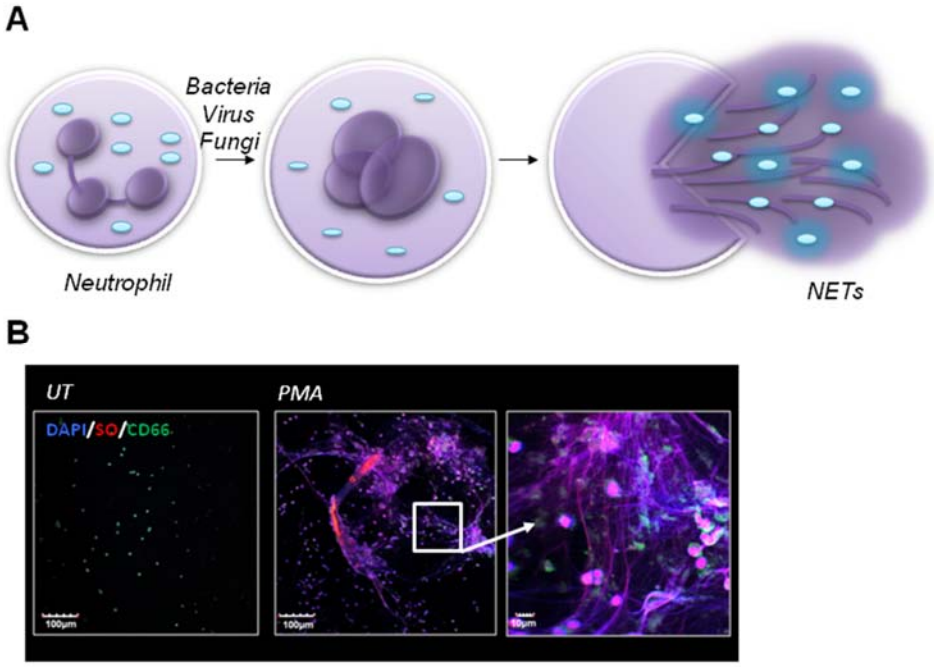

Figure 1.3 Visualizing NETosis.

(A) Schematic diagram representing resting neutrophils undergoing activation and NETs formation after encounter with pathogens. (B). Confocal microscopy of untreated (UT) or 100 nM PMA stimulated human neutrophils. The long extended NET structures following PMA are clearly visible with SytoxOrange (SO) and DAPI. Neutrophils are stained with anti-CD66-FITC. Images were acquired using 10X or 100X magnification on Olympus FV1000 confocal microscope. SO and DAPI bind DNA *(Zharkova et. al in preparation)*

1.3.5.5 MONOCYTES

CD14+ monocytes are significantly increased in patients with SLE (Mortezagholi, Babaloo et al. 2016). Furthermore, recent data has shown that anti-dsDNA antibodies activate the NLP3 inflammasome in monocytes from SLE patients, leading to the production of IL-1beta and subsequent inflammation and pathology (Zhang, Fu et al. 2016). Murine studies have also suggested a key role for monocytes mediating end organ inflammation (Marks, Williams et al. 2008). However, interestingly monocytes depletion did not result in a reduction of diminishing SLE symptoms in a Phase 1b clinical trial. (Masek-Hammerman, Peeva et al. 2016).

1.3.5.6 MACROPHAGES

Early experimental data from mice suggested that macrophages (MFs) play a key role in driving kidney inflammation in SLE (Chalmers, Chitu et al. 2015). Murine studies using clodronate liposomes demonstrated increased MF apoptosis triggered by CD4 T

cells, as well as impaired clearance of apoptotic debris leads to ANA formation (Denny, Chandaroy et al. 2006, Kavai and Szegedi 2007). Furthermore, SLE MFs secrete increased levels of pro-inflammatory cytokines and mediators including TNF– alpha, IL-10, IL-23, nitric oxide and type 1 IFNs (Byrne, Ni Gabhann et al. 2012).

Biopsies of cutaneous lesions and kidneys from SLE patients show have MF infiltration (Masek-Hammerman, Peeva et al. 2016). One of the key factors contributing to this may be MCP-1 (CCL2) produced by the SLE MF itself. MCP-1 is important in cells migration to the tissue, and is regulated by IFNs and LPS (Hill, Delahousse et al. 2001). Surprisingly, administration of an antibody to MCSF (macrophage colony stimulating factor) does not affect tissue MFs infiltration or clinical outcomes of patients with cutaneous lupus (Masek-Hammerman, Peeva et al. 2016).

A report from Li and colleagues demonstrated that enhanced macrophages polarization towards M2, expressing anti-inflammatory IL-10 cytokine, abrogates SLE induced in murine models (Li, Zhu et al. 2016). In the next experiment by Li it was demonstrated that M2 adoptive transfer reduced SLE activity in murine models (Li, Yang et al. 2015).

1.3.5.7 PLATELETS

There is emerging evidence suggesting that platelet-neutrophils interactions participate in inflammatory processes (Zarbock, Polanowska-Grabowska et al. 2007). During inflammation, platelets release activation molecules which enhance leukocyte adhesion, transmigration and the production of cytokines as well as reactive oxygen species (Davi and Patrono 2007). During SLE, platelets stimulate interferon production by pDCs and interact with ICs through their own Fc receptors as recently reviewed in (Boilard, Blanco et al. 2012).

Microarray data analysis of platelets of SLE patients demonstrated increase in IFN regulated gene mRNA (Lood, Amisten et al. 2010). Experiments in mouse blood revealed the presence of enhanced platelet activation in SLE (Blanco, Palucka et al. 2001).

1.3.5.8 SUMMARY OF INNATE IMMUNE SYSTEM IMBALANCE

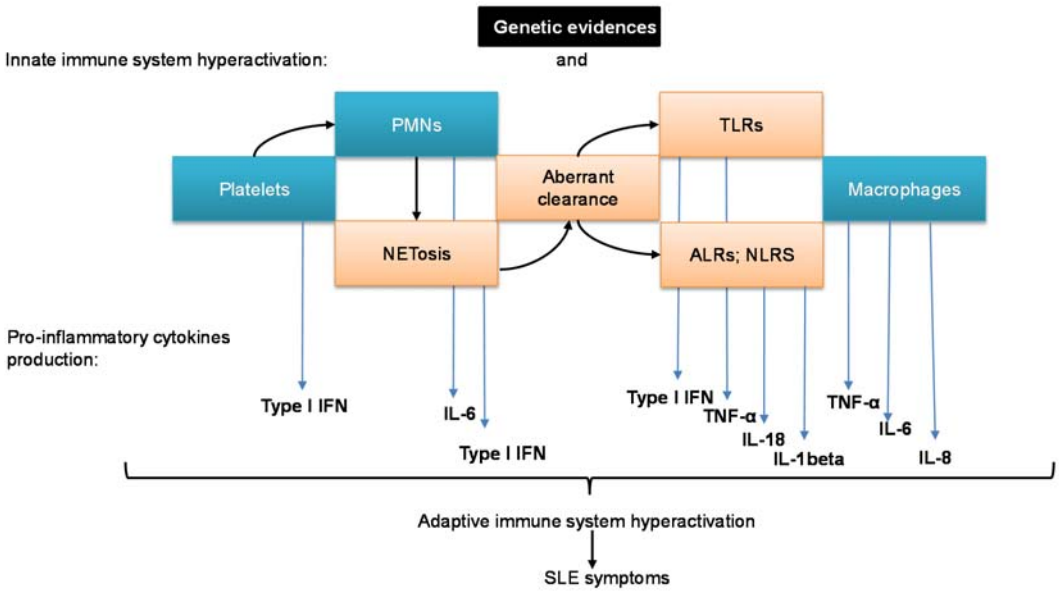

Figure 1.4 Schematic representation of innate immune system events resulting in SLE symptoms.

In attempt to summarize evidences from innate immune system about possible triggers of SLE development, available data were put in **Figure 1.4** Genetic predispositions affected by environmental challenges lead to hyperactivation of innate leukocytes such as PMNs, monocytes/macrophages trough receptors sensing nucleic acids, resulting in increased pro-inflammatory cytokines expression via activation of NF-Kb, IL-1beta and type 1 IFN secretion. This leads to hyperactivation of adaptive immune system, eventually resulting in the development of SLE symptoms.

1.3.6 ADAPTIVE IMMUNE SYSTEM HYPERACTIVATION

The immune system requires an intelligent strategy to protect the body from the enormous amount of pathological antigens. Somatic hypermutation and VDJ recombination are two major processes producing clonally expanded B and T cells with diverse B and T cell receptors which are able to protect against different antigens. However to prevent self-attack by these cells they should pass through several tolerance checkpoints during which almost 90% of T and B cells will be eliminated as autoreactive, undergo receptor editing or be suppressed by regulatory cells (Crispin, Liossis et al. 2010). In SLE patients either one or multiple of these mechanisms responsible for tolerance are impaired due to genetic mutations or other influencing factors (Schroeder, Herrmann et al. 2013) (Anolik 2007).

1.3.6.1 B CELLS

B cells are major players of adaptive immune system providing normal immune response to invading pathogens, however in SLE B cells function is impaired. Due to multiple factors, including genetic alterations the regulation of normal B cell is disturbed, resulting in ANA production, excessive cytokines secretion and antigen presentation to T cells. Abnormal T cells help subsequently cause increased in B cells proliferation, survival of autoreactive B cells and improper differentiation to long lived plasma cells (Dorner, Giesecke et al. 2011).

Genetic polymorphisms implicated in SLE include genes encoding kinases, phosphatases, as well as adaptor molecules participating in B cell intrinsic signalling (Kaul, Gordon et al. 2016). In one study the majority of lupus patients screened were found to have a polymorphism in the gene expressing the inhibitory FcγRIIb receptor resulting in the abnormal production of autoreactive B cells (Rahman, Alabyev et al. 2007, Li, Wu et al. 2013). Decreased expression of FcγRIIb receptor on memory B cells also alters cytokine production, activating other immune cells and worsening pathology (Mackay, Stanevsky et al. 2006).

The majority of SLE patients develop different types of autoantibodies, specifically against self DNA or RNA, produced by B cells. Circulating plasmablasts are the source of anti-dsDNA autoantibodies (Jacobi, Mei et al. 2010), while plasma cells resting in bone marrow are usually the source of anti-Ro and anti-Sm autoantibodies, due to the high availability of ligands (Hiepe, Dorner et al. 2011). Lastly, RNA within this complexes

activates TLR receptors and cells start a secretion of type I IFN (reviewed in (Kattah, Kattah et al. 2010).

1.3.6.2 REGULATORY B CELLS

A small subset of B cells which release IL-10 are termed B regulatory cells (Breg) (Katz, Parker et al. 1974). There are different Breg subsets identified by surface expression molecules which accumulate in different diseases. For example, in murine models of EAE they express MHC I, MHC II, and surface IgM and IgD (Yang, Rui et al. 2013) , in human SLE, they reportedly express CD19+CD24hiCD38hi (Blair, Norena et al. 2010)

Bregs decrease inflammation by secreting IL-10 and IL-35 which stimulates the Tregs population (Mauri and Bosma 2012). There are limited reports on Bregs in SLE. However, Palanichamy and colleagues determined that B cell therapy also resulted in eliminating a protective B cell compartment (Palanichamy, Barnard et al. 2009). Furthermore, others have shown that pDCs failed to promote Bregs development in patients with SLE due to altered STAT1 and STAT3 activation (Menon, Blair et al. 2016).

Taken together these data suggest that SLE pathology may derive from multiple immune populations. However, it is necessary to dissect a functional role of each population in order to resolve a complex task of SLE disease.

1.3.6.3 T CELL SUBSETS

The other major immune cell-type with multiple functions is T cells. In SLE the majority of T cells undergo hyperactivation, altered intracellular signaling and cytokine expression, excessive proliferation and clonal expansion of self-reactive T cells (Crispin, Kyttaris et al. 2010). Polymorphisms within MHC alleles are one of the direct links to SLE development, driving altered antigen presentation resulting in the loss of T cell tolerance (Green, Montasser et al. 1986, Gaffney, Kearns et al. 1998).

Although lupus patients have lymphocytopaenia, the amount of $CD3^{+}CD4^{-}CD8^{-}$ is increased, making kidney disease worse due to overproduction of IL-17 (Crispin, Oukka et al. 2008). CD4+ T cells, with high expression of CD44, drive excessive B cell differentiation by providing more help than required (Ettinger, Sims et al. 2007) (Gatto, Zen et al. 2013). T cells from lupus patients have increased expression of the

costimulatory molecule CD40, leading to excessive help to B cells (Koshy, Berger et al. 1996).

An expansion of CD8+ cells correlates with poor prognosis in SLE, however those CD8+ T cells possess lower cytotoxic ability (Mok and Lau 2003, Crispin, Kyttaris et al. 2008). Reports from clinical data on regulatory T cells (Treg) frequencies in SLE patients are conflicting with some data showing increases and others showing decreases. This may reflect the heterogeneity of the disease, ethnicity differences or the effects of the immunosuppressive medicine that the patients are on (Suarez, Lopez et al. 2006, Crispin, Oukka et al. 2008, Gerli, Nocentini et al. 2009).

Functional data has also suggested that Tregs from SLE patients a production of anti-inflammatory IL-10, IL-35 and iTGF-beta allowing the T effector cells avoid the suppression, escalating SLE symptoms (Banchereau, Pascual et al. 2012). The SLE IFN-alpha signature, is also associated with a decrease in suppression activity of Tregs and simultaneously decreased tolerogenic function of Tregs on DCs, (Mao, Wang et al. 2011). Furthermore, increased expression of TNF-alpha provokes downregulation of FoxP3, a key transcription factor in Treg development, resulting in decrease number of Tregs (Yamaguchi, Wing et al. 2011).

Lupus patients, as well as murine models of autoimmunity, demonstrate increased numbers of Tfh cells (Ma and Deenick 2014). Accumulation of follicular helper T cells (Tfh) in germinal centers correlates with ANA production in SLE, and increases upon IFN-ɣ secretion (Lee, Silva et al. 2012).

The intrinsic metabolism of T cells from lupus patients is also affected. Mitochondrial dysfunction results in the production of reactive oxygen species, reduced glutathione levels as well as ATP depletion (Fernandez and Perl 2009). A substitution of the T cell receptor component CD3ζ to CD3γ has been associated with abnormalities in calcium metabolism. This increases intracellular calcium flux, which affects TCR signaling resulting in T cells hyperactivation in SLE patients (Krishnan, Warke et al. 2003, Nambiar, Fisher et al. 2003).

1.3.7 PROPOSED MECHANISM OF SLE DEVELOPMENT

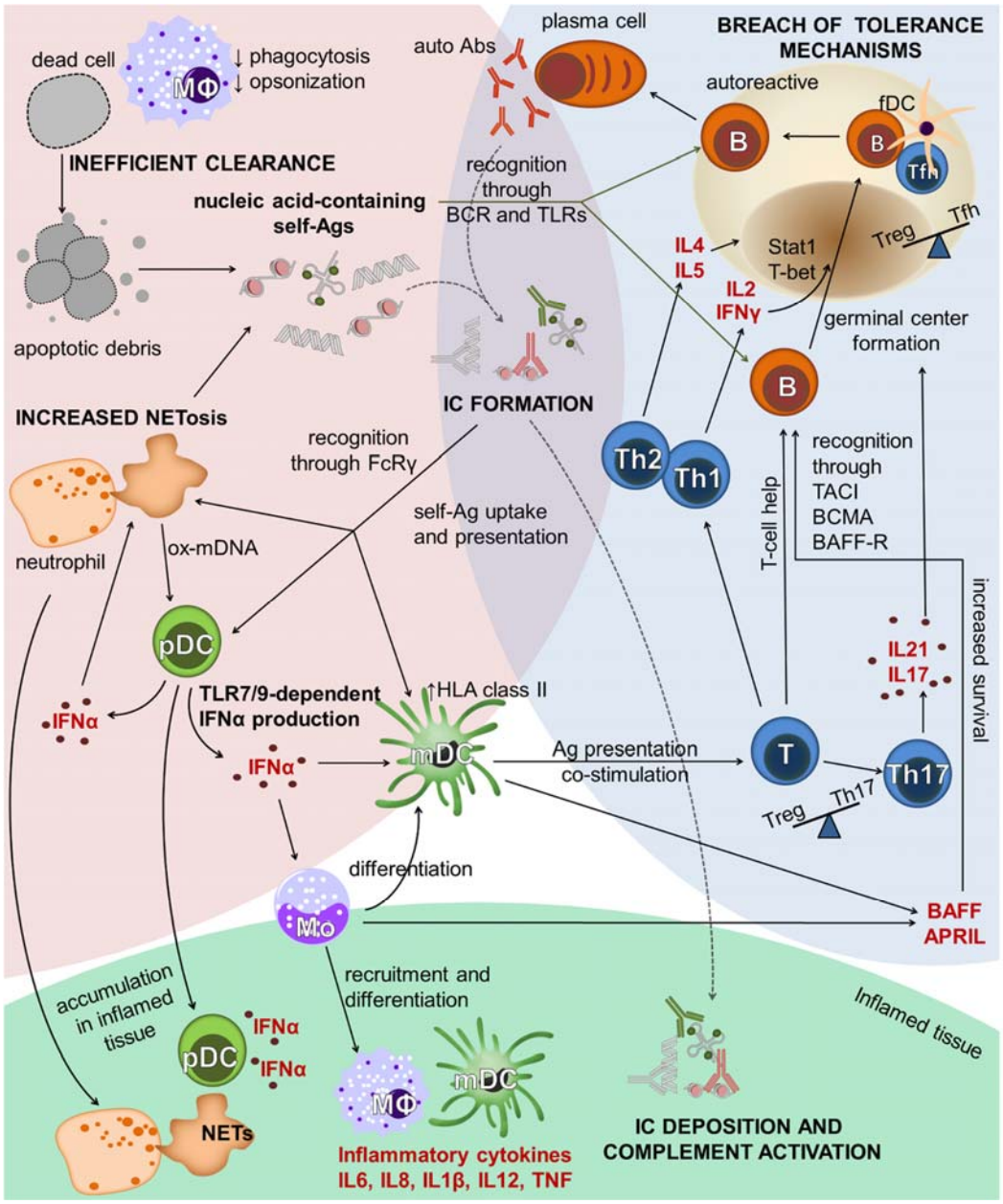

Figure 1.5 Mechanism of SLE development

Summarizing the above information, an inflammation as a symptom of SLE is developed due to high number of simultaneous pathological processes occurring in different cell-types from the innate to the adaptive immune system. In general there is a disturbance in the clearance of apoptotic debris, FC-gamma receptor mediated phagocytosis, antigen - presentation, alteration in numbers and dysregulation of function

of almost all leukocytes and soluble immune mediator production which spreads pathology even further and eventually results in tissue damage **(Figure 1.5)** . The current hypothesis of SLE development looks as follows: the availability of apoptotic remnants in the blood and tissue due to defective clearance by innate immune cells (macrophages etc.) will activate antigen-presenting cells (APCs) such as DCs or B cells. APCs will change phenotype and increase the production of soluble factors (cytokines, IFN) these will eventually lead to the production of auto-antibodies by B cells (Celhar, Magalhaes et al. 2012).

Excessive amounts of autoantibodies form immune complexes (ICs) with healthy cells and the deposition of these ICs, in particular in the skin and the kidneys, will lead to tissue damage and inflammation reported as the most common symptoms in SLE patients (Mannik, Merrill et al. 2003).

1.3.8 CURRENT SLE THERAPY

Due to the complexity and heterogeneity of the disease, approaches to SLE treatment are numerous, however not always efficient. Moreover, treatments often lead to impairment of a patient's health status and work productivity (Strand, Galateanu et al. 2013). Traditionally lupus therapy depends on non-specific immunosupressunts like steroids, cyclophosphamide, or anti-malaria drug Plaquenil (hydroxychloroquine). Immunosuppressive drugs, for example glucocorticoids such as prednisolone are associated with severe side effects and decreasing the quality of life. Also, aspirin have been approved by Food and drugs agency (FDA) of USA for SLE treatment since 1948.

In addition to their antibody-producing function, B cells are also antigen presenting cells. Therefore B cell depletion therapies were expected to help to treat SLE (Reff, Carner et al. 1994). For example, targeting CD20, a marker which is expressed in almost all lineages of B cells except pro-B cells and plasma cells, was found to be promising in treating murine lupus (Ahuja, Shupe et al. 2007, Bekar, Owen et al. 2010). However, recent data with Rituximab, an anti-human CD20 monoclonal antibody, did not have a significant effect in SLE patients (Merrill, Neuwelt et al. 2010) (Rovin, Furie et al. 2012). Furthermore, SLE flairs were reported following the trials, possibly due to elevated levels of circulating BAFF (B-cell-activating factor, also known as TNF ligand superfamily member 13B or BLyS), and a high proportion of plasmablasts within the B-cell pool(Carter, Isenberg et al. 2013).

The central importance of IFN-α in SLE makes it a favorable target for therapy, however the risk of side effects due to its physiological role in host defense is high (Craft 2011). Currently, several drugs as anti-IFN-α and anti-CD22 antibody showed promising

results in phase II clinical trials. Taking together, a current state of SLE medications suggests there is an overwhelming need for the new therapy approaches. However, the development of new drugs requires preclinical studies in animals, mice in particular.

1.4 Murine models of disease

The possibility to alter the murine genome and the relatively fast breeding cycle makes the usage of mice in particular a very useful tool in identification of lupus susceptibility genes and molecular mechanisms underlying the development of SLE. Mice with autoimmune-prone backgrounds develop symptoms of autoimmunity that highly resemble human lupus, including ANA development, lymphadenopathy, splenomegaly and kidney disease (Liu and Wakeland 2001) (Fairhurst, Wandstrat et al. 2006).

There are several induced and spontaneous mouse models of SLE available. Induced models include the pristane-induced model and the chronic graph-versus-host - disease models (Theofilopoulos and Dixon 1985).

Spontaneous lupus models include MRL/*lpr* mice, which carry a mutation in the *Fas* gene, disturbing apoptosis of B and T cells eventually resulting in severe autoimmunity (Vidal, Kono et al. 1998). The BXSB/*Yaa* strain is another spontaneous model, presenting with severe autoimmunity in male mice, due to a Y-linked *Yaa* loci expressing the *tlr7* gene (Murphy 1979) Historically the most widely used spontaneous model is the F1 female progeny of New Zealand Black (NZB) crossed to New Zealand White (NZW) (Fairhurst, Wandstrat et al. 2006).

1.5 (NZB × NZW) F1 female

The NZW mice do not present any overt autoimmunity traits unlike NZB (Fairhurst, Wandstrat et al. 2006). In NZB mice, ANAs and autoimmune haemolytic anaemia is reported. F1 generation of (NZB × NZW) demonstrates full autoimmune pathology with an increased production of class-switched ANAs, lymphadenopathy, splenomegaly and immune-complex mediated GN developing by the age of 5 - 6 months old which is ultimately fatal (Andrews, Eisenberg et al. 1978).

Following an accidental backcross of a NZB male with the F1 of (NZB × NZW) 27 fully inbred strains were generated named New Zealand Mix (NZM) (Rudofsky, Evans et al. 1993, Fairhurst, Wandstrat et al. 2006). The most severe pathology was reported in the strain NZM2140, where both males and females were affected, with 2-3 months delay

of onset of the disease in males. NZM2140 mice develop severe GN and ANAs (Rudofsky, Evans et al. 1993, Morel, Rudofsky et al. 1994).

Genotyping of NZM2140 revealed that 75% of its genome is derived from NZW, hence NZM2140 demonstrated 15% polymorphic differences in their autosomes and a slightly different phenotype, showing less severe GN, higher IL-4 expression and an increased number of marginal B cells in the spleen (Fairhurst, Wandstrat et al. 2006) (Rudofsky, Evans et al. 1993) (Morel, Rudofsky et al. 1994).

In order to investigate if a single susceptible gene was the pathology initiator, a large genetic study was done in E. Wakeland's lab using quantitative train linkage studies together with the derivation of multiple congenic mice strains for phenotype investigation. Four loci strongly associated with GN were identified on different chromosomes named *Sle1* on chromosome 1*, Sle2* on chromosome 4*, Sle3* on chromosome 7 and *Sle4* on chromosome 17 *(Morel and Wakeland 1998, Morel, Croker et al. 2000)*.

A congenic dissection approach was used to associate a specific phenotype to each locus. Of the 4 loci found to be associated with GN, *Sle4* was later renamed to *Sle1* suppressor (*Sles1*), due to the presence of this loci suppressing the pathology caused by the *Sle1* locus (Morel, Rudofsky et al. 1994). The presence of *Sle2* alters B cell function, making them hyperactive with an increased production of poly-reactive IgM antibodies (Mohan, Morel et al. 1997). The *Sle3* locus affects the function of T cells, provoking hyper-activated T cells with impaired apoptosis, however the incidence of GN is decreased to 18% (Mohan, Yu et al. 1999). *Sle1* is of particular interest due to its role in the initiation of pathology. A single *Sle1* locus will never trigger full fatal disease, however the phenotype shows an intrinsic activation of B and T cells with ANA development (Mohan, Morel et al. 1999, Sobel, Mohan et al. 1999, Sobel, Satoh et al. 2002).

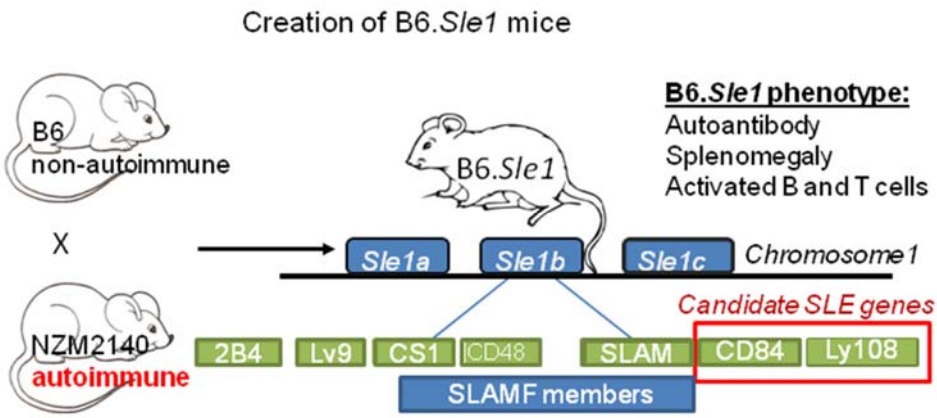

Figure 1.6 Genetic dissection of *Sle1* locus and creation B6.*Sle1* congenic autoimmune prone mouse model.

An investigation into the role of each locus gives insight into the initiation and development of lupus pathology, as well as epistatic interactions between *Sle1*, *Sle2* and *Sle3*, since triple congenic mice die from GN by the age of 12 months (Morel, Croker et al. 2000). The B6.*Sle123* highly resembles human lupus and arms scientists with a good *in vivo* model for further investigation into the role of polymorphisms in the breaking of tolerance.

Resemblance of lupus pathology in mice comes with the same problem as in human - multigenic background, making it challenging to identify specific autoimmunity susceptible genes. However, fine mapping and genetic linkage studies allow identify lupus step by step causing genes.

1.5.1 B6.*SLE1* MURINE MODEL OF BENIGN AUTOIMMUNITY

Mice that carry the *Sle1* locus on the C57BL6/J (B6) non-autoimmune background are characterised by overt autoimmune traits, as T and B cells activation, splenomegaly and ANAs development after 6 month of age **(Figure 1.7)**. For the development of severe disease their genome require other susceptibility loci such as *Sle2*, *Sle3* or *Yaa*. For example, mice from the B6.*Sle1*.Tg7 strain combine the *Sle1* locus with an additional copy of the TLR7 gene and develop severe autoimmunity (Hwang, Lee et al. 2012).

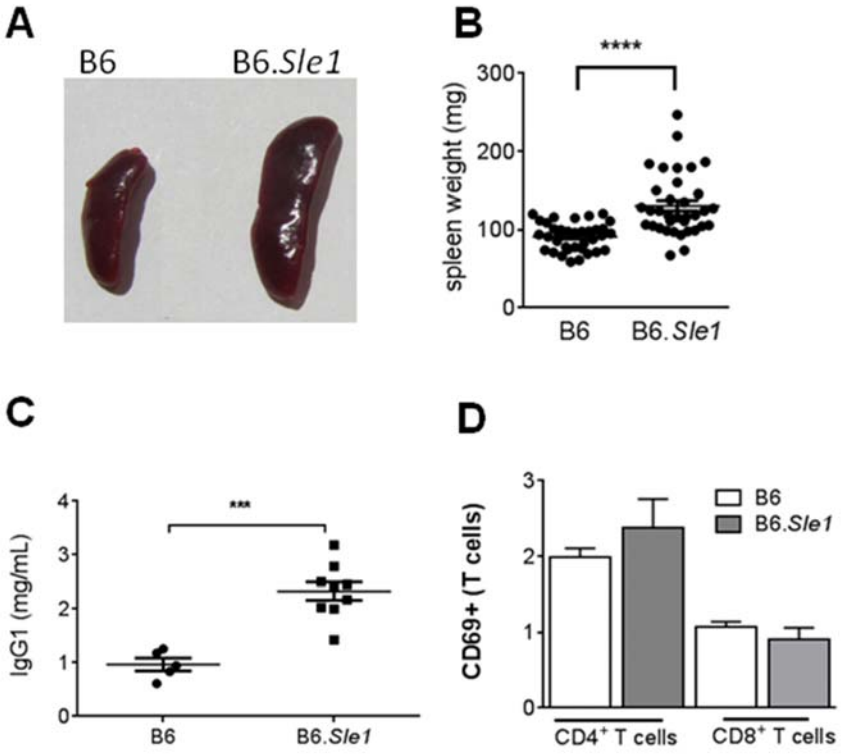

Figure 1.7 Female B6.*Sle1* mice phenotype

(A) Spleen size, (B) Spleen weight, (C) IgG1 titter, (D) T cells activation status of female 6 month old B6 and B6.*Sle1* mice. (Kindly provided by Dr.T.Celhar)

The *Sle1* region harbours 24 genes, most of them unrelated to immunology (Wandstrat, Nguyen et al. 2004). Dissection of the *Sle1* locus revealed 4 sub-loci named *Sle1a, b, c, d (cite)* (Table X.1). B6.*Sle1b* mice resemble the B6.*Sle1* phenotype the most (Morel, Blenman et al. 2001).

Genes encoding the signaling lymphocytic activation molecule family (SLAMF) members are the most potent candidates (for breaching immune tolerance within the *Sle1b sub*locus, since they are expressed in most types of immune cells and are highly polymorphic. Two main haplotypes of SLAMF genes are known: haplotype1 and haplotype2 (Wandstrat, Nguyen et al. 2004, Wang, Batteux et al. 2010). Mice carrying

haplotype1 do not develop autoimmunity, however the presence of the haplotype2 genes provokes autoimmune development (Bygrave, Rose et al. 2004).

Sub-loci	Phenotype	References
Sle1a	Higher IgG level over IgM; Increased B220+ cells; Decreased CD4+ and CD8+T cells;	(Morel, Blenman et al. 2001)
Sle1b	IgG ANA; Increased level of IgG and IgM; Splenomegaly; Activated B and T cells;	(Wandstrat, Nguyen et al. 2004) (Morel, Blenman et al. 2001)
Sle1c	Low penetrance for ANA; Lower IgM than in B6; Increased CD4+ memory T cells;	(Morel, Blenman et al. 2001)
Sle1d *not fully characterized	Nephritis pathology	(Morel, Blenman et al. 2001)

Table 1.1 Functional role of *Sle1* subloci.

In a very elegant study with the utilization of VH knock-in transgenic mouse line encoding dual specific BCR (HKIR) was determined that *Sle1* region breaching peripheral tolerance through the alteration during germinal centers checkpoint, however the exact molecular mechanism remains elusive (Vuyyuru, Mohan et al. 2009).

1.6 Biology of the SLAM family members

SLAMF became attractive targets for investigation due to their involvement in multiple immunological processes (Chan, Westcott et al. 2006) and pan-leukocyte expression (Wu and Veillette 2016). Major functions of these molecules are cell-to-cell contact of immune cells, cellular activation and regulation (Cannons, Tangye et al. 2011). There are currently 9 reported SLAMF members; historically some of the molecules were

given several names, meanwhile others have the same name in humans and mice. Usually one type of immune cell expresses 3 to 5 SLAMF members (Wu and Veillette 2016) .

SLAMF genetics

The genes encoding SLAMF receptors are located on the long arm of chromosome 1 in humans (1q23-24) within a 400 kilobase cluster and its syntenic region at 93.3 cM on murine chromosome 1. The SLAMF genes share a similar structure between each other consisting of several exons. The 5' UTR and signal peptide are encoded by exon 1, the exatracellular domain is encoded by exons 2 and 3, the transmembrane domain of the receptors encoded by exon 4 and the intracellular domain, which is usually expressed in different isoforms due to downstream splicing, is encoded by several more exons (Tangye, Phillips et al. 2000).

Structure

SLAM family members are distinct immune receptors, which are part of the larger CD2-superfamily of Ig-domain containing molecules. According to the structural classification, cluster of differentiation 2 (CD2) molecules belong to the immunoglobulin superfamily, since the extracellular region consists of two immunoglobulin-like domains (Yang, Ye et al. 2001). The CD2 molecule, which gave the family its name, is a cell adhesion molecule expressed on the surface of T cells and natural killer cells (NK cells) (Sanchez-Madrid, Krensky et al. 1982). The SLAMF members are type I cell surface glycoproteins that have a variable domain lacking a disulfide bond at the N-terminal end which is involved in ligand-binding and a C2 domain with 2 conserved disulfide bonds proximal to the membrane. The only exceptional member is Ly9 (SLAMF3) having 4 extracellular domains due to genetic duplication (Sandrin, Gumley et al. 1992).

The cytoplasmic regions of SLAMF members (with the exception of SLAMF2) possess one or several immunoreceptor tyrosine-based switch motifs (ITSMs) which mediate downstream signaling. The amino-acid sequence of an ITSM motif is T X Y X X V/I and it functions as a docking site for intracellular kinases, phosphatases, SLAM associated protein (SAP), or Ewing's sarcoma associated transcript 2 (EAT-2) and EAT-2 related transducer (ERT) dependent upon the cell type (Engel, Eck et al. 2003, Ma, Nichols et al. 2007).

Function

Hence, the SLAMF family includes mostly adhesion homotypic receptors that usually interact with other adhesive molecules and possesses co-stimulatory activity (Wilkins, Yang et al. 2003). These molecules are expressed on different types of immune cells and play various roles in the immune system such as (i) modulation of neutrophils

(PMNs) and macrophage (MF) functions, (ii) regulation of leukocyte adhesion, (iii) co-stimulation and cytokine production and (iv) development of innate T lymphocytes (Cannons, Tangye et al. 2011)

1.6.1 SLAMF DOWNSTREAM SIGNALLING.

Various immune cells express different types of adaptor protein which mediate SLAMF intracellular signaling. The three adaptor proteins SAP, EAT-2 and ERT interact with SLAMF members and transmit the extracellular signals primarily via a common Src homology (SH2) domain, through which those adaptor proteins bind to SLAM receptors and downstream molecules.

SAP is expressed in both mice and humans in T and NK cells; the SAP gene is located on the X chromosome and its structure consists of a SH2 domain and a short amino-acid tail. SAP plays a role in the regulation of Th2 differentiation, since it recruits the kinase Fyn and mediates Th2 cytokine production through NF-kB signaling (Li, Sofi et al. 2007). Knocking out SAP in murine models affects the T cell-dependent immune response only (Cannons, Yu et al. 2006), SAP deficiency in humans has a more dramatic result however of a fatal disease called Duncan's disease or X-linked lymphoproliferative disorder characterised by vasculitis, B cell lymphoma and dysgammaglobulinemia and infectious mononucleosis (Veillette 2006, Schwartzberg, Mueller et al. 2009, Cannons, Tangye et al. 2011).

SAP is important in SLE development; although it is not expressed in B cells, antibody production is impaired in SAP-deficient mice. EAT-2 is expressed in B cells**.** The gene encoding EAT-2 located on chromosome 1, next to the SLAMF members. EAT-2 is expressed in APCs, including B cells and NK cells (Cannons, Yu et al. 2006, Veillette 2006, Schwartzberg, Mueller et al. 2009).

The last adaptor protein is called ERT: it expressed in NK cells, CD8+ T cells and macrophages, and functionally similar to EAT-2, however posseses a different impact on NK cells, negatively regulating their function, but not their development (Cannons, Tangye et al. 2011). Unlike SAP, both EAT-2 and ERT are missing a domain which allows to interact with Fyn kinase and have been proposed to negatively regulate phosphorylation of their receptors (Roncagalli, Taylor et al. 2005).

Downstream signaling of SLAMF members is poorly understood, however it could play an important role in the development of pathologies. Impaired intracellular signaling

might arise from alterations in SLAMF structure or an alternative isoform, which could lead eventually to various disorders including autoimmunity.

1.6.2 SLAMF POLYMORPHISM, ISOFORMS, SNPS

Polymorphisms within the *Sle1b* region on Chromosome 1 give rise to isoforms in SLAMF members. In total 12 SNPs were reported within structural and regulatory regions of SLAMF members which distinguish the B6 and B6.*Sle1b* genome (Wandstrat, Nguyen et al. 2004). Further analysis has revealed a set of SNPs inherited as a single unit and was called a haplotype. Mild autoimmune traits in murine models where the *Sle1* locus was introduced on the B6 background, arise from a haplotype of SLAMF members suggesting that actually autoimmunity is a consequence of bad combinations of common alleles in a specific genomic context. Two distinct haplotypes of SLAMF/CD2 have been identified thus far, with haplotype 2 linked to SLE since it has been reported in autoimmune prone mouse models (Wang, Batteux et al. 2010).

Currently it is not known whether the isoform variations in several members of SLAMF originate from splice variants or from haplotype differences. (Wandstrat, Nguyen et al. 2004). A variety of isoforms has been suggested for almost each human and mouse SLAMF member according to ENSMBL and UniProt databases. For example, in mice SLAMF1 and SLAMF6 have 3 isoforms each and SLAMF5 has 5 reported isoforms (Palou, Pirotto et al. 2000). Moreover, in humans SLAMF3 is known to have 5 isoforms and the SLAMF5 protein has been predicted to be expressed in 7 isoforms.

Some haplotype differences in structure of SLAMF receptor is usually followed by a change in their functions. As an example, SLAMF molecule Ly-108-H1 encodes an additional tyrosine (Tyr) in its cytoplasmic domain, which is most probably involved in altering intracellular signaling. A structural change in this molecule results in an increase in the TCR-mediated immune response and a self-reactive immune system (Veillette 2006).

1.6.3 CD84 AND LY108 AS POTENTIAL CANDIDATES

Recent studies propose the role of Ly-108 and CD84 as prominent genes driving murine autoimmunity (Wang, Batteux et al. 2010). Mice heterozygous for *Sle1* demonstrate a reduction in penetrance of ANA (30%) compared to homozygous mice (90%). This property makes it possible to use bacteria artificial chromosome (BAC) transgenic strategy. One group used BAC carried B6 alleles of the *sle1b* causative genes subsequently introduced them into the B6.*Sle1b mice*. ANAs was measured after 9 to 12

months, allowin identification of causative genes for ANA production deriving from B6.*Sle1b*. Out of several BACs spanning the *sle1b* region, only a BAC carrying the CD84 and Ly108 genes demonstrated significant suppression of ANA production (Wong, Soni et al. 2015).

Extensive studies to dissect particular SLAMF members responsible for ANA production still have not revealed the exact molecule. Initially Ly108 was shown to be a key molecule in the peripheral tolerance maintenance, due to Ly108-H1 isoform, expressed only in B6 haplotype and inhibiting ANA development (Dutta and Schwartzberg 2012). However a BAC carried Ly108 only failed to suppress fully ANAs development in B6.*Sle1* mice. CD84 is important during follicular T helper cell development, for the proper interaction of B and T cells and for optimal germinal centre formation (Cannons, Qi et al. 2010). Furthermore, this data suggested the plausible role of one of CD84 isoforms or haplotype in ANAs suppression.

1.6.4 BIOLOGY OF MURINE CD84

1.6.4.1 CD84 GENE STRUCTURE

The human *CD84* gene was discovered almost two decades ago by the isolation of cDNA from B cell lymphoma cell line (de la Fuente, Pizcueta et al. 1997). The CD84 gene is located in long shoulder of chromosome 1, within the SLAM locus, at position 1q24 in human, and at 1H3 at 93.3 cM in the murine genome (de la Fuente, Pizcueta et al. 1997). The structure of the CD84 gene consists of 7 exons in human and 9 exons in mice **(Figure 1.8A)**; with 2 exons in murine CD84 remaining untranslated. Due to alternative splicing of exons and the use of cryptic splice sites, multiple isoforms of the protein are possible (Palou, Pirotto et al. 2000). Five isoforms of human CD84 were reported by Palou *et al.* (Palou, Pirotto et al. 2000), which differ mostly in their predicted cytoplasmic domains. Current information from the ENSEMBL browser (*www.ensembl.org*) suggests 7 putative isoforms for the human protein and 5 isoforms for the murine homolog (Figure 1.7 B). According to BLAST *(www.ncbi.nlm.nih.gov/blast)* human and murine CD84 has 58% amino-acid similarity.

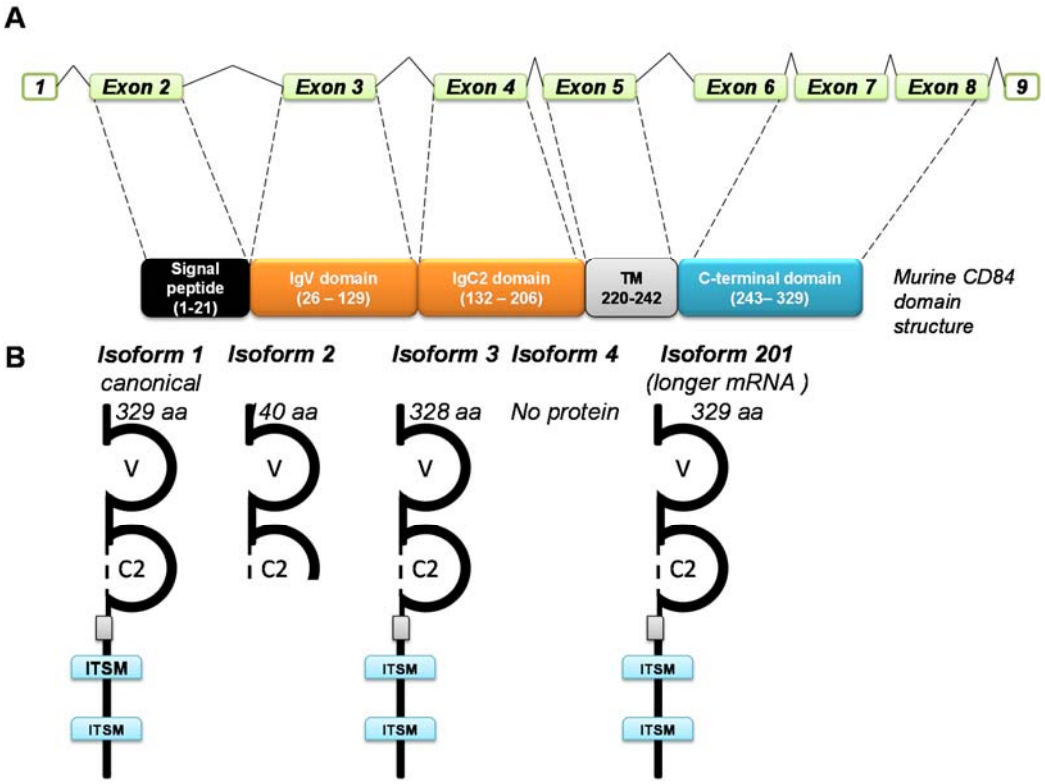

Figure 1.8 Murine CD84 gene and protein structure

(A) Genomic structure of the murine CD84 coding region. Exons 1 and 9 are untranslated (empty boxes), while exons 2-8 are translated (green filled boxes) to the indicated protein domains. (B) Schematic of the murine CD84 protein isoforms according to ENSEMBL browser. TM- transmembrane region; V – immunoglobulin V; IgC2 – immunoglobulin C2.

1.6.4.2 CD84 PROTEIN STRUCTURE

The CD84 protein is highly glycosylated, however the actual molecular weight is approximately 39 kDa (de la Fuente, Pizcueta et al. 1997). CD84 is a cell surface type-I transmembrane glycoprotein. Similar in mouse and humans, the protein has a 21 aa N-terminal extracellular part. Followed by 199 aa long IgV and IgC2 domains, a 25 aa transmembrane domain and a C-terminal intracellular domain which is 83 aa long (Figure 1.7 A). The C-terminal cytoplasmic domain encodes two ITSM motifs, where phosphorylation occurs, providing downstream signals inside the cell (de la Fuente, Pizcueta et al. 1997, Krause, Rehli et al. 2000, Palou, Pirotto et al. 2000). CD84 is a homotypic receptor binding CD84 on other immune cells or platelets (Nanda, Andre et al. 2005).

1.6.4.3 CD84 EXPRESSION

CD84 is expressed on various populations of immune cells, including granulocytes, dendritic cells, mast cells, monocytes, macrophages, B and T lymphocytes and platelets (de la Fuente, Pizcueta et al. 1997, Zaiss, Hirtreiter et al. 2003, Romero, Benitez et al. 2004, Nanda, Andre et al. 2005). CD84 is also expressed on pluripotent stem cells and its expression is upregulated upon differentiation to committed progenitors (Zaiss, Hirtreiter et al. 2003). CD84 has been particularly studied on CD27+ memory B cells express CD84 at a higher level than naïve B cells, however memory B cells have been shown to lose CD84 expression upon *in vitro* activation (Tangye, van de Weerdt et al. 2002).

Among other blood cells, platelets express the highest levels of CD84 (Nanda, Andre et al. 2005). In addition, the SLAMF member CD150 is expressed on the surface of platelets. During platelet activation, the cytoplasmic tail of the CD84 cell surface receptor undergoes tyrosine phosphorylation (Nanda, Andre et al. 2005). No aggregation of platelets was observed following inhibition of CD84 (Nanda, Andre et al. 2005).

1.6.4.4 CD84 DOWNSTREAM SIGNALING

The CD84 downstream signaling pathway has been partially elucidated. These studies have been performed on B cells and T cells, indicating differences in the downstream proteins involved in the different cell types. For example, antibody crosslinking of CD84 in T cells and platelets leads to ITSM phosphorylation and recruitment of SAP protein as an intracellular adaptor (Tangye, Nichols et al. 2003, Nanda, Andre et al. 2005).

While B cells and other antigen presenting cells do not express SAP, tyrosine phosphorylation has still been detected upon antibody-crosslinking with CD84. Another SH2-domain containing protein, EAT-2, is reported in B cells and macrophages to bind phosphorylated CD84 and enable intracellular signaling (Morra, Lu et al. 2001). To our knowledge, the intracellular adaptor molecule recruited following CD84 phosphorylation in granulocytes has not been studied yet in either in human or murine granulocytes.

1.6.4.5 CD84 KO MICE

Studies performed on CD84 knock out (KO) mice did not report alterations in platelet functions, and platelet–platelet interactions (Hofmann, Braun et al. 2014), however CD84 might be important in interactions of platelets with other immune cells.

Since lupus in multifactorial disease, the role of any cell-type should not be underestimated.

CD84 ko mice did not demonstrate any specific phenotype, however B - T cell interactions and germinal center formation are impaired in these mice (Cannons, Qi et al. 2010). This study highlights the importance of integrins in the initial B and T cell interactions, and the requirements of SAP and CD84 to sustain longer interactions (Cannons, Qi et al. 2010).

1.6.4.6 CD84 FUNCTION

Homophilic interactions of CD84 molecules on human leukocytes provoke increased IFN-γ signaling (Martin, Romero et al. 2001). Cross-linking of CD84 on T cells stimulated with anti-CD3 antibody lead to increased levels of T cell proliferation (Tangye, Nichols et al. 2003), suggesting that CD84 acts as a co-stimulatory molecule. The evidence of interactions of CD84 with TLR4 comes from a study demonstrating the role of CD84 in macrophage cytokine expression upon stimulation with the TLR4 ligand, LPS (Sintes, Romero et al. 2010). Platelets lose surface CD84 expression upon activation by calpain and ADAM10 enzymes (Hofmann, Vogtle et al. 2012).

If the functional role of CD84 expression has been partially addressed on B and T lymphocytes and platelets, innate immune leukocytes were omitted by scientists. However, a recent report about the role of CD84 in ANA formation brings more attention to this protein expressed by most of the immune system cells (Wong, Soni et al. 2015).

1.6.5 AN ASSOCIATION OF CD84 AND TLR7

The investigation in our laboratory using flow cytometry revealed that human PMNs selectively express only one SLAMF member - CD84; this was an unknown phenomenon for PMNs **(Figure 1.8 A).** However, the comparison of the frequency of this novel CD84+ subset between SLE patients and controls did not reveal any differences.

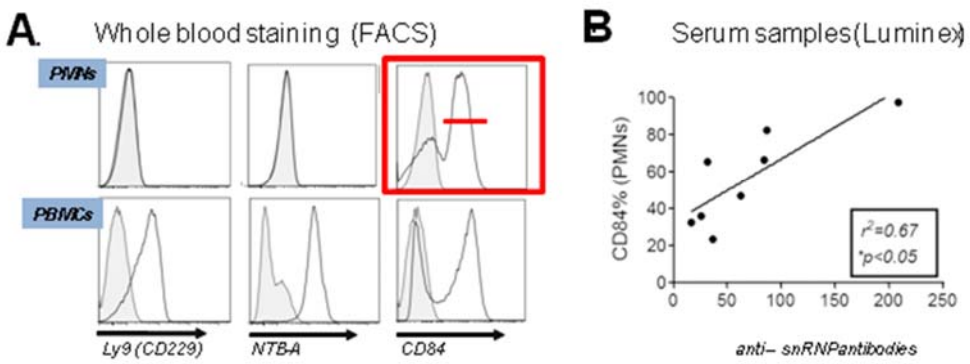

Figure 1.9 Correlation of CD84 on PMNs and anti-snRNP antibodies.
(A) SLAMF members expression on peripheral PMNs and PBMCs. (B) Correlation of CD84+ PMNs subset in patients with anti-snRNP ab titers. (Kindly provided by Lee HY)

Luminex analysis was used to detect ANAs from patients' samples. Luminex is a flow cytometry based technique allowing determination of multiple soluble proteins. The principle of this technology resides in combining fluorescent labelled specific antibodies with Multiplex beads (Carson and Vignali 1999). The data from Luminex obtained in our laboratory demonstrated positive association of CD84+ PMNs subset and the level of anti-snRNP antibodies only **(Figure 1.9 B).** Anti-snRNP antibodies form ICs with self-RNA further internalizing through the BCR on B cells or the FcγR on PMNs. RNA from these ICs may then activate TLRs, suggesting plausible intrinsic interactions between CD84 and TLR7.

Multiple murine studies provide evidence for the importance of TLR7 as a center al molecule for spontaneous GCs development (Soni, Wong et al. 2014), as well as the presence of SLAMF members with an extra copy of TLR7 results in fatal lupus disease, highlighting possible interactions of CD84 and TLR7 (Hwang, Lee et al. 2012) The BXSB murine models used in lupus research possess SLE-like phenotype due to aberrations in TLR7 gene(Morel, Croker et al. 2000).

Summarizing the data from SLE patients samples and mouse models of SLE, it is clear that TLR7 participates in pathogenesis of SLE; however the mechanism of its role during participation remains elusive.

1.6.6 Murine and human CD84

Murine and human CD84 receptor shares 58% homology when a BLAST search was conducted (https://www.ncbi.nlm.nih.gov/BLAST). Human CD84 expressed on the majority of immune cells (de la Fuente, Pizcueta et al. 1997), suggesting an involvement

of CD84 in multiple immunological functions. Furthermore, human CD84 might be used as maturation marker, as CD84 expression is increased upon maturation of CD34+ progenitor cells and CD27+ memory B cells (Tangye, van de Weerdt et al. 2002). Furthermore, both mice and human CD84 have been shown to be involved in the humoral immune response, through the interactions of T and B cells in the germinal centers (Cannons, Qi et al. 2010), thus may play an important role in the adaptive immune cells.

A report from Wang (Wang, Batteux et al. 2010) shows that polymorphism in human and murine CD84 is associated with lupus-like symptoms development in certain human populations and in mice. A work of Reindel and colleagues (Reindel, Bischof et al. 2014) described upregulation of CD84 gene in platelets and immune cells in Kawasaki disease, an autoimmune disease. Since CD84 is involved in T-B cells interactions (Cannons, Qi et al. 2010), it could influence ANA development by altering peripheral immune system checkpoints, for example in germinal center. Moreover, due to CD84 pan-leukocytic expression, its dysregulation may lead to multiple autoimmune pathologies; therefore, blocking or antagonizing CD84 might be a promising strategy to mitigate autoimmune diseases.

1.7 SUMMARY AND PROJECT AIMS

Data from our lab suggested a role of CD84 in the pathogenesis of SLE includes the correlation of serum anti-snRNP autoantibodies with PMN CD84 expression in SLE patients. Anti-snRNP-self RNA immune complexes stimulate TLR7 following internalization through either the BCR on B cells or the FcγR on innate immune cells, which ultimately activates IFN-α production by pDC and leads to disease progression.

Furthermore, the data from SLE murine models also demonstrates an important role for TLR7 in lupus pathogenesis. Polymorphisms within the *Sle1* region in autoimmune prone mice result in structural changes of SLAMF molecules leading to alterations in their functions. This has led to studies demonstrating that expression of auto-immune-prone Ly108 and CD84 SLAMF members results in ANA production(Wong, Soni et al. 2015). **We therefore hypothesize that the interaction of CD84 with the TLR7 pathway contributes to SLE progression.**

To address this hypothesis we established murine and human studies. We aimed to investigate CD84 expression at both the RNA, DNA and protein level in cohorts of young and aged mice. Furthermore, we wanted to examine the modulation of CD84 following various stimulations of PMNs and B cells. Furthermore, we wanted to assess platelet-PMN conjugate formation in steady state and upon stimulation in murine blood of both B6 and B6.*Sle1* mice. Lastly, we aimed to investigate the difference in NETosis level in autoimmune mice compared to conrol B6, and role of CD84 in NETosis. Since the robust method for NETosis quantification was missing, we developed a flow-cytometry based assay for NETs quantification, which is possible to apply to human and murine neutrophils. It is plausible that the upregulation of CD84, together with amplification of the TLR7 pathway, leads to immune system dysregulation and progression of SLE. Hence, the system to assign CD84 and TLR7 interactions was developed. I will address this initial dysregulation during my PhD studies.

Objective A – To assess CD84 cellular expression in murine leukocytes at the RNA and protein level:

1.1 To assess CD84 protein expression on leukocytes from the spleen and kidney of aged B6, B6.*Sle1*.

1.2 To assess CD84 protein expression on leukocytes from BM, spleen and whole blood of young B6 and B6.*Sle1* mice;

1.3 To identify sequence differences in genomic DNA in B6 versus B6.*Sle1* mice

1.4 To confirm sequence differences between CD84 mRNA in B6 and B6.*Sle1* mice by Illumina Technology;

Objective B – To examine the functional role of CD84 in B cells:

2.1 To assess CD84 expression on B cells upon stimulation with TLR ligands and IgM/IL-4;

2.2 To assess antibody production following TLR stimulation;

2.3 To assess CD84 expression on B cells upon homotypic stimulation with rCD84 or anti-CD84 ab.

Objective C – To evaluate the importance of CD84 haplotype and interactions with TLR7:

3.1 Develop a system allowing for evaluation of the role of CD84 haplotype *in vitro* and *in vivo*;

3.2 Investigate in vitro interactions of TLR7 with different haplotypes of CD84;

3.3 In vivo study of the CD84 haplotypes in B cells.

Objective D – To characterize the functional role of murine CD84 in PMNs

4.1 To characterize platelet-PMN conjugates in different tissues from B6 and B6.*Sle1* mice;

4.2 To assess CD84 expression on PMNs upon stimulation with TLR ligands;

4.3 To investigate apoptosis levels in murine PMNs in B6 and B6.*Sle1* mice

4.4 To investigate NETosis levels in murine PMNs in B6 and B6.*Sle1* mice

Objective E – To develop and optimize a quantitative method for murine and human NETosis evaluation:

5.1 Evaluation of existing methods for NETosis quantification;

5.2 Evaluation of new possible tools/equipment for the detection and further quantification of NETosis;

5.3 To validate antibodies for flow cytometry which could be used for NETosis detection;

5.4 To validate and compare a novel method for NETosis detection

with existing methods.

2 MATERIALS & METHODS

2.1 Mouse strains

Mice were bred and maintained in pathogen-free conditions at the Biomedical Resource Centre (BRC), A*STAR, Singapore. Breeding pairs for C57BL/6J (B6) mice were originally obtained from the Jackson Laboratory. The derivation of the B6.*Sle1* and B6.Tg7 strains has already been described (Morel, Croker et al. 2000, Celhar, Hopkins et al.). Breeding pairs were kindly donated by Ward Wakeland, UT Southwestern Medical Center, Dallas, USA.

For aging studies to detect the development of disease, mice were 6-9 months old. For all other studies mice were used at the age of 6-8 weeks. The care and use of laboratory animals conformed to the National Institutes of Health guidelines and all experimental procedures conformed to an IACUC approved animal protocol.

2.2 Verification of Strain identity by PCR genotyping

2.2.1 PREPARATION OF DNA FROM MOUSE TAIL LYSATES

To confirm the genotype of the mice, tails (0.5 cm or less) were processed for DNA extraction and genotyping by polymerase chain reaction (PCR). Tail snips were transferred to a 1.5 ml centrifuge tubes and 75 µL of alkaline lysis buffer (recipe in Appendix IV) per tail was added. The centrifuge tubes containing the tail and lysis buffer were heated at 95˚ C for 1 h. Following rapid cooling at 4˚ C for 5 min, 75 uL of neutralizing buffer was subsequently added. Lysed tails were vortexed and centrifuged 10 sec at 10000 g, room temperature (RT). Supernatant containing DNA was stored at 4˚ C.

2.2.2 PCR GENOTYPING

PCR reactions in a total volume of 25 µl contained 10-100 ng of template DNA, 200 µM of each of dNTP, 25 mM $MgCl_2$, reverse and forward primers at 660 nM in 10X reaction buffer (Taq polymerase buffer) diluted in distilled water to a 1 X final concentration. Cycle conditions were as follow: 35 cycles of 95 C for 30 seconds, 55-58 C for 30 seconds, 72°C for 1 minute.

		PCR Product size (bp)	
Strain	Marker	C57BL/6	B6.Sle1
B6.Sle1	D1Mit17 (1-17)	167	179
	D1Mit113 (1-113)	210	235
	D1Mit202 (1-202)	143	179

* Please refer to the reagents list for the sequences of the primers

Table 2.1 Primers and expected band sizes for B6.*Sle1* and B6.Tg7 mice:

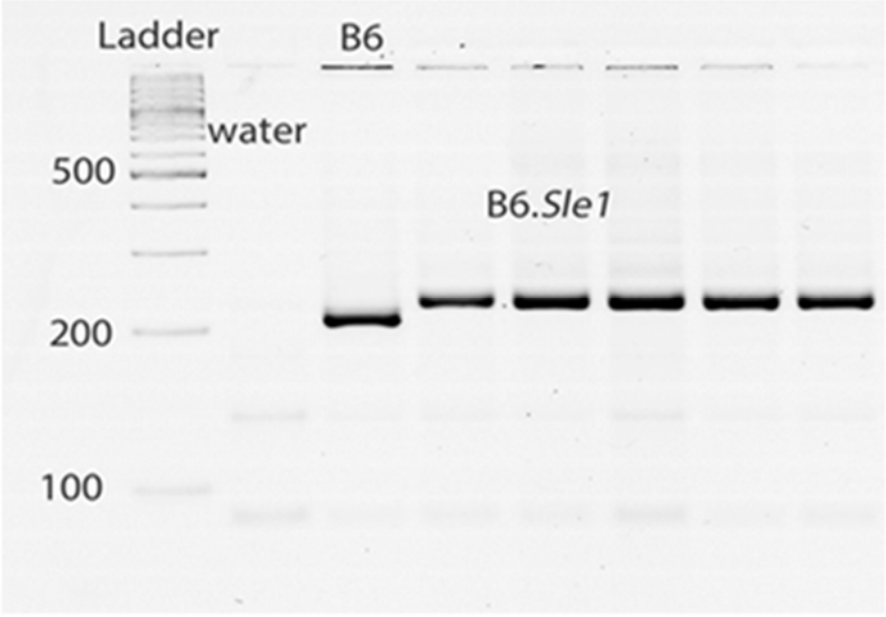

Figure 2.1 Example of 5% agarose gel with detected product.

2.3 Analysis of serum autoantibodies

Murine blood was collected retro-orbitally in serum tubes (approximately 200 µl per tube) for the detection of auto-antibodies. Blood was processed according to manufacturer instructions (Sarstedt AG & Co). In brief, collected samples were stored at 4º C for 2 h, they were centrifuged at 93000 g, 4º C, for 7 min in a table-top centrifuge.

The transparent soluble fraction was aliquoted and stored at -80º C. Auto-antibodies were detected using HEP-2 slides or ELISA.

2.3.1 ENZYME-LINKED IMMUNE SORBENT ASSAY (ELISA) FOR ANTI-BODIES PRODUCTION

ELISA was performed strictly according to manufacturer instruction. eBioscience anti-IgA, anti-IgM, IgG2a, IgG2b, IgG3, IgG1. In brief, 96-wells flat bottom plates were coated overnight with anti-bodies of interest diluted in coating buffer. Next day, plates were washed, samples in required dilution were added and incubated required amount of time (determined by manufacturer). Following incubation plates were washed and detection ab were added. After 1 h of incubation plated were washed 5 times and detection solution were added. Signal was allowed to develop for 15 min at room temperature (RT) and absorbance were measured at Envision plate-reader.

2.4 Murine tissue sample preparation

2.4.1 SPLEEN PROCESSING

Spleen was harvested, meshed and filtered immediately into chilled Roswell Park Memorial Institute-1640 (RPMI) media. Splenocytes were spun down at 1500 rpm for 5 minutes at 4ºC. Pellet was resuspended in 1 mL of RPMI for cell counting and viability was assessed by Trypan blue exclusion. Splenocytes were then diluted to a concentration of 2 x 10^6 cells/mL using RPMI.

2.4.2 BONE MARROW PROCESSING

Fibia and tibia was removed from the murine hip bones, leftover muscles and tissue were strip off with scissors and forceps, maintained in 70% EtOH followed by RPMI. Clean bones were placed in Petri dish with plane RPMI. The joint ends of the bones were cut off and crashed later. Long bones were flushed with plain RPMI using a 25 g needle/3 ml syringe. Cell pellets were crushed using the syringe and filter into a 50 ml conical through a 70 µM sterile sieve. Cells were spun down immediately at 1500rpm, 5min, at 4C.

2.4.3 WHOLE BLOOD PROCESSING AND STAINING

Mouse blood was collected in the plastic heparin tubes, volume 300 ul. Immediately after collection 100 ul of blood were seed to the Nunc™ *96-Well* Polystyrene *Round Bottom* Microwell Plates and stain with 100 µL antibody for flow-cytometry. After

incubation for 30 min on ice in the dark plate were spun down at 1200 rpm, 5 min. Then samples were lysed 5 min at room temperature with BD FACS lysis buffer, washed 2 times and transferred to flow-tubes.

2.4.4 KIDNEY PROCESSING

Following perfusion with warm PBS to remove excessive blood from the tissue both kidney was extracted and put in cRPMI. Connective tissue was removed using two curved forceps and one kidney was chopped by razor blade in 4 cm petri dish. After homogenize tissue was carefully transferred into 1.7 mL tube and plate was washed with 500 µL of ice-cold PBS. Samples were spun down at 13000 rpm, 7 min, 4 C. Supernatant was carefully aliquoted and store in -80 C freezer. Tissue was transferred to 50 mL falcon tube and incubated 30 min at 37C, 150 rpm with 10 mL collagenase A (Roche). After incubation cells were syringed with 23G 2 times and 21G 1 time and spun down at 4 C, 1500 rpm, 5 min. After washing syringing was repeated and cells were transferred trough 70 µn (micron) neilon mesh and toped up with fresh cRPMI to 20 ml. Cells suspension was layered over 40% percoll and spun down at 2000g no break, 20 min, in order to separate immune cells.

Following centrifugation supernatant was carefully aspirated and cells were wahed 2x with PBS. Ready cells were resuspended in 100 ul of SB and prepared for staining.

2.5 Specific cell isolation and culture

2.5.1 ISOLATION OF MURINE HEMATOPOETIC STEM CELLS (HSC)

Femurs and tibias of B6.*Sle1* or B6 mice were flushed and bone marrow cells were harvested in recommended media. Further cells were pelleted by centrifugation at 1500 rpm, 5 min, RT subsequently resuspended in recommended media. StemSep lin- (full name of the cells) mouse isolation kit was used according to manufacturer's instructions to isolate cells from 2-8 x 10^7 cells/ml. Isolated murine lin- stem cells were cultured in StemSpan SFEM serum-free medium supplemented with 1% (v/v) penicillin/streptomycin and cytokines (100 ng/ml mSCF, 100 ng/ml mFlt-3, 100 ng/ml mIL-11, 20 ng/ml mIL-3) using non-treated 24-well plates.

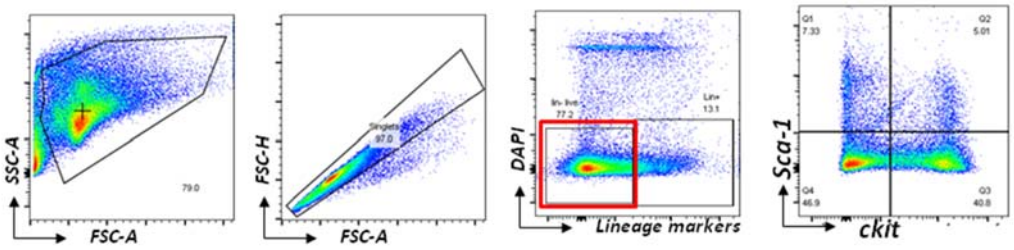

Figure 2.2 Isolation of hematopoetic stem cells.
The population of interest is in the red box.

2.5.2 ISOLATION OF SPLENIC MURINE B CELLS

Splenic B cells were isolated using a B cell isolation kit II, mouse, from Miltenyi or B cell negative selection kit from StemCell Technologies according to the manufacture instructions.

2.5.3 ISOLATION OF MURINE NEUTROPHILS FROM BONE MARROW

Fibia and tibia bones were flushed in cRPMI and pelleted by centrifugation at 1500 rpm, RT, 5 min. Cells were counted and resuspended at the concentration 1 x 10^8 in recommended media. Subsequently neutrophils were isolated using cells negative selection kit, EasySep (StemCell), carefully to prevent activation of cells. In brief, cells were resuspended in recommended media (receipe in Appendix III), blocked with rat serum and labeled with cocktail of ab for cells except neutrophils. Following 15 min incubation on ice cells were washed with recommender media and centrifuged at 300 g, 10 min, 4 C. Biotinilated magnetic particles were added, and using magnet pure neutrophil fraction was extracted in a clean tube. Cells were washed and counted.

2.5.4 ISOLATION OF MURINE NEUTROPHILS FROM BLOOD

Whole blood was collected to heparin tubes through retro-orbital bleeding. Isolated cells were washed with PBS and neutrophils were isolated using EasySep negative selection isolation kit. Yielded cells were counted and resuspended at the concentration 1 x 10^6 cell/mL.

2.6 Stimulants preparation

2.6.1 TLR-LIGANDS FOR MURINE B CELLS AND NEUTROPHILS STIMULATION

TLR4 agonist LPS, TLR7 agonist R848 and TLR9 agonist CpG-B ODN1826 (InvivoGen) were used for stimulation. These ligands were serial diluted accordingly to reach 2X their respective concentrations using RPMI supplemented with 10% fetal bovine serum (FBS) (Thermo Scientific), 15mM HEPES, 1% penicillin-streptomycin, 0.1 mM MEM non-essential amino acids (NEAA), 1mM sodium pyruvate and 0.16 µM beta-mercaptoethanol (Sigma-Aldrich). This is known as complete RPMI (cRPMI). All reagents are from Life Technologies, Gibco, unless otherwise stated.

2.6.2 MURINE RECOMBINANT CD84 AND ANTI-CD84 ANTIBODY

Murine recombinant CD84 (rCD84) from Sino Biological or Anti-CD84 antibodies, clone m.CD84.7, from Biolegend were used in serial dilution as mentioned above. The dilution was prepared in cRPMI as stated above.

Splenocytes were seeded at a density of 250 - 500 K/well into 96-well plate round-bottom (Costar). Ligands were subsequently added such that the final concentration is reduced to 1X. Splenocytes were then incubated for their respective time points at 37^{o}C. cRPMI was used as an untreated control. All conditions were performed in duplicates.

2.6.3 CARBOXYFLUORESCEIN SUCCINIMIDYL ESTER (CFSE) LABELING

CFSE (Life Technologies ^{TM}) was diluted with RPMI media in a 1:4000 ratio. Equal volume of diluted CFSE was added to the cells to be stained and the mixture was incubated in dark for 7 minutes. Equal volume of FBS was subsequently added and incubated for a minute. Stained splenocytes were washed twice with cRPMI and recounted. Splenocytes were then seeded at a density of 200 K/well for ligand stimulation and incubated for 72 hours.

2.6.4 CELL VIABILITY ASSAY

B cells or neutrophils were seeded in round-bottom 96-well plate in the density of 500 K per well, stimulant were added ad described in 2.5.1. After each timepoint (24 h, 48 h, 72 h) plates were span down at 450g, 4˚ C, 5 min. Subsequently, cells were stained with Annexin V and propidium iodide (PI) according to manufacturer instructions. Acquired cells were further analyzed using gating strategy provided on the Figure 2.3

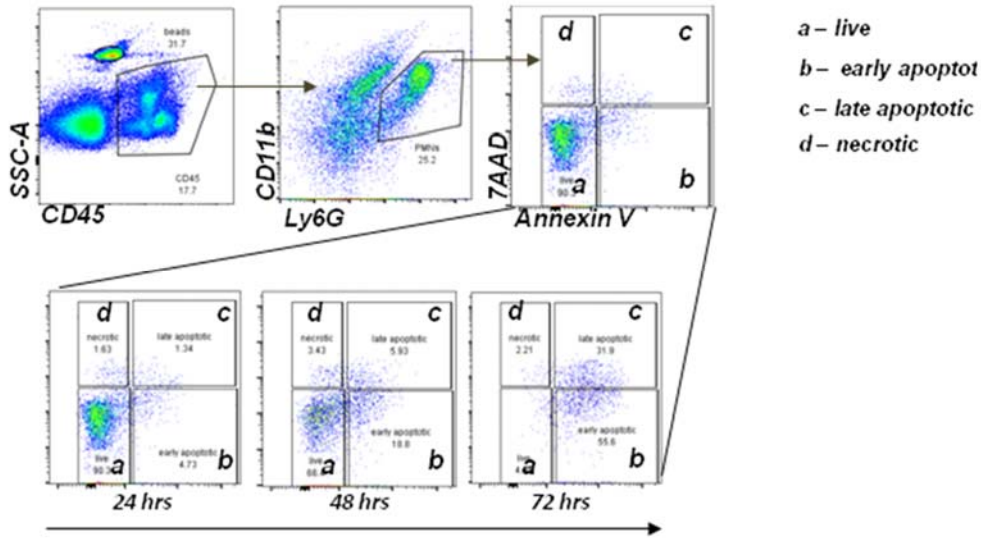

Figure 2.3 Apoptotic cells analysis.

2.7 Generation and culture of CD84-expressing HEK Blue cell lines

2.7.1 Propagation and maintenance of adherent cell lines

Complete Dulbecco's modified eagle medium (cDMEM) supplemented with 10% Fetal bovine serum (Gibco) and 1% (v/v) penicillin/streptomycin was used for maintenance of adherent cell lines. Selection antibiotics were added to engineered HEK-BLUE cell-line at 100 µg/mL. Cells were grown in T75 or T175 tissue culture flasks in 20 mL or 30 mL media respectively in 37ºC incubators in a 5% CO_2 atmosphere. Usually cells were passage around 70-80% confluency, for HELA and HEK293, HEK293ft 0.25% trypsin-EDTA solution was used for 5 min at 37 C.

Since trypsin may affect reporter gene expression in HEK-BLUE cell lines 10 mM EDTA at 37 C was used for 5 min in order to detached HEK-BLUE monolayers from tissue culture flask. Detached cells were washed with plain DMEM, centrifuged at 1500 rpm, 5 min, RT and resuspended in 10 mL fresh cDMEM. One to three mL of cells was transferred to a new flask.

2.7.2 Storage of cell lines

Cell lines stock was kept in liquid nitrogen. Before transfer to liquid nitrogen 5 – 10 x 10^6 cells were resuspended in 1 ml of freezing medium and transferred to 2 mL cryovials. Cryovials were stored at -80 freezer overnight to two weeks in Mr.Frosty containers

contained isopropanol to reduce cell death due to temperature shift, before transferred to liquid nitrogen tank.

To defrost a new batch of cells, vials were removed from liquid nitrogen into dry ice and directly placed in 37 C water bath for 2-3 min. After that cells were transferred to 25 ml of cDMEM and centrifuged at 1500 rpm, 5 min, RT in order to remove DMSO. Cells were resuspended in 10 ml of cDMEM without antibiotics and transfer to T75 tissue culture flask

2.7.3 HEK-BLUE ANALYSIS

Interaction of CD84 and TLR7 was assign using HEK-BLUE cells. According to manufacturer instructions sorted transfected cells expressing GFP cells were resaspended in SEAP media and plate to round-bottom 96 well plate in density 40 K/180 uL. Prior to cells seeding 20 uL of ligand or water was added to the plate. Cells were mixed with ligands carefully and incubated in 37 C, 5% CO_2 incubator for 14-16 h. The intensity of blue color was analysed using Envision plate reader. Absorbtion was recorded at 620 nm.

2.7.4 CD84 HAPLOTYPE-SPECIFIC PLASMID GENERATION

Lenti-viral plasmids were designed to carry one of two haplotypes (h) of CD84. CD84 h1 carried the non-autoimmune, B6 canonical sequence of CD84 (Q18PI6-1). The second plasmid, CD84-h2 expressed the sequence which was found from our analysis of B6.*Sle1* mice (Q18PI6-3)**.** This has a nonsynonymous variation in position 27 (Valine to Methionine).

A vector expressing only GFP (no CD84) was ordered as a control. In addition, a plasmid expressing the non-autoimmune Ly108 isoform, characterised previously in B6 mice (Dutta and Schwartzberg 2012) was also used (Genebank EU591721.1). The lentiviral plasmids were 3rd generation, ordered purchased from Addgene 2.0. Genes of interest were expressed under control of IRES promoters. Plasmid maps in Appendix figure 1-4

2.7.5 CD84-PLASMID TRANSFORMATION IN E.COLI

Bacteria *Escherichia coli* (*E.Coli*) were grown in liquid LB media supplemented with either kanamycin (50 µg/ml) or penicillin (100 µg/ml) at 37ºC, with shaking at 250-300 rpm. E.Coli were transformed by a heat shock method according to the manufacturer's instructions (Company). To the 10 µl of chemically competent bacteria cells (XL - gold or DH5α) approximately 100 ng of plasmid DNA was added. A mixture

was incubated 1 min on ice (4°C), following by heat shock at 42°C for 1 min. Subsequently 200 µl of LB was added and bacteria were plated on agar plates supplemented with 150 µg/ml ampicillin. They were then left at 37°C overnight (14-18 h). For long-term storage of transformed bacteria, 800ul of the overnight miniprep culture was vigorously mixed with 400 µl of 60% glycerol and stored at -80°C.

2.7.6 Isolation of CD84-plasmid DNA from E. coli

For low levels of plasmid, the Qiagen Mini-Prep kit was used to prepare plasmid DNA according to manufacturer's instructions from 5 ml of 6 h cultures. For large amounts of plasmid DNA, bacteria were cultured for 14-16 h in LB broth supplemented with required antibiotic. Subsequently DNA was extracted using the Qiagen Maxi-Prep according to the protocol supplied with the kit.

The concentration of plasmid and genomic DNA was measured in 1 ul of solution using NanoDrop ND-2000 spectrophotometer at wavelength of 260 nm (A_{260}). The quality of DNA was determined using the A260/A230 index: 1.85-1.95 index indicated good quality of DNA.

2.7.7 Validation of CD84 plasmid DNA by Restriction enzyme digest and agarose gel visualisation.

Approximately 1-3 µg of plasmid DNA was digested for 10-15 min at 37 C in a final volume of 50 µl. Restriction mixture consisted of distilled water, 10X enzyme compatible buffer diluted to 1X final concentration and 1 µl of restriction enzyme. Double or triple digestion was performed by addition of required enzyme to the mixture reducing the volume of distilled water. DNA digestion was verified by agarose gel electrophoresis.

For gel electrophoresis, an agarose gel was prepared by combining 1.5% low melting (Lonza) and 3.5% standard agarose (Lonza). 200 mL TAE buffer was added and the mixture was warmed using a microwave for 3min. The gel solution was cooled slightly and then GelRed (Biotium) was added at the manufacturer's recommended concentration. The gel solution was transferred into the gel tray and cooled until use. Xug of DNA was mixed with loading buffer and loaded onto the prepared gel. The gels were run at 60 min time and 90 min for 1% and 5% respectively.

For determination of DNA fragments size either 100 bp or 1 kb plus ladder was used in every gel. Separated DNA fragments were detected with either Typhoon™ FLA 9500 biomolecular imager or ultra-violet light using an UVIdoc gel documentation system.

2.7.8 VALIDATION OF CD84 PLASMIDS DNA BY SEQUENCING

In order to control for mutations in plasmids using for lenti-virus production, 10 µL (10µg total) of each plasmid: CD84-H1 and CD84-H2 were sent for sequencing using Axil Singapore. The sequencing results confirmed that the plasmids used in the study had the expected sequence of nucleotides. (Appendix X)

2.7.9 LENTIVIRUS PRODUCTION FOR *IN VITRO* AND *IN VIVO* WORK

The day before transfection 15 x 10^6 HEK293ft cells were plated in 15 cm round tissue culture plates in 13 mL cDMEM. After 24 h transfection mixture containing **40 µg** of lenti viral DNA and packaging plasmids as *pREV* (pRSV; addgene 12253) - **8 µg**, *pVSVG* envelope plasmid (pMD2,g; addgene 12259) - **8,5 µg,** *pMDL* packaging plasmid (pMDL9; addgene 12251) - **15,5 µg** was prepared**.** DNA was resuspended in serum-free OPTI-MEM media and mixed with equivalent amount of polyethylenimine (PIE) (10 mM) transfection reagent mixed with OPTI-MEM. After resuspension DNA and PIE mixtures were briefly vortexed and 1mL of PIE containing mixture was added to DNA.

The mixture was vortexed for 30 seconds and left for 20 min in RT until it became cloudy, then 2 mL of the prepared mixture was added to plate was added and mixed well. Viral supernatant were collected after 48 and 72 h, filtered through 0.45 nm filter and spun at 28000 rpm 2.5 – 3 h at 22 C using SW-28 rotor and Beckmann&Coulter ultracentrifuge. Pelleted virus was resuspended in serum-free StemSpam media, aliqoted and stored in -80.

2.7.10 LENTI-VIRUS TITRATION USING HELA OR HEK293FT CELL LINES

Viral titer was determined by transduction of either HEK293 or HELA cells (depends on experiment to be performed). 5 x 10^4 cells were seeded in cDMEM in 12-well plate 3 h before transduction. Later media was aspirated cells were washed with RT PBS and polybrene (increases virus adherence) in concentration 8 µg/mL was added. Serially diluted viral supernatant was added subsequently following 72 h incubation in

37C/5 % CO_2. Expression of GFP, RFP or gene of interest was analysed using flow cytometer and calculated by formula

T = (P*N)/(D*V)

T = titer (TU/mL)

P = % GFP positive cells according to the FACS (P= 0.2 for 20% GFP FACS) N = number of cells at the time of transduction)

D = dilution factor (10^{-3} = 0.001)

V = total volume of viral inoculum (1.50 mL)

2.7.11 TRANSDUCTION OF HEK-BLUE CELL – LINE

HEK-BLUE mTLR7 or control Null-2k cells were plate at 0.5 x 10^6 cells in 1.5 ml in 6-well plates. After 3 h supernatant was aliquoted, cells were washed with RT PBS and polybrene in concentration of 8 µg/mL were added. Viral supernatant in MOI 1 was added subsequently. Cells were left 72 h after initial transduction before further analysis. Subsequently transduced cells were kept in culture, since virus were integrated in there genome and used for further analysis.

2.7.12 TRANSDUCTION OF CD84 TRANSDUCED LENTI-VIRUS INTO ISOLATED HSCS

Cytokines for culturing HSCs were resuspended in 0.22 um filtered 0.1%BSA/PBS and 1500 µL was kept inside the tube for 30 min in RT to dissolve. Cytokines were aliquoted and stored in -20 C freezer.

HSCs were isolated as described in 2.4.1. and resuspended at 0.5–1 x 10^6 in StemSpam serum free media containing 1% of penicillin/streptomycin and the following cytokines: (mSCF (100 ng/ml), mFlt3 (100 ng/ml), mIL-3 (20 ng/ml), mIL-11 (100 ng/ml)). Cells were cultured in 24 well Non-treated plate (Costar).

Concentrated lenti-viral supernatant with TU of 1or above were added directly to the growth media, cells were kept in 37C, 5%CO_2, overnight. Next day cells were harvested and injected in lethaly irradiated recipient mouse, plated for methacult colony formation assay or pelleted and kept in -80 freezer for further analysis.

2.7.13 TRANSDUCTION OF TERMINALLY DIFFERENTIATED B CELLS

Isolated splenic murine B cells were plated in 12-well plate in concentration 0.3 - 0.5 x 10^6 in 500 ul cRPMI. Lenti-viral supernatant at MOI 2 was added to the media. In order to increase virus transduction B cells were spun down at 700 g, 1 h, 20 C. Cells were left 24 h in 37 C, 5% CO_2. Next day, B cells were transferred to 15 mL falcon tube,

12-well plate was washed with 10 mM EDTA and incubated 5 min in 37 C. 5% CO_2 in order to collect all cells. Subsequently cells were spun at 1200 rpm, no break, 5 min, RT and resuspended in 300 ul RPMI.

2.8 In vivo assessment of CD84 haplotype function.

2.8.1 Optimization of gamma - irradiation dose and engraftment experiment

In order to perform this experiment 6-8 week old mice were irradiated with different dose of gamma irradiation, start from lethal 6 Gy, sublethal 3 Gy, and half sublethal dose 1.5 Gy or left untouched. Doses were split on two days to decrease harmful effect of irradiation. CD45.1 cells were injected on the day of last irradiation.

Six days later cheek bleed were performed in order to determine the percentage of reconstitution. At day 21 the mice were sacrificed and spleen, whole blood were harvested in order to assign engraftment.

2.8.2 muMT B cells adoptive transfer

Sublethally irradiated over 2 days with 3 Gy B6.μMT (muMT) mice were i.v. injected with 1 x 10^6 lenti-viral transduced B cells resuspended in 300 ul RMPI using 27 G needle attached to tuberculin syringe.

2.8.3 Alum-ova challenge

For immune challenge of previously transferred lenti-virus transduced B cells mice were immunized with OVA, (Worthington) endotoxin level <0.001 μg/ml measured by limulus-amebocyte lysate assay (Biowhittaker), at doses 10 ug per mouse was used.

As an adjuvant Imject alum, a mixture of aluminium and magnesium hydroxide (Pierce Biochemicals) was mixed with OVA ag in saline in 1:20 ratio, followed by mixing no less than 4 h at RT. Mice were immunised with 200 ul of imject-alum solution containing 10 ug of OVA ag injected in the left lower part i.p. using 26 – gauge needle.

2.9 Single cell flow cytometry analysis

2.9.1 Leukocytes Surface Markers Staining

Plates were spun down at 1500 rpm for 5 minutes at 4°C. Supernatant was collected for cytokines analysis. Cells of the same stimulation conditions were pooled together. FcγII/III receptors of B cells were blocked with 25 μL of Fc-block (hybridoma

supernatant from 2.4G2 cell line producing anti- FcγII/III monoclonal Ab, produced in Dr. Anna-Marie Fairhurst's laboratory, SIgN) for 15 minutes. Cells were subsequently stained with a cocktail of antibodies which comprises of anti-CD4, anti-CD19, anti-CD84, anti-CD3, anti-CD69, anti-CD45 and anti-CD8 for 30 minutes in the dark. *Please refer to supplementary Table 3 for more details regarding antibodies*.

2.9.2 INTRACELLULAR STAINING

Cells stained with surface markers were washed 3 times in 150 ul of staining buffer and spun down at 1500 rpm, 4 C, 5 min. Subsequently cells were washed in 100 ul (1X) permeabilization buffer and stained for 30 min on ice with anti-bodies of interest diluted in 1X Fix/Perm buffer. After staining cells were washed 3 times in 1X Fix/Perm buffer spun down at 1500 rpm, 4 C, 5 min, resuspended in 200 ul of staining buffer and run in flow cytometer.

2.9.3 STAINING OF HUMAN WHOLE BLOOD LEUKOCYTES

Hundred uL of whole blood were pipetted out into U-bottom 96-well plate. Staining cocktail of antibodies in 2 times concentration was added for 30 min and left in the dark on ice. Subsequently 50 uL of staining buffer was added and 96-well plate was washed at 1200 rpm, 4 C, 5 min. Supernatant was carefully aspirated and 150 uL of BD Fix\lysis buffer was added in order to lyse red blood cells to diminish excessive autofluorescence. Cells were vigorously mixed with multi-channel pipette and left covered with aluminium foil at RT for 5 min. Cells were washed with addition of 100 uL staining buffer and spun down at 1200 rpm, 4 C, 5 min. Lyses was repeated if the pellet was too red. Following lysis plate were washed 3 times with staining buffer, stained cells were resuspended in 200 uL of SB and analysed on flow cytometer.

2.9.4 IDENTIFICATION OF PLATELET-LEUKOCYTES INTERACTIONS USING FLOW CYTOMETRY

Lysed whole blood was stained as described above with anti-bodies cocktail containing CD41, in order to identify platelets. Following gating strategy was used to target platelet-neutrophil complexes. Since platelets are much smaller then neutrophils exclusion of doublets wouldn't exclude platelet-neutrophil complexes. Cells were gated on neutrophils as CD66+, following by identification of 4 population CD84+Cd41+

(Neutrophils with platelets), CD84+CD41- (Neutrophils without platelets) Cd84-CD41- (population of CD84-Neutrophils) CD84-CD41+ (platelets alone).

2.9.5 Flow Cytometry Analysis

Stained cells were then washed twice with staining buffer (Phosphate saline buffer supplemented with HEPES and FBS). Finally, cells were resuspended in staining buffer containing 4', 6-diamidino-2-phenylindole (DAPI) for flow cytometry analysis. Fluorescence data were acquired using the 4-laser LSRFortessa flow cytometer system (BD Biosciences) and 10,000 events were recorded per sample based on live B cells. Data were analyzed using FlowJo version 10.1

2.9.6 Gating strategy

Compensation was checked on every sample, recompensation was done if necessary before analysis using FlowJo. Specific gating strategy for every experiment demonstrated in each figure, however general initial gating was applied to all samples.

First, doubles appearing on forward scatter (Figure 2.4) was excluded, by gate 1. Further live cells were gated on CD45+FSC-H parameters.

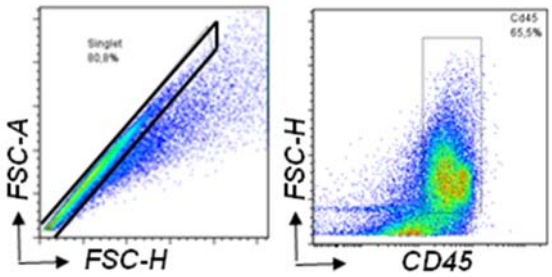

Figure 2.4 Initial gating strategy for live single cells identification

2.9.7 FMO CONTROL FOR MFI DETECTION IN FLOW CYTOMETRY

MFI or Median Fluorescence Intensity is a representation of amount of antibodies bind to the cell. The gating and subsequent calculation was performed based on FMO – fluorescence minus one control samples, where all the fluorochromes were added except, the fluorochrome of interest. Gating was set on positive values by the FMO.

2.10 Human sample processing

2.10.1 ETHICS STATEMENT AND HUMAN BLOOD SAMPLING

Human samples were collected and processed according to National University of Singapore Institutional Review Board "Blood from healthy donors collected in SIgN: Study of Blood Cell Subsets and their Products in Models of Infection, Inflammation and Immune Regulation", NUS-IRB 09-256**.** Peripheral blood was taken into a Vacutainer containing 3.8% EDTA (10%v/v; Becton Dickinson).

2.10.2 HUMAN PMNS ISOLATION

Neutrophils were isolated by density centrifugation as previously described (Paoliello-Paschoalato, Azzolini et al. 2014). Briefly, blood was mixed 1:1 with sterile pre-warmed PBS without calcium and magnesium. 20 mL of the mixture was layered onto a previously prepared separation media (10 ml Histopaque® 1077 on 10 ml Histopaque® 1119) and centrifuged at 800 *g* for 20 min, RT, brake off. The neutrophil layer above the red cell mass was removed using a pasteur pipette. Red cells were lysed with an equal volume (5-8 ml) of ACK lysing buffer for 5 min, RT. Following the incubation, an equal volume of PBS was added and the cells were spun at 450 *g*, 5 min, RT. ACK lysis was

repeated if necessary. The resultant cell pellet was resuspended in 1 ml RPMI-complete RPMI.

2.10.3 NETs IDENTIFICATION BY MICROSCOPY

NETosis was verified using an established fluorescent microscopy protocol with the following modifications (Brinkmann, Laube et al. 2010). Neutrophils were resuspended at 10^6 in 250 µl cRPMI and added to each well of a 12-well plate containing a 15 mm coverslip. An equal volume of PMA, etoposide or cRPMI was added, as described above, for up to 4 h, 37 C, 5% CO_2. Following stimulation, neutrophils were fixed using an equal volume of 2% PFA/PBS, 15 min, RT. The coverslip was then removed using forceps and placed carefully onto a prepared drop of staining cocktail consisting of CD66-FITC, clone B1.1/CD66, Sytox Orange and DAPI in PBS, as described above, for 15 min, RT, dark. Excess liquid was then removed by tapping the coverslip onto a Kimwipe tissue. The cover slip was prepared for microscopy by mounting onto a microscope slide with Fluorescence Mounting Medium.

2.10.4 NETs IDENTIFICATION BY FLOW-CYTOMETRY

For all the following procedures we maintained a timed SOP described in supplemental table 1. In addition, antibodies and dyes were carefully titrated to minimize washing steps, since these can disrupt the fragile structures of the NETs formed. Cells were stained with 100 µl of a staining cocktail consisting of antibodies or dyes to identify neutrophils and NETs respectively (Supplemental Fig. 1A). A volume was intentionally kept low to minimize long acquisition times on the flow cytometer. Following 15 min, RT incubation with the staining cocktail, samples were run immediately on a BD LSRFortessa®.

2.11 Statistical analysis

Results are presented as the arithmetic mean ± standard error of the mean (SEM). Significance was tested using Student's t-test, results were considered significant at *$p < 0.05$, P values of <0.05, <0.01, and <0.001 are depicted as *, **, and *** respectively. Prism 6.0 software (GraphPad) for Windows was used to perform the analyses. For time and dose response analyses, a 2-way ANOVA was completed with Dunnett's multiple comparison test.

2.11.1 DNA-SEQ SAMPLES PREPARATION

In collaboration with the Wakeland laboratory at UT Southwestern Medical Center (UTSW) in Dallas, Texas, USA the investigation of genomic and transcriptomic data was done. Genomic DNA from either B6 or B6.*Sle1* mice was isolated from tail DNA using in house protocol. The DNA (2 µg) was sheared with a Ultrasonicator and subsequently prepared using KAPA LTP library preparation kit (KAPA Biosystems, Wilmington, MA 01887). After hybrid capture, amplification and quality assessment, the samples were sequenced on Illumina NextSeq 500 using a standard 150-bp or HiSeq 2000 using 100-bp paired-end protocol. The image analysis and base calling were performed with an Illumina pipeline, using default settings.

The SNPs were extracted from the data and analyzed in Singapore using CLC genomics software and alignment was performed against reference genome.

2.11.2 RNA SEQ SAMPLES PREPARATION

B cell mRNA from either B6 or B6.*Sle1* mice was processed and analyzed using RNA-sequencing (RNA-seq) technology in collaboration with the Dr.Wakeland's laboratory at UTSW in Dallas. This technique allows evaluation of gene expression and differences in transcription.

B cells were isolated from the mouse spleen using EasySep™ Mouse CD19 Positive Selection Kit II. RNA was isolated from B cells using RNAeasy kit as per the manufacturer's protocol (Qiagen Corp. Valencia, CA) and RNA quality was verified using Agilent Bioanalyzer 2100 (Agilent Technologies). One µg of total RNA was used to perform RNA-SEQ using TruSeq RNA Sample Preparation kit v2 (Illumina) as per the manufacturer's instructions. The library from each sample was sequenced on GAIIx sequencer or Illumina Hiseq 2000 or NextSeq 500 (Illumina, San Diego, CA), using 50-bp or 36 bp single-end protocol. One sample is one replicate.

2.11.3 RNA SEQ SAMPLES ANALYSIS

Data was transferred to Singapore and sequence reads were mapped to the mouse genome (Mus Musculus strain MGSCv37, C57BL/6J) using Spliced Transcripts Alignment to a Reference (STAR) software, allowing up to 10 mismatches (Dobin, Davis et al. 2013). Of the total reads, 70% matched to unique genomic locations, 25% showed multiple matches, and 5% had no match to the genome. The unique reads were then mapped to known genes based on ENSMBL database. The quality of reads was

confirmed using FastQC software (Andrews 2010). Visualization and determination of Reads Per Kilobase of Exon per Million mapped reads (RPKM), and therefore gene expression was determined using SeqMonk (Ver. 0.27.0). **(Figure 2.5)**

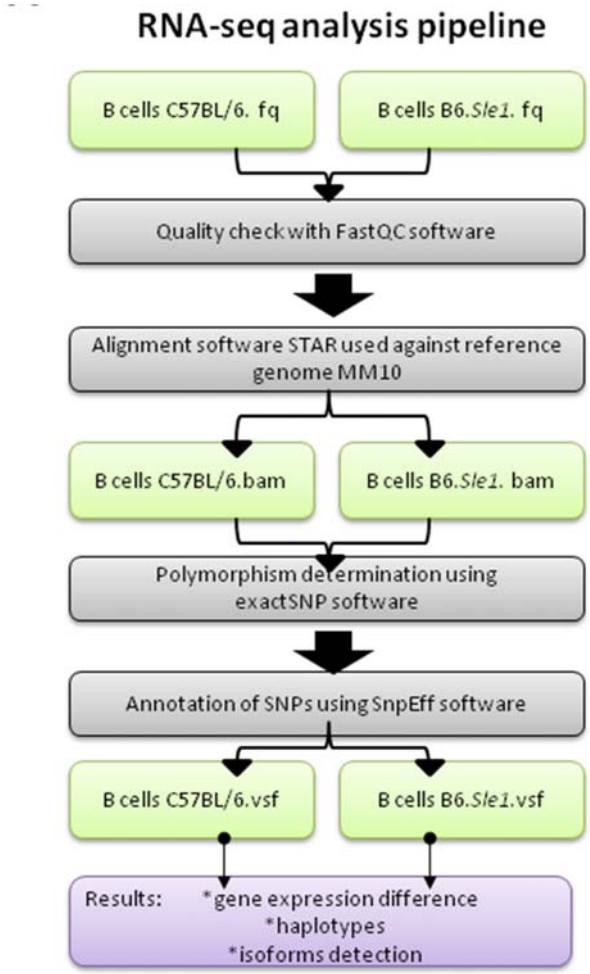

Figure 2.5 RNA seq analysis pipeline.

A pipeline of analysis of genomic and transcriptomic sequences from B6 and B6.*Sle1* mice.

3 RESULTS

3.1 Elevated surface expression of CD84 in aged auto-immune prone *Sle1* mice

The introduction of the *Sle1* locus into the genome of non-autoimmune mice, such as B6, causes benign autoimmunity characterized by splenomegaly, activated lymphocytes and ANA development by the age of 6 months (Morel, Blenman et al. 2001). To determine whether there were CD84 expression differences associated with disease, we examined CD84 surface expression in the spleen and kidney of aged 6 month old female B6 and B6.*Sle1* mice. The majority of *Sle1*-associated phenotypes have been described in the spleen and kidney disease rarely occurs in this strain.

We used a multi-flow cytometry approach to analyse surface CD84 expression across multiple leukocytes using the gating strategy described in **Figure 3.6 A**. We observed a significantly higher expression of CD84 on splenic B cells from aged B6.*Sle1* mice when compared to the control B6 strain. In contrast, PMNs from the spleens of B6.*Sle1* mice show decreased CD84 levels **(Figure 3.1 B)**. Our B cell findings are in contrast to those described by Wong and colleagues who report a decrease in splenic B cell CD84 expression in 8mos old mice using the B6.*Sle1* subcongenic with a shorter interval; B6.*Sle1b* (Wong, Soni et al. 2015).

Lymphocyte infiltration into the kidney is a sign of inflammation initiation. Hence a comparison of CD84 expression in the kidneys of B6 and B6.*Sle1* mice was performed. Consistent with our splenic B cell findings described above, we determined a significant upregulation of CD84 was found on B cells from B6.*Sle1* mice **(Figure 3.1C)**.

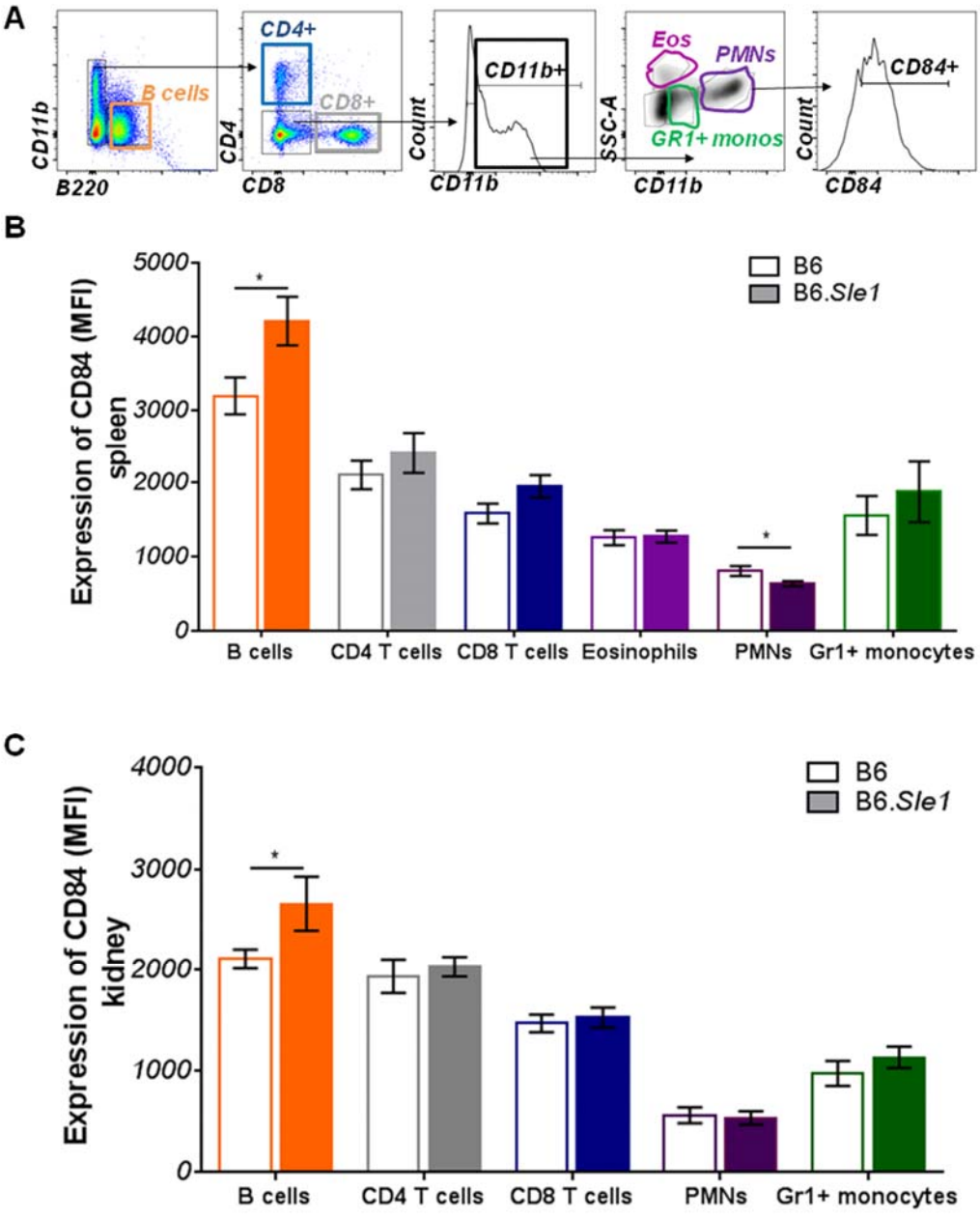

Figure 3.1 Surface expression of CD84 in aged 6 month old B6 and B6.Sle1 mice.

(A) Gating strategy for identification of B cells, CD4+ and CD8+ T cells, PMNs, Eosinophils, GR1+ monocytes. Expression of CD84 on each cell type in (B) spleen and (C) kidney. Statistical values were determined using an unpaired, nonparametric, Student's t test. Error bars represent mean ± SEM. *,P ≤ 0.05, **,P ≤ 0.01, ***,P ≤ 0.001, ****,P ≤ 0.0001. N=6-8 mice per genotype, two independent experiments.

Consistent with previous reports (Sintes, Romero et al. 2010) (Tangye, van de Weerdt et al. 2002) we determined that CD84 increases upon maturation from the bone marrow to the periphery, independent of the strain **(Figure 3.2 B, C)**. CD84 expression could be also used a maturation marker (Zaiss, Hirtreiter et al. 2003). Furthermore, young B6.*Sle1* mice expressed more surface CD84 in the periphery compared to B6 controls, in contrast to the bone marrow and spleen where levels were similar **(Figure 3.2 B, C)**.

Detailed analysis of CD84 median fluorescence intensity (MFI) shows increased amount of CD84 per cell from B6.*Sle1* mice, especially in blood **(Figure 3.2 B).** However, the significant increase of CD84 in splenic B and CD8+ T cells demonstrate intrinsic reasons for the upregulation of CD84. The percentage of leukocytes expressing CD84 was slightly increased in B6.*Sle1* mice, however did not reach statistical significance. Increased expression of CD84 in B6.*Sle1* mice was an interesting phenomenon. Therefore we decided to initiate an investigation to determine whether increased CD84 expression might affect functional differences in B cells, due to the role of CD84 in B and T cells interactions.

3.2 Upregulation of CD84 surface expression in young B6.*Sle1* mice

To ascertain whether the increases in B cell CD84 expression were disease related we went on to analyse expression of CD84 in young 6-8 week old B6 and B6.*Sle1* mice**.** In a similar manner, surface CD84 expression was evaluated on different leukocytes across different tissues using flow cytometry and the gating strategy provided in **Figure 3.2 A**.

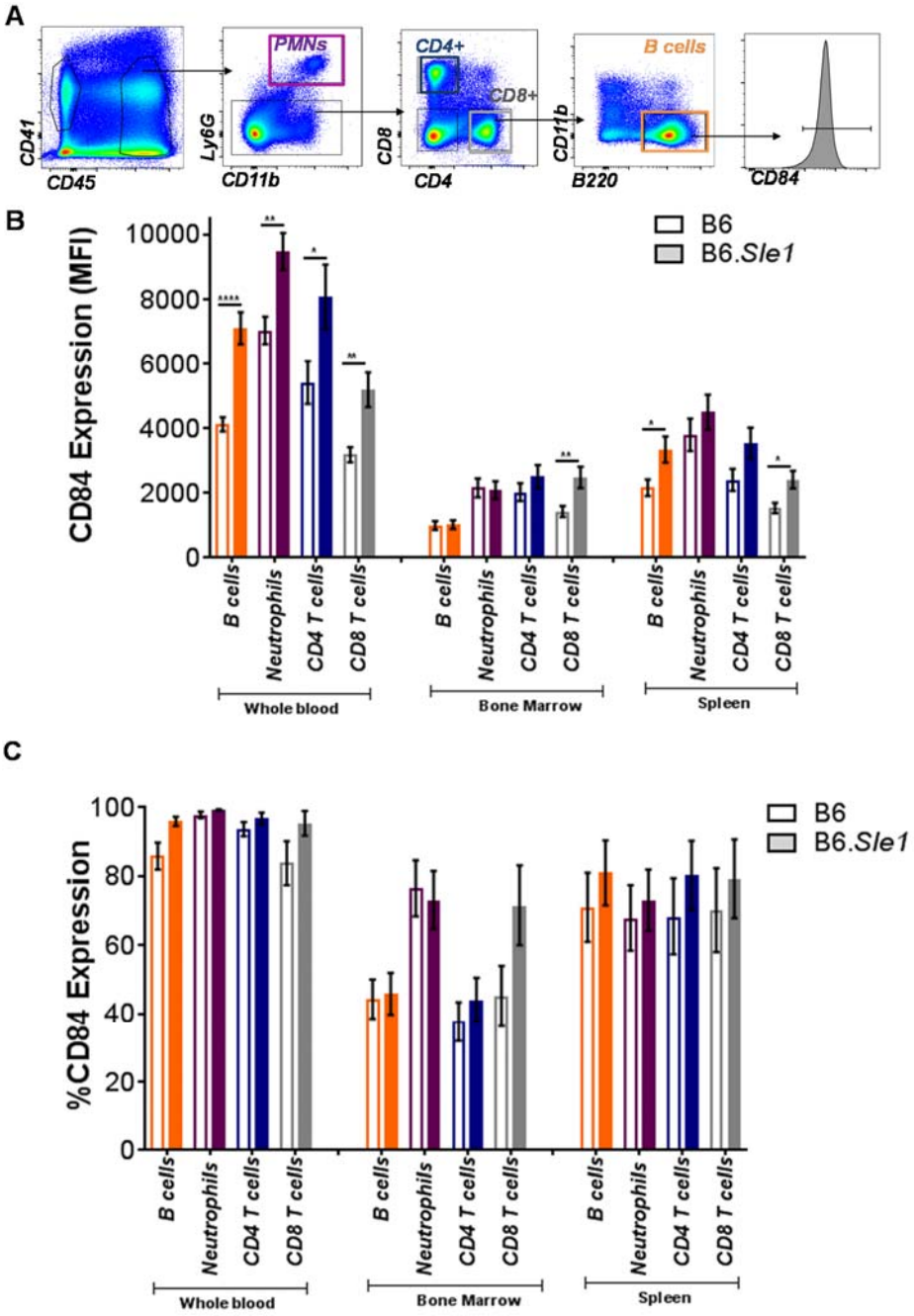

Figure 3.2 *Ex vivo* expression of CD84 in 2 month old B6 and B6.*Sle1* mice.

(A) Gating strategy for the identification of B cells, PMNs, CD4+ and CD8+ T cells and. CD84 expression (B) MFI and (C) percentage in each cell type in bone marrow, spleen and whole blood taking retro-orbitaly. Statistical values were determined using an unpaired, nonparametric, Student's *t* test. Error bars represent mean ± SEM.*,*P* ≤ 0.05, **,*P* ≤ 0.01, *,*P* ≤ 0.001, ****,*P* ≤ 0.0001. N=11-12 mice per genotype, four independent experiments.**

3.2.1 PLATELETS MAY EFFECT CD84 INCREASE ON BLOOD LEUKOCYTES

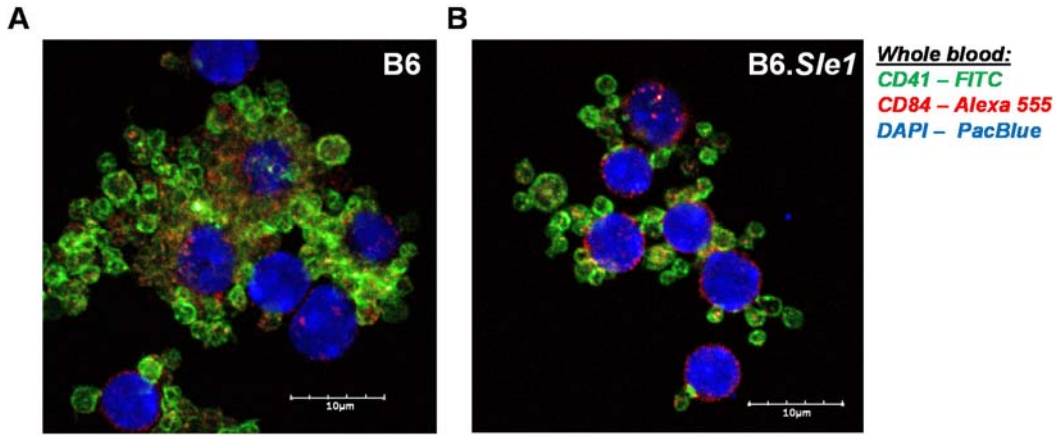

Figure 3.3 Platelets - neutrophils interactions in murine blood of (A) B6 and (B) B6.*Sle1* mice.

Figure 3.3 shows staining of murine leukocytes and platelets in whole blood. Neutrophils (PMNs) are known to bind platelets, and undergo further activation resulting in excessive NETosis and pro-inflammatory cytokines secretion. Since platelets highly express CD84 as well as it is a predominant cell type in murine blood, it is probable that the increase CD84 expression observed in B6.*Sle1* mice is due to platelet binding.

Indeed, our analysis of platelet binding in blood of B6.*Sle1* mice revealed an increase in neutrophil-platelet conjugates **(Figure 3.16)**, in contrast to the spleen where the majority of these cells were not bound to platelets. This data demonstrates that the PMNs express CD84 this is not an artefact of platelet binding, but the peripheral increases are probably due to platelet binding.

3.2.2 CD84 EXPRESSION ON B AND T CELL SUBSETS

In additional, we examined the expression of CD84 on different splenic B cell subsets in B6 and B6.*Sle1* mice. Total B cells are defined as (CD19+CD20+). Different B cell subsets could be further identified by the expression of Fas+ and GL7+ receptors (germinal center B cells) (Loder, Mutschler et al. 1999); marginal zone B cells are CD21+ CD23-; and transitional precursors (T1) and (T2) are IgM+CD21-CD23- and IgM+CD21+CD23+, respectively (Cerutti, Cols et al. 2013) (**Figure 3.4 A**). Memory B cells

are defined as (CD27+IgD+), activated B cells as (IgM+IgD+), and a population of IgM+ B cells was also identified.

Consistent with our previous data **(Figure 3.2 B)**, CD84 expression was higher on total B cells in B6.*Sle1* mice compare to B6 control. CD84 expression was also significantly higher on CD27+ memory and IgM+IgD+ activated B cells from B6.*Sle1* mice compared to B6 control (**Figure 3.4 B**). Interestingly, GC B cells from B6.*Sle1* mice showed significantly lower CD84 expression compared to B6 controls (**Figure 3.4 B**). Splenic B cells precursors and MZ B cells showed similar level of CD84 expression between the two groups (**Figure 3.4 B**).

In order to rule out the differences in MFI of CD84 was not attributed to differences in the number of cells examined, we quantified the frequency of different B cell subsets in the two mouse strains (**Figure 3.4 C**). We showed that the frequency of total B cells, GC, T1, T2 and MZ B cells were similar between the two trains of mice. Data presented here demonstrated that overall difference in CD84 expression on B cells derives from certain subpopulations of B cells, suggesting that *sle1* gene may only affects subpopulation of B cells at different stages of differentiation. Further study to investigate the expression level of *sle1* genes mRNA in different B cell populations may shed light into its role during B cell development.

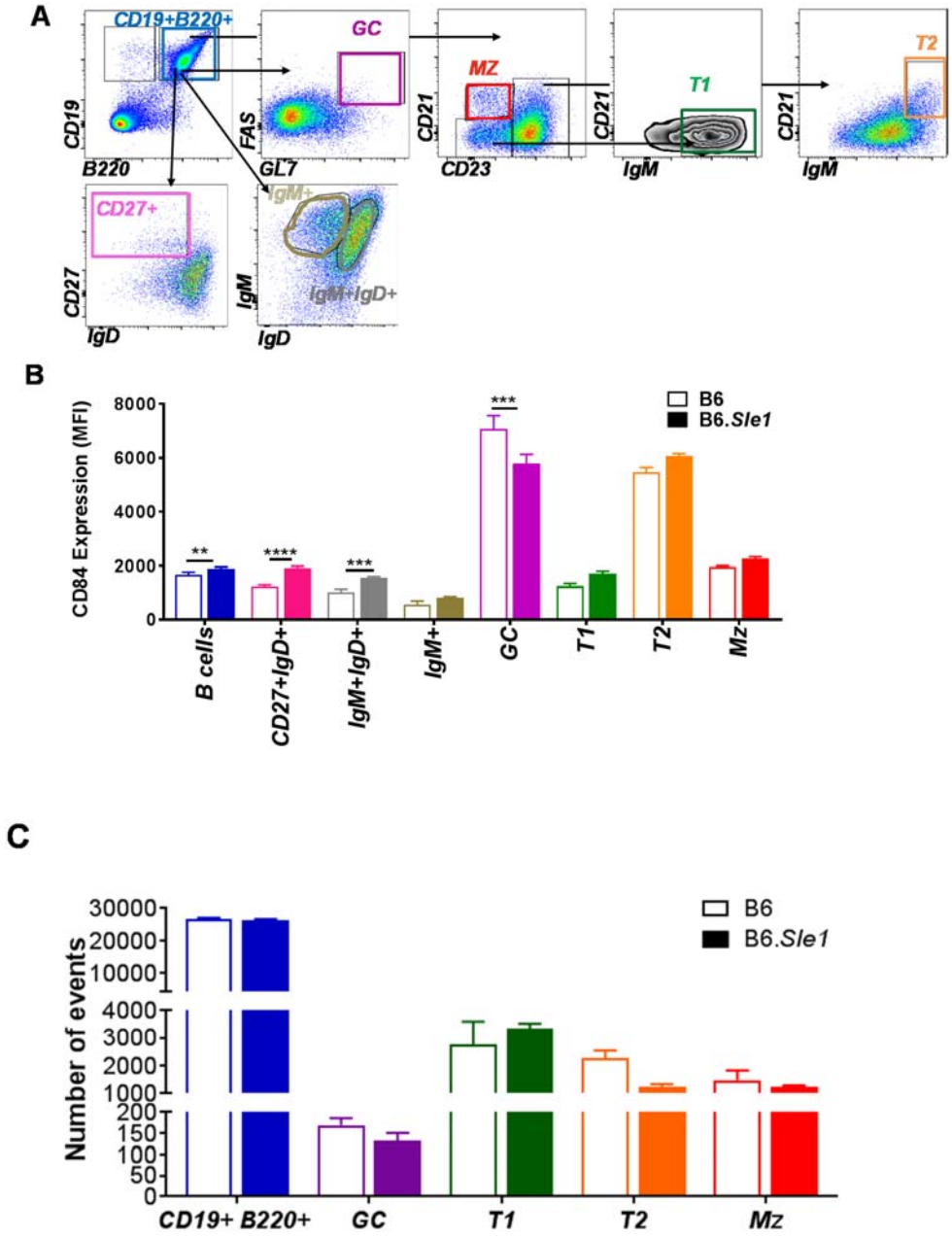

Figure 3.4 Expression of CD84 in various B cell subsets.

(A) Schematic of a gating strategy to determine B cells subsets in mice. (B) The median fluorescent intensity (MFI) of CD84 on various B cell subsets in B6 and B6.Sle1 mice are shown. (C) Number of events of B cell subsets in spleen of young B6 and B6.*Sle1* mice. Data represent mean ± SEM of 4 mice per group. Results were analysed by one-way ANOVA with multiple comparisons. ** $p < 0.01$, *** $p < 0.001$, **** $p < 0.0001$. NB: GC, germinal centre; MZ, marginal zone; T1&2, transitional precursor 1&2.

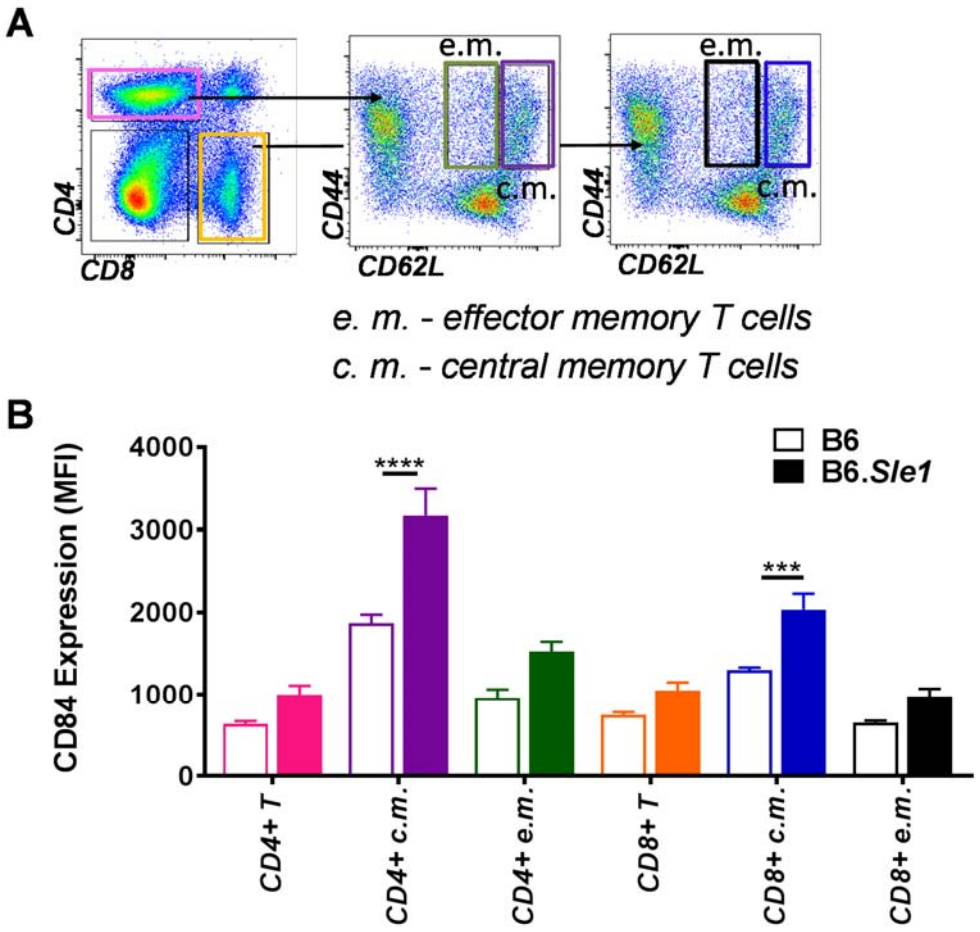

Figure 3.5 Expression of CD84 in various T cell subsets.

(A) Schematic of a gating strategy to determine T cells subsets in mice. (B) The median fluorescent intensity (MFI) of CD84 on various T cell subsets in B6 and B6.Sle1 mice. Data represent mean ± SEM of 4 mice per group. Results were analysed by one-way ANOVA with multiple comparisons. *** p < 0.001, **** p < 0.0001. NB: c.m. – central memory T cells; e.m. – effector memory T cells.

Total T cells are defined based on CD3 expression, which then subdivided into CD4+ and CD8+ T cells. For both populations, CD4+ and CD8+ T cells, effector memory T cells are identified as CD62L*lo*CD44+*hi* as described in (Gerberick, Cruse et al. 1997); central memory T cells are defined base on the expression of CD44*hi*CD62L*hi* as described in (Rosenblum, Way et al. 2016) and **(Figure 3.5 A)**. We have also determined the number of T cell subpopulation in these mice. Although there were similar frequency

of T cells in B6 and B6.*Sle1* mice (data not shown), CD84 was significantly upregulated on CD4+ and CD8+ central memory T cells from spleen of B6.*Sle1* compare to B6 mice (**Figure 3.5 B**). In contrast, expression of CD84 on regulatory T cells (Tregs) was similar between B6 and B6.*Sle1* mice (data not shown).

3.1 Functional assay of CD84 in murine B cells

3.1.1 SPLENOCYTES CELL NUMBER TITRATION

Having determined that CD84 expression was higher in B cells from B6.*Sle1* mice compared to B6 controls **(Figure 3.2 B, C),** we sought to determine whether leukocyte activation could increase CD84 expression. CD84 is a homotypic pan-leukocyte receptor. It plays a primary role in T-B cell interactions, particularly during germinal centre (GC) formation and normal humoral responses (Cannons, Qi et al. 2010). Therefore, since these receptors bind themselves, we first set out to ascertain whether the cell number in the culture could affect activation in the 2 strains.

The hallmark feature of SLE is the presence of anti-nuclear antibodies (ANAs), particularly anti-dsDNA and anti-RNA antibodies. These form immune complexes with their self-ligands (self nucleic acids) and are internalized through surface receptors such as FcγR or the BCR (Nundel, Busto et al. 2013). This enables ligation of the self nucleic acid with either TLR7 or TLR9. To study the function of CD84 *in vitro* during cell activation initially we performed titration with increasing numbers of splenocytes with TLR7 or TLR9 ligation or IgM/IL-4 stimulation. While a number of TLRs have been associated with lupus pathology, increases in TLR7 expression and function are known to drive leukocyte activation and severe disease in B6.*Sle1* mice (Celhar, Magalhaes et al. 2012, Hwang, Lee et al. 2012).

Total splenocytes from B6 and B6.*Sle1* mice were resuspended in different concentrations 0.2, 0.5, 0.75, 1 x 10^6 per 100 µL. B cell activation was determined by the upregulation of surface CD69 on CD19+ cells following 24 h exposure to CpGB; a TLR9 ligand, R848; a TLR7 ligand, or IgM/IL-4 which resembles activation of B cells with the help of T cells. The concentrations used were sub-maximal, chosen following initial optimization experiments. **(Figure 3.6 A, B, C).** Consistent with existing data, stimulation with any of these ligands upregulated the expression of CD69 on B cells. However, there were no differences attributed to cell number.

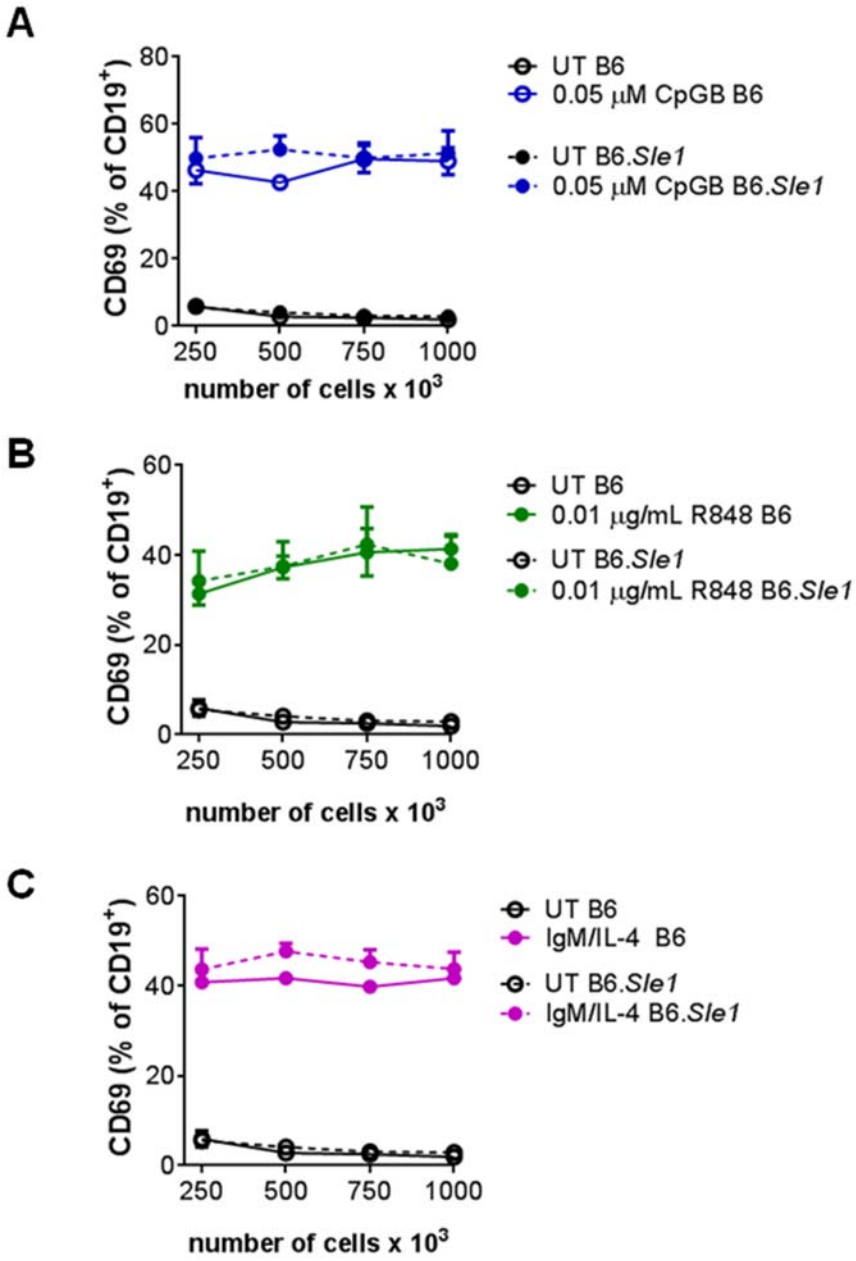

Figure 3.6. Cell number titration for activation of splenocytes upon TLR-ligands stimulation.

(A) 0.1 μM GpGB, (B) 0.1 μg/mL R848, and (C) 5 μg/mL IgM, 10 ng/mL IL-4 for 24 h. Comparison af difference between number of cells. Statistical values were determined using an unpaired, nonparametric, Student's t test. Error bars represent mean ± SEM.*,P ≤ 0.05, **,P ≤ 0.01, ***,P ≤ 0.001, ****,P ≤ 0.0001. N=6 mice per genotype, two independent experiments.

Analysis of CD84 expression determined a decrease in surface expression following either TLR7 or TLR9 ligation, however, the stimulation with IgM/IL4 had no effect on CD84 levels.

The percentage of CD84 on B cells decreased upon stimulation with CpGB in both strains of mice **(Figure 3.7 A),** with the increased number cells per well the percentage of CD84 expressed by B cells decreased almost to 30% compared to untreated, indicating either loss of CD84 or engagement in cell to cell interactions **(Figure 3.7 A)**. Expression of CD84 per cell is higher on B cells from B6.*Sle1* mice compared to B6, consistent with baseline findings. Furthermore, we determined a significant decrease in both strains following CpGB exposure **(Figure 3.7 A)**.

In contrast, stimulation with R848 **(Figure 3.7 B)**, or IgM/IL4 **(Figure 3.7 C)**, failed to induce a significant decrease in either strain, indicating possible activation of the cells through a different signaling cascade.

Following analysis of splenic B cells activation and surface CD84 expression the concentration of 0.5 x 10^6 cells per 100 µL was chosen as a working concentration for further experiments.

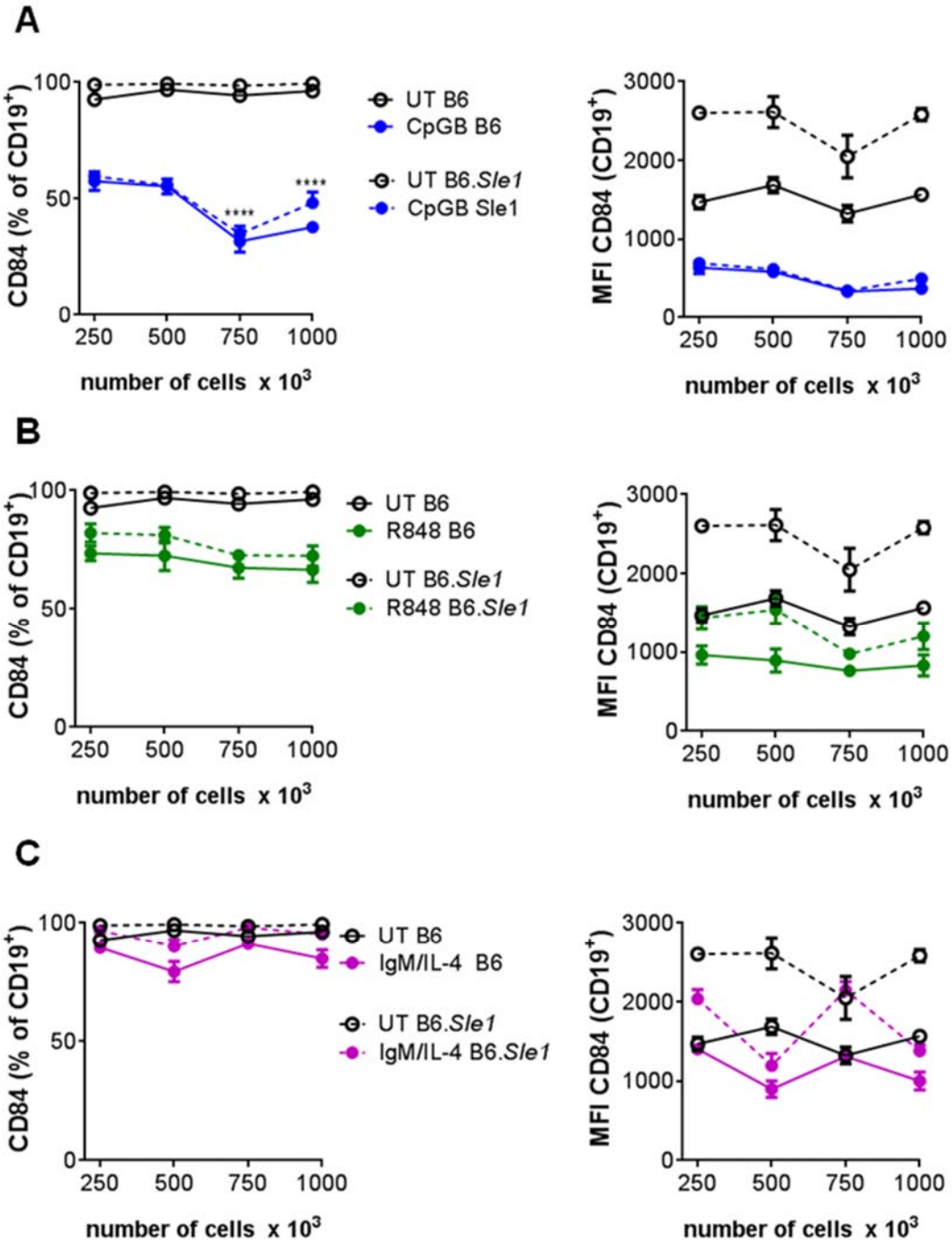

Figure 3.7 CD84 surface expression upon cell number titration for activation of splenocytes upon TLR-ligands stimulation

(A) 0.1 µM GpGB, (B) 0.1 µg/mL R848, and (C) 5 µg/mL IgM, 10 ng/mL IL-4 for 24 h. Statistical values were determined using an two-ways ANOVA with repeated measures. Error bars represent mean ± SEM.*,$P \leq 0.05$, **,$P \leq 0.01$, ***,$P \leq 0.001$, ****,$P \leq 0.0001$. N=6 mice per genotype, two independent experiments.

3.1.2 CD84 EXPRESSION AND B CELLS PROLIFERATION UPON ACTIVATION WITH TLR LIGANDS

After the optimal cell number was determined we went on to optimize the optimal concentrations of stimuli. Splenocytes were stimulated with various concentrations of LPS (TLR4), R848 (TLR7) or CpGB (TLR9). Activation and proliferation of the cells were analysed by flow cytometry after 24 and 72 hrs of stimulation respectively. The upregulation of surface CD69 and CD86 was used as a marker of activation. Proliferation was assessed using dilution of CFSE as described previously (Quah, Warren et al. 2007). *In vitro* antibody production was determined using several Ig ELISAs 96 h following stimulation.

Stimulation of splenocytes with 1, 3, 5 and 10 µg/mL of LPS, demonstrated gradual upregulation of CD69 and CD86 expression at 24 h, confirming the activated status of the cells. Both, B6 and B6.*Sle1* showed activation in a dose-dependent manner **(Figure 3.8 A, B)**. Similar to the untreated splenocytes, CD84 expression was increased in B6.*Sle1* mice, and decreased with increasing LPS concentrations **(Figure 3.8 C, D).**

Furthermore, analysis at 72 h showed that each dose of LPS induced B cell proliferation: a representative plot is shown in **(Figure 3.8 E).** However, similar to our previous findings at 24h, the expression of surface CD84 decreased following cellular activation. The higher levels of surface CD84 was maintained on B cells from B6.*Sle1* mice compared to B6 controls, even with the decreased expression **(Figure 3.8 F, G)**. 1 and 3 µg/mL of LPS were chosen as working concentrations for subsequent experiments.

In the next experiment we investigated the activation of splenic B cells upon 24 h stimulation with different doses of TLR7 ligand - R848. The concentrations were 0.1, 0.3 and 1 µg/mL and activation of B cells was detected by elevation of CD69 and CD86as before **(Figure 3.9 A, B).** B6 splenocytes showed more activation compared to B6.*Sle1*, however CD84 expression upon the stimulation was slightly lower in B6 mice. Although, overall trend demonstrated loss of surface CD84 expression, the difference of CD84 expression on B cells stimulated with high and low concentrations of R848 was not significant **(Figure 3.9 C, D).**

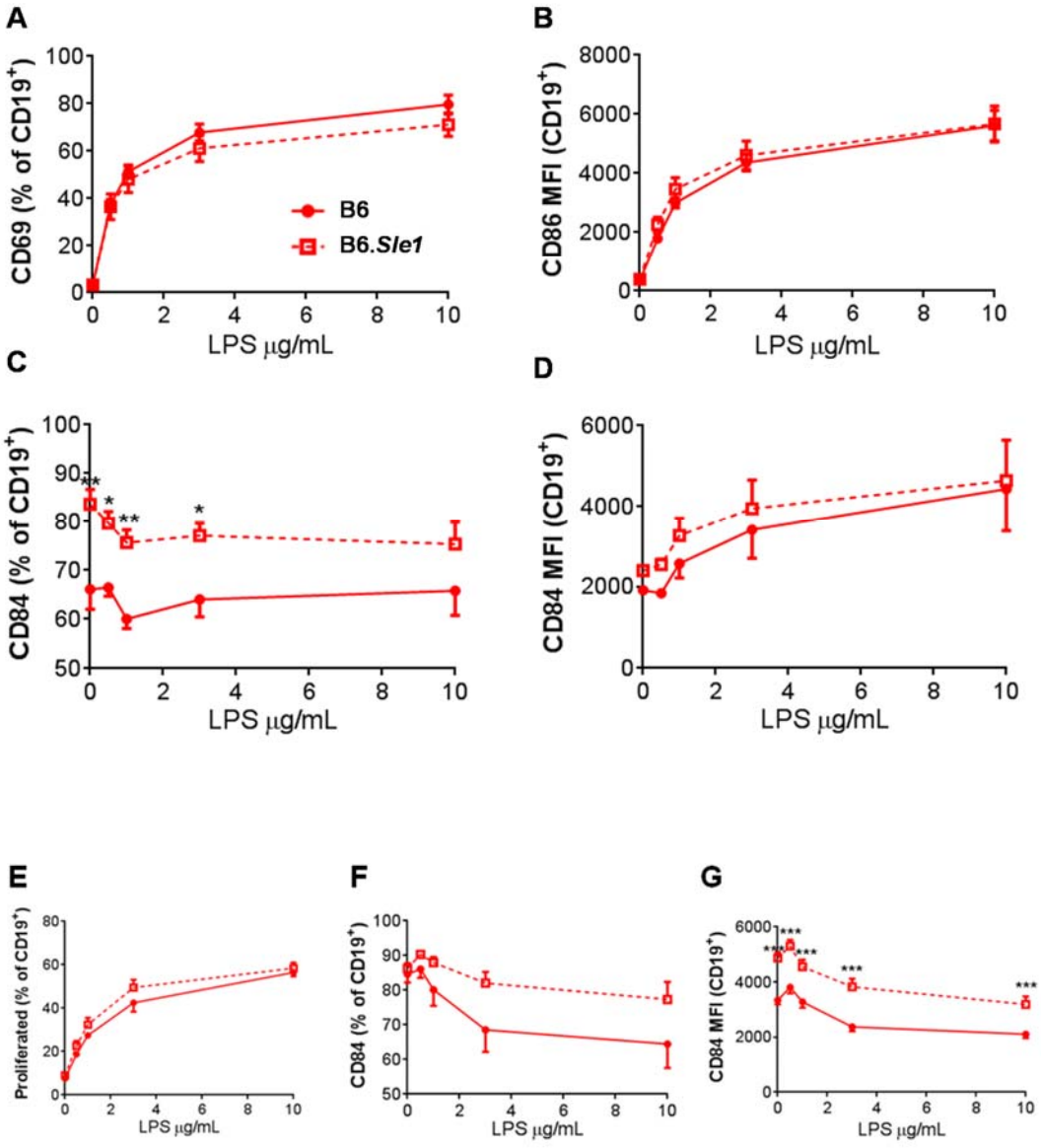

Figure 3.8 Splenic B cells stimulation with TLR4 ligand.

(A,B) Activation of splenic B cells (C,D) CD84 expression upon 24 h stimulation with 1, 3, 5 and 10 µg/mL of LPS. (E) Proliferation of splenic B cells, (F,G) CD84 expression upon 72 h of stimulation with 1, 3, 5 and 10 µg/mL of LPS. Statistical values were determined using an two-ways ANOVA with repeated measures. Error bars represent mean ± SEM.*,*P* ≤ 0.05, **,*P* ≤ 0.01, *,*P* ≤ 0.001, ****,*P* ≤ 0.0001. N=6 mice per genotype, two independent experiments.**

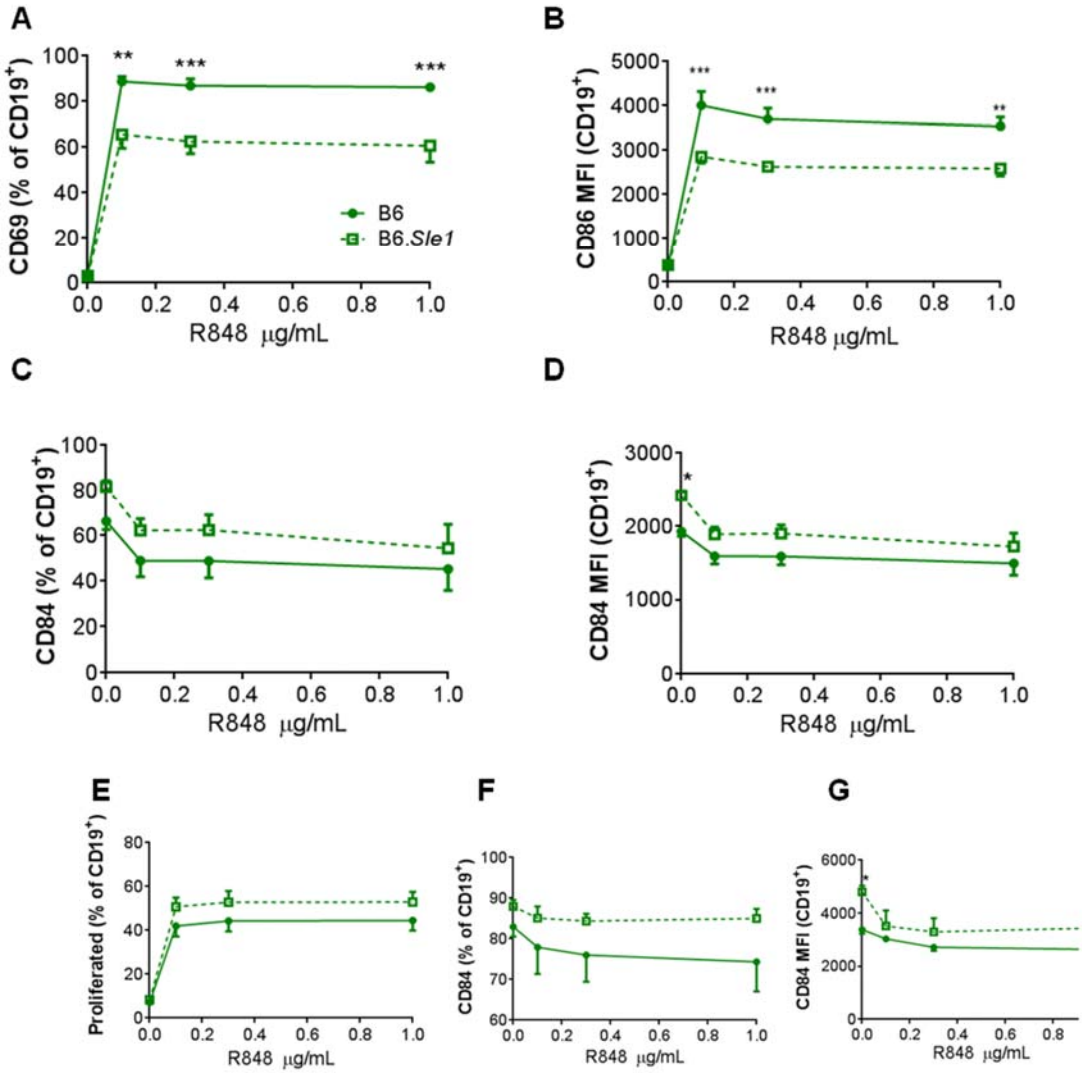

Figure 3.9 Splenic B cells stimulation with TLR7 ligand

(A,B) Activation of splenic B cells, (C,D) CD84 expression upon 24 h stimulation with 0.1, 0.3 and 1 µg/mL of R848. (E) Proliferation of splenic B cells, (F,G) CD84 expression upon 72 h of stimulation with 0.1, 0.3 and 1 µg/mL of R848. Statistical values were determined using an two-ways ANOVA with repeated measures. Error bars represent mean ± SEM.*,*P* ≤ 0.05, **,*P* ≤ 0.01, *,*P* ≤ 0.001, ****,*P* ≤ 0.0001. N=6 mice per genotype, two independent experiments.**

All R848 concentrations used increased the proliferation of B cells at 72 h regardless of strain **(Figure 3.9 E).** The expression of CD84 was also higher on B6.*Sle1* with slight lose upon stimulation compared to B6, as observed previously, **(Figure 3.9 F, G)**. The optimal dose of R848 was 0.1 µg/mL.

Stimulation with CpGB (TLR9 ligand) resulted in a significantly higher activation of B6 B cells compared to B6.*Sle1*after 24h of stimulation, as determined by CD69 and CD86 upregulation **(Figure 3.10 A, B)**. Expectedly, CD84 expression still was increased on B cells from B6.*Sle1* mice, although the difference did not reach statistical significance in these studies **(Figure 3.10 C, D)**. B6.*Sle1* splenocytes demonstrated more proliferation compared to B6 control at 72 h following CpGB stimulation **(Figure 3.10 C, D)**.

Surface expression analysis at 72 h revealed higher CD84 levels on splenic B cells from B6.*Sle1* mice compared to B6 controls. Furthermore, in a similar manner to TLR4 or TLR7 stimulation, CD84 expression decreased with increasing concentrations of stimulant (Figure 3.7F, G). The optimal dose for TLR9 ligand, CpGB was determined at 0.03 µM.

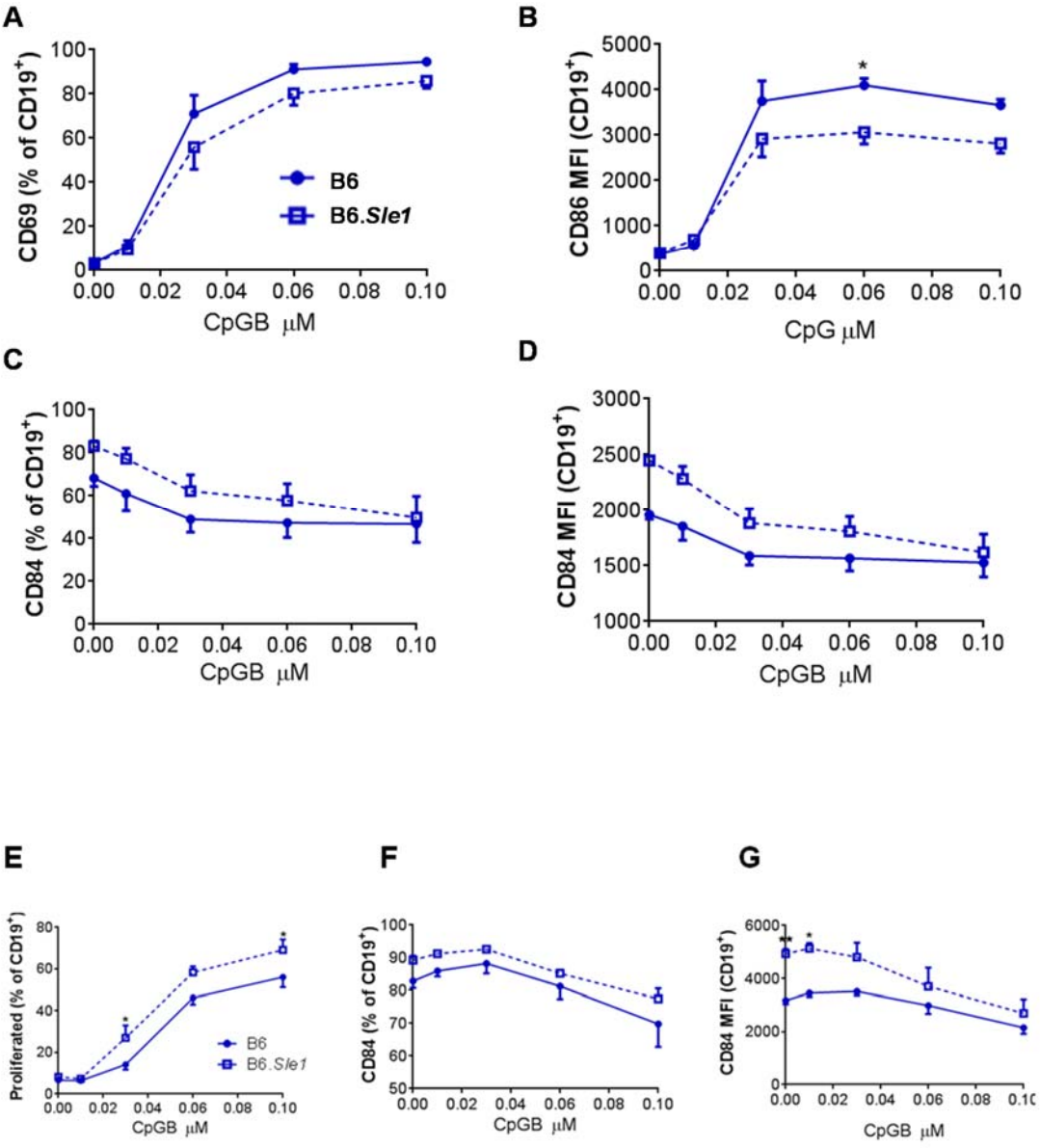

Figure 3.10 Splenic B cell stimulation with TLR9 ligand

(A,B) Activation of splenic B cells, (C,D) CD84 expression upon 24 h stimulation with 0.01, 0.03, 0.06 and 0.1 μM of GpGB. (E) Proliferation of splenic B cells, (F,G) CD84 expression upon 72 h of stimulation with 0.01, 0.03, 0.06 and 0.1 μM of CpGB. Statistical values were determined using an two-ways ANOVA with repeated measures. Error bars represent mean ± SEM.*,*P* ≤ 0.05, **,*P* ≤ 0.01, *,*P* ≤ 0.001, ****,*P* ≤ 0.0001. N=6 mice per genotype, two independent experiments.**

3.1.3 ANTIBODY RESPONSE TO STIMULATION WITH TLR LIGANDS

ANAs, are usually class-switched antibodies produced by plasma cells following by the priming of B cells with the wrong, self-antigen, in GCs. To investigate the difference in class switched antibody production in the response to TLR ligands between B6 and B6.*Sle1* mice splenic B cells were stimulated with various doses of TLR4, 7 and 9 ligands for 96 h *in vitro*. After the stimulation supernatants were collected and the production of antibodies was analyzed by ELISA.

Stimulation of Splenocytes with LPS resulted in a higher level of IgA in the supernatant from B6 mice compared to B6.*Sle1* mice **(Figure 3.11 A)**. Levels of IgA were inconsistent following CpGB stimulation and beyond the level of detection with R848 in both strains. Therefore, requires further evaluation **(Figure 3.11 A)**.

Secreted IgM antibodies were detected in supernatants following stimulation with all 3 TLR ligands used **(Figure 3.11 B)**, with B6 B cells consistently secreting higher levels when compared to B6.*Sle1*. Further analysis of class-switched antibodies was performed. However, IgG1, IgG2a and IgG2b antibodies were not detected in supernatants of stimulated B cells from spleen of B6 as well as B6.*Sle1* mice using this cell number **(Figure 3.11 C)**. The only class-switched antibodies detected at significant level were IgG3. There were no significant differences determined between B6 and B6.*Sle1* mice for IgG3 production. These findings from Ig secretion studies need to be repeated for further validation.

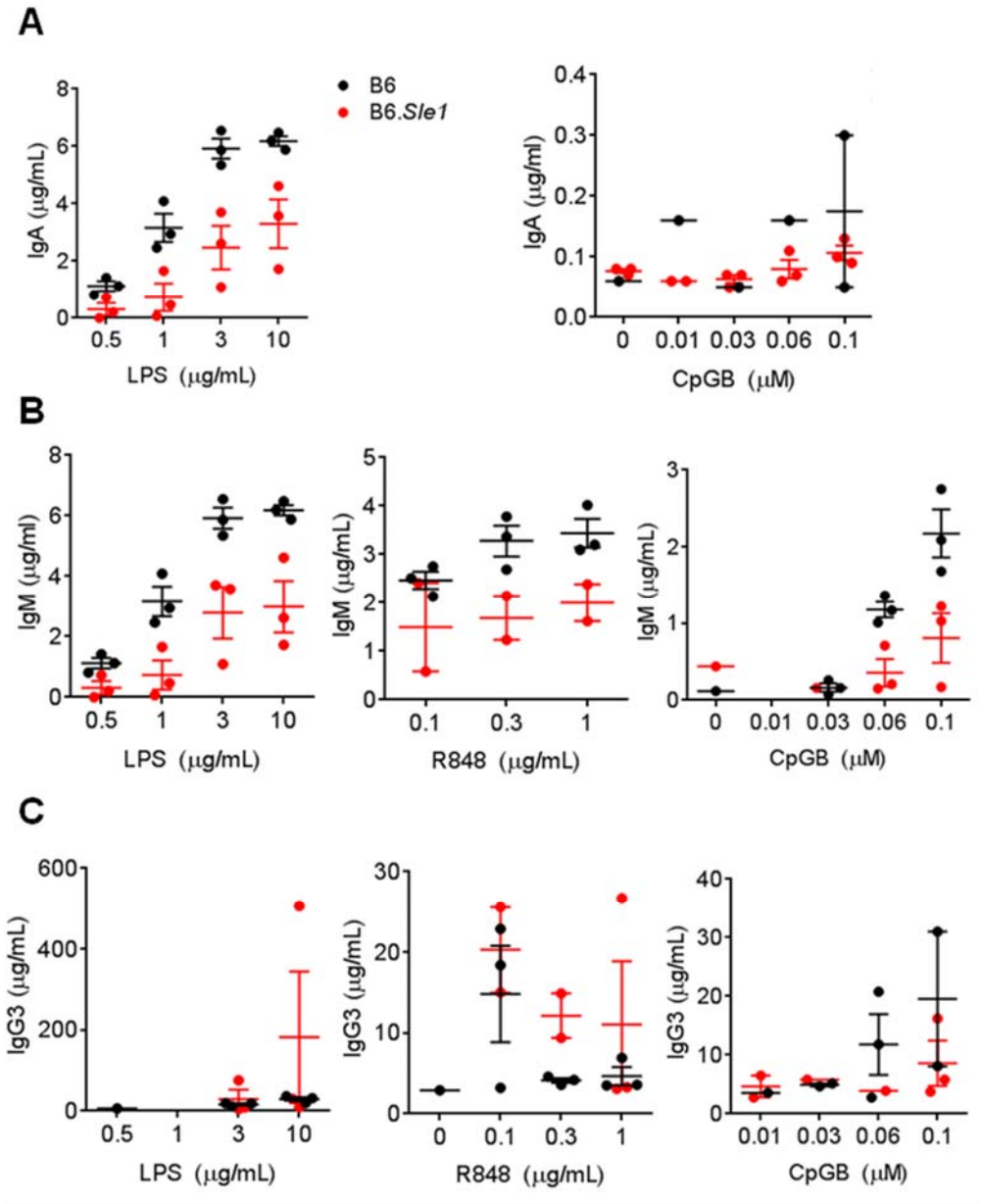

Figure 3.11 The concentrations of antibodies upon TLR stimulation.

The concentration of (A) IgA, (B) IgM, (C) IgG3 in the supernatants of splenic B cells cultures upon stimulation with various concentrations of LPS, R848 and CpGB. Statistical values were determined using an two-ways ANOVA with repeated measures. Error bars represent mean ± SEM.*,$P \leq 0.05$, **,$P \leq 0.01$, ***,$P \leq 0.001$, ****,$P \leq 0.0001$. N=3 mice per genotype, a representative experiment.

3.1.4 BLOCKING OF CD84 ON B CELLS

CD84 is a homophilic cell-surface receptor, expressed by nearly 100% of B cells**(Figure 3.2 C)**. To assign functional role of CD84 upon ligation with anti-CD84 antibodies or recombinant CD84 (rCD84) the concentrations of anti-CD84 antibodies, isotype controls and rCD84 were tested. Since CD84 participates in cell to cell interactions we tested both 250,000 and 500,000 cells per well in a 96 well culture plate.

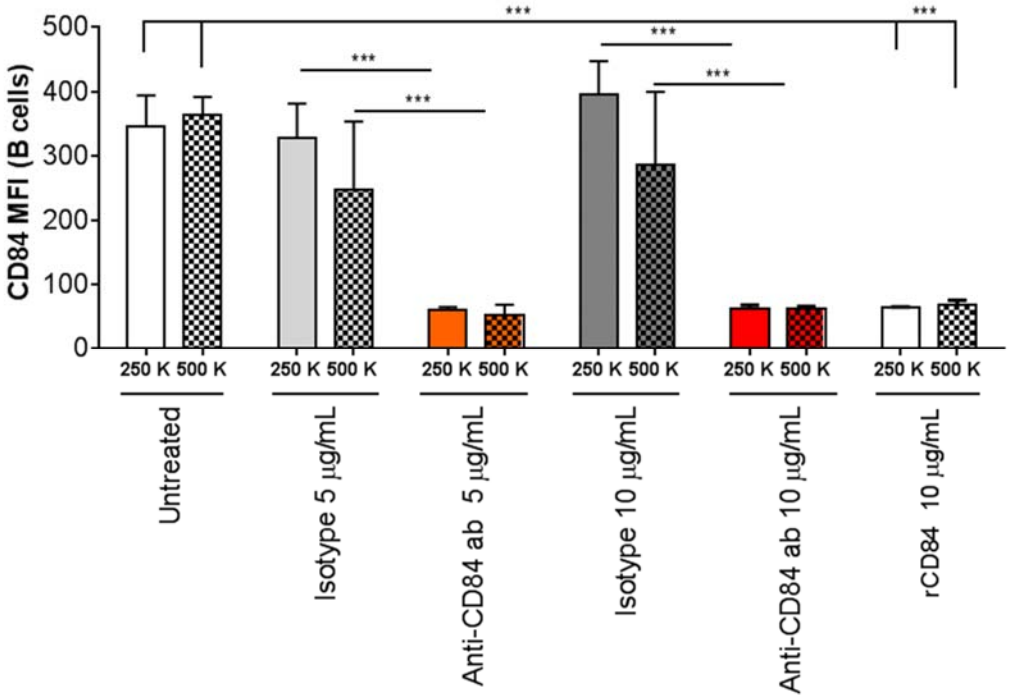

Figure 3.12 Blocking of CD84 with anti-CD84 antibodies or rCD84.
(A) CD84 expression after blocking B cells with different concentrations of anti-CD84 antibodies and isotype controls, or recombinant CD84 (rCD84) upon cell number titration. Statistical values were determined using a two-ways ANOVA with repeated measures. Error bars represent mean ± SEM.*,P ≤ 0.05, **,P ≤ 0.01, ***,P ≤ 0.001, ****,P ≤ 0.0001. N=6 only B6 mice were used, two independent experiments.

SepInocytes at the 2 different concentrations were incubated with either 5 or 10 µg/mL of anti-CD84 (clone CD84.7) or corresponding isotype control or 10 µg/mL rCD84 for 30 min at 37º C. Post stimulation, cells were stained with anti-CD84-PE (Clone mCD84.7). We detected a decrease in CD84 expression, indicating that the antibodies used for incubation bind to surface CD84 **(Figure 3.12)**. The optimal cell number to use

in subsequent experiments was determined at 0.5 x 10^6, in order to maintain consistency with the experiments with TLR stimulation.

Since CD84 is a homophilic receptor, it was reported that CD84 is activated upon CD84-CD84 interactions (Martin, Romero et al. 2001). Thus, murine B cells were then assessed for activation following ligation with either anti-CD84 antibodies or isotype control for 24 h. We demonstrated that the antibodies bound to CD84 but did not activate the B cells as determined by CD69 expression **(Figure 3.13 A)**. Subsequently we set out to determine whether the anti-CD84 antibody could inhibit activation of a known stimulus, such as TLR7 ligand R848. Whilst we did detect the decrease in CD84 expression which demonstrated binding **(Figure 3.13 B),** we did not find any decrease in activation, as determined by CD69 expression **(Figure 3.13 A)**.

Since the antibodies to CD84 did not activate or inhibit activation of B cells, we then examined the effect of rCD84 protein to CD84. Similar to the previous experiment we observed a significant decrease in the detection of surface expression of CD84, following 24 hours incubation with rCD84 **(Figure 3.13 B)**. However, we did not detect any evidence of B cell activation **(Figure 3.13 A)**. Furthermore, co-incubation of rCD84 with TLR7 ligand did not reveal any inhibiting or stimulating effect of rCD84 on CD69 expression **(Figure 3.13 A)** though B cells CD84 expression were decreased showing rCD84 was binding to surface CD84 **(Figure 3.13 B).**

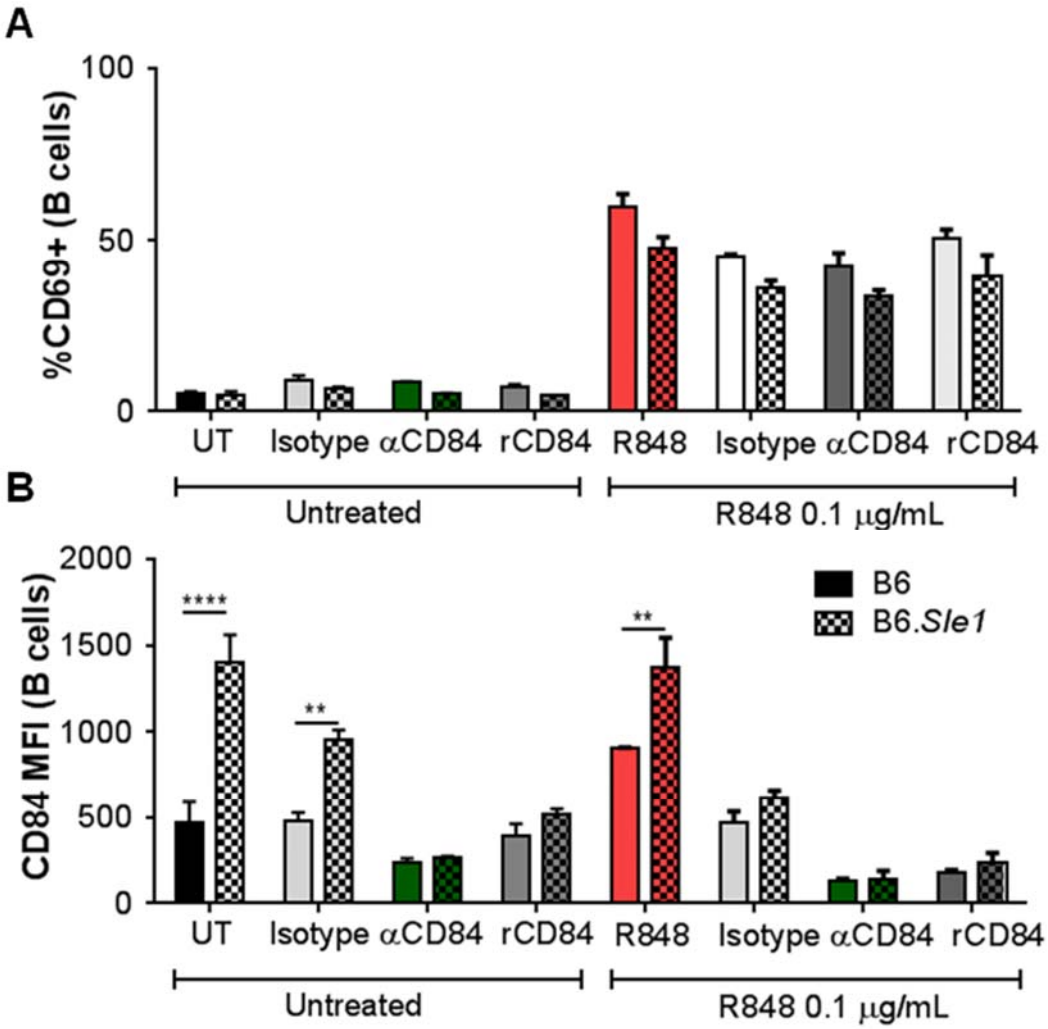

Figure 3.13 CD84 expression upon CD84 blocking following the stimulation.

(A) Activation of B cells (*** of untreated samples compared to R848 stimulated, B6 and B6.*Sle1* mice) and (B) CD84 expression following incubation with anti-CD84 antibodies, recombinant CD84 (rCD84) or combination of 0.1μg/mL R848 with anti-CD84, isotype control rCD84. Column with pattern represent B6.Sle1 mice. Statistical values were determined using a two-ways ANOVA with repeated measures. Error bars represent mean ± SEM.*,P ≤ 0.05, **,P ≤ 0.01, ***,P ≤ 0.001, ****,P ≤ 0.0001. N=6 per genotype, two independent experiments.

3.1.5 APOPTOSIS DIFFERENCE IN SPLENIC B CELLS OF B6 AND B6.*SLE1* MICE

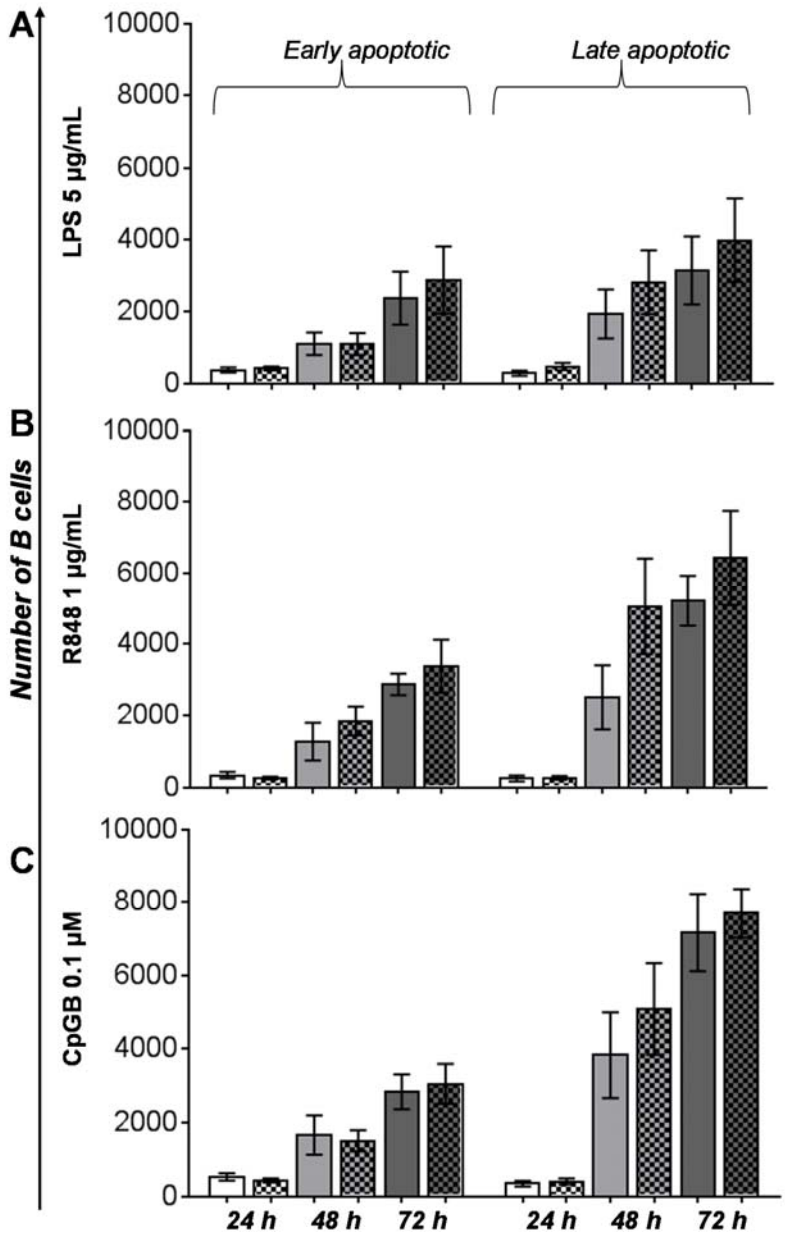

Figure 3.14 B cells apoptosis.

A comparison of B cell numbers in early or late apoptotic stages upon stimulation with (A) LPS, (B) R848, (C) CpGB in B6 (no pattern) or B6.*Sle1*(white pattern) mice at different time points. Statistical values were determined using an unpaired, nonparametric, Student's *t* test. Error bars represent mean ± SEM.*,*P* ≤ 0.05, **,*P* ≤ 0.01, ***,*P* ≤ 0.001, ****,*P* ≤ 0.0001. N=6 mice per genotype, two independent experiments.

Follicular dendritic cells are able to activate autoreactive B cells with B cells receptor after somatic hypermutations in GCs by picking apoptotic remnants within GC. Hence, we investigated the amount of cells in different stages of apoptosis in spleen (Munoz, Lauber et al. 2010).

No difference was reported in the number of cells between strains, highlighting that cells undergoing excessive apoptosis and providing ligands for APC in not the B cells, but might be other cell types **(Figure 3.14).**

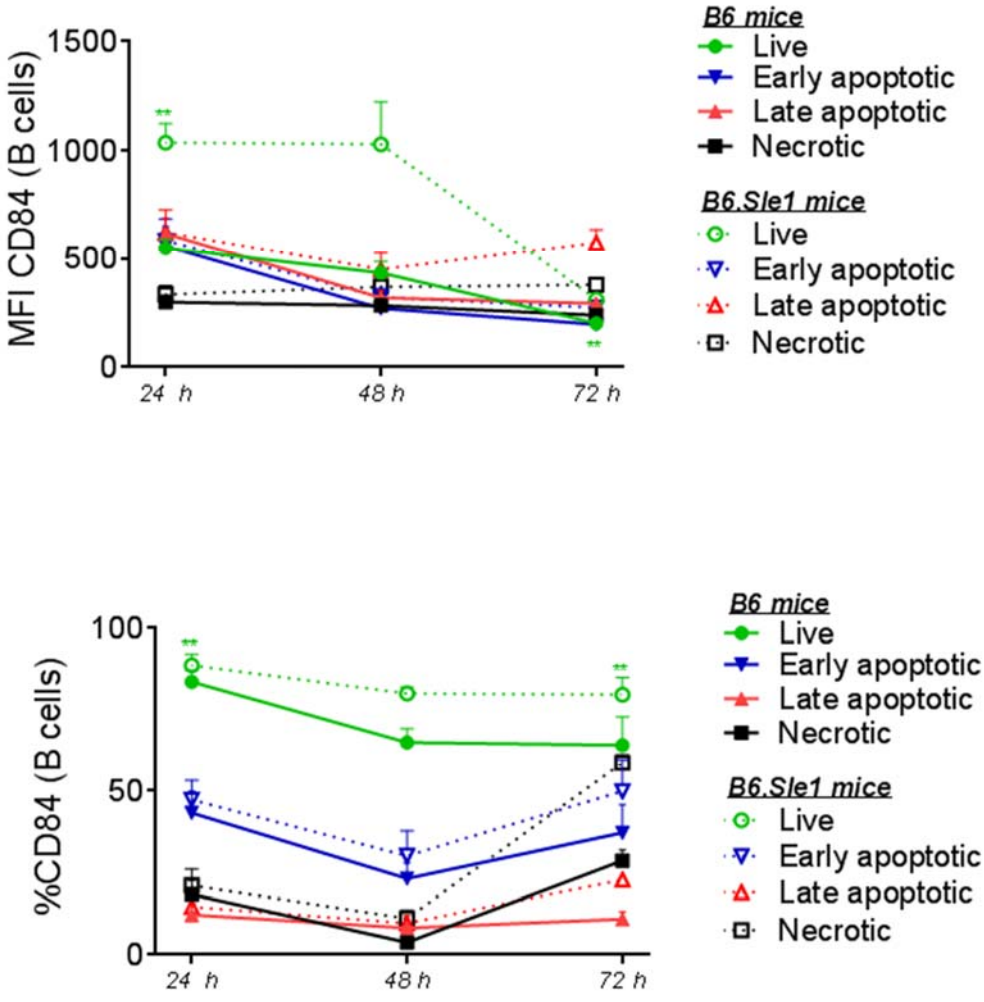

Figure 3.15 CD84 expression on B cells upon apoptosis.
CD84 expression (MFI and %) upon different stage of apoptosis in B cells from B6 and B6.Sle1 mice.

B6.*Sle1* mice have higher CD84 expression, confirmed by **Figure 3.15**, which are lost although different stage of apoptosis, reporting that CD84 as any surface molecule shaded and lost upon apoptosis. It is suggesting that CD84 might not be important in

apoptosis of B cells. Possibly, it plays role in PMNs apoptosis, since these cells are more likely to provide self ligands for APC.

Summary of B cell results

B cells are one of the main players in ANA production in SLE. Furthermore, recent report from Wong and colleagues (Wong, Soni et al. 2015) postulated an important role of CD84 and Ly108 expression on B cells and preventing ANA production. However, a single Ly108 has failed completely suppress ANA production leave the gap in understanding the role of CD84 in this process.

Initially we compared CD84 surface expression on splenic and renal B cells. Since we determined an upregulation of CD84 in B6.*Sle1* mice, we sought out to examine which functional differences it could provoke. Since CD84 is a homotypic receptor cell number titration was performed to chose 0.5 x 10^6 optimal cell concentrations for further experiments.

TLR receptors are also important in the SLE. Stimulation with TLR7 and TLR9 ligands resulted in a loss in B cell surface CD84 expression in both B6 and Sle1 strains. The comparison of antibody production revealed slight decrease of in IgM and IgA production by B6.*Sle1* mice. However further research is needed in this area.

Furthermore, we showed that ligation of surface CD84 receptor did not decrease or increase activation of cells upon R848 stimulation. Finally, apoptosis of B cells did not show any differences between B6 and B6.*Sle1* mice

3.2 Functional assay of CD84 in murine neutrophils

Recent data, reviewed in (Kaplan 2013) has shown an important role for neutrophils and TLR receptors in the development of SLE. Neutrophils play a putative role in providing self-ligand for perpetuating the inflammatory response and ANA production through a number of pathways culminating in cell death, **(Figure 1.3)**. We determined an increase in CD84 expression in neutrophils from 2 months old B6.*Sle1* mice. Given these findings we decided to investigate the functional differences in B6 and B6.*Sle1* mice in response to TLR ligand stimulation.

3.2.1 INCREASED MURINE NEUTROPHILS - PLATELET BINDING THROUGH CD84

It was reported previously (Nanda, Andre et al. 2005) that platelet CD84 expression is one of the highest among other blood cells. Neutrophils interact with platelets and form heterogeneous complexes which are further circulating in the blood (Li, Hu et al. 2000). Furthermore platelets have been shown to be essential for NETosis reviewed in (Zawrotniak and Rapala-Kozik 2013), a process believed to be fundamental in the generation of self-nucleic acids and stimulation of leukocytes in SLE (Garcia-Romo, Caielli et al. 2011). Therefore, we set out to determine if there was a relationship between platelets and neutrophils through CD84.

To assess binding to platelets, we stained peripheral blood and gated neutrophils from live leukocytes, using Gr-1 and Ly6-G as shown earlier **(Figure 3.16 A)**. We then examined the expression of CD84 in relation to CD41 this is a specific platelet marker. We used the CD84 FMO stain to assess positivety for CD84 **(Figure 3.16 A)**. In these studies we examined CD84 expression in B6 and B6.*Sle1* mice.

Based on our experiments the majority of neutrophils expressed CD84 (>90%) in both murine strains. Interestingly, approximately 45% of CD84+ neutrophils bound platelets in B6 mice, while in B6.*Sle1* this percentage was significantly higher **(Figure 3.16 B)**. There was no difference in binding of platelets in CD84 negative neutrophils (data not shown). B cells from peripferal blood did not show high level of platelet binding, suggesting it is neutrophil spesific phenomen in the blood **(Figure 3.16 B)**

We then investigated platelet - neutrophils interactions in spleen since there are very few platelets in this lymphoid organ. We determined approximately the same percentage of CD84 positive neutrophils in the spleen compare to the peripheral blood. Furthermore, as expected, the majority of these cells were not bound to platelets. This demonstrates that the PMNs CD84 expression is not an artifact of platelet binding.

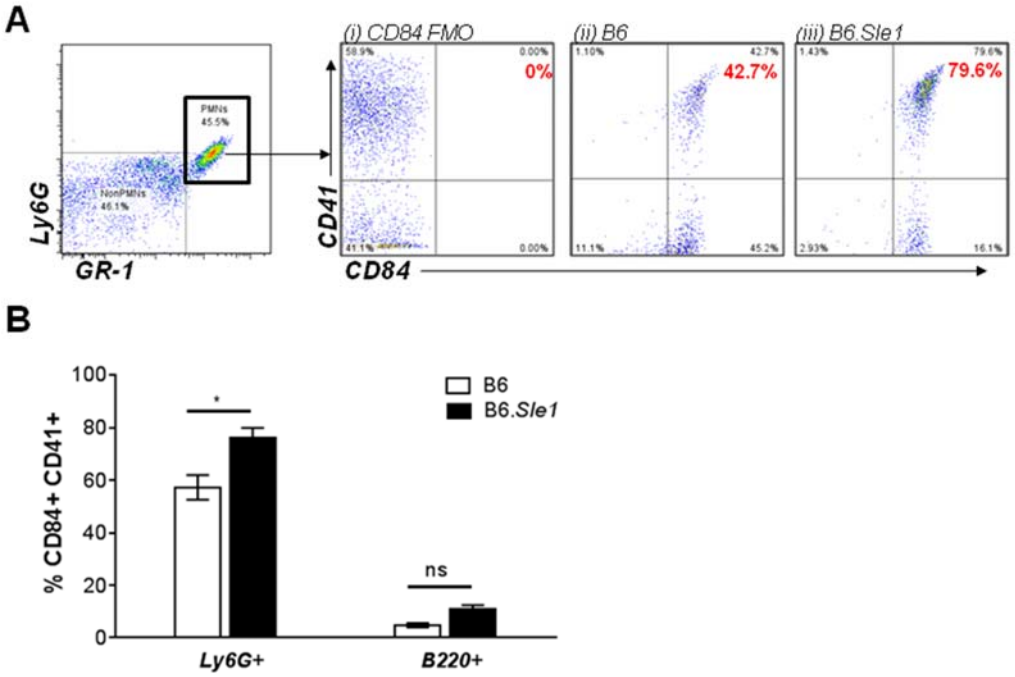

Figure 3.16 Murine platelet-PMNs interactions in peripheral blood and spleen of B6 and B6.Sle1 mice.

(A) CD84 FMO in peripheral blood and platelet-PMNs conjugates. (B) Percentage of CD84+ PMNs in peripheral blood. *P ≤ 0.05 paired t-test. The bars represent the mean ± SEM of four mice. The values indicate % of at least three independent experiments.

3.2.2 INCREASED APOPTOSIS IN BONE MARROW NEUTROPHILS OF B6.*SLE1* MICE

Abberant clearence of apoptotic cells is a reported sign of initiation of autoimmune pathology, especially SLE (Kruse, Janko et al. 2010). However, it is not clear yet which cells of innate or adaptive immune system contribute to this process the most. Since our investigation of murine B cells apoptosis did not reveal any alterations between B6 and B6.*Sle1* mice we sought out to evaluate apoptosis in murine bone marow neutrophils (BM-neutrophils).

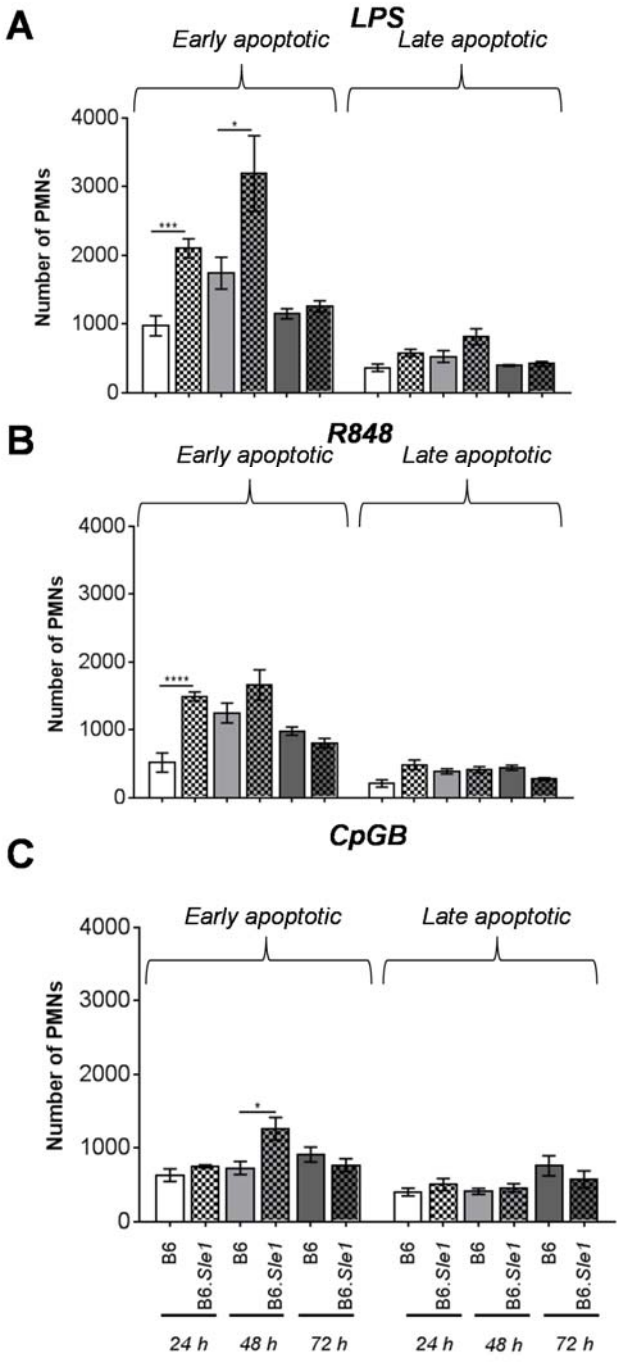

Figure 3.17 Apoptosis of BM-neutrophils in B6 and B6.*Sle1* mice.

Comparison of numbers of neutrophils in early or late apoptotic stages upon stimulation with (A) LPS, (B) R848, (C) CpGB in B6 or B6.*Sle1* mice at different time points. Statistical values were determined using an unpaired, nonparametric, Student's *t* test. Error bars represent mean ± SEM.*,$P \leq 0.05$, **,$P \leq 0.01$, ***,$P \leq 0.001$, ****,$P \leq 0.0001$. N=6 mice per genotype, two independent experiments.

Dying cells provide self-material which is recognized by autoreactive immune cells, further chaging there phenotype and start a production of cytokines or other soluble molecules leading to the tissue inflammation and production of ANAs (Manea, Mueller et al. 2009). Since apoptosis is one of the factors initiating autoimmunity, it was important to evaluate the difference between non-autoimmune mice and autoimmune- prone mice. In the assay used in this study cells were stained with annexin V and PI and analyzed at 24, 48 and 72 h **(Figure 3.17)**.

Therefore, the number of the cells in different apoptotic states was compared, mostly focused on early and late apoptotic stage over live and necrotic neutrophils. Non-stimulated neutrophils became necrotic within 24 h, hence the evaluation was performed upon stimulation with TLR ligands, LPS, R848 and CpGB **(Figure 3.17)**.

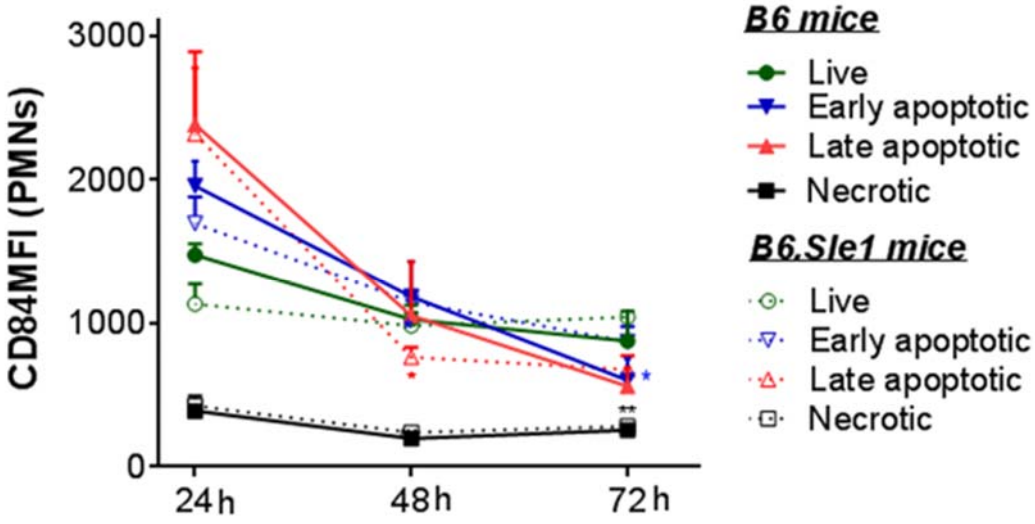

Figure 3.18 CD84 expression on BM-neutrophils upon apoptosis.
CD84 expression in B6 and B6.*Sle1* mice though out different stages of apoptosis.

Cells were stained for apoptosis at 24h, 48 and 72 h following stimulation and the cell numbers were calculated using Spherotec counting beads which were added prior to flow cytometry acquisition. The analysis was performed using the gating strategy outlines in the (material & methods, Figure 2.3.) BM-neutrophils derived from B6.*Sle1* mice showed significantly higher number of cells been in early apoptotic phase compared to B6 control **(Figure 3.17 A, B)**. Neutrophils stimulated with CpGB demonstrated increased number of cells in early apoptotic phase at later 48 h timepoint, suggesting that stimulation with TLR9 ligand shifts the alterations in B6.*Sle1* PMNs functions further in time. The

increased number of neutrophils in the early apoptotic stage together with impaired apoptotic debris clearance may provide enough self-ligands to initiate inflammation and immune response against self.

Since CD84 expression was initially increased in B6.*Sle1* neutrophils, therefore further analysis was performed on the changing in CD84 surface expression through different stages of apoptosis. Upon apoptosis cells usually lose surface markers, it was exactly reported in our study. Regardless of murine strain and stage of apoptosis BM-neutrophils were losing slowly CD84 expression with every further timepoint **(Figure 3.18)**, suggesting that CD84 has a minor role in apoptotic aberrations reported in B6.*Sle1* mice.

Although, CD84 might not be involved in apoptosis, and apoptosis might not be the key factor of initiation of autoimmunity, aberrations in another other type of neutrophil cell death, called NETosis might be key to understanding a primary mechanism of disease. This is supported by evidence of this process from human SLE patients which shows a higher rate of NETosis compared to controls (Garcia-Romo, Caielli et al. 2011). Therefore, in the next step the evaluation of NETosis in B6 and B6.*Sle1* was performed.

3.3 Rationale for a novel method NETosis evaluation

Traditional methods for measuring NETosis use microscopy, which does not enable large sample sizes or rapid analysis. Furthermore, ELISA plate reader based protocols are often used to assess NET remnants in solution (Barrientos, Marin-Esteban et al. 2013, Handono, Sidarta et al. 2014, Soderberg, Kurz et al. 2015). Given the emerging role of NETs across different pathologies, there is a need for a fast, reproducible and quantitative method for measuring active NETosis. Hence, before the evaluation of NETosis in B6 and B6.*Sle1* mice, we had to develop a method to detect NETosis by flow cytometry. We started our optimization using fluorescent nucleic acid dyes that have previously been used for microscopic quantification in human PMNs due to the availability of biological material (Berkes, Oehmke et al. 2014).

3.3.1 Choice and titration of antibodies and dyes for NETosis assay using flow cytometry.

We isolated neutrophils using density centrifugation as described in materials and methods, section 2.10.2. Since flow cytometry can analyze multiple parameters within a heterogenous population in a time-efficient manner. An added advantage of this method is the ability to broaden the staining panel to further characterize the cell population under investigation. To optimize a flow cytometry method we began by assessing a series of fluorescently-labelled antibodies to distinguish between untreated and PMA-treated neutrophils. We discriminated PMNs from other possible leukocytes using a combination of antibodies to several cell-surface markers, including CD14, CD16, CD115, CD193 and Siglec-10 **(Figure 3.19 A and data not shown)**. An anti-CD66 antibody was subsequently selected, since it labels both inactivated and activated PMNs clearly and can be used for both flow cytometry and microscopy (Ducker and Skubitz 1992). We chose a FITC-conjugated antibody at a concentration of 0.1 µg per 1 x 10^5 cells to eliminate overlap and avoid compensation issues.

During NETosis, specific cellular components are released including nucleic acids and enzymes. Our strategy was therefore to choose cell impermeable dyes or antibodies for the detection of nucleic acid to avoid unspecific labelling of intracellular or apoptotic DNA. We tested a series of dyes and antibodies previously used in microscopy (Brinkmann, Laube et al. 2010, Akong-Moore, Chow et al. 2012) to label neutrophils following mild fixation with PFA (2% final concentration for 15 min). This method enables visualization of the tangled DNA mesh of NETs expelled from the cells. We determined

several of these reagents to be specific for NETosis, with minimal labelling of apoptotic cells **(Figure 3.19 A)**.

A

Neutrophils identification		*NETs identification*	
Siglec 10		Elastase	
CD14		Histone 1	
CD16		SytoxOrange	+
CD66	+	Calcein AM	
CD115		DAPI	+
CD193			

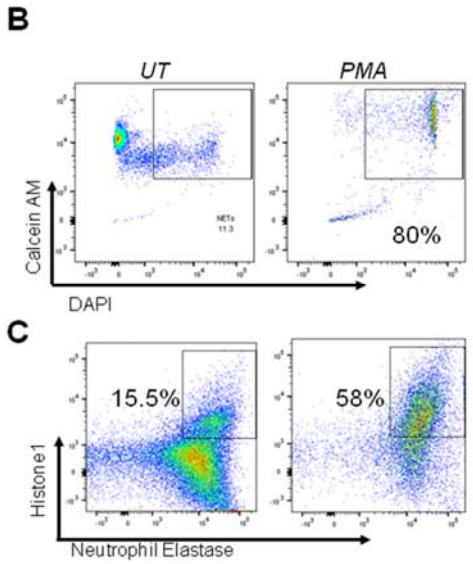

Figure 3.19 The choice of dyes for detection of neutrophils or neutrophil remnants and NETs.

(A) List of various antibodies and dyes to be used for neutrophils and NETs identification following stimulation with PMA. Dyes and antibodies used in this manuscript denoted with "+". Detection of NETs production by untreated (left panel) or treated (right panel) PMNs using (B) 2.5 μM Calcein AM and 0.3 nM DAPI or (C) anti-Histone 1 (1:300 ul) and anti-elastase (1:400 ul) antibodies following stimulation for 4 h with 100 nM PMA acquired using BD LSR Fortessa®.

For detection of NET-DNA we selected 4′,6-diamidino-2-phenylindole (DAPI), which binds to adenine-thymine clusters within the minor groove of DNA (Kubista, Akerman et al. 1987) and is excluded by a competent plasma membrane when the cell is alive. We used an optimized concentration of 0.3 nM which gave a bright signal, can be used immediately in a single staining step, and can be detected in the UV channel thus avoiding compensation issues. We also chose Sytox Orange (SO) at the optimized concentration of 2.5 μM. SO belongs to the Sytox group of molecules which emit increased fluorescence upon dsDNA binding.

3.3.2 Gating strategy to determine the percentage of neutrophils undergoing NETs.

Our optimized gating strategy is detailed in the **Figure 3.20**. Samples were gated on FSC-A/FSC-H and SSC-H/SSC-A to identify single cells **(Figure 3.20A)**. Neutrophils were then identified based on their high granularity (SSC-hi) and surface expression of CD66 **(Figure 3.20B)**. Cells undergoing NETosis were double positive for DAPI and SO. The mild fixative conditions used minimized the porosity of the neutrophils and decreased staining of intracellular material, which gave a background reading between 10 to 30% NETs.

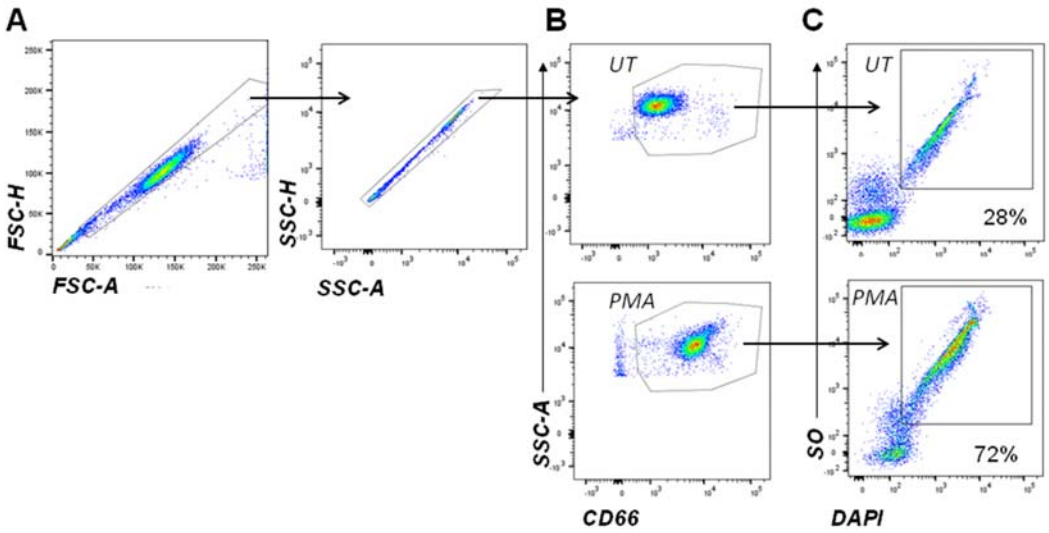

Figure 3.20 Gating Strategy for quantifying NETosis using flow cytometry
(A) Single cells were detected using forward scatter (FSC) and side scatter (SSC) area and height. (B) The neutrophil population was identified by high SSC and CD66 +. (C) NETs detection by DAPI and SytoxOrange (SO) positivity in untreated (UT) and PMA (100nM) stimulated samples.

3.3.3 Evaluation and comparison of the flow cytometry NETosis protocol with microscopy

Since flow cytometry is a relatively new method for NETosis evaluation, we set out to validate our protocol with microscopy, which is established and acknowledged methodology for detection (Brinkmann, Reichard et al. 2004, Clark, Ma et al. 2007, Naccache and Fernandes 2016). We assessed NETosis following PMA exposure of neutrophils over a time-course and examined samples in parallel using microscopy

(Figure 3.21A) and flow cytometry **(Figure 3.21 B)**. NETosis was monitored hourly by dual detection with SO and DAPI staining.

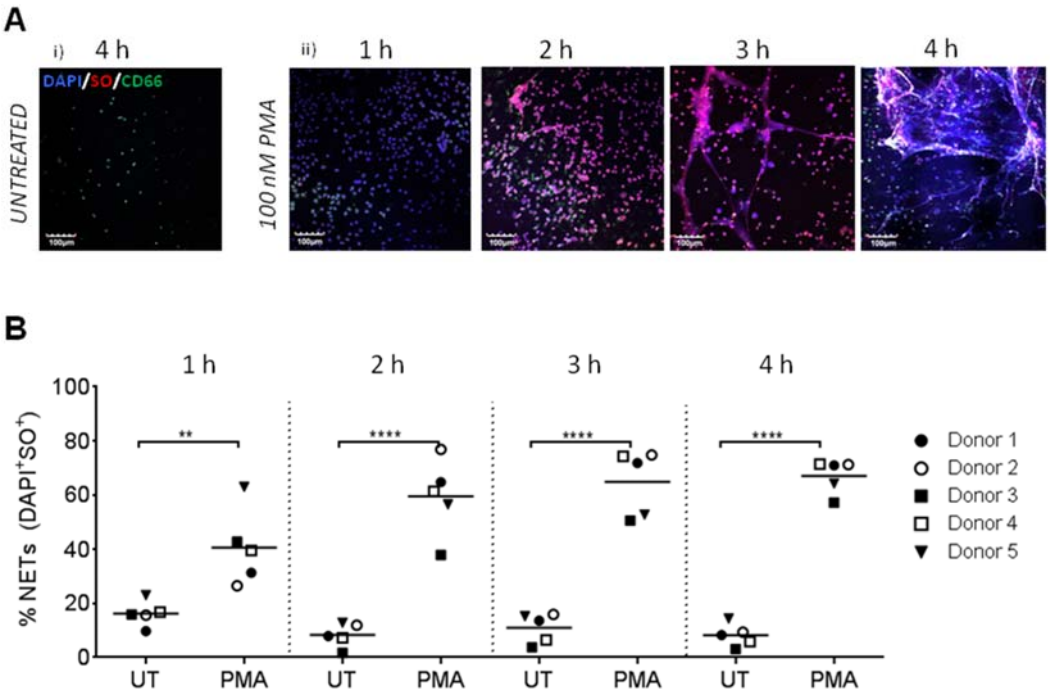

Figure 3.21 Validation of the novel flow cytometry assay using microscopy .

Neutrophils were stimulated with 100 nM PMA and prepared for quantification of NETosis as described in the methods and SOP. (A) Representative imaging of (i) untreated and (ii) PMA-stimulated neutrophils from one of five donors, acquired every hour. DNA was labeled with DAPI (blue), neutrophils remnants with CD66 (green), extracellular DNA stained with Sytox Orange (red) (B) At the same time NETosis formation was measured using flow cytometry in the same individuals. Graphs show the frequencies of NET-associated neutrophils following stimulation with 100 nM PMA every hour from 5 healthy donors.

At 1 h untreated neutrophils did not adhere to the cover slip and therefore few were visible under the microscope (data not shown). Adherence increased over time so that at 4h untreated neutrophils could clearly be observed using this protocol **(Figure 3.21 Ai)**. Addition of PMA increased adherence and enabled visible NET detection by DAPI and SO at 1 h, with full NETosis being observed at 3 and 4 h **(Figure 3.21 Aii)**. Analysis of NETosis using flow cytometry showed at 1 h a significant increase in the frequency of SO^+DAPI^+ neutrophils following 100 nM PMA compared to untreated cells **(Figure 3.21 B)**. This was also evident at 2, 3 and 4 h post stimulation, with the frequency of NETosis

by the neutrophils increasing with time **(Figure 3.21 B)**. All 5 donors responded to PMA, with maximal detection of NETosis at 3 and 4 h.

Furthermore, NETs could be observed under higher microscopic magnification, which is useful for colocalization studies **(Figure 3.22).**

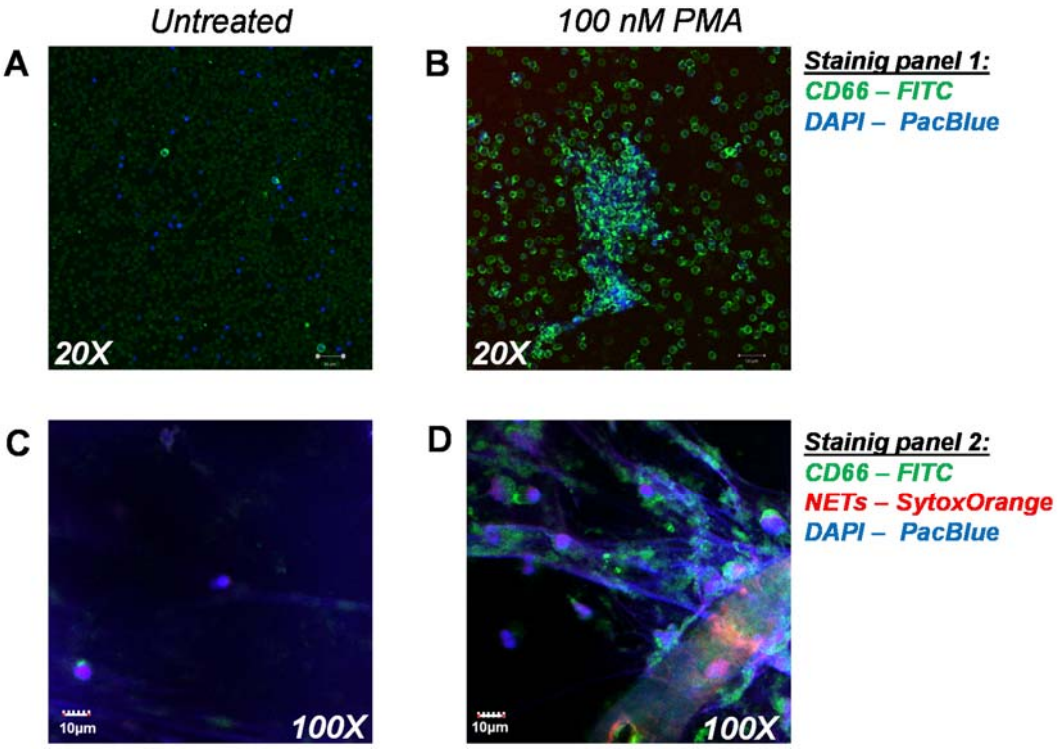

Figure 3.22 NETosis under high magnification.
Human neutrophils untreated (A; C) or stimulated with PMA for 4 h (B; D). Magnification of 20X (A and B) and 100X for (C and D) was used.

3.3.4 Flow cytometry detects NETosis at low concentrations of PMA

We developed this protocol using published concentrations of PMA (30 nM-100 nM). To assess the sensitivity of our method however, we went on to examine the effects of decreasing concentrations of PMA and measured levels of NETosis by flow cytometry. Isolated neutrophils from five different donors were stimulated with the indicated concentrations of PMA and analyzed hourly for up to 4 h **(Figure 3.23 A)**. Using our method, we observed a significant level of NETosis compared to untreated as early as 1 h following stimulation with the maximum concentration of PMA (30 nM) **(Figure 3.23 A)**.

A significant increase in the percentage of NETs was detected for PMA concentrations between 1 and 30 nM at 2 h. All concentrations of PMA stimulated a

significant level of NETosis at 3 and 4 h, with NETosis progressively increasing with higher concentrations of PMA and time. Detection of NETosis was maximal at 3 h with 1-30 nM of PMA. In contrast, exposure to etoposide which is a chemical that stimulates apoptosis, did not result in increased levels of NETosis **(Figure 3.23 B)**.

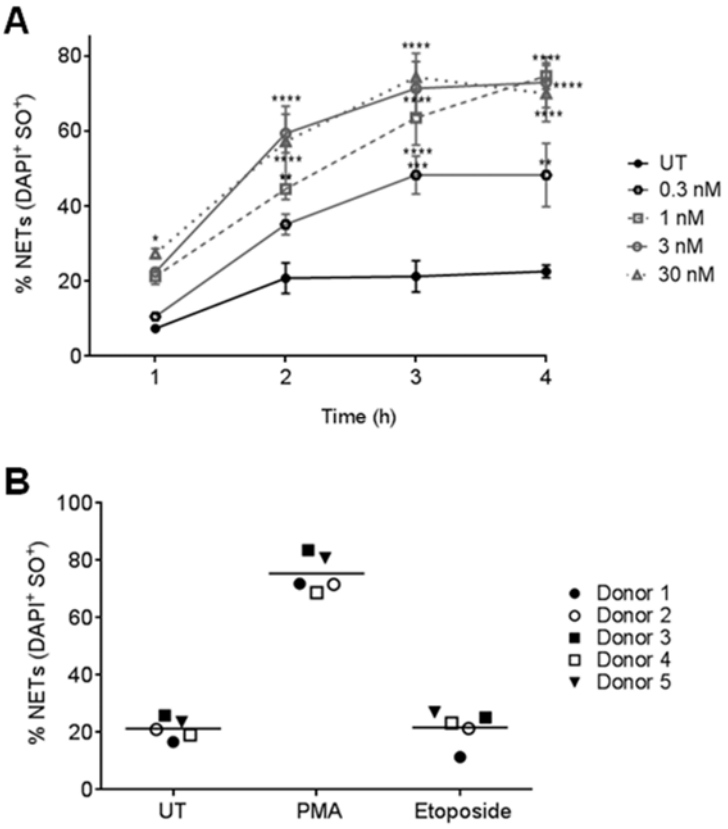

Figure 3.23 Flow cytometry provides a sensitive and specific method for detecting NETosis.

(A) NETosis can be detected as early as 1 h following the high concentration of PMA shown and after 2 h with all concentrations used. A 2-way ANOVA with repeated measures was used to determine significant differences compared to the untreated (UT). (*p<0.05 for 30 nM at 1 h, ***p<0.01 for 1 nM and ****p<0.001 for 3 and 30 nM at 2 h; p<0.01 for all concentrations at 3 h and 4 h)(n=5). (B) Stimulation with 30 μM etoposide did not result in an increase in DAPI+SO+ neutrophils.

3.3.5 NETOSIS IN B6 AND B6.*SLE1* MICE

Neutrophil death through NETosis is known to provide self ligands for APC, which is followed by activation of T and B cells and Ig production. Hence, the evaluation of NETosis level in B6.*Sle1* mice was the next step in our research. Our novel flow cytometry method developed and optimized for human neutrophils was then applied to murine leukocytes. Whole blood was lysed using Ack lysis buffer as described in the materials and methods section 2.10.2 cells were stimulated with PMA or the TLR7 ligand, R848.

Following 4 h stimulation cells were stained with SO, DAPI to identify NETs and Ly6G to identify neutrophils. Cells were analysed using flow cytometry and the gating strategy shown below **(Figure 3.24 A)**.

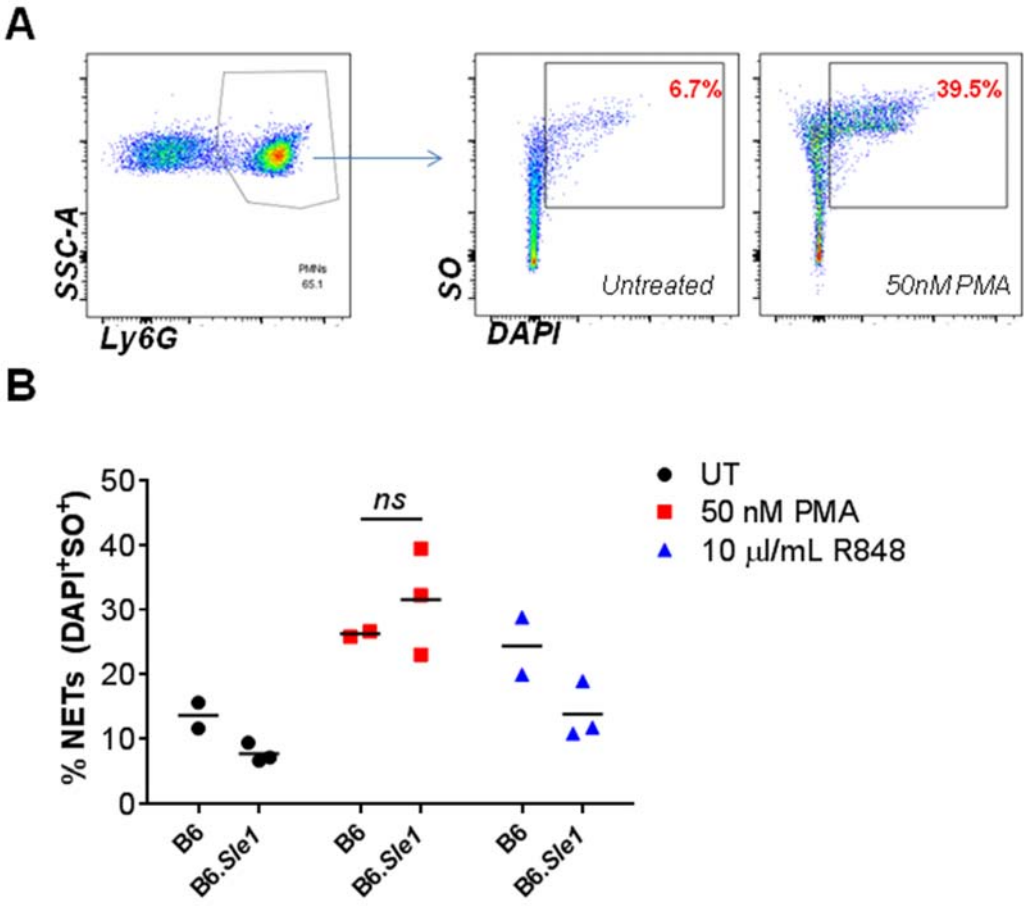

Figure 3.24 NETosis in B6 and B6.*Sle1.*
(A) Gating strategy for NETs identification, gated first on Ly6G+ high SSC, following by SO+DAPI+ population, defined as NETs. (B) NETs formation from murine peripheral neutrophils of B6 and B6.*Sle1* mice upon stimulation with PMA or R848. Statistical values were determined using an unpaired, nonparametric, Student's *t* test.. N=2-3 mice per genotype, a representative experiment.

B6.*Sle1* neutrophils showed decreased levels of NETs on their neutrophils compared to B6 mice, however this did not reach statistical significance **(Figure 3.24 B).** More mice should be evaluated in order to draw any conclusions. Surprisingly, murine neutrophils were forming NETs upon stimulation with R848, a TLR7 ligand. According to Immgen (https://www.immgen.org/), unlike human, neutrophils from mice express TLR7. Furthermore, TLR8 is a pseudogene and therefore it is possible that in murine models of SLE, stimulation with TLR7 ligand, as single strand RNA (ssRNA), initiate pathology development. Meanwhile in human, TLR8 might play dual role and become activated, undergo NETosis resulting in self ligand availability for APC. B6.*Sle1* neutrophils were less responsive to stimulation with TLR ligands similar to the results demonstrated by

B6.*Sle1* B cells, which were also slower in response to TLR7 ligand stimulation. Therefore it is possible, that slower responses to stimulation results in higher amounts of autoreactive cells, escaping checkpoints and avoiding anergy. Similar results were determined by others who showed B cells from B6.*Sle1* mice have a slower response proposing this is the of the key factor in disease initiation (Wong, Soni et al. 2015).

A future direction for these studies would be to evaluate the role of CD84 in NETosis. The hypothesis is that excessive binding of lupus platelets might activate neutrophils, making them produce self ligands and make it available for APCs. Since we reported that lupus neutrophils bind platelets 30% more, hence it could be possible trigger for NETosis activation. With the developed method to evaluate NETosis by flow cytometry, it will be possible to identify changes of CD84 expression and propose the role of CD84 in increased NETosis in murine models of autoimmunity and lupus patients.

Since we had determined expression differences and some functional changes in B6.*Sle1* B cells and neutrophils we went on to compare sequence differences between these 2 strains to further evaluation possible differences in cellular activation.

Summary PMNs

Recent data has shown that neutrophils may play an important role in the initiation of lupus pathology, however this has not been fully elucidated Since initially we determined an increase in CD84 expression in neutrophils we went on to examine how differential expression of CD84 on neutrophils affect the functional differences. We determined that B6.*Sle1* mice bind 30% more platelets in blood compared to B6 control. Next, increased number of early apoptotic cells were reported in B6.*Sle1* mice. In attempt to analyse NETosis a new flow cytometry based assay was developed, and NETosis in B6 and B6.*Sle1* mice was analysed, however in order to make a strong statement more mice from both strains should be assessed.

Hence, reported functional differences in B cells and PMNs between control and B6.*Sle1* mice did not give full answers for the reasons of pathology initiation in B6.*Sle1* mice, we went on to examine the genetic differences in CD84 in B6 and B6.*Sle1* mice.

3.4 The differences in CD84 haplotypes

3.4.1 NOVEL SNPS DETECTED BY DNA SEQUENCING

To assess whether there are differences in CD84 structure between B6 and B6.*Sle1* mice, we examined DNA and RNA. Murine DNA from B cells of both strains was isolated and sequenced. The sequencing data was aligned and analyzed for single nucleotide polymorphism (SNPs) as described in material and methods section 2.11.3. Most of the SNPs were found to be located within intronic regions or within the 5' and 3' untranslated regions. However two reported SNPs were located in exonic regions as described in **Figure 3.25 A.**

Nonsynonymous mutations resulted in alterations of amino acid sequencing, and therefore were the most interesting. The first exonic SNP is nonsynonymous and affected the change at position 27. In the B6.*Sle1* this results in the expression of a methionine residue instead of valine at position 27 (compared to B6) **(Figure 3.25 B)**. This has been predicted previously by (Wandstrat, Nguyen et al. 2004) using the protein analysis. The CD84 protein structure consists of 5 domains **(Figure 3.25 B)**: two extracellular domains, a transmembrane domain and an intracellular domain. The SNPs is located in the N-terminal variable domain region, participating mostly in the homotypic interactions with CD84 expressed on the other cell (Yan, Malashkevich et al. 2007). It is tempting to speculate that changing an amino acid in this region alters binding property of CD84 which resulted in possibly longer cell to cell interactions, provoking excessive antibody formation.

The second SNP detected in an exonic region resulted in a synonymous mutation from T to C maintaining a tyrosine residue at position 245 **(Figure 3.25 A, B)**. It is located right on top of the ITSM motif, which undergo phosphorylation, however this residue have not been reported to participate in phosphorylation. Since this is synonymous mutations aminoacid sequence has not been changed. The last SNPs resulted in nonsynonymous mutation at position 293 leading to the substitution of Lysine (K) aminoacid in the B6 strain to Glutamic acid (E) in B6.*Sle1* **(Figure 3.25 B).**

The polymorphism of Ly108 was reported previously (Wandstrat, Nguyen et al. 2004) and further investigated to reveal the difference in function Ly108-1 and Ly108-2 isoforms (Zhong and Veillette 2008). The data from DNA seq revealed SNPs in B6.*Sle1* mice resulting in nonsynonymous mutation in the position 126 **(Figure 3.25 A, C)**. The other SNPs reported in the position 328 do not alter the Ly108 protein sequencing. Amino

acid replacement in the position 126 located within first IgV domain of Ly108 and plausibly important in homotypical interactions and antibody binding.

A

SLAMF	Position in gene	Reference genome NM_001289470	B6.*Sle1* genome NM_013489	Codon change	Mutation	Position in protein	Aminoacid change
CD84	171851835	G	*A*	exonic	nonsynonymous	27	V to M
	171852430	T	*C*	3' UTR			
	171873408	T	*C*	exonic	synonymous	245	Y to Y
	171885586	A	*G*	exonic	nonsynonymous	293	K to E
Ly108	171934390	C	*T*	exonic	nonsynonymous	126	T to I
	171942580	C	*T*	exonic	synonymus	328	A to A

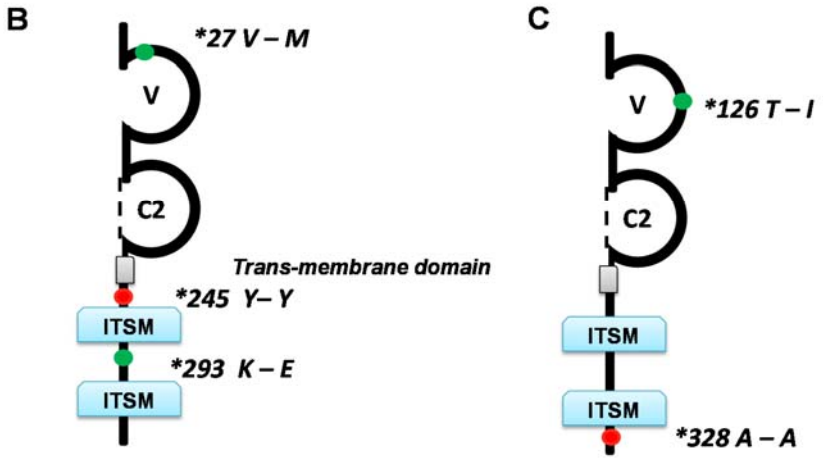

Figure 3.25 Analysis of genomic and transcriptomic sequences from B6 and B6.Sle1 mice.

(A) Positions with altered sequences in B6.*Sle1* mice with reported data. (B) Schematic structure of murine CD84 protein, based on Uniprot database with the location of SNPs reported by DNA sequencing. V- valine, M - methionin, Y - tyrosine, K - lysine, E - glutamic acid. V - Immunoglobuline variable domain, C2 - Imunoglobuline constant domain, ITSM - Immunotyrosine switch motif.

According to the ENSEMBL database, this SNPs has been previously reported in the literature, however not in B6.*Sle1* mice, thus it is a novel SNP associated with this autoimmune mouse model. The location of mutation is within the intracellular domain in the position 293 which might influence the downstream protein binding and alter intracellular signaling.

3.4.2 INCREASED MURINE CD84 TRANSCRIPTION IN B6.*SLE1* MICE

To confirm the differences in CD84 expression between B6 and B6.*Sle1* mice we also examined RNA. Analysis of whole transcriptome shotgun sequencing (RNA-seq) revealed splenic B cells from B6.*Sle1* mice express 40% more (1.4 fold change) CD84 RNA when compared to age- and gender-matched B6 controls **(Figure 3.26 C)**. Subsequent isoforms analyses demonstrated between 1.4 and 1.75 fold differences across each of the five isoforms in B6.*Sle1* mice compared to B6 control **(Figure 3.26 B)**.

Analysis of the five isoforms using ENSEMBL and the VEGA genome browser (www.ensembl.org) revealed that only 4 isoforms are reportedly translated to protein.

Next, we asked whether the SNPs reported by DNA sequencing analysis were present in B cells in B6.*Sle1* mice. Two SNPs (one at position 27 and one at position 245) were confirmed at the RNA level in B6.*Sle1* mice **(Figure 3.26 A)**. However, the lysine to glutamic acid change at position 293 was not confirmed by RNA seq **(Figure 3.26 A)**. As RNAseq data represents only one mouse per genotype further analysis would be required to confirm the presence or absence of this SNP in the genome of B6.*Sle1* mice.

A

Position	Reference genome NM_001289470	B6.Sle1 genome NM_013489	Codon change	Mutation	Position in protein	Aminoacid change
171851835	G	A	GTG to ATG	nonsynonymous	27	V to M
171873408	T	C	TAT yo TAC	synonymus	245	Y to Y
171888736	C	T	3' UTR			
171888772	A	C	3' UTR			

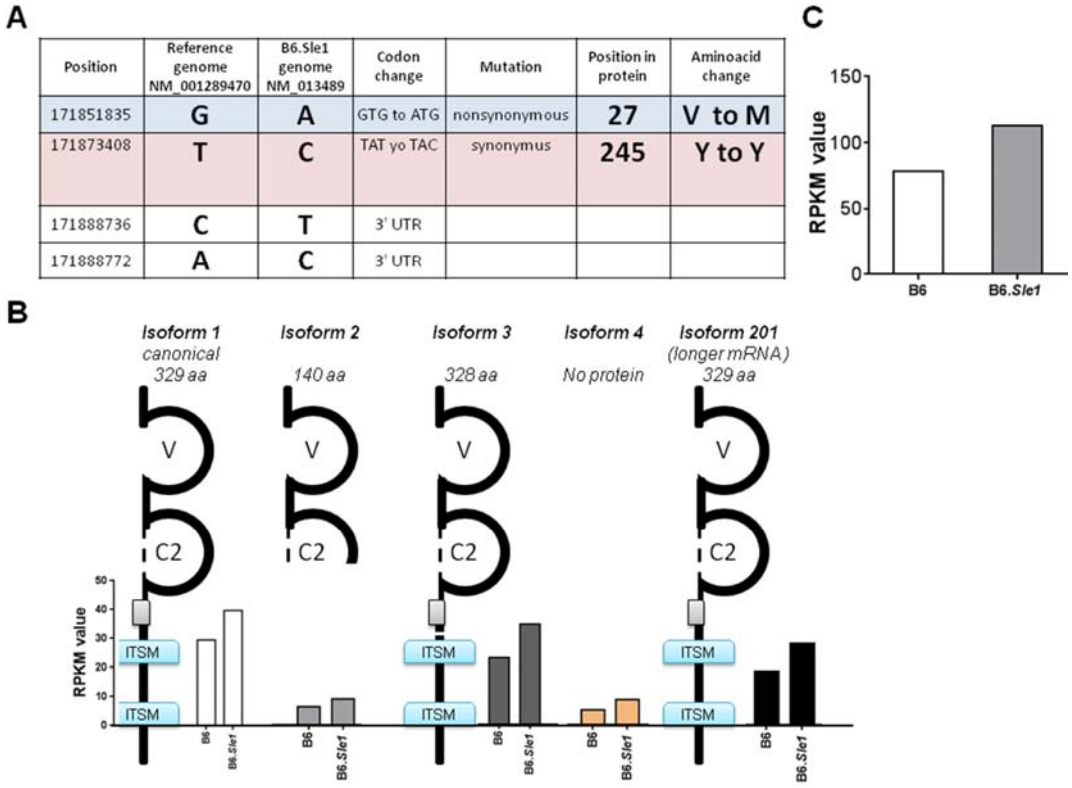

Figure 3.26 Increased CD84 expression in RNA level in B6.*Sle1* mice.
(A) Mutations in Cd84 protein identified by RNAseq. (B) Comparison of CD84 isoforms transcription in B6 and B6.*Sle1* mice with the structures of isoforms presented. (C) A comparison of total murine CD84 level of expression in B cell splenocytes.

B6.*Sle1* carrying an extra copy of TLR7 exhibit severe lupus phenotypes (Hwang, Lee et al. 2012). Therefore, we hypothesised that CD84 interacts with the TLR7 signalling pathway, provoking hyperactivation of TLR7 and subsequent severe pathology. Hence, to determine how sequence alterations in CD84 from B6.*Sle1* mice will affect the functional properties of the molecule and interaction with TLR7 we adopted a lentivirus approach and the use of a HEK-BLUE cell line engineered to express TLR7.

HEK-BLUE Cells

Previous studies have showed the importance of TLR7 in the formation of germinal centers and furthermore the development of ANAs, resulting in the initiation of autoimmunity (Soni, Wong et al. 2014). Data from mouse models has also demonstrated the development of severe lupus pathology by the addition of an extra copy of TLR7 to the genome of mice carrying the auto-immune prone haplotype of SLAMF (Hwang, Lee et al. 2012). This information brings about the hypothesis that harmful interactions of SLAMF members with TLR7 may result in autoimmune pathology.

In order to investigate the interaction of TLR7 with different haplotypes of SLAMF we employed an engineered cell line called HEK-BLUE from Invivogen. The cell line is based on human embryonic kidney 293 cells (HEK293), which are stably transfected with a murine TLR7 gene and an inducible secreted embryonic alkaline phosphatase (SEAP) gene mTLR7-HEK-BLUE. The SEAP gene is placed under the control of the IL-12 p40 minimal promoter and fused to five NF-κB and AP-1-binding sites. Upon stimulation with TLR7 ligands, NF-kB and AP-1 become activated and induce the secretion of SEAP.

For analysis, cells are resuspended in special SEAP detection media containing a substrate for the alkaline phosphatase enzyme which changes the color from pink to purple upon the SEAP secretion and makes detection possible by the naked eye **(Figure 3.27 A)**. The control cell line is transfected with null plasmid and called NULL-2K-HEK-BLUE (Null-2k). HEK-BLUE cells have to be grown in special media supplemented with selective antibiotics: zeocin for Null-2k and zeocin plus blasticidin for mTLR7.

For more precise measurement of SEAP secretion and hence TLR7 activation, it is possible to measure plate absorption using plate-readers at 620 nm **(Figure 3.27 B)**. The obtained values may then be graphed for analysis **(Figure 3.27 C)**.

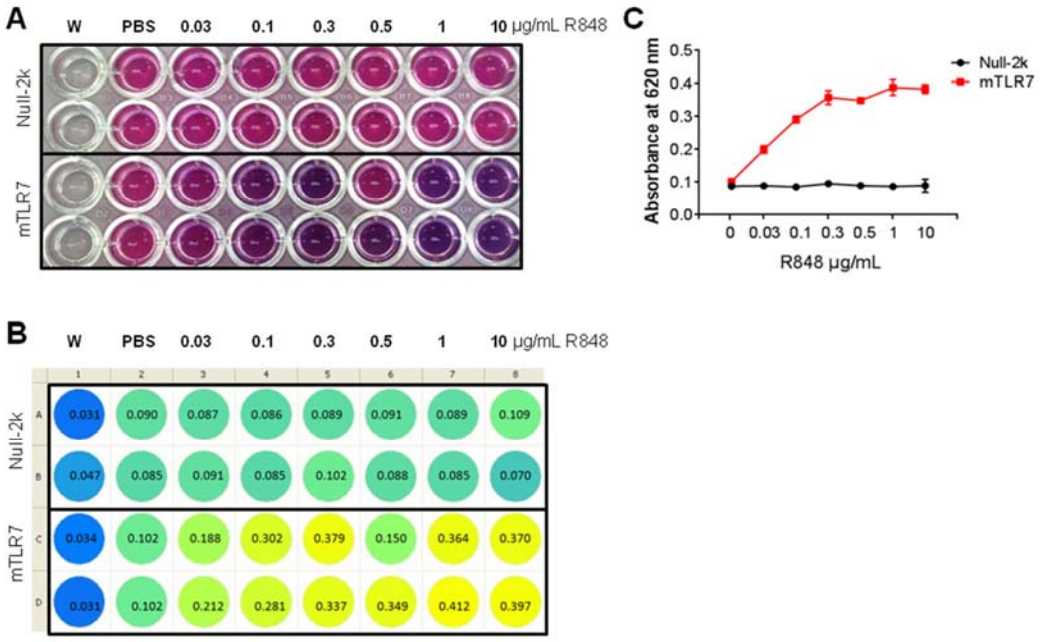

Figure 3.27 TLR7 ligand titration using engineered HEK-BLUE cell line.
(A) SEAP secretion detection by naked eye with HEK-BLUE detection media in HEK-BLUE transfected with null plasmid (Null-2k) or with plasmid expressing murine TLR7 (mTLR7) cell line upon 16 h stimulation with a titration of TLR7 ligand (R848). (B) Optical density reading of (A) at 620 nm using an Envision plate (C) Graphical representation of the results.

Lentivirus approach for transduction of HEK-BLUE cells with gene of interest

Initially several attempts to use the plasmid expressing different CD84 haplotypes to transfect HEK-BLUE cell line was performed (data not shown). However due to the fact that plasmids are not episomally maintained, as well as time constraints (since the development of stable cell lines takes a long time), we decided to imply lentiviral approach.

Lentiviral constructs have been widely used in research as fast, relatively cheap tools to deliver stable transgene expression as they integrate into the host cell genome (Trono 2001, Woods, Mikkola et al. 2001). Lentiviral vectors also offer the advantage that they are able to deliver genes into non-dividing cells and are therefore convenient for transducing hematopoetic stem cells without pre-stimulation (which may cause the cells to differentiate *in vitro*) (Sherman and Greene 2002).

Lentiviral vector plasmids were therefore designed to express the two different haplotypes of CD84: haplotype 1, the canonical sequence of CD84 (CD84-H1) and

haplotype 2, or the autoimmune-prone haplotype, with the alteration of the amino-acid at position 27 (CD84-H2) (Wandstrat, Nguyen et al. 2004). A plasmid expressing solely eGFP was ordered as a negative control. Please refer to the Appendix 1. for plasmid information.

For a fast assess of transduction efficiency with microscopy or flow cytometry the vectors have been designed to express fluorescent GFP signal for CD84-H1 and CD84-H2 or RFP signal for Ly108. It was achieved by using the internal ribosome entry site (IRES) vector, a bicistronic system allowing the transcription of multiple proteins from one long RNA. In our case, the transcription of CD84 will correlate with GFP, hence the vector expressed only GFP is a necessary control.

The IRES vectors allow simultaneous translation of multiple proteins under the same promoter, the human housekeeping gene promoter elongation factor-1 alpha (EF-1α) was chosen(Qin, Zhang et al. 2010). It gives a stable long-term expression and is active in multiple cell-lines as well as in a progenitor cell, like hematopoietic stem cells (HSC)(Varma, Janic et al. 2011).

Since an initial study demonstrated a potential pairing role of CD84 and Ly108 in decreasing ANA development (Wong, Soni et al. 2015), a lentiviral vector expressing the Ly108-H1 isoform, known to suppress autoimmune response, was also ordered (Dutta and Schwartzberg 2012). This construct was designed to co-express red fluorescent protein (RFP) as a reporter gene (see Appendix 1).

Lentivirus was produced and concentrated by ultracentrifugation to obtain a necessary titre around 1 x 10^7. Subsequently the Null-2K and mTLR7 HEK-blue cell lines were transduced and defined the titre of virus obtained.

3.4.3 TRANSDUCTION OF HEK-BLUE CELLS WITH CD84 AND LY108

To compare a functional effect of SNP which resulted in amino acid change at position 27 the HEK-BLUE cells were transduced with lentiviral vectors encoding either empty GFP **(Figure 3.28 A)**, Ly108-H1 **(Figure 3.28 B)**, CD84–H1 or CD84-H2 **(Figure 3.28 C, D** respectively) at a multiplicity of infection (MOI) 1. The low MOI was chosen to prevent the incorporation of multiple genes in the genome, hence to compare the effect of SNP rather than compare the copy number effect. The expression of GFP at less than 30% indicated incorporation of 1 virus into a genome (Trono 2001).

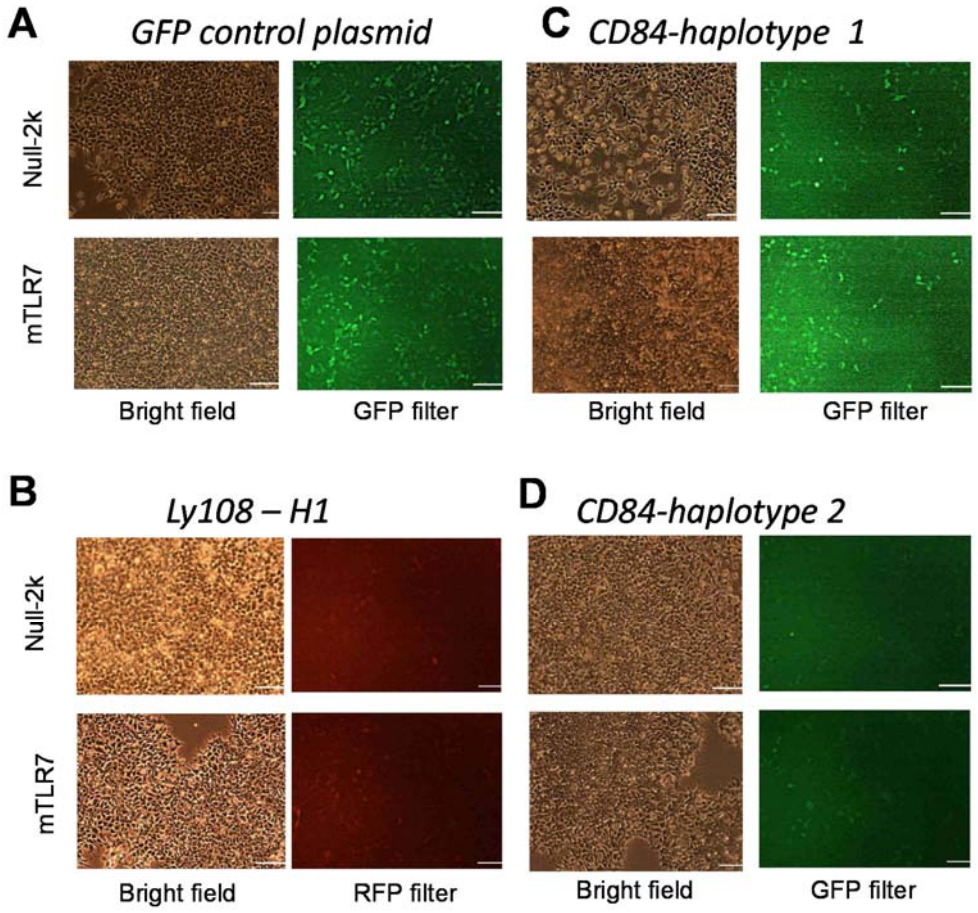

Figure 3.28 Lentiviral transduction of HEK-Blue cells.
Fluorescence microscopy demonstrating transduction efficiency of Null-2K or mTLR7 HEK-BLUE cell lines after 72 h. Lentiviral vectors carrying either (A) empty GFP, (B) Ly108–H1, (C) CD84-H1 or (D) CD84–H2 genes were used for transduction.Size bar 100 μm.

Fluorescence microscopy was used initially for the assessment of transduction efficiency after 72 h. However high background, as in the **Figure 3.28 B and C** and difficult to quantify drove us to imply flow cytometry for more precise evaluation of the transduction efficiency.

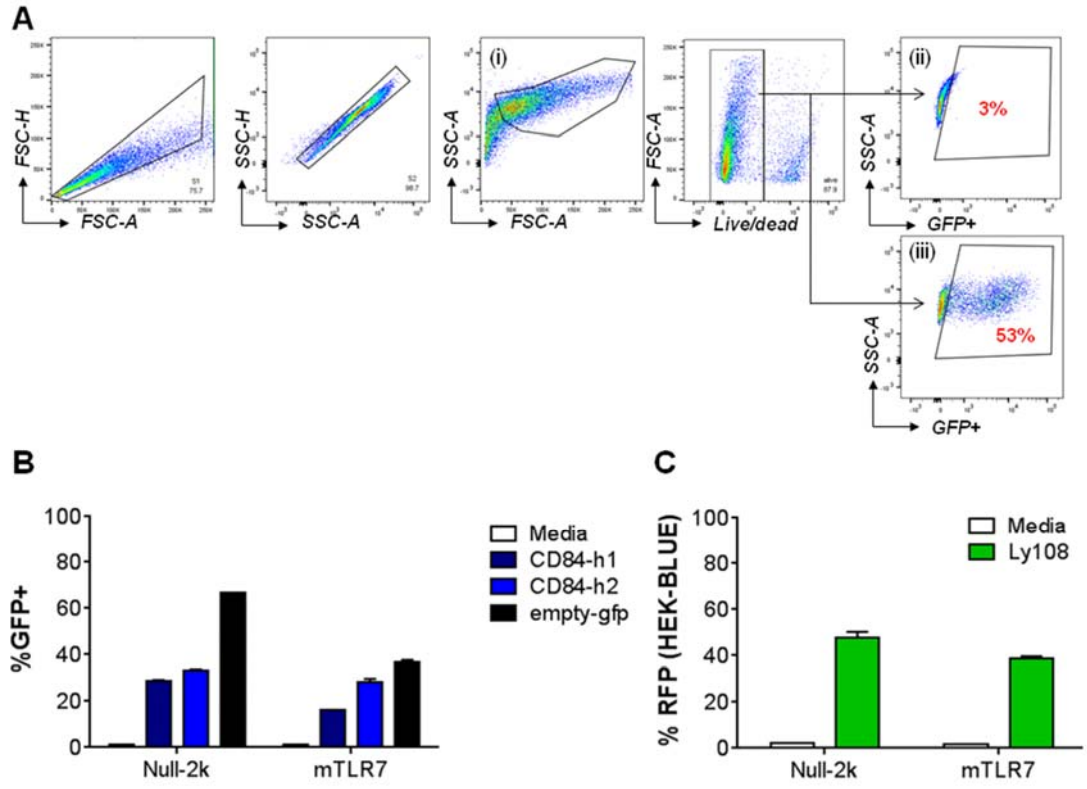

Figure 3.29 Flow cytometry analysis of lentiviral transduction of HEK-Blue cells.

(A) Gating strategy for the detection of transduction efficiency of HEK-BLUE cell line (i), monitored by GFP expression. Cells were transduced with either (ii) media, CD84-H1 or CD84-H2 lentiviral vectors or (iii) control empty GFP lentiviral vector. (B) Percentage of GFP expression by transduced Null–2k or mTLR7. (C) RFP expression by transduced Null-2K and mTLR7.

At first, GFP (Figure 3.29 B) or RFP (Figure 3.29 C) expression was determined using the depicted gating strategy (Figure 3.29 A). GFP+ cells were gated based on untransduced HEK-BLUE cells (Figure 3.29 Aii). Null-2k cells demonstrated slightly higher transduction efficiencies as compared to the mTLR7 cell line, however this did not affected the overall system workflow. (Null-2k was still non-responsive to TLR7 ligand stimulation).

A transduction with the empty GFP control vector showed the highest efficiency likely due to the smaller size of the vector and that in this backbone the GFP reporter gene is transcribed directly from the EF1-α promoter as opposed to in the bicistronic vectors in which it is well-documented that expression of the second transgene is reduced

(Mizuguchi, Xu et al. 2000). The GFP signal from cells transduced with CD84-H1 was lower than CD84-H2, however it did not reach statistical significance **(Figure 3.29 B)**.

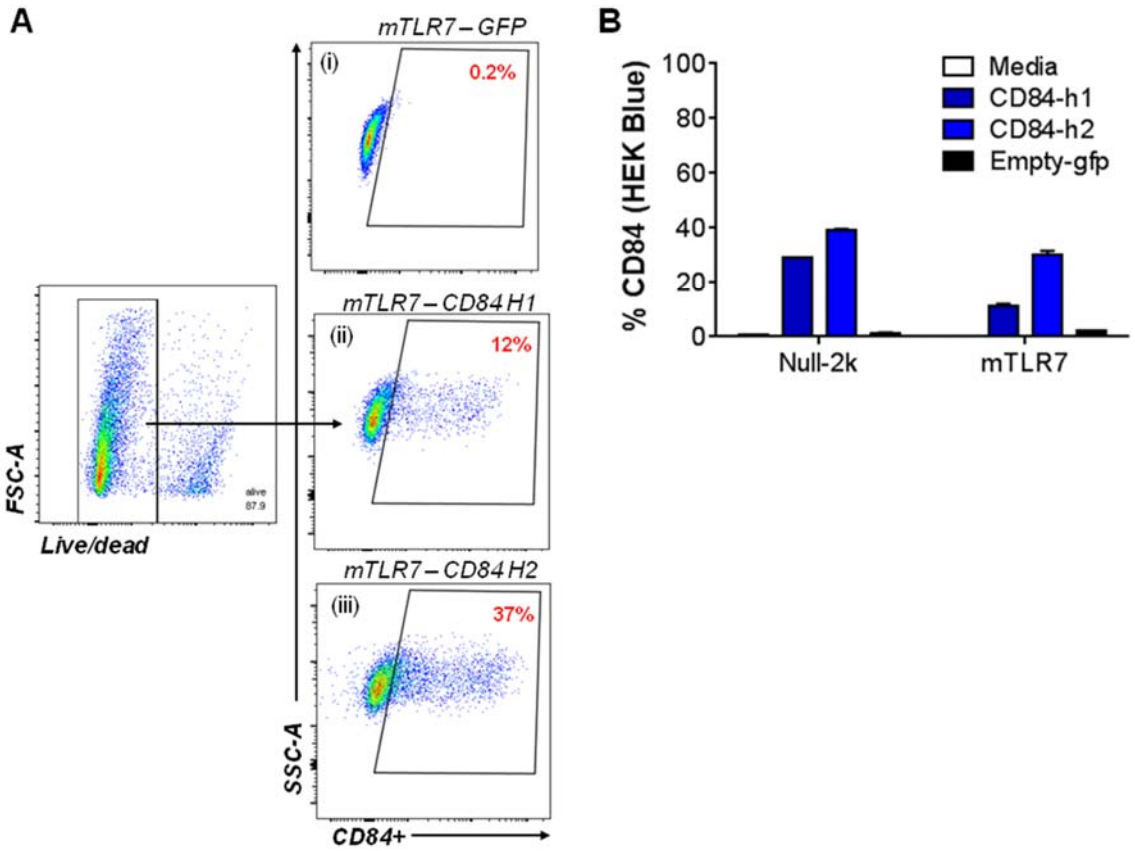

Figure 3.30 CD84 expression in HEK-BLUE cells after lentiviral transduction. (A) Gating strategy for the detection of CD84 expression on live HEK-BLUE cells (i) mock transfected or (ii) CD84-H1transduced and (iii) CD84–H2 transduced. (B) CD84 and expression by Null-2k or mTLR7 cell lines after transduction.

Ly108 expression was evaluated by RFP expression only, since an anti-Ly108 antibody was only available conjugated to phycoerythrin (PE), which would clash with RFP expression. Similarly to the GFP expression, the Null-2k cell line was found to express higher levels of Ly108 **(Figure 3.29 C)**, however these were still unresponsive to TLR7 stimulation.

In the next step, surface expression of CD84 was also assessed using flow cytometry. Following the previous example, CD84 expression was determined based on non-transduced mTLR7 cells following staining with an anti-CD84 antibody **(Figure 3.30 A)**. CD84-H2 expression was observed to be slightly higher than CD84-H1 **(Figure 3.30 B)**. Initially, the virus titre might be not detected precise enough to use in comparison

study. Hence, more quantitative technique, like RT-PCR should be used for the control of transduction level.

3.4.4 STIMULATION OF TRANSDUCED NULL-2K AND MTLR7 CELL LINES WITH TLR7 LIGAND (R848)

To determine the influence of CD84 haplotype and possible interactions between CD84 and TLR7, the transduced cells were subsequently stimulated with different concentrations of R848. As a control for stimulation, non-transduced mTLR7 cells were chosen. The response time for untransduced cells is around 14-16 h following the stimulation with R848 **(Figure 3.31 A)**. In contrast, untransduced Null-2K cells, which do not express TLR7, failed to exhibit any media colour change following stimulation with R848 **(Figure 3.31 A)**.

Following transduction with the genes of interest, mTLR7 HEK-BLUE cells demonstrated a faster response to the TLR7 ligand, with maximal absorbance reached by 12 h compared to 16 h for untransduced cells. Murine TLR7 cells transduced with either empty GFP **(Figure 3.31 B)** or Ly108-H1 **(Figure 3.31 C)** showed dose dependent response upon stimulation with different concentration of R848 ligand.

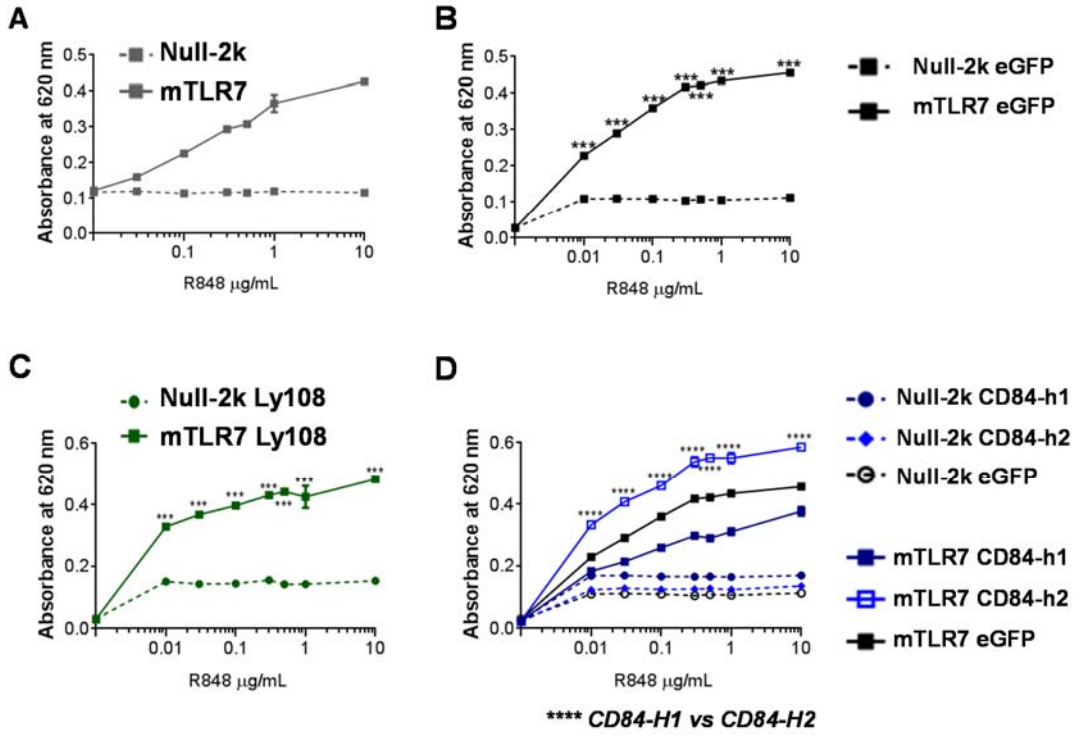

Figure 3.31 Stimulation of transduced HEK–BLUE cells with R848.
A dose-response to TLR7 ligand of (A) HEK-BLUE Null–2k cells (dotted line) versus mTLR7 cells (solid line). (B) HEK-BLUE cells transduced with empty GFP plasmid. (C) HEK-BLUE transduced with Ly108-H1 gene. (D) A comparison of absorbance between HEK-BLUE expressing CD84-H1 or CD84–H2 with GFP as a control. Statistical values were determined using an unpaired, nonparametric, Student's *t* test. Error bars represent mean ± SEM.*,$P \leq 0.05$, **,$P \leq 0.01$, ***,$P \leq 0.001$, ****,$P \leq 0.0001$. N=2, two independent experiments.

Further comparison of the response to the stimulation cells transduced with either CD84-H1 or Cd84-H2 **(Figure 3.31 D)** demonstrated statistically significant increase in response to R848 stimulation in HEK-BLUE cells transduced with CD84–H2. It is appeared that CD84 - H1 isoform has slight suppressing effect on the stimulation with TLR7 ligand **(Figure 3.31 D)**, since the response is lower than the response of cells transduced with empty vector. These results need to be interpreted with caution due to possible unequal amount of CD84 initially integrated into genome upon transduction.

Since lentivirus incorporated into the genome of cells of interest, cells became stably express the gene of interest. To perform more precious experiment the transduced

cells were sorted on GFP+ and RFP+ following gating strategy demonstrated in **Figure 3.32 A** and **B** respectively.

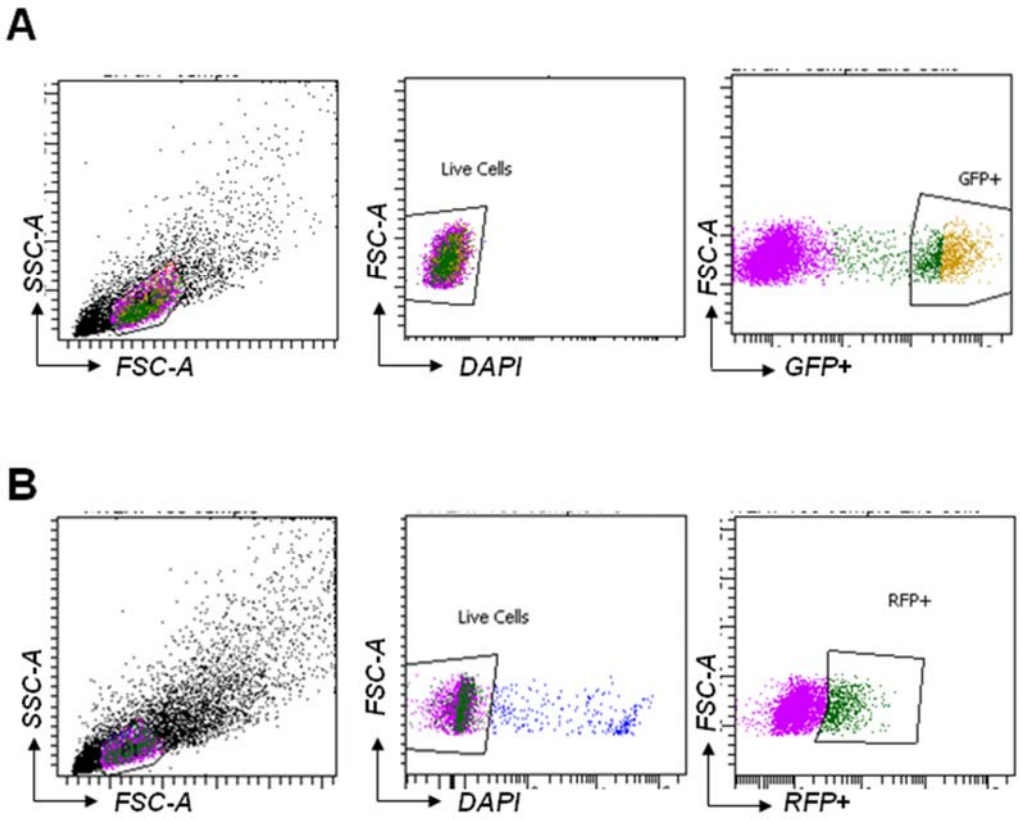

Figure 3.32 Sorting of transduced HEK-BLUE cells.
HEK-BLUE Null – 2K and mTLR7 cells (A) transduced with either CD84-H1, CD84-H2, or empty GFP lentivirus were sorted for GFP+ and GFP-, (B) transduced with Ly108 were sorted for RFP+ and RFP- .

3.4.5 Stimulation of sorted homogeneous GFP+ or RFP+ HEK-BLUE cells with R848

Our previous experiments showed that mTLR7 transduced with CD84-H2 enhanced the TLR7 response upon R848 stimulation **(Figure 3.31 D)**. To test further this finding, transduced cells were sorted and subsequent experiments were performed on only the homogeneous population of GFP+ or RFP+ cells.

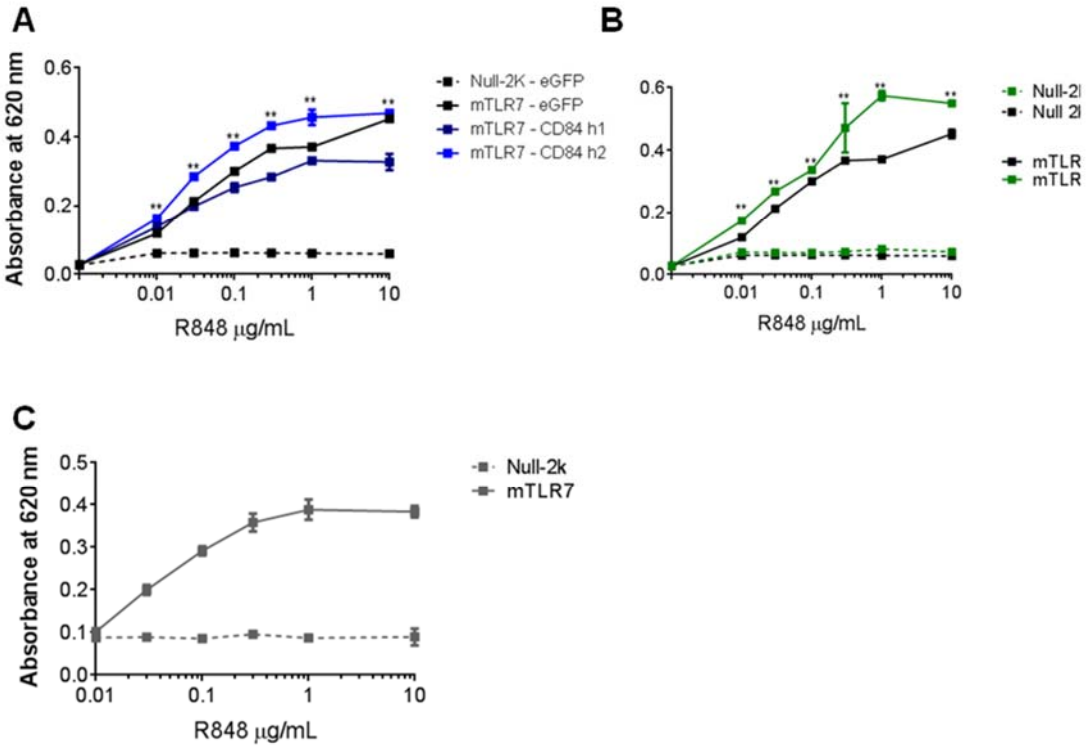

Figure 3.33 Post–sorting dose response to R848 stimulation of transduced HEK-BLUE cells.

(A) CD84-H1 versus CD84-H2 versus empty GFP. (B) Ly108+ versus empty GFP. (C) Control mTLR7 versus Null – 2k. Response time shortened to 12 h instead of 16 h. Statistical values were determined using an unpaired, nonparametric, Student's *t* test. Error bars represent mean ± SEM.*,*P* ≤ 0.05, **,*P* ≤ 0.01, ***,*P* ≤ 0.001, ****,*P* ≤ 0.0001. N=2, two independent experiments.

To validate our previous finding, sorted cells transduced with CD84-H1 or CD84-H2 or empty GFP were stimulated with different doses of R848 **(Figure 3.33 A)**. Concurrently, cells transduced with Ly108-H1, sorted based upon RFP positivity were also stimulated **(Figure 3.33 B)**. The sorted transduced with GFP only Null-2K and mTLR7 cells were used as a control **(Figure 3.33 A dotted line).** Since Null-2K transduced with either CD84-H1 or CD84-H2 or demonstrated similar no response as GFP only transduced NUll-2k **(Figure 3.31 D)** and sorting time is limited, only Null-2K cells transduced with GFP was used in further experiments. Untransduced, non-sorted mTLR7 and Null-2K was used as a control of TLR7 expression **(Figure 3.33 C)**, since manufacturer emphasize the importance of usage of cells in early passages.

Sorting of the transduced cells makes the population more homogeneous, hence neglecting the differences arised from not precise detection of virus titer or cell death. In

agreement with the previous data **(Figure 3.31)**, sorted cells carrying the CD84-H2 gene showed a higher response to stimulation with the TLR7 ligand compared to the cells transduced with the CD84-H1 vector or GFP alone **(Figure 3.33 A).** These results are in line with the initial hypothesis that the autoimmune prone haplotype of CD84 hyperactivates TLR7. Hyperactivation of TLR7 is a well-documented reason for SLE initiation (Celhar, Magalhaes et al. 2012).

Although sorting helps to make the population of cells homogeneous, however there is a possibility of a different copy numbers incorporated into the genome. Hence, in the next step we decided to sort the cells expressing high and low level of GFP and RFP.

3.4.6 SORTING OF HEK-BLUE CELLS FOR HIGH OR LOW LEVEL OF GFP OR FRP EXPRESSION

Subsequently we sought out to determine whether the responsiveness of transduced mTLR7 cells will depend on the amount of copy numbers of the gene incorporated into the genome. To test this, we performed an additional sorting of previously sorted GFP+ or RFP+ transduced cells into two populations expressing either low or high levels of RFP expression **(Figure 3.34 A)** or GFP **(Figure 3.34 B).**

The yield of cells after sorting was very low, hence some time was required for the cells to expand to the necessary amount to perform further analysis. After 20 days in culture with the selective antibiotics, the cells sorted for high or low expression of GFP were assessed for GFP expression by flow cytometry **(Figure 3.34C).**

The mTLR7 cells expressing low amount of RFP did not survive manipulations while sorted, hence only RFP expressing cells were used for further analysis. Meanwhile, Null-2K and mTLR7 transduced with GFP only and expressed high (bright green gate) and low (dark green gate) amount of GFP represents clear difference in GFP expression, even 20 days after the initial sorting. Murine TLR7 cells transduced with CD84-H1 or CD84-H2 also demonstrated two population expressing different level of GFP, however GFP signal was lower compared to cells transduced with GFP only, due to the reasons discussed above.

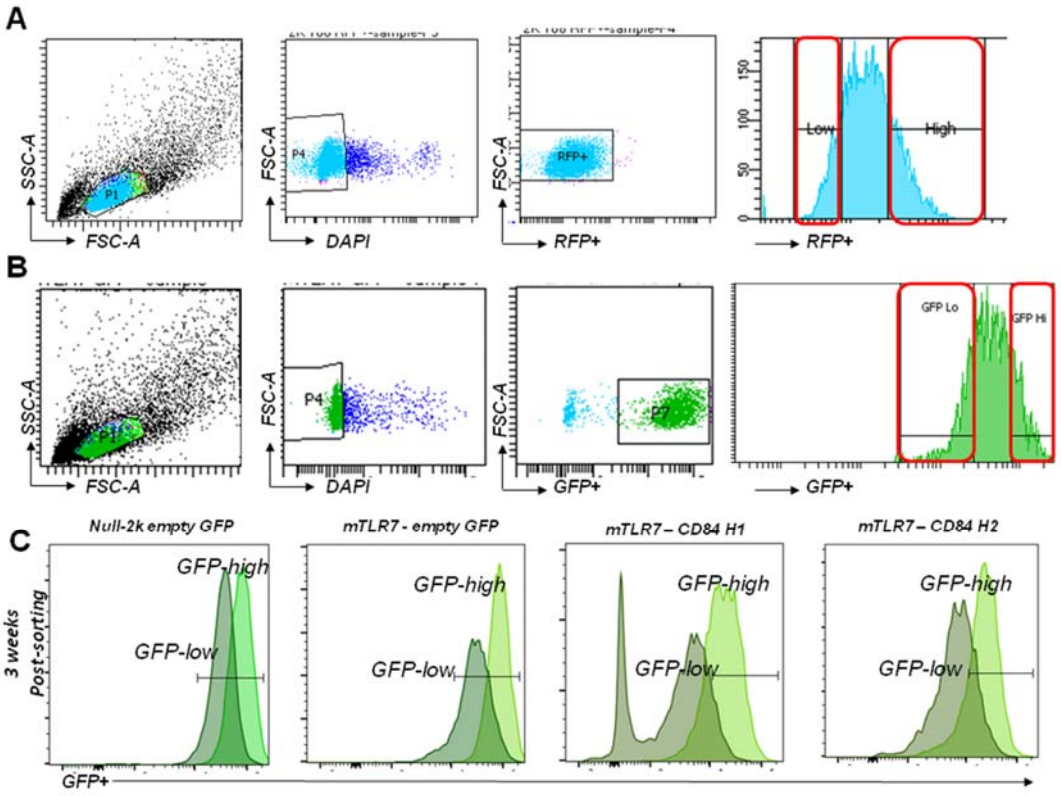

Figure 3.34 Sorting of GFP/RFP expressing cells.
Sorting strategy for collection of 2 different populations with different level of (A) GFP and (B) RFP expression. (C) Flow cytometry assay of the cells expressing different level of GFP after growing in culture for 20 days.

Also, within the cells transduced with CD84-H1 and expressing low level of GFP the negative population occurs. It might be due to initial contamination with GFP- cells while sorting or due to possible silencing of the gene, known for IRES vectors. An addition step was performed in order to quantify the CD84 expression within transduced cells and further investigate the interactions of CD84 and TLR7.

In the next step real-time PCR (qPCR) and flow cytometry was performed in order to quantify the expression level of the genes of interest (CD84). The expression of CD84 mRNA in the cells transduced with CD84-H1 and CD84-H2 and expressing high level of GFP was at equivalent levels **(Figure 3.35 A).** Whilst CD84 expression was almost two-fold lower for the cells transduced with CD84-H1 and expressed low GFP expression compared to CD84-H1 high GFP **(Figure 3.35 A).**

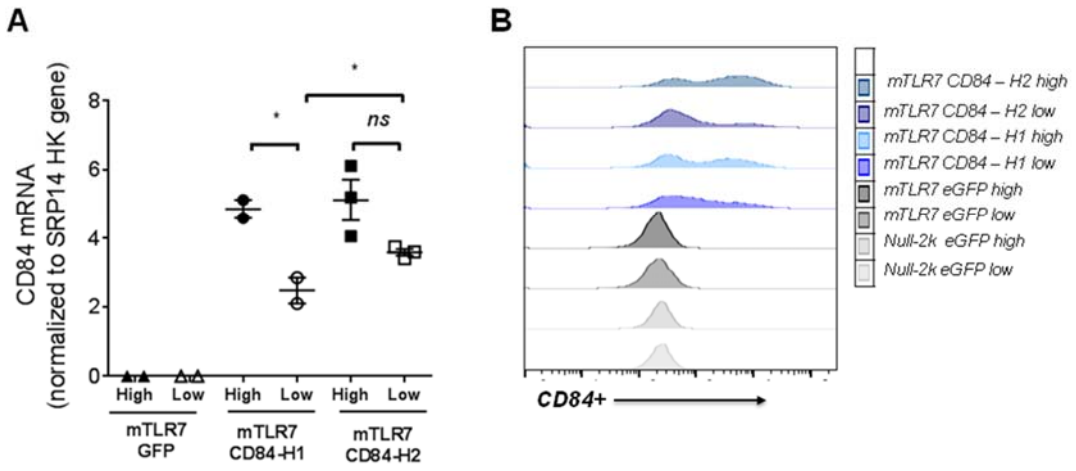

Figure 3.35 Amount of CD84 expressed by transduced mTLR7 cells.
(A) HEK-BLUE mTLR7 cells expressing high or low GFP were analyzed for genomic expression of CD84 gene, which were normalized to SPR14 house-keeping gene, done in triplicates. (B) Flow cytometric analysis of CD84 expression level (MFI) on lentivirally-transduced mTLR7 cells. Statistical values were determined using an unpaired, nonparametric, Student's *t* test. Error bars represent mean ± SEM.*,*P* ≤ 0.05, **,*P* ≤ 0.01, ***,*P* ≤ 0.001, ****,*P* ≤ 0.0001. N=2, two independent experiments.

The difference in copy numbers was not significant between the cells transduced with CD84-H2 expressing high and low GFP level. Surprisingly, the CD84 expression was significantly lower in CD84-H1 transduced cells compared to CD84-H2, possibly due to the presence of GFP- population within the cells, expressing lower GFP. To avoid this issue in future, the gate for GFP low expressing cells should be shifted towards brighter cells.

Flow cytometry staining with an anti-CD84 antibody confirmed the expression of CD84 only in transduced cells **(Figure 3.35 B)**. The CD84 expression level detected by flow correlated with the level of GFP expressed by the cells **(Figure 3.35 B)**.

3.4.7 STIMULATION OF HEK-BLUE CELLS EXPRESSING HIGH OR LOW LEVEL OF GFP

The initial goal of these experiments was to investigate possible interactions between the SLAMF members, CD84 and Ly108, and TLR7. Therefore, the above transduced and sorted cells were next stimulated with different concentrations of the TLR7 ligand, R848.

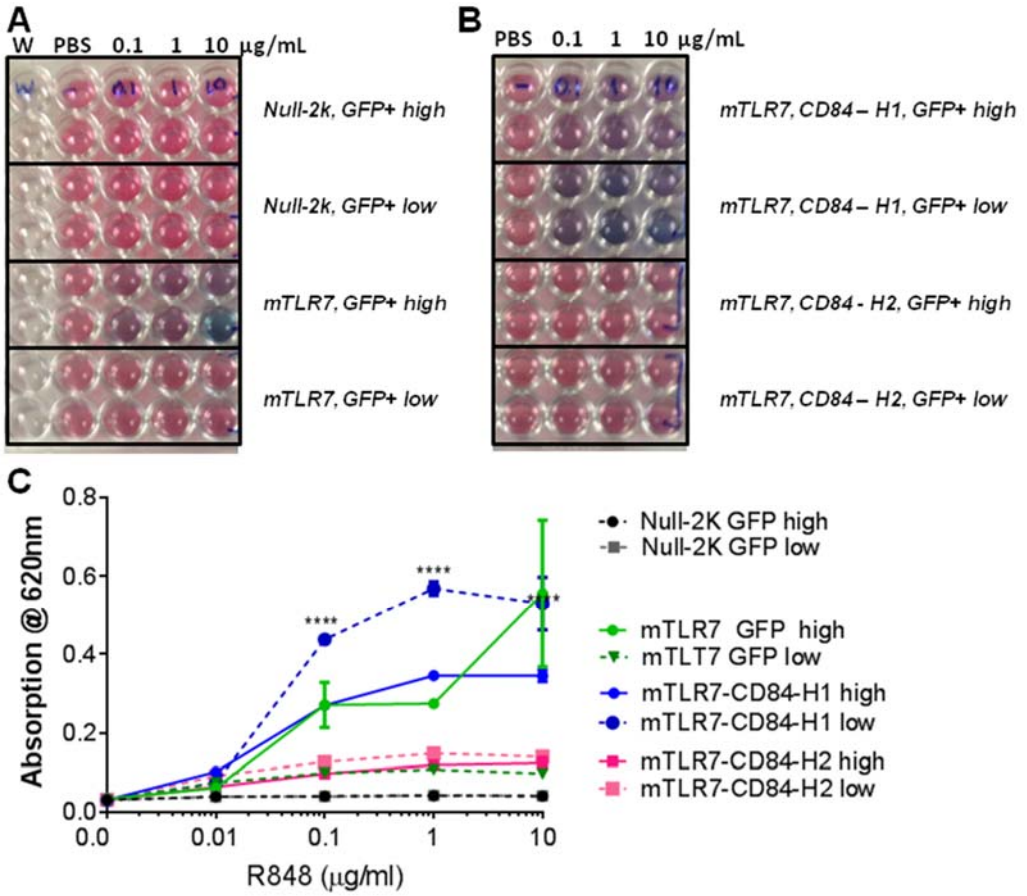

Figure 3.36 Dose dependent differences in CD84 haplotype function.
SEAP secretion detection by naked eye upon stimulation of different dose of R848 in (A) Null-2K and mTLR7 transduced with empty GFP and (B) mTLR7 transduced with CD84-H1 and CD84-H2. Statistical values were determined using an two-way ANOVA with repeated measurements. Error bars represent mean ± SEM.*,$P \leq 0.05$, **,$P \leq 0.01$, ***,$P \leq 0.001$, ****,$P \leq 0.0001$. The stars represent the comparison between CD84-H1 low versus CD84-H1 high and CD84-H1 high versus GFP-high. N=2, two independent experiments.

The dose of TLR7 ligand was chosen from the previous experiments **(Figure 3.31 A)**, which demonstrated the highest differences between CD84-H1 and CD84-H2. As predicted, Null-2K cells expressing either high or low levels of GFP did not respond to stimulation with R848, with the media maintaining its pink colour **(Figure 3.36 A)**. Control

murine TLR7 cells sorted for high GFP expression demonstrated a higher response rate to the stimulation as compared to the same cells expressing lower levels of GFP **(Figure 3.36 A).**

The media in the wells with the cells expressing low level of CD84-H1 turned to dark blue color indicating a very high activity of SEAP, which means high NF-kB activation. Although the color of the media in the cells with low level of CD84-H1 expression turned to a light purple, demonstrating NF-kB activation it was significantly lower **(Figure 3.36 B, C).** The media in murine TLR7 cells transduced with CD84-H2 and mTLR7-GFP low remains pink color even after 24 h of stimulation, showing that cells are no longer responding to the TLR7 stimulation **(Figure 3.36 B).**

The experiment was repeated 2 times demonstrating similar results, indicating the loose of response of mTLR7 – CD84-H2 and low expressing GFP TLR7-GFP to the stimulation with TLR7 ligand. A possible reason is the high number of passages cells has gone through, which resulted in loss of TLR7. The manufacture is not recommended to use the cells for the analysis after 15-20 passages, since stable transfection of TLR7 might be affected. By the last two experiment cells reach 16 passage, also counting many manipulations and sorting could affect the integrity of TLR7 plasmid and function. Since the major optimization has been performed, the experiment should be repeated with one sorting after transduction.

3.4.8 *IN VIVO* STUDY OF DIFFERENT CD84 HAPLOTYPES USING LENTIVIRUS APPROACH

It was hypothesized that CD84 haplotype 2 transduced stem cells will give rice to B cells producing ANA. However, using irradiation for chimera mice creation could affect ANA development due to effect of whole body irradiation on autoimmunity development (Kaminitz, Mizrahi et al. 2009). Previous studies have used successfully myeloblast transplantation after irradiation to cure autoimmunity in MRL/lpr or BXSB mice (Ikehara, Good et al. 1985).

Previous studies have demonstrated the influence of dose of irradiation on IgG production (Nossal and Pike 1975) demonstrated that naive B cells will develop tolerance rather than autoimmunity. After irradiation of the host, even auto-immune prone host, mostly cells will be HSC, containing pre-B. Hence, the dose used in the experiments for testing role of CD84 haplotype should be carefully chosen, in order to avoid the prevention of ANA development due to high dose of irradiation used. Since the recovery from radiation resembles the state of immunological immaturity resembling newborn, when it

is highly susceptible to tolerance induction (Ada, Nossal et al. 1965, Dresser and Mitchison 1968).

Although a very helpful tool for biological research, cell-lines have many limitations compared to direct *in vivo* investigations. Hence, in the next step we attempted to investigate the functional differences between two haplotypes of CD84 *in vivo.* Most of the *in vivo* experiments on the immune system require lethal or sublethal irradiation in order to replace it with the immune system of interest. However, it is known that irradiation prevents autoimmunity (Nossal and Pike 1975, Kaminitz, Mizrahi et al. 2009).

Since the initial hypothesis postulated that the haplotype 2 of CD84 provokes ANA secretion by B cells, it is important during tasting it in vivo, eliminate factors which alters a native condition of immune cells. In order to prevent the elimination effect of irradiation we sought out to titrate a dose of the irradiation, which will neglect the presence of the recipient immune system and allow the reconstitution to occur.

The irradiation titration was performed using two mice per group, forming 4 groups. Mice in the first group were not irradiated and received 150 ul of media during the mock injection. The mice from the second group received the dose of radiation equivalent to 1.5 Gy, the mice from the third group – 3 Gy, and the mice from the last group received 6 Gy. All doses were introduced within 2 days and were split by half for each day **(Figure 3.37 A)**.

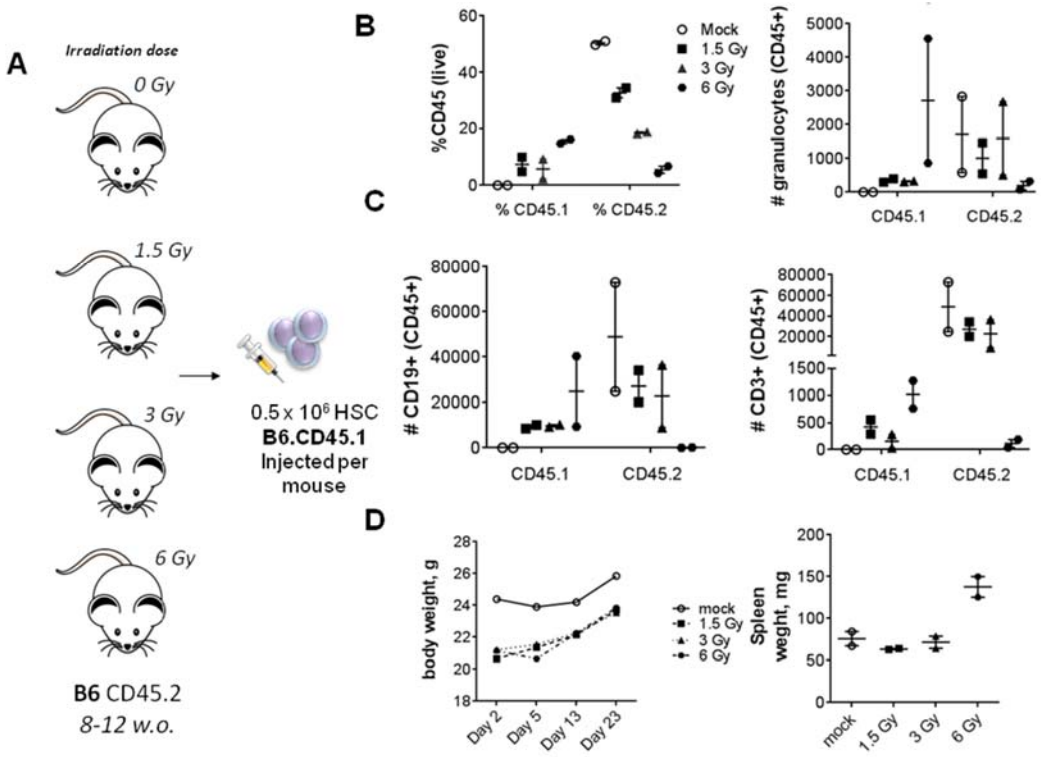

Figure 3.37 Optimization of chimerism and autoimmunity development after irradiation.

(A) Irradiation of mice with different dose in order to check reconstitution and cell activation. (B) Percentage of reconstituted cells 3 weeks post irradiation. (C) Activation status of injected cells versus host cells. (D) Mouse body weight and spleen weight.

Each recipient of B6 background received 0.5 x 10^6 HSC CD45.1 following irradiation **(Figure 3.37 A).** Based on work of Duran-Struuc (Duran-Struuck and Dysko 2009) which reported that full reconstitution occurs after 21 day after the injection of HSC, the day for phenotype investigation was set up in 22 days. The amount of CD45.2 cells gradually decreased with the increase of irradiation dose **(Figure 3.37 B)**. Hence, the amount of donor cells present in the spleen of irradiated mice increased with increasing radiatioin.

In the next step, the reconstitution of cells by cell type was assigned. Regardless of the cell type, either B, T cells or granulocytes, we determined that the best reconstitution was after the irradiation dose of 6 Gy **(Figure 3.37 B, C).** After 6Gy irradiation the amount of donor CD45.2 cells were very low, and the amount of CD45.1 cells were increased compared to the 3 and 1.5 Gy **(Figure 3.37 B, C).**

The activation of leukocytes also were assessed by CD69 expression. Cells from the recipient mice were more activated compared to injected HSC. Cells in mice receiving

3 and 6 Gy demonstrate higher CD69 expression, meaning slightly higher activation, however the difference did not reach statistical significance. In addition, the MFI of CD69 was assigned demonstrating higher values in donor cells injected in mice received 3 and 6 Gy (data not shown).

The weight is affected by radiation, hence this reading was measured flowing irradiation. No striking difference was reported except common weight loss by all irradiated animals regardless of dose of irradiation **(Figure 3.37 D)**. Also, the weight of spleen was obtained, as well did not show any statistical significance between the different radiation doses **(Figure 3.37 D)**.

3.4.9 OPTIMIZATION OF B CELLS LENTIVIRUS TRANSDUCTION FOLLOWED BY OVA-CHALLENGE IN MUMT MICE

Given the role of B cells in ANA production, we asked whether CD84 haplotype is a crucial element in losing tolerance to self. We sought out to test this in vivo using mouse model lacking mature B cells, B6. $Igh^{mtm1Cgn}$, (B6.mμMT). However, B cells are terminally differentiated cells hence very hard to transduce, to our knowledge there is only one successful work reported up to date (Warncke, Vogt et al. 2004). The protocol described in the study was implemented in our experiments.

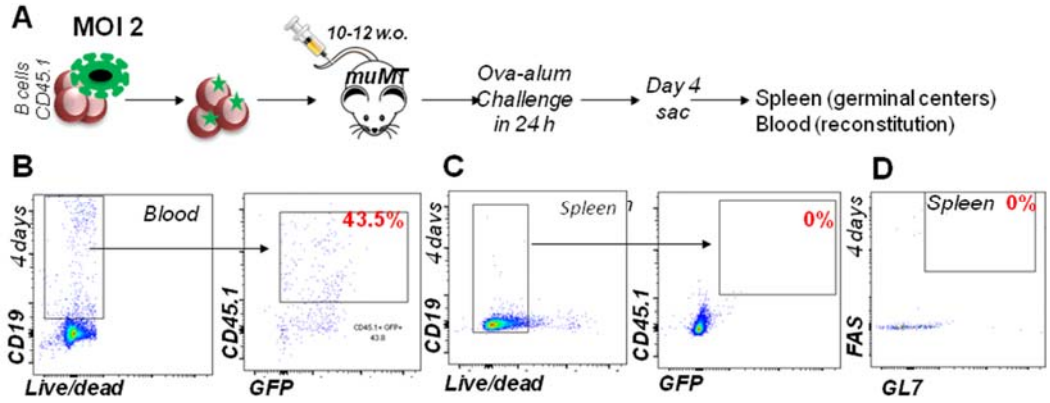

Figure 3.38 Optimization of lentivirus B cells transduction.
(A) Creation of B6.muMT B cells chimera mice. Reconstitution of muMT mice with B cells 5 days after transduced cells injection, 4 days after immune challenge in (B) spleen, (C) whole blood. (D) Activation of B cells at day 4 following alum-ova challenge.

In order to test the protocol and MOI of lentivirus optimal for B cells transduction the trail experiment was performed. B cells isolated from B6.CD45.1 mice were transduced with lentivirus expressing GFP only by applying 45 min centrifugation at 700 g. Subsequently, 24 h after transduced B cells were injected in sublethally (3 Gy) irradiated 10-12 w.o. B6.muMT female mice. In 24h after transduced B cells injection the mice were immunized with 10 ug OVA-Alum, and sacrificed 4 days later, in order to check B cells reconstitution, activation and formation of germinal centers in spleen **(Figure 3.38 A)**.

The complication we encountered was the lentivirus transduction of terminally differentiated B cells. After an overnight transduction, almost 60% were dead, the rest of the cells, 0.3-0.5 x 10^6 were injected. No B cells were detected in spleen 4 days after reconstitution **(Figure 3.35 B)**. However, slightly less than 50% of CD19+ cells in blood were GFP positive **(Figure 3.35 C)**, indicating probably longer time is required for homing of transduced B cells into spleen. Since no B cells were detected in spleen, no germinal centers or germinal centers B cells were detected in spleen of muMT mice **(Figure 3.38 D)**.

The data from this experiment indicated that in order to perform a successful transduction of B cells more optimization has to be done. The increased number of B cells as well as utilization of chemicals like polybrene polyethanolamine sulfate will result in better outcome.

3.4.10 Optimization of HSC lentivirus transduction followed by ova-challenge in muMT mice

In the next step, to investigate of the role of CD84 haplotype we used HSC transduced with lentivirus followed by subsequent injection into B6.muMT mice and OVA-alum challenge in 2 months. HSC are much easier to transduce and the protocol for HSC transduction is well established (Modlich, Navarro et al. 2009).

Murine HSC supplemented with cytokines and antibiotic were transduced overnight. The next day RFP or GFP expression was detected using fluorescent microscopy **(Figure 3.36 A, B respectively).**

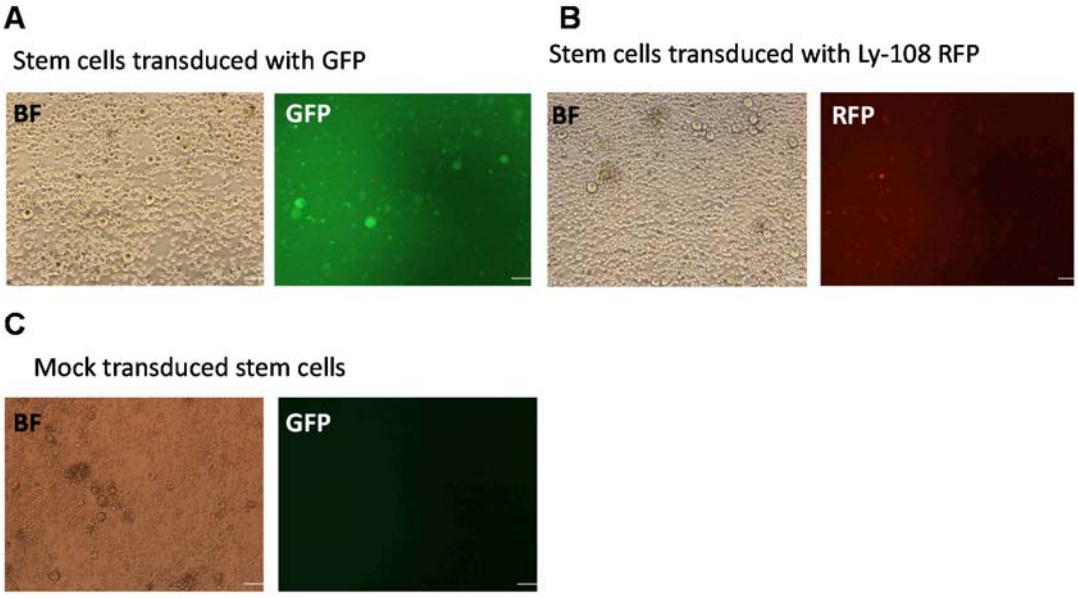

Figure 3.39 Stem cells transduction with lentivirus at MOI 1.
Murine HSC or transduced with (A) GFP and (A) Ly108 – RFP or (C) mock-transduced . *BF – bright field microscopy. Size bars 100 µm*

Mock transfected cells did not show any fluorescence **(Figure 3.39 C)**. The transduced cells were subsequently injected into lethally irradiated (6Gy) B6.muMT mice in order to optimize the MOI for stem cells and ova-alum challenge **(Figure 3.40 A)**.

The reconstitution at one month after the injections demonstrated 99% of B cells were CD45.1, however GFP expression indicating successful transduction was very low **(Figure 3.40 B)**, hence mice were left for another month before ova-alum challenge has to be performed. The reason why GFP expression was not detected in transduced cells is because of probability of silencing, which is known for IRES vectors, since GFP is a second protein expressing by the ORF. In this optimization experiment the lentivirus

expressing empty GFP was used, indicating that probably MOI of virus initially should be increased to MOI 5-10.

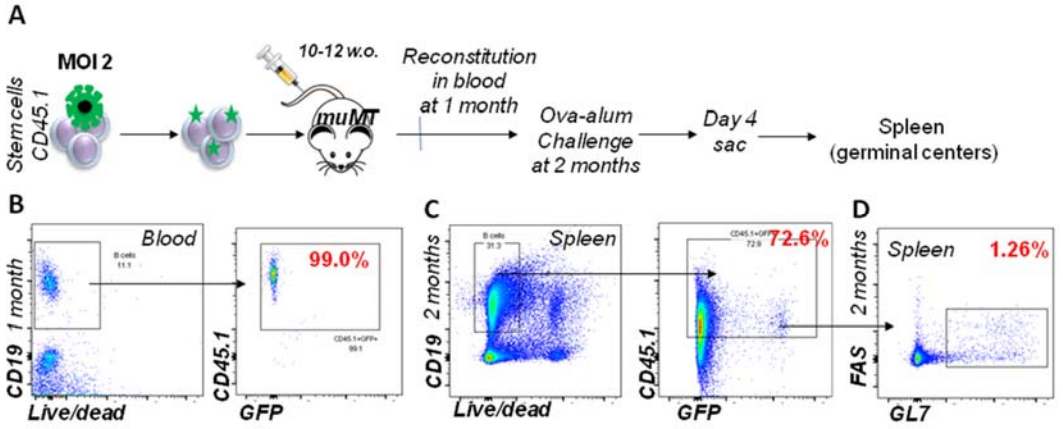

Figure 3.40 Optimization of lentivirus HSC transduction.
(A) Creation of B6.muMT bone marrow chimera mice. Reconstitution of muMT mice with HSC (B) 1 month after transduced cells injection in blood, (C) 2 months after injection in spleen. (D) Activation of B cells at day 4 following alum-ova challenge.

Four days before the intending day of the experiment mice were immunized with 10 ug ova-alum. In the next step reconstitution of B cells in spleen were monitored, demonstrating 72.6 % of CD19+ cells were CD45.1 and only very small population had GFP expression **(Figure 3.40 C)**, indicating MOI of virus should be increased and titrated for optimal results. Less than 2% of germinal centers B cells were detected following ova-alum challenge **(Figure 3.40 D)**.

Data obtained from two experiments above indicated that further optimization is required in order to perform in vivo experiment which will answer the question of the role of CD84 haplotype in ANA development. Meanwhile two experiment are proposed in order to answer the question.

3.4.11 PROPOSED *IN VIVO* EXPERIMENTS TO INVESTIGATE CD84 HAPLOTYPE DIFFERENCE

In the first proposed experiment, described in **Figure 3.41** we will examine whether B cells from B6.*Sle1* mice are more reactive to immune challenge with ova-alum. To answer the question B6.muMT bone marrow chimera mice will be injected with transduced HSC, consisting of 80% of muMT bone marrow and 20% of B6.*Sle1* mice HSC. Meanwhile, HSC will be transduced with CD84-H1 or CD84-H2 or GFP **(Figure 3.41**

A). After 2 months of the reconstitution ova-alum challenge will be done, and subsequently spleen and lymph node germinal centers formation will be analyzed **(Figure 3.41).**

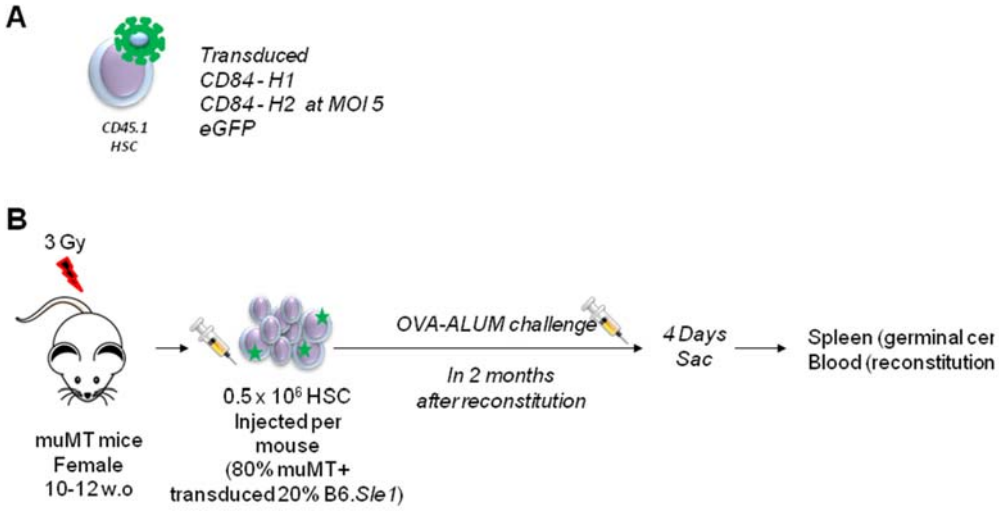

Figure 3.41 A proposed experiment to assess B cells activation difference in B6 and B6.*Sle1* mice.

(A) Transduction of HSC with genes of interest and a control. (B) Experiment outline.

Secondly, a long term experiment is planned, evaluating the role of the two CD84 haplotypes in ANA development. This will require B6.*Sle1* CD45.1 bone marrow HSC to be transduced with different haplotypes of CD84 or the control vector **(Figure 3.42 A)** and injected back in B6.*Sle1* mice **(Figure 3.42 B)**. Since, SLE onset and ANA development is a long process, the first ANA test will be performed in 2 months after the reconstitution, when mice are 4 month of age. The subsequent sera collection for ANA to be done at 7-9 months of age. The final experiment in which ANAs, splenomegaly and germinal centers formation will be tested will be performed at approximate age of 9-12 months.

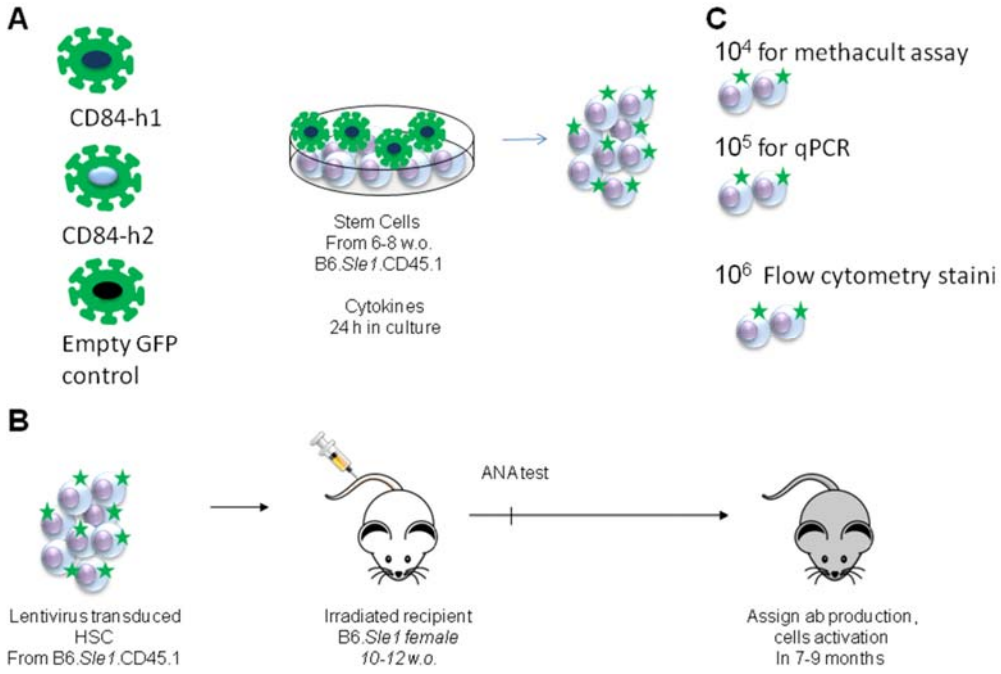

Figure 3.42 Plan of in vivo investigation of CD84 haplotype influence on auto-antibodies development.

(A) Transduction of HSC with genes of interest and a control. (B) Experiment outline. (C) Methods of monitoring the amount of gene expressing by transduced cells.

A very careful control should be done on the amount of CD84 gene expressed by the cells after transduction, to avoid the effect of excessive amount of expression. The methacult assay, real-time PCR as well as flow cytometry should be used to check the amount of CD84 expressed by the cells **(Figure 3.42)**.

Summary of CD84 haplotype investigation

A nonsynonymous mutation, which resulted in a single amino acid alteration at position 27 was identified in DNA and RNA of B6.*Sle1* mice, confirming the difference between haplotype 1 and haplotype 2 of CD84. The second nonsynonymous mutation, resulted in single amino acid change at position 293 was reported in DNA, however was not detected by RNA sequencing.

To test the functional differences of 2 different haplotypes of CD84 series in vitro experiments using HEK-BLUE cell line were performed. Preliminary data reporting increased TLR7 activation upon the presence of CD84 haplotype 2, and slight suppression of the activation upon the presence of CD84 haplotype 1. However, further studies have to be done to validate current statements.

In the series of in vivo experiments, we attempted to optimize terminally differentiated cells lentivirus transduction, in order to study role of CD84 in antibody transduction. However more extensive optimization has to be performed before initiation of the experiments.

4 DISCUSSION

There is emerging evidence suggesting that adaptive immune cell dysfunction, together with defects in innate immunity, are critical in the initiation and progression of SLE. Over the years, research has focused on the importance of B cells in driving pathogenesis with more recent trends investigating innate cells, including DCs (Ganguly, Haak et al. 2013), macrophages (Orme and Mohan 2012) and PMNs (Garcia-Romo, Caielli et al. 2011, Kaplan 2013). In particular, accumulating evidence suggests that innate pathogen recognition receptors, such as TLRs, ALRs and NLRs play an important role.

Data from murine models has shown that SLAMF polymorphisms contribute to adaptive immune dysfunction, resulting in loss of tolerance to self. In fact, the murine genetic region encompassing this family of receptors has been associated with the development of SLE in the majority of known lupus prone strains reviewed in (Celhar, Magalhaes et al. 2012). On the B6 non-autoimmune background, this NZW-derived *Sle1* lupus susceptibility region confers various polymorphisms including a polymorphism within murine SLAMF members – referred to as haplotype 2. This results in B and T cell activation and the development of ANAs.

Several other groups recently reported that intrinsic inactivation of IFN-ɣ production by B cells due to the impaired signaling through T-bet or BCL-6 transcription factors ceases ANA development (Domeier, Chodisetti et al. 2016, Jackson, Jacobs et al. 2016). A further question will be about the regulation of the IFN-ɣ production system, which in healthy individuals is present and do not lead to the production of ANA. Although, one more study from Lee (Lee, Silva et al. 2012) postulated that IFN-ɣ dependent ANA production occurs because of accumulation of Tfh cells and the subsequent formation of germinal centers, one more time highlighting the importance of the regulation of this system.

Since humoral immunity is dependent on B-T cell interactions we were looking for the genes within the *Sle1* region which could impair the normal function of T and B cells, leading eventually to germinal center formation and ANA secretion. The most prominent candidates were SLAMF members, which are highly polymorphic (up to 5 isoforms per member) and participate as co-receptors within B-T cell interactions. An elegant work of Wong and colleagues shed light on the importance of polymorphisms in two particular SLAMF members, Ly108 and CD84, which resulted in pathology (Wong, Soni et al. 2015). The authors replaced haplotype 2 genes of the *Sle1* locus with a BAC carrying CD84-Ly108 haplotype 1, which resulted in ANA suppression to the same level as in B6 mice. Further research has shown that B6 mice express a third isoform of Ly108, Ly108-H1, which suppresses autoimmunity (Keszei, Detre et al. 2011). However, the BAC carrying

only Ly108 (haplotype1) did not show such a decrease in ANA production as the BAC carrying both Ly108 and CD84 of haplotype 1 (Wong, Soni et al. 2015).

CD84 became a candidate molecule following a focused study of association of SLAMF genes with autoimmunity, where CD84 sequence differences were identified in autoimmune-prone mice (Wang, Batteux et al. 2010). However, the functional role of CD84 in mechanisms of ANA development has yet to be established. Hence, we initiated phenotypical and functional studies of murine CD84 using B6 and B6.*Sle1* mice.

Previous reports have shown differences in surface CD84 expression across different types of immune cells (Zaiss, Hirtreiter et al. 2003, Romero, Benitez et al. 2004). However, most data has been focused on CD84 in B and T cells (Tangye, van de Weerdt et al. 2002, Yan, Malashkevich et al. 2007, Cannons, Qi et al. 2010, Ding, Liang et al. 2012). A broader leukocyte examination or an investigation into expression and function in the context of autoimmunity are lacking.

Initially we examined the expression of CD84 across different cell types within the spleen and kidneys of aged 6-month old mice. At this age, the B6.*Sle1* mice display a phenotype of benign autoimmunity characterized by mild splenomegaly, B and T cell activation and the production of ANAs. CD84 expression was higher on B cells from B6.*Sle1* mice, irrespective of the tissue examined, while in PMNs the expression levels were lower. Our initial hypothesis was that this upregulation within the lymphoid population was most likely due to disease. The data from Wong (Wong, Soni et al. 2015) reported no difference in CD84 expression between aged B6 and B6.*Sle1* mice, however they analysed 8 month old mice, indicating a possible involvement of CD84 in germinal centre formation.

B6.*Sle1* female mice develop benign autoimmune phenotypes at around 6-9 months of age. It is characterized by elevated ANA levels, severe kidney disease, activated T and B cells and mild splenomegaly. However, little is known about SLAMF member expression, including CD84, in young and aged B6.*Sle1* mice. Previous reports suggested that CD84 is a maturation marker (Tangye, van de Weerdt et al. 2002).

One hypothesis is that CD84 increases cell-to-cell communication and activation, stimulating cellular hyperactivation and driving autoimmunity. We addressed this hypothesis initially by evaluating CD84 expression in older B6.*Sle1* mice with detectable autoimmune traits (Figure 3.1), and young mice which had minimal evidence of autoimmunity (Figure 3.2). The increased of CD84 was reported only on B cells, however the other leukocytes had similar CD84 expression (Figure 3.1A). Therefore, we went on to examine whether the difference in CD84 expression was due to disease progression

and evaluate CD84 expression in young mice, before autoimmunity symptoms onset (Figure 3.2).

We reported increase in CD84 expression in multiple immune cell types (Figure 3.2A), which suggested that the presence of *sle1* gene is affected increased CD84 expression rather than increased expression is a consequence of phenotype development.

Analysis of CD84 expression of different b cells subsets presented here demonstrated that overall difference in CD84 expression on B cells derives from certain subpopulations of B cells, suggesting that *sle1* gene may only affects subpopulation of B cells at different stages of differentiation. Further study to investigate the expression level of *sle1* genes mRNA in different B cell populations may shed light into its role during B cell development. Similarly to B cell CD84 expression, only certain subsets of T cells demonstrated upregulation in CD84, therefore it is tempting to speculate of these populations as pathology drivers.

The other cells, could drive autoimmune pathology are macrophages (MF) from the renal biopsies of lupus-prone mice, which demonstrated mixed phenotype expressing markers for both M1 and M2 populations (Sahu, Bethunaickan et al. 2014). A shift towards inflammatory macrophages (MF) M1 population has been proposed as one of the factor of increased inflammation in SLE (Anders and Ryu 2011, Orme and Mohan 2012) and we hypothesize that it could potentially lead to increase in CD84 expression in macrophages from B6.*Sle1* mice, however further study are required to test this hypothesis. Since murine MF are known to drive kidney pathology, it will be interesting to determine the expression of CD84 on kidney MF, and to quantify the level M1/M2 MF in B6 versus B6.*Sle1* mice.

The highest difference in CD84 expression between control and B6.*Sle1* lupus prone mice was observed in blood PMNs. These short lived innate cells are the first responders at the site of injury or infection. Their dysfunction in SLE is widely described, with current hypotheses suggesting that they contribute the self-ligand important for autoreactive B and T cell activation (Kaplan 2013). Our future studies will continue to examine the role of CD84 in this cell type.

Taken together, our results so far show that autoimmune prone mice express higher levels of CD84 protein in blood leukocytes Furthermore, CD84 expression is increased on B cells of aged mice.

In conclusion, increase in expression of CD84 on leukocytes of B6.Sle1 mice are likely derived from certain subpopulations of immune cells such as memory CD27+ B cells, or central memory T cells. Determining the function of CD84 in these specific cell

subpopulations and demonstrate how that could contribute to the development of SLE should be the focus of the future work. Functional studies are required to determine the significance of these findings.

4.1 Functional studies of CD84 in B cells and neutrophils

Few studies have investigated the functional role of CD84 in the immune system, and have addressed its function in autoimmunity. A report from Sintes and colleagues demonstrated a role for CD84 in the modulation of TLR4-induced activation of a macrophage cell line (Sintes, Romero et al. 2010).

Based on this work and our findings of altered expression in disease, we investigated whether CD84 expression could be modulated by TLR stimulation. TLR7 and TLR9 are known to be important in the progression of disease (reviewed in (Celhar, Magalhaes et al. 2012). We examined B cells and PMNs since these leukocytes express TLR4, TLR7 and TLR9 and have been recently been implicated in SLE disease progression. Our experiments show that CD84 expression is unaffected by over-night TLR ligation on splenic B cells, despite the cells being activated (Figure 3.8-10 A-D). Additionally, longer incubation with TLR ligands, which induce B cell proliferation, failed to alter CD84 expression (Figure 3.8-10 E-G).

Stimulation of splenic B cells with TLR ligands demonstrated slight decrease in CD84 (Figure 3.8-3.10), compared to results obtained by Cannons (Cannons, Qi et al. 2010), where the stimulation was performed on B220+CD43+ purified pro-B cells, the majority of these cells are derived from bone marrow, suggesting they are at development stage (Allende, Tuymetova et al. 2010). Furthermore, CD84 is a potential maturation marker, plausibly CD43+ B cells increased CD84 upon stimulation, resembling maturation process. In our experiment whole splenocytes, fully differentiated cells, were used and number of cells per well were carefully titrated (Figure 3.6.) to show optimal proliferation and activation.

In addition, in work by Cannons the concentration of LPS is not stated, making the comparison between our experiments difficult. One of the other possible explanations of decreased CD84 expression due to either loss of CD84 upon activation of B cells or due to engagement in homophilic interactions with other splenocytes, which is reported previously by Martin and colleagues (Martin, Romero et al. 2001, Deenick and Ma 2011).

Since a characteristic feature of SLE is ANA production by B cells, we evaluated TLR stimulated release of Ab production by B cells *in vitro* (Figure 3.11). CD84 might be responsible for pathological class switch, hence ELISA for ab subtypes was performed.

In these experiments, we did detect all IgG Ab subtypes. A possible explanation can be because stimulation with either of TLRs ligands, 4, 7 or 9, does not lead to pathological class switching. Alternatively, it may be due to the young age of the mice, and that these changes occur later in disease development. Alternatively, our assay may not be sensitive enough to detect changes in antibody production. Further studies would include the utilization of an ELISPOT to assess IgG production on a per cell basis.

Work from Mittereder and colleagues suggested that pathological Ab switches occur in the GC of B6.*Sle1* mice due to ICOS, which is expressed on GC T cells (Mittereder, Kuta et al. 2016). Therefore, further work should investigate the expression of CD84 on T cells and its effects on B-T cell coupling and activation.

CD84 blocking on B cells

One of the key characteristics of SLAMF members is that they are homotypic receptors, binding themselves for the activation of a signalling cascade. Limited data from Tangye *et al* is available about B cell stimulation using an anti-CD84 Ab (Tangye, van de Weerdt et al. 2002). They reported activation and proliferation upon CD84 ligation only for activated naïve B cells. This data, together with studies on the expression of CD84 in developmental stages of the cells, suggests that CD84 is upregulated with B cell maturity.

In contrast to Tangye and colleagues, we observed a downregulation of CD84 on naïve B cells following 24hr stimulation with anti-CD84 (Figure 3.12). In our experiments we used mouse primary immune cells, however Tangye and colleagues performed their experiments either on human primary immune cells or cell-lines derived from human cells. These contradictory results could arise from fundamental differences in mouse and human biology, as well as differences between metabolism rates in primary cells and cell-lines.

We assessed whether blocking CD84 with either anti-CD84 antibodies or rCD84 protein would influence the TLR-induced activation of B cells (Figure 3.13). In a similar manner to the inhibitory antibody, the recombinant protein prevented detection by a fluorescently conjugated antibody, demonstrating effective binding. Despite this, we did not detect any change in TLR-induced stimulation of B cells.

Our data are in contrast to investigations of CD84 homophilic interactions by Oliver-Vila and colleagues using the human basophilic leukemia cell line RBL-2H3 (Oliver-Vila, Saborit-Villarroya et al. 2008). In their report, they demonstrated functional changes in the form of decreased degranulation by eosinophils and basophils in response to CD84 homo-interactions. It may be that homotypic interactions are important in other functions that we did not assess, including cell-to cell interactions with other leukocytes (B-T cell

interactions). Additionally, it may be that CD84 - CD84 homophilic interactions are cell-type specific.

Additionally, CD84 might affect pathology through preventing apoptosis, since impaired clearance of apoptotic debris has been implied in the initial stages of SLE (Munoz, Lauber et al. 2010). Wong and colleagues reported decreased B cell apoptosis levels in B6.*Sle1* mice compared to B6 upon stimulation with IgM/CD40 (Wong, Soni et al. 2015). We observed a decrease in B-cell CD84 expression with every next stage of apoptosis (Figure 3.14), as expected since cells usually lose surface receptors upon apoptosis.

An increase in the number of early apoptotic neutrophils was detected in B6.*Sle1* mice (Figure 3.17), suggesting that an excessive amount of early apoptotic cells might eventually provide self-debris for the antigen presenting cells and stimulating pathology development in these mice. Similar to B cells, the neutrophils were losing CD84 surface expression with every further stage of apoptosis regardless of murine strain (Figure 3.18). However, in contrast to Wong et al, stimulation with TLR ligands resulted in similar levels of early and late apoptotic and necrotic B cells in both strains (Figure 3.15). It may be that utilization of caspase detection as a marker of apoptosis used by Wong et al. is a more sensitive method, compared to staining with Annexin V and PI used in our experiments.

CD84 on neutrophils

We have shown that B6.*Sle1* neutrophils bind 30% more platelets than B6 neutrophils; however a physiological role of this binding is not yet clear. We showed the presence of CD41+CD84+ conjugates in mouse blood (Ly6G+), demonstrating that platelet-neutrophil conjugates exist preferentially with CD84+ neutrophils. The percentage of these conjugates was significantly higher in the blood of lupus-prone B6.*Sle1* mice compared to control B6 mice.

Limited data is available about platelet-neutrophil interactions through SLAMF members, especially in the context of SLE. However, activated neutrophils might represent the main source of auto-antigens in the blood of SLE patients (Garcia-Romo, Caielli et al. 2011) Thus it is tempting to speculate that neutrophils may be activated by platelet binding. Functional assays are needed to confirm the role of CD41+CD84+ conjugates in inflammation and pathogenesis of SLE.

CD84 is a homotypic receptor, thus easily interacting with CD84 on other immune cells (Martin, Romero et al. 2001). Increased binding of platelets to PMNs activates PMNs leading to pro-inflammatory cytokines release and NETs formation (Sreeramkumar, Adrover et al. 2014), CD84 might participate in binding. Furthermore NETs could be a

double-sword of innate immunity: provide self-antigens upon DNA release, and forcing cardiovascular complications (Pieterse and van der Vlag 2014).

Activated platelets are known to initiate and develop thrombosis, leading to complications and death (Meikle, Kelly et al. 2016). Furthermore, SLE patients are prone to vascular damage even before the cardiovascular disease onset occurring due to excessive cytokines expression, NETs formation, autoantibody formation, immune complexes deposition, etc. (Mak and Kow 2014). Cardiovascular disease is a major co-morbidity of SLE (Manzi, Meilahn et al. 1997). The increased binding of platelets to PMNs through CD84 may shed a light for initiation and triggers of this pathology.

An interesting study could be performed using platelets depletion with antibody to see whether it will affect functional activity of PMNs from B6.*Sle1* mice. This will allow to further speculate whether platelets binding to PMNs through CD84 in human give rise to cardiovascular pathologies in human SLE patients. Moreover, an experiment where platelets binding to PMNs will be blocked using anti-CD84 or anti-P-selecting antibodies, may give answer for the role of CD84 in NETosis.

Clark and colleagues reported that platelets activate neutrophils in the periphery following TLR4 ligation, driving the formation of platelet-neutrophil conjugates and NET formation (Clark, Ma et al. 2007). Therefore, we sought to compare NETosis levels between B6 and B6.*Sle1* mice, however we faced the problem of lacking a reliable and robust method for NETs detection and quantification.

4.2 A development and optimisation of a method for NETosis quantification using flow cytometry

Therefore, we have developed, tested and validated a novel rapid and robust method for NETs identification using flow cytometry. We used an anti-CD66 antibody together with two nucleic acid binding-dyes, namely SytoxOrange and DAPI, to quantify NETs released by neutrophils following stimulation. This method is fast and more sensitive than existing protocols, enabling the evaluation of NETosis in large sample sizes with lower concentrations of PMA at earlier time points. Furthermore, this method minimizes user bias which can occur in microscopy.

Our approach uses DNA dyes which are non-fluorescent until they bind DNA, therefore reducing washing steps. This is important, since the NETs formed are fragile and can easily degrade following cellular manipulation or increased incubation time. By detecting extracellular DNA with cell impermeable dyes, we also minimized non-specific detection of apoptosis. Using our novel assay, we observed between 10-30% detectable NETs in untreated samples. This is at the similar level as has been previously described in salivary unstimulated neutrophils where 20-30% of NETosis was observed (Mohanty, Sjogren et al. 2015). In these studies Mohanty and colleagues quantified NETosis following microscopy. The majority of other studies have utilised plate based protocols to quantify free NET formation (Garcia-Romo, Caielli et al. 2011, Lande, Ganguly et al. 2011, Demers, Krause et al. 2012, Barrientos, Marin-Esteban et al. 2013, Dieker, Tel et al. 2016).

We also attempted a flow cytometry protocol from a previous report (Gavillet, Martinod et al. 2015). However, in concordance with another laboratory, we found limitations in this method in terms of sample throughput and reproducibility (Manda-Handzlik, Ciepiela et al. 2016). We adopted several strategies to enhance the reliability, sensitivity and reproducibility of the NETosis detection protocol, including the use of 96-well plates to decrease incubation time prior to stimulation. Furthermore, we decreased centrifugation speed in an attempt to maintain NET attachment to neutrophils. Careful and precise implementation of the developed gating strategy also eliminated the potential for false inclusion of debris.

A representative experiment performed by using the newly developed flow cytometry based assay for NETosis showed an increase in NETs formation in B6.*Sle1* compared to B6 control. NETs were also detected on neutrophils upon stimulation with a

TLR7 ligand; more experiments should be performed to confirm the role of TLR7 in NETs formation and possibly initiation of the disease.

Among different immune cell types, CD84 is highly expressed on platelets (Nanda, Andre et al. 2005) and it is known to be a homophilic receptor (Martin, Romero et al. 2001). Platelets are well known to interact with leukocytes in blood, particularly with neutrophils (Nagasawa, Matsuno et al. 2013). An excessive interaction between platelets and PMNs leads to spontaneous PMNs activation, further resulting in IFN-alpha secretion (Lindau, Mussard et al. 2014).

These happens via activation of signaling pathways leading to NETosis and eventually releasing DNA in the blood (Carestia, Kaufman et al. 2016). The available nuclear material that is picked up by dendritic cells, provokes IFN-alpha expression and leads to antigen presentation following by immune response to its own DNA (Garcia-Romo et al., 2011; Lande et al., 2011; Villanueva et al., 2011 Banchereau and Pascual, 2006; Elkon and Stone, 2011). Therefore, we hypothesize that increased expression of CD84 might prolong platelet interactions with PMNs starting the cascade of the reactions resulting in pathology.

4.3 CD84 haplotype study

The observed differences in CD84 expression and function in B cells and neutrophils, did not provide any evidence for CD84 being crucial for ANA production by B6.*Sle1* B cells. Since CD84 knockout mice do not develop germinal centers and humoral immunity, we hypothesized that B6.*Sle1* mice develop ANAs due to a polymorphism in CD84. Hence, we investigated the difference of the *cd84* genomic sequence between B6 and B6.*Sle1* mice.

We have identified a nonsynonymous mutation in B6.*Sle1* mice leading to the change of the amino acid valine to methionine at the N-terminal end of CD84 molecule, at the position 27. This mutation might result in alterations of the binding properties of the CD84 molecule, since it is a homotypic receptor. Another mutation was identified in the intracellular part of CD84 next to the ITSM (intracellular phosphorilation site) motif, which might influence downstream CD84 signaling. The mutation at the position 27 was confirmed at the RNA level,

Comparison of total RNA from splenic B cells of young B6 and B6.*Sle1* mice revealed a significant increase in CD84 mRNA expression in B6.*Sle1* mice. However, our

subsequent studies on splenic B cell protein expression did not reveal any difference. This may be because gene expression does not always correlate with protein levels.

Polymorphisms in SLAMF members are associated with different haplotypes and these might confer the loss of tolerance to chromatin. It is important to know which isoforms of CD84 could potentially be associated with the autoimmune prone strain, if any. Analysis of isoform usage identified almost twice the level of each of the five reported isoforms, with isoform 3 showing the greatest increase in B6.*Sle1* B cells compared to the B6 control (Figure 3.23). The alterations in CD84 isoforms affect the intracellular segment of the molecule, resulting in changes to the intracellular signaling (Morra, Lu et al. 2001, Tangye, Nichols et al. 2003). Our data did not reveal any striking difference in CD84 isoform usage between the two strains, aside from the overall increase in total expression.

A previous study utilizing a BAC strategy demonstrated that haplotype 1 of CD84 and Ly108, expressed in B6 mice, decreased ANA production (Wong, Soni et al. 2015). In order to address the role of CD84 we used a lentivirus approach to perform initial *in vitro* experiments and optimization.

B cells of B6.*Sle1* mice showed less activation upon stimulation with TLR ligands, however multiple studies have suggested a role of TLR7 (Soni, Wong et al. 2014) in ANA production. B6.Sle1.Tg7 mice carrying *Sle1* locus together with additional copies of TLR7 demonstrated aggressive fatal disease (Hwang, Lee et al. 2012), likely due to interactions of genes within S*le1* locus and TLR7 signaling. To understand the proposed interactions of TLR7 with different haplotypes of CD84 we used an engineered HEK-BLUE cell line, expressing TLR7, which allows fast detection of NF-kB dependent activation of TLR7 upon the stimulation with TLR7 ligands. CD84 haplotype 1 or CD84 haplotype 2 was introduced into the genome of this cell line using lentiviral transduction and subsequently cells were stimulated with R848, a TLR7 ligand, in order to study the possible interactions between TLR7 and CD84.

Preliminary data from the experiments utilizing the above model demonstrated suppression of TLR7 signaling by CD84-H1 compared to an empty GFP control; at the same time, CD84-H2 accelerated the response of TLR7 to the stimulation. Conceivably, due to these plausible interactions the B6.*Sle1*.Tg7 mice exhibit severe pathology. A report from Sintes and colleagues (Sintes, Romero et al. 2010) revealed the interactions between CD84 and TLR4, hence it is possible that interactions between CD84 and other TLRs also exist. The system to investigate an interaction of CD84 and TLR7 was developed and optimized, however further studies are required to prove the hypothesis.

The aim of any research is eventually a treatment or prevention of diseases. An extensive investigation of murine CD84 aims to discover new potential therapeutic target

or diagnostic marker. Hence, findings described in this thesis, both phenotypic and functional are of a potential benefit for SLE treatment.

The current literature suggests that CD84 is important in B-T cells interactions, during antibody production by adoptive immune system (Cannons, Qi et al. 2010). Hence CD84 is potentially a key molecule involved in ANA production during SLE. In order to test CD84 as a potential drug target to prevent ANA formation, blocking of CD84 on either B or T cells should be conducted in our mouse model. CD84 might be the main regulatory switch of immune cells, i.e. overexpression of CD84 haplotype 1 might prevent ANA development (Wong, Soni et al. 2015). The lenti-virus approach and bone marrow chimera technique could be used to confirm this hypothesis. The results would be for potential used for a diagnostic biomarker and a targetable drug development aimed at CD84.

Summary

In summary, we have shown that CD84 expression is increased in autoimmune-prone mice at both the RNA and protein level, however it is tissue and cell type specific. CD84 from B6.*Sle1* has sequence alterations at amino-acid position 27, which possibly affects the function of the molecule. A lower activation of B cells as a response to TLR ligand stimulation from autoimmune mice could predict their slow reactivity hence the possibility to avoid clearance during the tolerance checkpoints.

The optimisation of a new method of NETosis evaluation has taken a significant step towards developing a valuable innovative and robust approach for NETs detection. There is burgeoning data on the role of NETs across multiple diseases; therefore a simple, robust and comparable tool for examining NETosis will be beneficial in many fields from basic science to medicine.

An attempt to investigate interactions of TLR7 and CD84 could reveal a new mechanism of interactions between these molecules, as well as a possible mechanism of the influence of a single amino-acid change in the development of pathology.

5 CONCLUSIONS

Taken together, the findings of this study reinforce and highlight the importance of CD84 haplotypes in ANA secretion, which further leads to SLE development. The nonsynonymous mutation identified in CD84 expressed by autoimmune-prone mice demonstrates the fundamental differences in CD84 from B6 and B6.*Sle1* mice, suggesting a possible reason why B6.*Sle1* develops ANAs. Our preliminary *in vitro* data suggests evidence of an interaction of CD84 with TLR7. However, further *in vivo* studies are required to confirm these interactions, as well as to elucidate their functional outcome.

CD84 is a homotypic receptor involved in B-T cells interactions upon germinal centres formation. Hence, we performed an investigation of the functional role of CD84 on B cells, which pointed to the fact that increased CD84 expression alone on autoimmune-prone mice is not sufficient to activate the cells and drive them to pathological disease. Meanwhile, increased CD84 expression on neutrophils from autoimmune-prone mice showed 30% increased of platelets binding.

To study further CD84 function in neutrophils, since there are not much data available, we have also devised a methodology for the detection, assessment and quantification of NETs formation. This simple, fast and robust method allows the comparison and quantification of NETs formation in both human and mice samples, facilitating further investigation of the role of NETs in multiple pathologies, including SLE.

6 REFERENCES

Abu-Shakra, M. and V. Novack (2012). "Mortality and multiple causes of death in systemic lupus erythematosus -- role of the death certificate." J Rheumatol **39**(3): 458-460.

Ada, G. L., G. J. Nossal and J. Pye (1965). "Antigens in Immunity. Xi. The Uptake of Antigen in Animals Previously Rendered Immunologically Tolerant." Aust J Exp Biol Med Sci **43**: 337-344.

Ahuja, A., J. Shupe, R. Dunn, M. Kashgarian, M. R. Kehry and M. J. Shlomchik (2007). "Depletion of B cells in murine lupus: efficacy and resistance." J Immunol **179**(5): 3351-3361.

Akong-Moore, K., O. A. Chow, M. von Kockritz-Blickwede and V. Nizet (2012). "Influences of chloride and hypochlorite on neutrophil extracellular trap formation." PLoS One **7**(8): e42984.

Allende, M. L., G. Tuymetova, B. G. Lee, E. Bonifacino, Y. P. Wu and R. L. Proia (2010). "S1P1 receptor directs the release of immature B cells from bone marrow into blood." J Exp Med **207**(5): 1113-1124.

Amezcua-Guerra, L. M., V. Higuera-Ortiz, U. Arteaga-Garcia, S. Gallegos-Nava and C. Hubbe-Tena (2015). "Performance of the 2012 Systemic Lupus International Collaborating Clinics and the 1997 American College of Rheumatology classification criteria for systemic lupus erythematosus in a real-life scenario." Arthritis Care Res (Hoboken) **67**(3): 437-441.

Anders, H. J. and M. Ryu (2011). "Renal microenvironments and macrophage phenotypes determine progression or resolution of renal inflammation and fibrosis." Kidney Int **80**(9): 915-925.

Andrews (2010). "FastQC: A quality control tool for high throughput sequence data. ." http://www.bioinformatics.babraham.ac.uk/projects/fastqc/.

Andrews, B. S., R. A. Eisenberg, A. N. Theofilopoulos, S. Izui, C. B. Wilson, P. J. McConahey, E. D. Murphy, J. B. Roths and F. J. Dixon (1978). "Spontaneous murine lupus-like syndromes. Clinical and immunopathological manifestations in several strains." J Exp Med **148**(5): 1198-1215.

Anolik, J. H. (2007). "B cell biology and dysfunction in SLE." Bull NYU Hosp Jt Dis **65**(3): 182-186.

Arnson, Y., Y. Shoenfeld and H. Amital (2010). "Effects of tobacco smoke on immunity, inflammation and autoimmunity." J Autoimmun **34**(3): J258-265.

Banchereau, J., V. Pascual and A. O'Garra (2012). "From IL-2 to IL-37: the expanding spectrum of anti-inflammatory cytokines." Nat Immunol **13**(10): 925-931.

Barrientos, L., V. Marin-Esteban, L. de Chaisemartin, V. L. Le-Moal, C. Sandre, E. Bianchini, V. Nicolas, M. Pallardy and S. Chollet-Martin (2013). "An

improved strategy to recover large fragments of functional human neutrophil extracellular traps." Front Immunol **4**: 166.

Baugh, C. W., P. M. Kirol and M. V. Sachs (1960). "Demonstration and Titration of Anti-Nuclear Antibodies in Systemic Lupus Erythematosus." Can Med Assoc J **83**(11): 571-580.

Baumann, I., W. Kolowos, R. E. Voll, B. Manger, U. Gaipl, W. L. Neuhuber, T. Kirchner, J. R. Kalden and M. Herrmann (2002). "Impaired uptake of apoptotic cells into tingible body macrophages in germinal centers of patients with systemic lupus erythematosus." Arthritis Rheum **46**(1): 191-201.

Bekar, K. W., T. Owen, R. Dunn, T. Ichikawa, W. Wang, R. Wang, J. Barnard, S. Brady, S. Nevarez, B. I. Goldman, M. Kehry and J. H. Anolik (2010). "Prolonged effects of short-term anti-CD20 B cell depletion therapy in murine systemic lupus erythematosus." Arthritis Rheum **62**(8): 2443-2457.

Bennett, L., A. K. Palucka, E. Arce, V. Cantrell, J. Borvak, J. Banchereau and V. Pascual (2003). "Interferon and granulopoiesis signatures in systemic lupus erythematosus blood." J Exp Med **197**(6): 711-723.

Berkes, E., F. Oehmke, H. R. Tinneberg, K. T. Preissner and M. Saffarzadeh (2014). "Association of neutrophil extracellular traps with endometriosis-related chronic inflammation." Eur J Obstet Gynecol Reprod Biol **183**: 193-200.

Blair, P. A., L. Y. Norena, F. Flores-Borja, D. J. Rawlings, D. A. Isenberg, M. R. Ehrenstein and C. Mauri (2010). "CD19(+)CD24(hi)CD38(hi) B cells exhibit regulatory capacity in healthy individuals but are functionally impaired in systemic Lupus Erythematosus patients." Immunity **32**(1): 129-140.

Blanco, P., A. K. Palucka, M. Gill, V. Pascual and J. Banchereau (2001). "Induction of dendritic cell differentiation by IFN-alpha in systemic lupus erythematosus." Science **294**(5546): 1540-1543.

Boilard, E., P. Blanco and P. A. Nigrovic (2012). "Platelets: active players in the pathogenesis of arthritis and SLE." Nat Rev Rheumatol **8**(9): 534-542.

Brinkmann, V., B. Laube, U. Abu Abed, C. Goosmann and A. Zychlinsky (2010). "Neutrophil extracellular traps: how to generate and visualize them." J Vis Exp(36).

Brinkmann, V., U. Reichard, C. Goosmann, B. Fauler, Y. Uhlemann, D. S. Weiss, Y. Weinrauch and A. Zychlinsky (2004). "Neutrophil extracellular traps kill bacteria." Science **303**(5663): 1532-1535.

Brunelleschi, S. (2016). "Immune response and auto-immune diseases: gender does matter

and makes the diff erence." Ital J Gender-Specific Med **2**(1): 5-14.

Bygrave, A. E., K. L. Rose, J. Cortes-Hernandez, J. Warren, R. J. Rigby, H. T. Cook, M. J. Walport, T. J. Vyse and M. Botto (2004). "Spontaneous

autoimmunity in 129 and C57BL/6 mice-implications for autoimmunity described in gene-targeted mice." PLoS Biol **2**(8): E243.

Byrne, J. C., J. Ni Gabhann, E. Lazzari, R. Mahony, S. Smith, K. Stacey, C. Wynne and C. A. Jefferies (2012). "Genetics of SLE: functional relevance for monocytes/macrophages in disease." Clin Dev Immunol **2012**: 582352.

Cannons, J. L., H. Qi, K. T. Lu, M. Dutta, J. Gomez-Rodriguez, J. Cheng, E. K. Wakeland, R. N. Germain and P. L. Schwartzberg (2010). "Optimal germinal center responses require a multistage T cell:B cell adhesion process involving integrins, SLAM-associated protein, and CD84." Immunity **32**(2): 253-265.

Cannons, J. L., S. G. Tangye and P. L. Schwartzberg (2011). "SLAM family receptors and SAP adaptors in immunity." Annu Rev Immunol **29**: 665-705.

Cannons, J. L., L. J. Yu, D. Jankovic, S. Crotty, R. Horai, M. Kirby, S. Anderson, A. W. Cheever, A. Sher and P. L. Schwartzberg (2006). "SAP regulates T cell-mediated help for humoral immunity by a mechanism distinct from cytokine regulation." J Exp Med **203**(6): 1551-1565.

Carestia, A., T. Kaufman and M. Schattner (2016). "Platelets: New Bricks in the Building of Neutrophil Extracellular Traps." Front Immunol **7**: 271.

Carson, R. T. and D. A. Vignali (1999). "Simultaneous quantitation of 15 cytokines using a multiplexed flow cytometric assay." J Immunol Methods **227**(1-2): 41-52.

Carter, L. M., D. A. Isenberg and M. R. Ehrenstein (2013). "Elevated serum BAFF levels are associated with rising anti-double-stranded DNA antibody levels and disease flare following B cell depletion therapy in systemic lupus erythematosus." Arthritis Rheum **65**(10): 2672-2679.

Cedervall, J. and A. K. Olsson (2015). "NETosis in cancer." Oncoscience **2**(11): 900-901.

Cedervall, J., Y. Zhang, H. Huang, L. Zhang, J. Femel, A. Dimberg and A. K. Olsson (2015). "Neutrophil Extracellular Traps Accumulate in Peripheral Blood Vessels and Compromise Organ Function in Tumor-Bearing Animals." Cancer Res **75**(13): 2653-2662.

Celhar, T., R. Hopkins, S. I. Thornhill, R. De Magalhaes, S. H. Hwang, H. Y. Lee, H. Yasuga, L. A. Jones, J. Casco, B. Lee, T. P. Thamboo, X. J. Zhou, M. Poidinger, J. E. Connolly, E. K. Wakeland and A. M. Fairhurst (2015). "RNA

sensing by conventional dendritic cells is central to the development of lupus nephritis." Proc Natl Acad Sci U S A **112**(45): E6195-6204.

Celhar, T., R. Magalhaes and A. M. Fairhurst (2012). "TLR7 and TLR9 in SLE: when sensing self goes wrong." Immunol Res **53**(1-3): 58-77.

Cerutti, A., M. Cols and I. Puga (2013). "Marginal zone B cells: virtues of innate-like antibody-producing lymphocytes." Nat Rev Immunol **13**(2): 118-132.

Chalmers, S. A., V. Chitu, M. Ramanujam and C. Putterman (2015). "Therapeutic targeting of macrophages in lupus nephritis." Discov Med **20**(108): 43-49.

Chan, A. Y., J. M. Westcott, J. M. Mooney, E. K. Wakeland and J. D. Schatzle (2006). "The role of SAP and the SLAM family in autoimmunity." Curr Opin Immunol **18**(6): 656-664.

Cheng, O. Z. and N. Palaniyar (2013). "NET balancing: a problem in inflammatory lung diseases." Front Immunol **4**: 1.

Clark, S. R., A. C. Ma, S. A. Tavener, B. McDonald, Z. Goodarzi, M. M. Kelly, K. D. Patel, S. Chakrabarti, E. McAvoy, G. D. Sinclair, E. M. Keys, E. Allen-Vercoe, R. Devinney, C. J. Doig, F. H. Green and P. Kubes (2007). "Platelet TLR4 activates

neutrophil extracellular traps to ensnare bacteria in septic blood." Nat Med **13**(4): 463-469.

Concetta Ferretti, A. L. C. (2012). Systemic Lupus Erythematosus Basic, Applied and Clinical Aspects. Department of Medicine, University of California Los Angeles, Los Angeles, CA, USA.

Cooper, G. S., M. L. Bynum and E. C. Somers (2009). "Recent insights in the epidemiology of autoimmune diseases: improved prevalence estimates and understanding of clustering of diseases." J Autoimmun **33**(3-4): 197-207.

Cooper, G. S. and C. G. Parks (2004). "Occupational and environmental exposures as risk factors for systemic lupus erythematosus." Curr Rheumatol Rep **6**(5): 367-374.

Cooper, G. S., C. G. Parks, E. L. Treadwell, E. W. St Clair, G. S. Gilkeson and M. A. Dooley (2004). "Occupational risk factors for the development of systemic lupus erythematosus." J Rheumatol **31**(10): 1928-1933.

Costenbader, K. H., D. Feskanich, M. J. Stampfer and E. W. Karlson (2007). "Reproductive and menopausal factors and risk of systemic lupus erythematosus in women." Arthritis Rheum **56**(4): 1251-1262.

Costenbader, K. H., D. J. Kim, J. Peerzada, S. Lockman, D. Nobles-Knight, M. Petri and E. W. Karlson (2004). "Cigarette smoking and the risk of systemic lupus erythematosus: a meta-analysis." Arthritis Rheum **50**(3): 849-857.

Crispin, J. C., V. C. Kyttaris, Y. T. Juang and G. C. Tsokos (2008). "How signaling and gene transcription aberrations dictate the systemic lupus erythematosus T cell phenotype." Trends Immunol **29**(3): 110-115.

Crispin, J. C., V. C. Kyttaris, C. Terhorst and G. C. Tsokos (2010). "T cells as therapeutic targets in SLE." Nat Rev Rheumatol **6**(6): 317-325.

Crispin, J. C., S. N. Liossis, K. Kis-Toth, L. A. Lieberman, V. C. Kyttaris, Y. T. Juang and G. C. Tsokos (2010). "Pathogenesis of human systemic lupus erythematosus: recent advances." Trends Mol Med **16**(2): 47-57.

Crispin, J. C., M. Oukka, G. Bayliss, R. A. Cohen, C. A. Van Beek, I. E. Stillman, V. C. Kyttaris, Y. T. Juang and G. C. Tsokos (2008). "Expanded double

negative T cells in patients with systemic lupus erythematosus produce IL-17 and infiltrate the kidneys." J Immunol **181**(12): 8761-8766.

Crow, M. K., M. Olferiev and K. A. Kirou (2015). "Targeting of type I interferon in systemic autoimmune diseases." Transl Res **165**(2): 296-305.

Davi, G. and C. Patrono (2007). "Platelet activation and atherothrombosis." N Engl J Med **357**(24): 2482-2494.

de la Fuente, M. A., P. Pizcueta, M. Nadal, J. Bosch and P. Engel (1997). "CD84 leukocyte antigen is a new member of the Ig superfamily." Blood **90**(6): 2398-2405.

Deenick, E. K. and C. S. Ma (2011). "The regulation and role of T follicular helper cells in immunity." Immunology **134**(4): 361-367.

Demers, M., D. S. Krause, D. Schatzberg, K. Martinod, J. R. Voorhees, T. A. Fuchs, D. T. Scadden and D. D. Wagner (2012). "Cancers predispose neutrophils to release extracellular DNA traps that contribute to cancer-associated thrombosis." Proc Natl Acad Sci U S A **109**(32): 13076-13081.

Denny, M. F., P. Chandaroy, P. D. Killen, R. Caricchio, E. E. Lewis, B. C. Richardson, K. D. Lee, J. Gavalchin and M. J. Kaplan (2006). "Accelerated macrophage apoptosis induces autoantibody formation and organ damage in systemic lupus erythematosus." J Immunol **176**(4): 2095-2104.

Dieker, J., J. Tel, E. Pieterse, A. Thielen, N. Rother, M. Bakker, J. Fransen, H. B. Dijkman, J. H. Berden, J. M. de Vries, L. B. Hilbrands and J. van der Vlag (2016). "Circulating Apoptotic Microparticles in Systemic Lupus Erythematosus Patients Drive the Activation of Dendritic Cell Subsets and Prime Neutrophils for NETosis." Arthritis Rheumatol **68**(2): 462-472.

Ding, S., Y. Liang, M. Zhao, G. Liang, H. Long, S. Zhao, Y. Wang, H. Yin, P. Zhang, Q. Zhang and Q. Lu (2012). "Decreased microRNA-142-3p/5p expression causes CD4+ T cell activation and B cell hyperstimulation in systemic lupus erythematosus." Arthritis Rheum **64**(9): 2953-2963.

Dobin, A., C. A. Davis, F. Schlesinger, J. Drenkow, C. Zaleski, S. Jha, P. Batut, M. Chaisson and T. R. Gingeras (2013). "STAR: ultrafast universal RNA-seq aligner." Bioinformatics **29**(1): 15-21.

Domeier, P. P., S. B. Chodisetti, C. Soni, S. L. Schell, M. J. Elias, E. B. Wong, T. K. Cooper, D. Kitamura and Z. S. Rahman (2016). "IFN-gamma receptor

and STAT1 signaling in B cells are central to spontaneous germinal center formation and autoimmunity." J Exp Med **213**(5): 715-732.

Dorner, T., C. Giesecke and P. E. Lipsky (2011). "Mechanisms of B cell autoimmunity in SLE." Arthritis Res Ther **13**(5): 243.

Dresser, D. W. and N. A. Mitchison (1968). "The mechanism of immunological paralysis." Adv Immunol **8**: 129-181.

Du, J., L. M. Johnson, S. E. Jacobsen and D. J. Patel (2015). "DNA methylation pathways and their crosstalk with histone methylation." Nat Rev Mol Cell Biol **16**(9): 519-532.

Ducker, T. P. and K. M. Skubitz (1992). "Subcellular localization of CD66, CD67, and NCA in human neutrophils." J Leukoc Biol **52**(1): 11-16.

Duran-Struuck, R. and R. C. Dysko (2009). "Principles of bone marrow transplantation (BMT): providing optimal veterinary and husbandry care to irradiated mice in BMT studies." J Am Assoc Lab Anim Sci **48**(1): 11-22.

Dutta, M. and P. L. Schwartzberg (2012). "Characterization of Ly108 in the thymus: evidence for distinct properties of a novel form of Ly108." J Immunol **188**(7): 3031-3041.

Edwards, S. W. and M. B. Hallett (1997). "Seeing the wood for the trees: the forgotten role of neutrophils in rheumatoid arthritis." Immunol Today **18**(7): 320-324.

Elfving, P., K. Puolakka, H. Kautiainen, L. J. Virta, T. Pohjolainen and O. Kaipiainen-Seppanen (2014). "Mortality and causes of death among incident cases of systemic lupus erythematosus in Finland 2000-2008." Lupus **23**(13): 1430-1434.

Engel, P., M. J. Eck and C. Terhorst (2003). "The SAP and SLAM families in immune responses and X-linked lymphoproliferative disease." Nat Rev Immunol **3**(10): 813-821.

Ettinger, R., G. P. Sims, R. Robbins, D. Withers, R. T. Fischer, A. C. Grammer, S. Kuchen and P. E. Lipsky (2007). "IL-21 and BAFF/BLyS synergize in stimulating plasma cell differentiation from a unique population of human splenic memory B cells." J Immunol **178**(5): 2872-2882.

Fadini, G. P., L. Menegazzo, M. Rigato, V. Scattolini, N. Poncina, A. Bruttocao, S. Ciciliot, F. Mammano, C. D. Ciubotaru, E. Brocco, M. C. Marescotti, R. Cappellari, G. Arrigoni, R. Millioni, S. Vigili de Kreutzenberg, M. Albiero and A.

Avogaro (2016). "NETosis delays diabetic wound healing in mice and humans." Diabetes.

Fairhurst, A. M., A. E. Wandstrat and E. K. Wakeland (2006). "Systemic lupus erythematosus: multiple immunological phenotypes in a complex genetic disease." Adv Immunol **92**: 1-69.

Fei, Y., X. Shi, F. Gan, X. Li, W. Zhang, M. Li, Y. Hou, X. Zhang, Y. Zhao, X. Zeng and F. Zhang (2014). "Death causes and pathogens analysis of systemic lupus erythematosus during the past 26 years." Clin Rheumatol **33**(1): 57-63.

Fernandez, D. and A. Perl (2009). "Metabolic control of T cell activation and death in SLE." Autoimmun Rev **8**(3): 184-189.

Ferucci, E. D., J. M. Johnston, J. R. Gaddy, L. Sumner, J. O. Posever, T. L. Choromanski, C. Gordon, S. S. Lim and C. G. Helmick (2014). "Prevalence and incidence of systemic lupus erythematosus in a population-based registry of American Indian and Alaska Native people, 2007-2009." Arthritis Rheumatol **66**(9): 2494-2502.

Flower, C., A. J. Hennis, I. R. Hambleton, G. D. Nicholson, M. H. Liang and G. Barbados National Lupus Registry (2012). "Systemic lupus erythematosus in an African Caribbean population: incidence, clinical manifestations, and survival in the Barbados National Lupus Registry." Arthritis Care Res (Hoboken) **64**(8): 1151-1158.

Franchi, L., N. Warner, K. Viani and G. Nunez (2009). "Function of Nod-like receptors in microbial recognition and host defense." Immunol Rev **227**(1): 106-128.

Fuchs, T. A., A. Brill, D. Duerschmied, D. Schatzberg, M. Monestier, D. D. Myers, Jr., S. K. Wrobleski, T. W. Wakefield, J. H. Hartwig and D. D. Wagner (2010). "Extracellular DNA traps promote thrombosis." Proc Natl Acad Sci U S A **107**(36): 15880-15885.

Gaffney, P. M., G. M. Kearns, K. B. Shark, W. A. Ortmann, S. A. Selby, M. L. Malmgren, K. E. Rohlf, T. C. Ockenden, R. P. Messner, R. A. King, S. S. Rich and T. W. Behrens (1998). "A genome-wide search for susceptibility genes in human systemic lupus erythematosus sib-pair families." Proc Natl Acad Sci U S A **95**(25): 14875-14879.

Ganguly, D., S. Haak, V. Sisirak and B. Reizis (2013). "The role of dendritic cells in autoimmunity." Nat Rev Immunol **13**(8): 566-577.

Garcia-Romo, G. S., S. Caielli, B. Vega, J. Connolly, F. Allantaz, Z. Xu, M. Punaro, J. Baisch, C. Guiducci, R. L. Coffman, F. J. Barrat, J. Banchereau and V.

Pascual (2011). "Netting neutrophils are major inducers of type I IFN production in pediatric systemic lupus erythematosus." Sci Transl Med **3**(73): 73ra20.

Gatto, M., M. Zen, A. Ghirardello, S. Bettio, N. Bassi, L. Iaccarino, L. Punzi and A. Doria (2013). "Emerging and critical issues in the pathogenesis of lupus." Autoimmun Rev **12**(4): 523-536.

Gavillet, M., K. Martinod, R. Renella, C. Harris, N. I. Shapiro, D. D. Wagner and D. A. Williams (2015). "Flow cytometric assay for direct quantification of neutrophil extracellular traps in blood samples." Am J Hematol.

Geering, B. and H. U. Simon (2011). "Peculiarities of cell death mechanisms in neutrophils." Cell Death Differ **18**(9): 1457-1469.

Gerberick, G. F., L. W. Cruse, C. M. Miller, E. E. Sikorski and G. M. Ridder (1997). "Selective modulation of T cell memory markers CD62L and CD44 on murine draining lymph node cells following allergen and irritant treatment." Toxicol Appl Pharmacol **146**(1): 1-10.

Gerli, R., G. Nocentini, A. Alunno, E. B. Bocci, R. Bianchini, O. Bistoni and C. Riccardi (2009). "Identification of regulatory T cells in systemic lupus erythematosus." Autoimmun Rev **8**(5): 426-430.

Giltiay, N. V., C. P. Chappell, X. Sun, N. Kolhatkar, T. H. Teal, A. E. Wiedeman, J. Kim, L. Tanaka, M. B. Buechler, J. A. Hamerman, T. Imanishi-Kari, E. A. Clark and K. B. Elkon (2013). "Overexpression of TLR7 promotes cell-intrinsic expansion and autoantibody production by transitional T1 B cells." J Exp Med **210**(12): 2773-2789.

Gonzalez, L. A., S. M. Toloza and G. S. Alarcon (2014). "Impact of race and ethnicity in the course and outcome of systemic lupus erythematosus." Rheum Dis Clin North Am **40**(3): 433-454, vii-viii.

Green, J. R., M. Montasser and J. C. Woodrow (1986). "The association of HLA-linked genes with systemic lupus erythematosus." Ann Hum Genet **50**(Pt 1): 93-96.

Gualtierotti, R., M. Biggioggero, A. E. Penatti and P. L. Meroni (2010). "Updating on the pathogenesis of systemic lupus erythematosus." Autoimmun Rev **10**(1): 3-7.

Gupta, A. K., M. B. Joshi, M. Philippova, P. Erne, P. Hasler, S. Hahn and T. J. Resink (2010). "Activated endothelial cells induce neutrophil extracellular traps and are susceptible to NETosis-mediated cell death." FEBS Lett **584**(14): 3193-3197.

Handono, K., Y. O. Sidarta, B. A. Pradana, R. A. Nugroho, I. A. Hartono, H. Kalim and A. T. Endharti (2014). "Vitamin D prevents endothelial damage induced

by increased neutrophil extracellular traps formation in patients with systemic lupus erythematosus." Acta Med Indones **46**(3): 189-198.

Harlan, J. M., B. R. Schwartz, M. A. Reidy, S. M. Schwartz, H. D. Ochs and L. A. Harker (1985). "Activated neutrophils disrupt endothelial monolayer integrity by an oxygen radical-independent mechanism." Lab Invest **52**(2): 141-150.

Hiepe, F., T. Dorner, A. E. Hauser, B. F. Hoyer, H. Mei and A. Radbruch (2011). "Long-lived autoreactive plasma cells drive persistent autoimmune inflammation." Nat Rev Rheumatol **7**(3): 170-178.

Hill, G. S., M. Delahousse, D. Nochy, P. Remy, F. Mignon, J. P. Mery and J. Bariety (2001). "Predictive power of the second renal biopsy in lupus nephritis: significance of macrophages." Kidney Int **59**(1): 304-316.

Hochberg, M. C. (1997). "Updating the American College of Rheumatology revised criteria for the classification of systemic lupus erythematosus." Arthritis Rheum **40**(9): 1725.

Hofmann, S., A. Braun, R. Pozgaj, M. Morowski, T. Vogtle and B. Nieswandt (2014). "Mice lacking the SLAM family member CD84 display unaltered platelet function in hemostasis and thrombosis." PLoS One **9**(12): e115306.

Hofmann, S., T. Vogtle, M. Bender, S. Rose-John and B. Nieswandt (2012). "The SLAM family member CD84 is regulated by ADAM10 and calpain in platelets." J Thromb Haemost **10**(12): 2581-2592.

Hwang, S. H., H. Lee, M. Yamamoto, L. A. Jones, J. Dayalan, R. Hopkins, X. J. Zhou, F. Yarovinsky, J. E. Connolly, M. A. Curotto de Lafaille, E. K. Wakeland and A. M. Fairhurst (2012). "B cell TLR7 expression drives anti-RNA autoantibody production and exacerbates disease in systemic lupus erythematosus-prone mice." J Immunol **189**(12): 5786-5796.

Ikehara, S., R. A. Good, T. Nakamura, K. Sekita, S. Inoue, M. M. Oo, E. Muso, K. Ogawa and Y. Hamashima (1985). "Rationale for bone marrow transplantation in the treatment of autoimmune diseases." Proc Natl Acad Sci U S A **82**(8): 2483-2487.

Ines, L., C. Silva, M. Galindo, F. J. Lopez-Longo, G. Terroso, V. C. Romao, I. Rua-Figueroa, M. J. Santos, J. M. Pego-Reigosa, P. Nero, M. Cerqueira, C. Duarte, L. C. Miranda, M. Bernardes, M. J. Goncalves, C. Mourino-Rodriguez, F. Araujo, A. Raposo, A. Barcelos, M. Couto, P. Abreu, T. Oton-Sanchez, C. Macieira, F. Ramos, J. C. Branco, J. A. Silva, H. Canhao, J. Calvo-Alen, R. Rheumatic Diseases Registry of the Portuguese Society of and R. Registry of Systemic Lupus Erythematosus Patients of the Spanish Society of (2015). "Classification of Systemic Lupus Erythematosus: Systemic Lupus International Collaborating Clinics Versus American College of Rheumatology Criteria. A

Comparative Study of 2,055 Patients From a Real-Life, International Systemic Lupus Erythematosus Cohort." Arthritis Care Res (Hoboken) **67**(8): 1180-1185.

Iwasaki, A. (2012). "A virological view of innate immune recognition." Annu Rev Microbiol **66**: 177-196.

J., W. D. (1995). The Lupus Book: A Guide for Patients and Their Families. . 1st edition New York: Oxford University Press. **47-51:** 159-163.

Jackson, S. W., H. M. Jacobs, T. Arkatkar, E. M. Dam, N. E. Scharping, N. S. Kolhatkar, B. Hou, J. H. Buckner and D. J. Rawlings (2016). "B cell IFN-gamma receptor signaling promotes autoimmune germinal centers via cell-intrinsic induction of BCL-6." J Exp Med **213**(5): 733-750.

Jacobi, A. M., H. Mei, B. F. Hoyer, I. M. Mumtaz, K. Thiele, A. Radbruch, G. R. Burmester, F. Hiepe and T. Dorner (2010). "HLA-DRhigh/CD27high plasmablasts indicate active disease in patients with systemic lupus erythematosus." Ann Rheum Dis **69**(1): 305-308.

Javierre, B. M., A. F. Fernandez, J. Richter, F. Al-Shahrour, J. I. Martin-Subero, J. Rodriguez-Ubreva, M. Berdasco, M. F. Fraga, T. P. O'Hanlon, L. G. Rider, F. V. Jacinto, F. J. Lopez-Longo, J. Dopazo, M. Forn, M. A. Peinado, L. Carreno, A. H. Sawalha, J. B. Harley, R. Siebert, M. Esteller, F. W. Miller and E. Ballestar (2010). "Changes in the pattern of DNA methylation associate with twin discordance in systemic lupus erythematosus." Genome Res **20**(2): 170-179.

Ju, J. H., S. H. Yoon, K. Y. Kang, I. J. Kim, S. K. Kwok, S. H. Park, H. Y. Kim, W. C. Lee and C. S. Cho (2014). "Prevalence of systemic lupus erythematosus in South Korea: an administrative database study." J Epidemiol **24**(4): 295-303.

Kaminitz, A., K. Mizrahi, I. Yaniv, D. L. Farkas, J. Stein and N. Askenasy (2009). "Low levels of allogeneic but not syngeneic hematopoietic chimerism

reverse autoimmune insulitis in prediabetic NOD mice." J Autoimmun **33**(2): 83-91.

Kaplan, M. J. (2013). "Role of neutrophils in systemic autoimmune diseases." Arthritis Res Ther **15**(5): 219.

Kattah, N. H., M. G. Kattah and P. J. Utz (2010). "The U1-snRNP complex: structural properties relating to autoimmune pathogenesis in rheumatic diseases." Immunol Rev **233**(1): 126-145.

Katz, S. I., D. Parker and J. L. Turk (1974). "B-cell suppression of delayed hypersensitivity reactions." Nature **251**(5475): 550-551.

Kaul, A., C. Gordon, M. K. Crow, Z. Touma, M. B. Urowitz, R. van Vollenhoven, G. Ruiz-Irastorza and G. Hughes (2016). "Systemic lupus erythematosus." Nat Rev Dis Primers **2**: 16039.

Kavai, M. and G. Szegedi (2007). "Immune complex clearance by monocytes and macrophages in systemic lupus erythematosus." Autoimmun Rev **6**(7): 497-502.

Keszei, M., C. Detre, S. T. Rietdijk, P. Munoz, X. Romero, S. B. Berger, S. Calpe, G. Liao, W. Castro, A. Julien, Y. Y. Wu, D. M. Shin, J. Sancho, M. Zubiaur, H. C. Morse, 3rd, L. Morel, P. Engel, N. Wang and C. Terhorst (2011). "A novel isoform of the Ly108 gene ameliorates murine lupus." J Exp Med **208**(4): 811-822.

Kim, Y. K., J. S. Shin and M. H. Nahm (2016). "NOD-Like Receptors in Infection, Immunity, and Diseases." Yonsei Med J **57**(1): 5-14.

Kirou, K. A., C. Lee, S. George, K. Louca, M. G. Peterson and M. K. Crow (2005). "Activation of the interferon-alpha pathway identifies a subgroup of systemic lupus erythematosus patients with distinct serologic features and active disease." Arthritis Rheum **52**(5): 1491-1503.

Komatsuda, A., H. Wakui, K. Iwamoto, M. Ozawa, M. Togashi, R. Masai, N. Maki, T. Hatakeyama and K. Sawada (2008). "Up-regulated expression of Toll-like receptors mRNAs in peripheral blood mononuclear cells from patients with systemic lupus erythematosus." Clin Exp Immunol **152**(3): 482-487.

Koshy, M., D. Berger and M. K. Crow (1996). "Increased expression of CD40 ligand on systemic lupus erythematosus lymphocytes." J Clin Invest **98**(3): 826-837.

Krause, S. W., M. Rehli, S. Heinz, R. Ebner and R. Andreesen (2000). "Characterization of MAX.3 antigen, a glycoprotein expressed on mature macrophages, dendritic cells and blood platelets: identity with CD84." Biochem J **346 Pt 3**: 729-736.

Kruse, K., C. Janko, V. Urbonaviciute, C. T. Mierke, T. H. Winkler, R. E. Voll, G. Schett, L. E. Munoz and M. Herrmann (2010). "Inefficient clearance of dying

cells in patients with SLE: anti-dsDNA autoantibodies, MFG-E8, HMGB-1 and other players." Apoptosis **15**(9): 1098-1113.

Kubista, M., B. Akerman and B. Norden (1987). "Characterization of interaction between DNA and 4',6-diamidino-2-phenylindole by optical spectroscopy." Biochemistry **26**(14): 4545-4553.

Kuhn, A., V. Ruland and G. Bonsmann (2010). "Photosensitivity, phototesting, and photoprotection in cutaneous lupus erythematosus." Lupus **19**(9): 1036-1046.

Lande, R., D. Ganguly, V. Facchinetti, L. Frasca, C. Conrad, J. Gregorio, S. Meller, G. Chamilos, R. Sebasigari, V. Riccieri, R. Bassett, H. Amuro, S. Fukuhara, T. Ito, Y. J. Liu and M. Gilliet (2011). "Neutrophils activate plasmacytoid dendritic cells by releasing self-DNA-peptide complexes in systemic lupus erythematosus." Sci Transl Med **3**(73): 73ra19.

Laustrup, H., A. Voss, A. Green and P. Junker (2010). "SLE disease patterns in a Danish population-based lupus cohort: an 8-year prospective study." Lupus **19**(3): 239-246.

Lee, S. K., D. G. Silva, J. L. Martin, A. Pratama, X. Hu, P. P. Chang, G. Walters and C. G. Vinuesa (2012). "Interferon-gamma excess leads to pathogenic accumulation of follicular helper T cells and germinal centers." Immunity **37**(5): 880-892.

Li, F., Y. Yang, X. Zhu, L. Huang and J. Xu (2015). "Macrophage Polarization Modulates Development of Systemic Lupus Erythematosus." Cell Physiol Biochem **37**(4): 1279-1288.

Li, F., X. Zhu, Y. Yang, L. Huang and J. Xu (2016). "TIPE2 Alleviates Systemic Lupus Erythematosus Through Regulating Macrophage Polarization." Cell Physiol Biochem **38**(1): 330-339.

Li, N., H. Hu, M. Lindqvist, E. Wikstrom-Jonsson, A. H. Goodall and P. Hjemdahl (2000). "Platelet-leukocyte cross talk in whole blood." Arterioscler Thromb Vasc Biol **20**(12): 2702-2708.

Li, W., M. H. Sofi, S. Rietdijk, N. Wang, C. Terhorst and C. H. Chang (2007). "The SLAM-associated protein signaling pathway is required for development of CD4+ T cells selected by homotypic thymocyte interaction." Immunity **27**(5): 763-774.

Li, X., J. Wu, T. Ptacek, D. T. Redden, E. E. Brown, G. S. Alarcon, R. Ramsey-Goldman, M. A. Petri, J. D. Reveille, R. A. Kaslow, R. P. Kimberly and J.

C. Edberg (2013). "Allelic-dependent expression of an activating Fc receptor on B cells enhances humoral immune responses." Sci Transl Med **5**(216): 216ra175.

Licht, R., J. W. Dieker, C. W. Jacobs, W. J. Tax and J. H. Berden (2004). "Decreased phagocytosis of apoptotic cells in diseased SLE mice." J Autoimmun **22**(2): 139-145.

Lim, S. S., A. R. Bayakly, C. G. Helmick, C. Gordon, K. A. Easley and C. Drenkard (2014). "The incidence and prevalence of systemic lupus erythematosus, 2002-2004: The Georgia Lupus Registry." Arthritis Rheumatol **66**(2): 357-368.

Lindau, D., J. Mussard, A. Rabsteyn, M. Ribon, I. Kotter, A. Igney, G. J. Adema, M. C. Boissier, H. G. Rammensee and P. Decker (2014). "TLR9 independent interferon alpha production by neutrophils on NETosis in response to circulating chromatin, a key lupus autoantigen." Ann Rheum Dis **73**(12): 2199-2207.

Liu, H. B., K. K. Loo, K. Palaszynski, J. Ashouri, D. B. Lubahn and R. R. Voskuhl (2003). "Estrogen receptor alpha mediates estrogen's immune protection in autoimmune disease." J Immunol **171**(12): 6936-6940.

Liu, K. and E. K. Wakeland (2001). "Delineation of the pathogenesis of systemic lupus erythematosus by using murine models." Adv Exp Med Biol **490**: 1-6.

Loder, F., B. Mutschler, R. J. Ray, C. J. Paige, P. Sideras, R. Torres, M. C. Lamers and R. Carsetti (1999). "B cell development in the spleen takes place in discrete steps and is determined by the quality of B cell receptor-derived signals." J Exp Med **190**(1): 75-89.

Lood, C., S. Amisten, B. Gullstrand, A. Jonsen, M. Allhorn, L. Truedsson, G. Sturfelt, D. Erlinge and A. A. Bengtsson (2010). "Platelet transcriptional profile and protein expression in patients with systemic lupus erythematosus: up-regulation of

the type I interferon system is strongly associated with vascular disease." Blood **116**(11): 1951-1957.

Ma, C. S. and E. K. Deenick (2014). "Human T follicular helper (Tfh) cells and disease." Immunol Cell Biol **92**(1): 64-71.

Ma, C. S., K. E. Nichols and S. G. Tangye (2007). "Regulation of cellular and humoral immune responses by the SLAM and SAP families of molecules." Annu Rev Immunol **25**: 337-379.

Mackay, I. R. (2000). "Science, medicine, and the future: Tolerance and autoimmunity." BMJ **321**(7253): 93-96.

Mackay, M., A. Stanevsky, T. Wang, C. Aranow, M. Li, S. Koenig, J. V. Ravetch and B. Diamond (2006). "Selective dysregulation of the FcgammaIIB receptor on memory B cells in SLE." J Exp Med **203**(9): 2157-2164.

Mak, A. and N. Y. Kow (2014). "Imbalance between endothelial damage and repair: a gateway to cardiovascular disease in systemic lupus erythematosus." Biomed Res Int **2014**: 178721.

Man, S. M., R. Karki and T. D. Kanneganti (2016). "AIM2 inflammasome in infection, cancer, and autoimmunity: Role in DNA sensing, inflammation, and innate immunity." Eur J Immunol **46**(2): 269-280.

Manda-Handzlik, A., O. Ciepiela, M. Ostafin, W. Bystrzycka, S. Sieczkowska, A. Moskalik and U. Demkow (2016). "Flow cytometric quantification of neutrophil extracellular traps: Limitations of the methodological approach." Am J Hematol **91**(3): E9-E10.

Mannik, M., C. E. Merrill, L. D. Stamps and M. H. Wener (2003). "Multiple autoantibodies form the glomerular immune deposits in patients with systemic lupus erythematosus." J Rheumatol **30**(7): 1495-1504.

Manzi, S., E. N. Meilahn, J. E. Rairie, C. G. Conte, T. A. Medsger, Jr., L. Jansen-McWilliams, R. B. D'Agostino and L. H. Kuller (1997). "Age-specific incidence rates of myocardial infarction and angina in women with systemic lupus erythematosus: comparison with the Framingham Study." Am J Epidemiol **145**(5): 408-415.

Mao, C., S. Wang, Y. Xiao, J. Xu, Q. Jiang, M. Jin, X. Jiang, H. Guo, G. Ning and Y. Zhang (2011). "Impairment of regulatory capacity of CD4+CD25+ regulatory T cells mediated by dendritic cell polarization and hyperthyroidism in Graves' disease." J Immunol **186**(8): 4734-4743.

Marks, S. D., S. J. Williams, K. Tullus and N. J. Sebire (2008). "Glomerular expression of monocyte chemoattractant protein-1 is predictive of poor renal prognosis in pediatric lupus nephritis." Nephrol Dial Transplant **23**(11): 3521-3526.

Martin, M., X. Romero, M. A. de la Fuente, V. Tovar, N. Zapater, E. Esplugues, P. Pizcueta, J. Bosch and P. Engel (2001). "CD84 functions as a

homophilic adhesion molecule and enhances IFN-gamma secretion: adhesion is mediated by Ig-like domain 1." J Immunol **167**(7): 3668-3676.

Marx, J. L. (1987). "Oxygen free radicals linked to many diseases." Science **235**(4788): 529-531.

Masek-Hammerman, K., E. Peeva, A. Ahmad, S. Menon, M. Afsharvand, R. Peng Qu, J. B. Cheng, J. Syed, Y. Zhan, S. P. O'Neil, S. Pleasic-Williams, L. A. Cox and D. Beidler (2016). "Monoclonal antibody against macrophage colony-stimulating factor suppresses circulating monocytes and tissue macrophage function but does not alter cell infiltration/activation in cutaneous lesions or clinical outcomes in patients with cutaneous lupus erythematosus." Clin Exp Immunol **183**(2): 258-270.

Mauri, C. and A. Bosma (2012). "Immune regulatory function of B cells." Annu Rev Immunol **30**: 221-241.

McGrogan, A., S. Sneddon and C. S. de Vries (2010). "The incidence of myasthenia gravis: a systematic literature review." Neuroepidemiology **34**(3): 171-183.

Medzhitov, R. and C. A. Janeway, Jr. (2002). "Decoding the patterns of self and nonself by the innate immune system." Science **296**(5566): 298-300.

Meikle, C. K., C. A. Kelly, P. Garg, L. M. Wuescher, R. A. Ali and R. G. Worth (2016). "Cancer and Thrombosis: The Platelet Perspective." Front Cell Dev Biol **4**: 147.

Menon, M., P. A. Blair, D. A. Isenberg and C. Mauri (2016). "A Regulatory Feedback between Plasmacytoid Dendritic Cells and Regulatory B Cells Is Aberrant in Systemic Lupus Erythematosus." Immunity **44**(3): 683-697.

Merrill, J. T., C. M. Neuwelt, D. J. Wallace, J. C. Shanahan, K. M. Latinis, J. C. Oates, T. O. Utset, C. Gordon, D. A. Isenberg, H. J. Hsieh, D. Zhang and P. G. Brunetta (2010). "Efficacy and safety of rituximab in moderately-to-severely active systemic lupus erythematosus: the randomized, double-blind, phase II/III systemic lupus erythematosus evaluation of rituximab trial." Arthritis Rheum **62**(1): 222-233.

Mittereder, N., E. Kuta, G. Bhat, K. Dacosta, L. I. Cheng, R. Herbst and G. Carlesso (2016). "Loss of Immune Tolerance Is Controlled by ICOS in Sle1 Mice." J Immunol **197**(2): 491-503.

Mizuguchi, H., Z. Xu, A. Ishii-Watabe, E. Uchida and T. Hayakawa (2000). "IRES-dependent second gene expression is significantly lower than cap-dependent first gene expression in a bicistronic vector." Mol Ther **1**(4): 376-382.

Modlich, U., S. Navarro, D. Zychlinski, T. Maetzig, S. Knoess, M. H. Brugman, A. Schambach, S. Charrier, A. Galy, A. J. Thrasher, J. Bueren and C.

Baum (2009). "Insertional transformation of hematopoietic cells by self-inactivating lentiviral and gammaretroviral vectors." Mol Ther **17**(11): 1919-1928.

Mohan, C., L. Morel, P. Yang and E. K. Wakeland (1997). "Genetic dissection of systemic lupus erythematosus pathogenesis: Sle2 on murine chromosome 4 leads to B cell hyperactivity." J Immunol **159**(1): 454-465.

Mohan, C., L. Morel, P. Yang, H. Watanabe, B. Croker, G. Gilkeson and E. K. Wakeland (1999). "Genetic dissection of lupus pathogenesis: a recipe for nephrophilic autoantibodies." J Clin Invest **103**(12): 1685-1695.

Mohan, C., Y. Yu, L. Morel, P. Yang and E. K. Wakeland (1999). "Genetic dissection of Sle pathogenesis: Sle3 on murine chromosome 7 impacts T cell activation, differentiation, and cell death." J Immunol **162**(11): 6492-6502.

Mohanty, T., J. Sjogren, F. Kahn, A. H. Abu-Humaidan, N. Fisker, K. Assing, M. Morgelin, A. A. Bengtsson, N. Borregaard and O. E. Sorensen (2015). "A novel mechanism for NETosis provides antimicrobial defense at the oral mucosa." Blood **126**(18): 2128-2137.

Mok, C. C. and C. S. Lau (2003). "Pathogenesis of systemic lupus erythematosus." J Clin Pathol **56**(7): 481-490.

Morel, L., K. R. Blenman, B. P. Croker and E. K. Wakeland (2001). "The major murine systemic lupus erythematosus susceptibility locus, Sle1, is a cluster of functionally related genes." Proc Natl Acad Sci U S A **98**(4): 1787-1792.

Morel, L., B. P. Croker, K. R. Blenman, C. Mohan, G. Huang, G. Gilkeson and E. K. Wakeland (2000). "Genetic reconstitution of systemic lupus erythematosus immunopathology with polycongenic murine strains." Proc Natl Acad Sci U S A **97**(12): 6670-6675.

Morel, L., U. H. Rudofsky, J. A. Longmate, J. Schiffenbauer and E. K. Wakeland (1994). "Polygenic control of susceptibility to murine systemic lupus erythematosus." Immunity **1**(3): 219-229.

Morel, L. and E. K. Wakeland (1998). "Susceptibility to lupus nephritis in the NZB/W model system." Curr Opin Immunol **10**(6): 718-725.

Morra, M., J. Lu, F. Poy, M. Martin, J. Sayos, S. Calpe, C. Gullo, D. Howie, S. Rietdijk, A. Thompson, A. J. Coyle, C. Denny, M. B. Yaffe, P. Engel, M. J. Eck and C. Terhorst (2001). "Structural basis for the interaction of the free SH2 domain EAT-2 with SLAM receptors in hematopoietic cells." EMBO J **20**(21): 5840-5852.

Mortezagholi, S., Z. Babaloo, P. Rahimzadeh, M. Ghaedi, H. Namdari, S. Assar, M. Azimi Mohamadabadi and E. Salehi (2016). "Evaluation of PBMC Distribution and TLR9 Expression in Patients with Systemic Lupus Erythematosus." Iran J Allergy Asthma Immunol **15**(3): 229-236.

Mosca, M., C. Tani, M. Aringer, S. Bombardieri, D. Boumpas, R. Cervera, A. Doria, D. Jayne, M. A. Khamashta, A. Kuhn, C. Gordon, M. Petri, M. Schneider, Y. Shoenfeld, J. S. Smolen, R. Talarico, A. Tincani, M. M. Ward, V. P. Werth and

L. Carmona (2011). "Development of quality indicators to evaluate the monitoring of SLE patients in routine clinical practice." Autoimmun Rev **10**(7): 383-388.

Munoz, L. E., K. Lauber, M. Schiller, A. A. Manfredi and M. Herrmann (2010). "The role of defective clearance of apoptotic cells in systemic autoimmunity." Nat Rev Rheumatol **6**(5): 280-289.

Murphy, E. D., and Roths, J. B. (1979). "A Y chromosome associated factor in strain BXSB producing accelerated autoimmunity and lymphoproliferation." Arthritis Rheum **22**: 1188–1194.

Naccache, P. H. and M. J. Fernandes (2016). "Challenges in the characterization of neutrophil extracellular traps: The truth is in the details." Eur J Immunol **46**(1): 52-55.

Nagasawa, A., K. Matsuno, S. Tamura, K. Hayasaka, C. Shimizu and T. Moriyama (2013). "The basis examination of leukocyte-platelet aggregates with CD45 gating as a novel platelet activation marker." Int J Lab Hematol **35**(5): 534-541.

Nanda, N., P. Andre, M. Bao, K. Clauser, F. Deguzman, D. Howie, P. B. Conley, C. Terhorst and D. R. Phillips (2005). "Platelet aggregation induces platelet aggregate stability via SLAM family receptor signaling." Blood **106**(9): 3028-3034.

Niewold, T. B., J. A. Kelly, M. H. Flesch, L. R. Espinoza, J. B. Harley and M. K. Crow (2008). "Association of the IRF5 risk haplotype with high serum interferon-alpha activity in systemic lupus erythematosus patients." Arthritis Rheum **58**(8): 2481-2487.

Nossal, G. J. and B. L. Pike (1975). "Evidence for the clonal abortion theory of B-lymphocyte tolerance." J Exp Med **141**(4): 904-917.

Nundel, K., P. Busto, M. Debatis and A. Marshak-Rothstein (2013). "The role of Bruton's tyrosine kinase in the development and BCR/TLR-dependent activation of AM14 rheumatoid factor B cells." J Leukoc Biol **94**(5): 865-875.

O'Reilly, S. (2015). "Pound the alarm: danger signals in rheumatic diseases." Clin Sci (Lond) **128**(5): 297-305.

Orme, J. and C. Mohan (2012). "Macrophage subpopulations in systemic lupus erythematosus." Discov Med **13**(69): 151-158.

Palanichamy, A., J. Barnard, B. Zheng, T. Owen, T. Quach, C. Wei, R. J. Looney, I. Sanz and J. H. Anolik (2009). "Novel human transitional B cell populations revealed by B cell depletion therapy." J Immunol **182**(10): 5982-5993.

Palanichamy, A., J. W. Bauer, S. Yalavarthi, N. Meednu, J. Barnard, T. Owen, C. Cistrone, A. Bird, A. Rabinovich, S. Nevarez, J. S. Knight, R. Dedrick, A. Rosenberg, C. Wei, J. Rangel-Moreno, J. Liesveld, I. Sanz, E. Baechler, M. J. Kaplan and J. H. Anolik (2014). "Neutrophil-mediated IFN activation in the bone

marrow alters B cell development in human and murine systemic lupus erythematosus." J Immunol **192**(3): 906-918.

Palou, E., F. Pirotto, J. Sole, J. H. Freed, B. Peral, C. Vilardell, R. Vilella, J. Vives and A. Gaya (2000). "Genomic characterization of CD84 reveals the existence of five isoforms differing in their cytoplasmic domains." Tissue Antigens **55**(2): 118-127.

Paoliello-Paschoalato, A. B., A. E. Azzolini, M. F. Cruz, L. F. Marchi, L. M. Kabeya, E. A. Donadi and Y. M. Lucisano-Valim (2014). "Isolation of healthy individuals' and rheumatoid arthritis patients' peripheral blood neutrophils by the gelatin and Ficoll-Hypaque methods: comparative efficiency and impact on the neutrophil oxidative metabolism and Fcgamma receptor expression." J Immunol Methods **412**: 70-77.

Pathak, S. and C. Mohan (2011). "Cellular and molecular pathogenesis of systemic lupus erythematosus: lessons from animal models." Arthritis Res Ther **13**(5): 241.

Petri, M., A. M. Orbai, G. S. Alarcon, C. Gordon, J. T. Merrill, P. R. Fortin, I. N. Bruce, D. Isenberg, D. J. Wallace, O. Nived, G. Sturfelt, R. Ramsey-Goldman, S. C. Bae, J. G. Hanly, J. Sanchez-Guerrero, A. Clarke, C. Aranow, S. Manzi, M. Urowitz, D. Gladman, K. Kalunian, M. Costner, V. P. Werth, A. Zoma, S. Bernatsky, G. Ruiz-Irastorza, M. A. Khamashta, S. Jacobsen, J. P. Buyon, P. Maddison, M. A. Dooley, R. F. van Vollenhoven, E. Ginzler, T. Stoll, C. Peschken, J. L. Jorizzo, J. P. Callen, S. S. Lim, B. J. Fessler, M. Inanc, D. L. Kamen, A. Rahman, K. Steinsson, A. G. Franks, Jr., L. Sigler, S. Hameed, H. Fang, N. Pham, R. Brey, M. H. Weisman, G. McGwin, Jr. and L. S. Magder (2012). "Derivation and

validation of the Systemic Lupus International Collaborating Clinics classification criteria for systemic lupus erythematosus." Arthritis Rheum **64**(8): 2677-2686.

Pieterse, E. and J. van der Vlag (2014). "Breaking immunological tolerance in systemic lupus erythematosus." Front Immunol **5**: 164.

Pillinger, M. H. and S. B. Abramson (1995). "The neutrophil in rheumatoid arthritis." Rheum Dis Clin North Am **21**(3): 691-714.

Pons-Estel, G. J., G. S. Alarcon, L. Scofield, L. Reinlib and G. S. Cooper (2010). "Understanding the epidemiology and progression of systemic lupus erythematosus." Semin Arthritis Rheum **39**(4): 257-268.

Qin, J. Y., L. Zhang, K. L. Clift, I. Hulur, A. P. Xiang, B. Z. Ren and B. T. Lahn (2010). "Systematic comparison of constitutive promoters and the doxycycline-inducible promoter." PLoS One **5**(5): e10611.

Quah, B. J., H. S. Warren and C. R. Parish (2007). "Monitoring lymphocyte proliferation in vitro and in vivo with the intracellular fluorescent dye carboxyfluorescein diacetate succinimidyl ester." Nat Protoc **2**(9): 2049-2056.

Rahman, Z. S., B. Alabyev and T. Manser (2007). "FcgammaRIIB regulates autoreactive primary antibody-forming cell, but not germinal center B cell, activity." J Immunol **178**(2): 897-907.

Ravetch, J. V. and J. P. Kinet (1991). "Fc receptors." Annu Rev Immunol **9**: 457-492.

Rees, F., M. Doherty, M. Grainge, G. Davenport, P. Lanyon and W. Zhang (2016). "The incidence and prevalence of systemic lupus erythematosus in the UK, 1999-2012." Ann Rheum Dis **75**(1): 136-141.

Reeves, W. H., P. Y. Lee, J. S. Weinstein, M. Satoh and L. Lu (2009). "Induction of autoimmunity by pristane and other naturally occurring hydrocarbons." Trends Immunol **30**(9): 455-464.

Reff, M. E., K. Carner, K. S. Chambers, P. C. Chinn, J. E. Leonard, R. Raab, R. A. Newman, N. Hanna and D. R. Anderson (1994). "Depletion of B cells in vivo by a chimeric mouse human monoclonal antibody to CD20." Blood **83**(2): 435-445.

Reindel, R., J. Bischof, K. Y. Kim, J. M. Orenstein, M. B. Soares, S. C. Baker, S. T. Shulman, E. J. Perlman, M. W. Lingen, A. J. Pink, C. Trevenen and A. H. Rowley (2014). "CD84 is markedly up-regulated in Kawasaki disease arteriopathy." Clin Exp Immunol **177**(1): 203-211.

Rivera, T. L., H. M. Belmont and G. Weissmann (2009). "Systemic lupus erythematosus in 6 male cocaine users at Bellevue hospital." J Rheumatol **36**(12): 2854-2855.

Romero, X., D. Benitez, S. March, R. Vilella, M. Miralpeix and P. Engel (2004). "Differential expression of SAP and EAT-2-binding leukocyte cell-surface

molecules CD84, CD150 (SLAM), CD229 (Ly9) and CD244 (2B4)." Tissue Antigens **64**(2): 132-144.

Roncagalli, R., J. E. Taylor, S. Zhang, X. Shi, R. Chen, M. E. Cruz-Munoz, L. Yin, S. Latour and A. Veillette (2005). "Negative regulation of natural killer cell function by EAT-2, a SAP-related adaptor." Nat Immunol **6**(10): 1002-1010.

Rosenblum, M. D., S. S. Way and A. K. Abbas (2016). "Regulatory T cell memory." Nat Rev Immunol **16**(2): 90-101.

Rovin, B. H., R. Furie, K. Latinis, R. J. Looney, F. C. Fervenza, J. Sanchez-Guerrero, R. Maciuca, D. Zhang, J. P. Garg, P. Brunetta, G. Appel and L. I. Group (2012). "Efficacy and safety of rituximab in patients with active proliferative lupus nephritis: the Lupus Nephritis Assessment with Rituximab study." Arthritis Rheum **64**(4): 1215-1226.

Rudofsky, U. H., B. D. Evans, S. L. Balaban, V. D. Mottironi and A. E. Gabrielsen (1993). "Differences in expression of lupus nephritis in New Zealand mixed H-2z homozygous inbred strains of mice derived from New Zealand black and New Zealand white mice. Origins and initial characterization." Lab Invest **68**(4): 419-426.

Sahu, R., R. Bethunaickan, S. Singh and A. Davidson (2014). "Structure and function of renal macrophages and dendritic cells from lupus-prone mice." Arthritis Rheumatol **66**(6): 1596-1607.

Sanchez-Madrid, F., A. M. Krensky, C. F. Ware, E. Robbins, J. L. Strominger, S. J. Burakoff and T. A. Springer (1982). "Three distinct antigens associated with human T-lymphocyte-mediated cytolysis: LFA-1, LFA-2, and LFA-3." Proc Natl Acad Sci U S A **79**(23): 7489-7493.

Sandrin, M. S., T. P. Gumley, M. M. Henning, H. A. Vaughan, L. J. Gonez, J. A. Trapani and I. F. McKenzie (1992). "Isolation and characterization of cDNA clones for mouse Ly-9." J Immunol **149**(5): 1636-1641.

Santer, D. M., B. E. Hall, T. C. George, S. Tangsombatvisit, C. L. Liu, P. D. Arkwright and K. B. Elkon (2010). "C1q deficiency leads to the defective

suppression of IFN-alpha in response to nucleoprotein containing immune complexes." J Immunol **185**(8): 4738-4749.

Schmidt, C. W. (2011). "Questions persist: environmental factors in autoimmune disease." Environ Health Perspect **119**(6): A249-253.

Schroder, K. and J. Tschopp (2010). "The inflammasomes." Cell **140**(6): 821-832.

Schroeder, K., M. Herrmann and T. H. Winkler (2013). "The role of somatic hypermutation in the generation of pathogenic antibodies in SLE." Autoimmunity **46**(2): 121-127.

Schwartzberg, P. L., K. L. Mueller, H. Qi and J. L. Cannons (2009). "SLAM receptors and SAP influence lymphocyte interactions, development and function." Nat Rev Immunol **9**(1): 39-46.

Scofield, R. H., G. R. Bruner, B. Namjou, R. P. Kimberly, R. Ramsey-Goldman, M. Petri, J. D. Reveille, G. S. Alarcon, L. M. Vila, J. Reid, B. Harris, S. Li, J. A. Kelly and J. B. Harley (2008). "Klinefelter's syndrome (47,XXY) in male systemic lupus erythematosus patients: support for the notion of a gene-dose effect from the X chromosome." Arthritis Rheum **58**(8): 2511-2517.

Sester, D. P., V. Sagulenko, S. J. Thygesen, J. A. Cridland, Y. S. Loi, S. O. Cridland, S. L. Masters, U. Genske, V. Hornung, C. E. Andoniou, M. J. Sweet, M. A. Degli-Esposti, K. Schroder and K. J. Stacey (2015). "Deficient NLRP3 and AIM2 Inflammasome Function in Autoimmune NZB Mice." J Immunol **195**(3): 1233-1241.

Shaw, P. J., M. F. McDermott and T. D. Kanneganti (2011). "Inflammasomes and autoimmunity." Trends Mol Med **17**(2): 57-64.

Sherman, M. P. and W. C. Greene (2002). "Slipping through the door: HIV entry into the nucleus." Microbes Infect **4**(1): 67-73.

Shin, M. S., Y. Kang, N. Lee, E. R. Wahl, S. H. Kim, K. S. Kang, R. Lazova and I. Kang (2013). "Self double-stranded (ds)DNA induces IL-1beta production from human monocytes by activating NLRP3 inflammasome in the presence of anti-dsDNA antibodies." J Immunol **190**(4): 1407-1415.

Sintes, J., X. Romero, J. de Salort, C. Terhorst and P. Engel (2010). "Mouse CD84 is a pan-leukocyte cell-surface molecule that modulates LPS-induced cytokine secretion by macrophages." J Leukoc Biol **88**(4): 687-697.

Sobel, E. S., C. Mohan, L. Morel, J. Schiffenbauer and E. K. Wakeland (1999). "Genetic dissection of SLE pathogenesis: adoptive transfer of Sle1

mediates the loss of tolerance by bone marrow-derived B cells." J Immunol **162**(4): 2415-2421.

Sobel, E. S., M. Satoh, Y. Chen, E. K. Wakeland and L. Morel (2002). "The major murine systemic lupus erythematosus susceptibility locus Sle1 results in abnormal functions of both B and T cells." J Immunol **169**(5): 2694-2700.

Soderberg, D., T. Kurz, A. Motamedi, T. Hellmark, P. Eriksson and M. Segelmark (2015). "Increased levels of neutrophil extracellular trap remnants in the circulation of patients with small vessel vasculitis, but an inverse correlation to anti-neutrophil cytoplasmic antibodies during remission." Rheumatology (Oxford) **54**(11): 2085-2094.

Somers, E. C., W. Marder, P. Cagnoli, E. E. Lewis, P. DeGuire, C. Gordon, C. G. Helmick, L. Wang, J. J. Wing, J. P. Dhar, J. Leisen, D. Shaltis and W. J. McCune (2014). "Population-based incidence and prevalence of systemic lupus erythematosus: the Michigan Lupus Epidemiology and Surveillance program." Arthritis Rheumatol **66**(2): 369-378.

Soni, C., E. B. Wong, P. P. Domeier, T. N. Khan, T. Satoh, S. Akira and Z. S. Rahman (2014). "B cell-intrinsic TLR7 signaling is essential for the development of spontaneous germinal centers." J Immunol **193**(9): 4400-4414.

Sreeramkumar, V., J. M. Adrover, I. Ballesteros, M. I. Cuartero, J. Rossaint, I. Bilbao, M. Nacher, C. Pitaval, I. Radovanovic, Y. Fukui, R. P. McEver, M. D. Filippi, I. Lizasoain, J. Ruiz-Cabello, A. Zarbock, M. A. Moro and A. Hidalgo (2014). "Neutrophils scan for activated platelets to initiate inflammation." Science **346**(6214): 1234-1238.

Stolwijk, C., A. Boonen, A. van Tubergen and J. D. Reveille (2012). "Epidemiology of spondyloarthritis." Rheum Dis Clin North Am **38**(3): 441-476.

Strand, V., C. Galateanu, D. S. Pushparajah, E. Nikai, J. Sayers, R. Wood and R. F. van Vollenhoven (2013). "Limitations of current treatments for systemic lupus erythematosus: a patient and physician survey." Lupus **22**(8): 819-826.

Suarez, A., P. Lopez, J. Gomez and C. Gutierrez (2006). "Enrichment of CD4+ CD25high T cell population in patients with systemic lupus erythematosus treated with glucocorticoids." Ann Rheum Dis **65**(11): 1512-1517.

Takeuchi, O. and S. Akira (2010). "Pattern recognition receptors and inflammation." Cell **140**(6): 805-820.

Tan, E. M., A. S. Cohen, J. F. Fries, A. T. Masi, D. J. McShane, N. F. Rothfield, J. G. Schaller, N. Talal and R. J. Winchester (1982). "The 1982 revised criteria for the classification of systemic lupus erythematosus." Arthritis Rheum **25**(11): 1271-1277.

Tangye, S. G., K. E. Nichols, N. J. Hare and B. C. van de Weerdt (2003). "Functional requirements for interactions between CD84 and Src homology 2

domain-containing proteins and their contribution to human T cell activation." J Immunol **171**(5): 2485-2495.

Tangye, S. G., J. H. Phillips and L. L. Lanier (2000). "The CD2-subset of the Ig superfamily of cell surface molecules: receptor-ligand pairs expressed by NK cells and other immune cells." Semin Immunol **12**(2): 149-157.

Tangye, S. G., B. C. van de Weerdt, D. T. Avery and P. D. Hodgkin (2002). "CD84 is up-regulated on a major population of human memory B cells and recruits the SH2 domain containing proteins SAP and EAT-2." Eur J Immunol **32**(6): 1640-1649.

Theofilopoulos, A. N. and F. J. Dixon (1985). "Murine models of systemic lupus erythematosus." Adv Immunol **37**: 269-390.

Trono, D. (2001). "Lentiviral vectors for the genetic modification of hematopoietic stem cells." Ernst Schering Res Found Workshop(33): 19-28.

Tsokos, G. C. (2011). "Systemic lupus erythematosus." N Engl J Med **365**(22): 2110-2121.

Vance, R. E. (2016). "Cytosolic DNA Sensing: The Field Narrows." Immunity **45**(2): 227-228.

Vanden Berghe, T., A. Linkermann, S. Jouan-Lanhouet, H. Walczak and P. Vandenabeele (2014). "Regulated necrosis: the expanding network of non-apoptotic cell death pathways." Nat Rev Mol Cell Biol **15**(2): 135-147.

Varma, N., B. Janic, M. Ali, A. Iskander and A. Arbab (2011). "Lentiviral Based Gene Transduction and Promoter Studies in Human Hematopoietic Stem Cells (hHSCs)." J Stem Cells Regen Med **7**(1): 41-53.

Veillette, A. (2006). "Immune regulation by SLAM family receptors and SAP-related adaptors." Nat Rev Immunol **6**(1): 56-66.

Verthelyi, D. and S. A. Ahmed (1994). "17 beta-estradiol, but not 5 alpha-dihydrotestosterone, augments antibodies to double-stranded deoxyribonucleic acid in nonautoimmune C57BL/6J mice." Endocrinology **135**(6): 2615-2622.

Vidal, S., D. H. Kono and A. N. Theofilopoulos (1998). "Loci predisposing to autoimmunity in MRL-Fas lpr and C57BL/6-Faslpr mice." J Clin Invest **101**(3): 696-702.

Villanueva, E., S. Yalavarthi, C. C. Berthier, J. B. Hodgin, R. Khandpur, A. M. Lin, C. J. Rubin, W. Zhao, S. H. Olsen, M. Klinker, D. Shealy, M. F. Denny, J. Plumas, L. Chaperot, M. Kretzler, A. T. Bruce and M. J. Kaplan (2011). "Netting neutrophils induce endothelial damage, infiltrate tissues, and expose

immunostimulatory molecules in systemic lupus erythematosus." J Immunol **187**(1): 538-552.

Vuyyuru, R., C. Mohan, T. Manser and Z. S. Rahman (2009). "The lupus susceptibility locus Sle1 breaches peripheral B cell tolerance at the antibody-forming cell and germinal center checkpoints." J Immunol **183**(9): 5716-5727.

Wandstrat, A. E., C. Nguyen, N. Limaye, A. Y. Chan, S. Subramanian, X. H. Tian, Y. S. Yim, A. Pertsemlidis, H. R. Garner, Jr., L. Morel and E. K. Wakeland (2004). "Association of extensive polymorphisms in the SLAM/CD2 gene cluster with murine lupus." Immunity **21**(6): 769-780.

Wang, A., F. Batteux and E. K. Wakeland (2010). "The role of SLAM/CD2 polymorphisms in systemic autoimmunity." Curr Opin Immunol **22**(6): 706-714.

Warnatsch, A., M. Ioannou, Q. Wang and V. Papayannopoulos (2015). "Inflammation. Neutrophil extracellular traps license macrophages for cytokine production in atherosclerosis." Science **349**(6245): 316-320.

Warncke, M., B. Vogt, J. Ulrich, M. D. von Laer, W. Beyer, H. Klump, B. Micheel and A. Sheriff (2004). "Efficient in vitro transduction of naive murine B cells with lentiviral vectors." Biochem Biophys Res Commun **318**(3): 673-679.

Wen, H., E. A. Miao and J. P. Ting (2013). "Mechanisms of NOD-like receptor-associated inflammasome activation." Immunity **39**(3): 432-441.

Wilkins, A. L., W. Yang and J. J. Yang (2003). "Structural biology of the cell adhesion protein CD2: from molecular recognition to protein folding and design." Curr Protein Pept Sci **4**(5): 367-373.

Wong, E. B., C. Soni, A. Y. Chan, P. P. Domeier, Shwetank, T. Abraham, N. Limaye, T. N. Khan, M. J. Elias, S. B. Chodisetti, E. K. Wakeland and Z. S.

Rahman (2015). "B cell-intrinsic CD84 and Ly108 maintain germinal center B cell tolerance." J Immunol **194**(9): 4130-4143.

Woods, N. B., H. Mikkola, E. Nilsson, K. Olsson, D. Trono and S. Karlsson (2001). "Lentiviral-mediated gene transfer into haematopoietic stem cells." J Intern Med **249**(4): 339-343.

Wu, N. and A. Veillette (2016). "SLAM family receptors in normal immunity and immune pathologies." Curr Opin Immunol **38**: 45-51.

Wu, Z., X. Li, H. Qin, X. Zhu, J. Xu and W. Shi (2013). "Ultraviolet B enhances DNA hypomethylation of CD4+ T cells in systemic lupus erythematosus via inhibiting DNMT1 catalytic activity." J Dermatol Sci **71**(3): 167-173.

Yadav, P., H. Tran, R. Ebegbe, P. Gottlieb, H. Wei, R. H. Lewis, A. Mumbey-Wafula, A. Kaplan, E. Kholdarova and L. Spatz (2011). "Antibodies elicited in response to EBNA-1 may cross-react with dsDNA." PLoS One **6**(1): e14488.

Yamaguchi, T., J. B. Wing and S. Sakaguchi (2011). "Two modes of immune suppression by Foxp3(+) regulatory T cells under inflammatory or non-inflammatory conditions." Semin Immunol **23**(6): 424-430.

Yan, Q., V. N. Malashkevich, A. Fedorov, E. Fedorov, E. Cao, J. W. Lary, J. L. Cole, S. G. Nathenson and S. C. Almo (2007). "Structure of CD84 provides

insight into SLAM family function." Proc Natl Acad Sci U S A **104**(25): 10583-10588.

Yang, C. A., S. T. Huang and B. L. Chiang (2015). "Sex-dependent differential activation of NLRP3 and AIM2 inflammasomes in SLE macrophages." Rheumatology (Oxford) **54**(2): 324-331.

Yang, J. J., Y. Ye, A. Carroll, W. Yang and H. W. Lee (2001). "Structural biology of the cell adhesion protein CD2: alternatively folded states and structure-function relation." Curr Protein Pept Sci **2**(1): 1-17.

Yang, M., K. Rui, S. Wang and L. Lu (2013). "Regulatory B cells in autoimmune diseases." Cell Mol Immunol **10**(2): 122-132.

Yeh, K. W., C. H. Yu, P. C. Chan, J. T. Horng and J. L. Huang (2013). "Burden of systemic lupus erythematosus in Taiwan: a population-based survey." Rheumatol Int **33**(7): 1805-1811.

Zaiss, M., C. Hirtreiter, M. Rehli, A. Rehm, L. A. Kunz-Schughart, R. Andreesen and B. Hennemann (2003). "CD84 expression on human hematopoietic progenitor cells." Exp Hematol **31**(9): 798-805.

Zarbock, A., R. K. Polanowska-Grabowska and K. Ley (2007). "Platelet-neutrophil-interactions: linking hemostasis and inflammation." Blood Rev **21**(2): 99-111.

Zawrotniak, M. and M. Rapala-Kozik (2013). "Neutrophil extracellular traps (NETs) - formation and implications." Acta Biochim Pol **60**(3): 277-284.

Zerhouni, E. (2002) Autoimmune Diseases Research Plan

Zhang, H., R. Fu, C. Guo, Y. Huang, H. Wang, S. Wang, J. Zhao and N. Yang (2016). "Anti-dsDNA antibodies bind to TLR4 and activate NLRP3 inflammasome in lupus monocytes/macrophages." J Transl Med **14**(1): 156.

Zhong, M. C. and A. Veillette (2008). "Control of T lymphocyte signaling by Ly108, a signaling lymphocytic activation molecule family receptor implicated in autoimmunity." J Biol Chem **283**(28): 19255-19264.

7 APPENDICES

Appendix I: Reagent List (In alphabetical order)

293fectin	Invitrogen (Carlsbad, CA, USA)
7-AAD viability staining solution	Biolegend (San Diego, CA, USA)
Agarose	Invitrogen (Carlsbad, CA, USA)
Alamar Blue	Invitrogen (Carlsbad, CA, USA)
Ampicillin	SIGMA-Aldrich (St. Louis, MO, USA)
Annexin V APC apoptosis assay	BD Bioscience (San Diege, CA, USA)
B -mercaptoethanol	Invitrogen (Carlsbad, CA, USA)
Bovine Serum Albumine (for lenti-virus work)	Gibco, Thermo Fisher Scientific (Waltham, MA, USA)
Calcein AM	Thermo Fisher Scientific (Waltham, MA, USA)
Calcium chloride (CaCl2)	Kanto Chemical&Co (Tokyo, Japan)
Carboxyfluorescein succinimidyl ester (CFSE)	Invitrogen (Carlsbad, CA, USA)
Compensation beads	Becton Dickinson (Fanklin Lakes, NJ, USA)
DAPI (4',6-Diamidino-2-Phenylindole, Dilactate)	Thermo Fisher Scientific (Waltham, MA, USA)
Dulbecco's Modified Eagle Medium (DMEM)	Thermo Fisher Scientific (Waltham, MA, USA)
Dimethyl sulfoxide (DMSO)	SIGMA-Aldrich (St. Louis, MO, USA)
GelRed	Biotium (California, USA)
ECL	GE Healthcare (Buckinghamshire, UK)
Ethanol (CH3CH2OH)	Merck (Kenilworth, NJ,USA)
Ethylenediaminetetraacetic acid (EDTA)	1st Base/Axil Scientific (Singapore)
Faramount Aqeous Mounting Medium	DAKO, Agilent Technology (Singapore)
Ficoll - Paque Premium	GE Healthcare (Little Chalfont, UK)
Glycerol	SIGMA-Aldrich (St. Louis, MO, USA)
LIVE/DEAD® Fixable Dead Cell Stains	Thermo Fisher Scientific (Waltham, MA, USA)
Hepes	SIGMA-Aldrich (St. Louis, MO, USA)
Histopaque®-1077	SIGMA-Aldrich (St. Louis, MO, USA)
Histopaque®-1119	SIGMA-Aldrich (St. Louis, MO, USA)

HyClone™ Fetal Bovine Serum (U.S.), Characterized (for tissue culture work)	GE Healthcare Life Sciences (South Logan, Utah, USA)
Hydrogen chloride (HCL)	Merck (Kenilworth, NJ,USA)
Isopropanol ((CH3)2CHOH)	Merck (Kenilworth, NJ,USA)
Kanamycin	A.G. Scientific Inc. (San Diego, CA, USA)
Lysogeny broth (LB) Agar	ASTAR (Singapore)
Lysogeny broth (LB) liquid medium	ASTAR (Singapore)
L-Glutamine	Invitrogen (Carlsbad, CA, USA)
Lipofectamin	Invitrogen (Carlsbad, CA, USA)
Laemmli buffer	Bio-Rad Laboratories Inc., (Hercules, USA)
Magnesium chloride ($MgCl_{2)}$	SIGMA-Aldrich (St. Louis, MO, USA)
Milk Powder, low fat	Anlene/Fontarra (Auckland, New Zealand)
Miniprep / Maxiprep	Quiagen (Venlo, Limburg, Netherlands)
B cell isolation kit	Stemcell (Singapore)
B cell isolation kit	Miltenyi (Bergisch Gladbach, Germany)
Non Essential Amino Acids (NEAA)	Invitrogen (Carlsbad, CA, USA)
Opti-MEM I Reduced Serum Media	Life Technologies (Carlsbad, CA, USA)
Penicilline/ Streptamycin	Invitrogen (Carlsbad, CA, USA)
Percoll	SIGMA-Aldrich (St. Louis, MO, USA)
Phosphate buffered saline (DPBS)	ASTAR (Singapore)
Potassium chloride (KCl)	SIGMA-Aldrich (St. Louis, MO, USA)
Protease inhibitor Pill	Thermo Fisher Scientific (Waltham, MA, USA)
Rat Serum	Invitrogen (Carlsbad, CA, USA)
Roswell Park Memorial Institute medium (RPMI)	Thermo Fisher Scientific (Waltham, MA, USA)
S.O.C medium	Invitrogen (Carlsbad, CA, USA)
Sodium Acetate (CH3COONa)	SIGMA-Aldrich (St. Louis, MO, USA)
Sodium Azide (NaN3)	SIGMA-Aldrich (St. Louis, MO, USA)
Sodium bicarbonate ($NaHCO_{3)}$	SIGMA-Aldrich (St. Louis, MO, USA)
Sodium Bicarbonate (NaHCO3)	Life Technologies (Carlsbad, CA, USA)

Sodium carbonate anhydrous (Na2CO3)	SIGMA-Aldrich (St. Louis, MO, USA)
Sodium Cholide (NaCl)	1st Base/Axil Scientific (Singapore)
Sodium citrate (HOC(COONa)(CH2COONa)2 2H2O)	SIGMA-Aldrich (St. Louis, MO, USA)
Sodium dodecyl sulfate (SDS)	1st Base/Axil Scientific (Singapore)
Sodium hydroxide (NaOH)	SIGMA-Aldrich (St. Louis, MO, USA)
Sodium phosphate dibasic anhydrous ($Na_2HPO_{4)}$	SIGMA-Aldrich (St. Louis, MO, USA)
Sodium Pyruvate (CH3COCOONa)	Invitrogen (Carlsbad, CA, USA)
Streptavidin-HRP	Biolegend
SYTOX Green Nucleic Acid Stain	Thermo Fisher Scientific (Waltham, MA, USA)
SYTOX® Red	Thermo Fisher Scientific (Waltham, MA, USA)
SYTOX® Orange Nucleic Acid Stain	Thermo Fisher Scientific (Waltham, MA, USA)
Tetramethylbenzidine (TMB)	Surmodix Bio FX (Eden Prairie, USA)
Tris	1st Base/Axil Scientific (Singapore)
Tris Acetate-EDTA buffer (TAE)	1st Base/Axil Scientific (Singapore)
Tris-EDTA buffer (TE)	1st Base/Axil Scientific (Singapore)
Triton-X-100	VWR Poole BDH (Radnor, PA)
Trypan Blue	SIGMA-Aldrich (St. Louis, MO, USA)
Trypsin	SIGMA-Aldrich (St. Louis, MO, USA)
Tween	Promega (Madison, WI, USA)
Water (ddH_2O)	A*STAR (Singapore)

Plasmids

pD2109-EFs: EF1a-ORF, Lenti-ElecD	DNA 2.0 (**Newark,** USA)
pD2109- EFs- 03 EF1a- GFP, Lenti	DNA 2.0 (**Newark,** USA)
pRSV-Rev	Addgene (Cambridge, USA)
pMDLg/pRRE	Addgene (Cambridge, USA)
pMD2.G	Addgene (Cambridge, USA)
pCMV6-AC-GFP	Origene (Rockville, USA)
CD84 (GFP-tagged)	
Bacteria	
E.coli XL10 gold	Stratagene (La Jolla, CA, USA)
DH5α Competent Cells	Invivogen (USA)
Cell-lines	
HEK293	ATCC (Manassas, USA)
HEK293ft	ATCC (Manassas, USA)
HELA	ATCC (Manassas, USA)
HEK-Blue™ Null2K	Invivogen (San Diego, USA)
HEK-Blue™ TLR7	Invivogen (San Diego, USA)
Primers	

Primer name	Sequence 5' --> 3'
D1Mit17 (1-17)	
Forward	GTGTCTGCCTTTGCACCTTT
Reverse	CTGCTGTCTTTCCATCCACA
D1Mit113 (1-113)	
Forward	CCTCAAAATCAGGATTAAAAGGG
Reverse	ACATGGGGTGGACTTGTGAT
D1Mit202 (1-202)	
Forward	CCATAAGCCTCCTCTTTCCC
Reverse	AAAATGAACTCAGCGGGTTG

Appendix II: Antibodies

Antibodies for flow cytometry

anti- CD3, PE, HIT3a	Becton Dickinson (Fanklin Lakes, NJ, USA)
anti- CD3, BUV 395, UCHT1	Becton Dickinson (Fanklin Lakes, NJ, USA)
anti- CD4, Fitc, RPA-T4	Biolegend (San Diego, CA, USA)
anti- CD4, V500, RPAT4	Becton Dickinson (Fanklin Lakes, NJ, USA)
anti- CD8,BV421, RPA-T9	Becton Dickinson (Fanklin Lakes, NJ, USA)
anti- CD8, APC-Cy7, SK1	Biolegend (San Diego, CA, USA)
Anti- Cd11b, PE, BM8	BD Pharmingen™ (Fanklin Lakes, NJ, USA)
Anti- CD14,	
anti- CD16, APC-Cy7, 3G8	Biolegend (San Diego, CA, USA)
anti- CD19, PE-Cy7, H1B19	Biolegend (San Diego, CA, USA)
anti- CD19, PE TxRd, J3-119	Beckman coulter (Brea, CA, USA)
anti- CD25, FITC, BC96	Biolegend (San Diego, CA, USA)
anti- CD28, PE, CD28.2	Biolegend (San Diego, CA, USA)
Anti- CD34, APC, MEC14.7	Biolegend (San Diego, CA, USA)
Anti- CD41, FITC, eBioMWReg30	E-Bioscience (San Diege, CA, USA)
Anti- CD45, Brilliant Violet 605™, 30-F11	Biolegend (San Diego, CA, USA)
anti- CD45, AF700, HI30	Biolegend (San Diego, CA, USA)
anti- CD45RA, PECy7, HI100	Biolegend (San Diego, CA, USA)
Anti- CD45R/B220, FITC, RA3-6B2	E-Bioscience (San Diege, CA, USA)
Anti- CD45.1, PE-Cy7, A20	Biolegend (San Diego, CA, USA)
Anti- CD45.2, FITC, 104	Biolegend (San Diego, CA, USA)
anti- CD56, PECy5, HCD56	Biolegend (San Diego, CA, USA)
Anti- CD62L, FITC, MEL-14	BD Pharmingen™ (Fanklin Lakes, NJ, USA)
Anti- CD66, Fitc, B1.1/CD66	BD Pharmingen™ (Fanklin Lakes, NJ, USA)
anti- CD69, APC, FN50	E-Bioscience (San Diege, CA, USA)
Anti- CD84, APC, CD84.7	E-Bioscience (San Diege, CA, USA)
Anti- CD84, PE, mCD84.7	Biolegend (San Diego, CA, USA)
Anti- CD86, FITC, GL-1	E-Bioscience (San Diege, CA, USA)
Anti- CD115, PE, AFS98	Biolegend (San Diego, CA, USA)
Anti- Histone H1 antibody	Abcam (Cambridge, UK)
anti- ICOS, PE-EFluor 610, ISA-3	E-Bioscience (San Diege, CA, USA)
Anti- L108, PE, 330-AJ	Biolegend (San Diego, CA, USA)
Anti- Ly-6A/E (Sca-1), FITC, D7	BD Pharmingen™ (Fanklin Lakes, NJ, USA)
Anti- Ly6G, PerCPCy5.5, 1A8	BD Pharmingen™ (Fanklin Lakes, NJ, USA)

Anti- Ly6G, AlexaFlour700, GR1	BD Pharmingen™ (Fanklin Lakes, NJ, USA)
Anti- MHC II, PerCPCy5.5, 551	Biolegend (San Diego, CA, USA)
Anti- MHC II (IA/IE), FITC, M5/114.15.2.	Biolegend (San Diego, CA, USA)
Anti-Neutrophil Elastase antibody	Abcam (Cambridge, UK)
Anti- SLAM150, PerCPCy5.5, TC15-12F12.2	Biolegend (San Diego, CA, USA)
Anti- Ter-119, AlexaFluore700, Ter119	Biolegend (San Diego, CA, USA)
Fc-block antibody	AMF lab (Singapore)

Antibodies for ELISA

Anti-IgM	eBioscience (San Diego, CA, USA)
Anti-IgA	eBioscience (San Diego, CA, USA)
Anti-IgG	eBioscience (San Diego, CA, USA)
Anti-IgG2a	eBioscience (San Diego, CA, USA)
Anti-IgG2b	eBioscience (San Diego, CA, USA)
Anti-IgG3	eBioscience (San Diego, CA, USA)

Antibodies for microscopy

Anti-CD66-FITC	Abcam (Cambridge, UK)
Anti-FITC-Alexa 488	Abcam (Cambridge, UK)
Anti-CD84 PE	Biolegend (San Diego, CA, USA)
Anti-PE Alexa 555	Abcam (Cambridge, UK)
Microscopy slides	
Cover slips	

Appendix III: Reagent recipes

DPBST

0.05% Tween 20
in PBS

Complete RPMI (cRPMI)
450 mL RPMI 1640
10% FBS (HyClone) Characterised
1 mM sodium pyruvate
15 mM HEPES
0.1 mM MEM NEAA
1% PenStrep
2 mM L-glutamine
0.16 µM 2-mercaptoethanol

Trypsin solution
20mM Tris pH8
15mM NaCl
2mM CaCl2
dissolve ~1mg Trypsin

Complete DMEM (cDMEM)
10% FBS (Gibco)
1% PenStrep
DMEM

FACS buffer
5% FBS
1.5% HEPES
DPBS

HEK BLUE growth medium
DMEM
10% FBS (Gibco)

1% PenStrep
2 µg/ml Normocin™
1 µg/ml Blasdicidine
1 µg/ml Zeocine™

SEAP detection media
50 g of SEAP powder
50 mL endotoxin free water

1X PBS, pH 7.4
137 mM NaCl
2.7 mM KCl
10 mM Na2HPO4
2 mM KH2PO4

LB medium
120 ug/ml Penicillin
25 ug/ml Kanamycin (optional)
2% glucose (optional)
1.5% Agar (optional)
LB

2XYT medium
120ug/ml Penicillin
1.5% Agar (optional)
2XYT medium

Recomended media (B cell isolation)
PBS w/o Ca^{2+} Mg^{2+}
1 mM EDTA
1% FBS

Freezing media
90% DMSO
10% FBS

Appendix IV: Software

Photoshop elements 9.0	Adobe (USA)
VEctor NTI	Thermo Fisher Scientific (Waltham, MA, USA)
FACS Diva	Becton Dickinson (Fanklin Lakes, NJ, USA)
FloJo X10	Tree Star (Ashland, Oregon, USA)
Imaris	Bitplane (USA)
ImageJ	NIH (USA)
Lasergene 8	DNASTAR (Singapore)
MS Office 2010	Microsoft (Redmond, WA, USA)
Foldit	University of Washington's Center for Game Science
Prism	Graphpad (La Jolla, CA, USA)
SeqMonk	Babraham Bioinformatics (the UK)

Appendix V: Machines and equipment

3510 pH meter	Jenway (Staffordshire, UK)
Biological Safety Cabinet Class II	Gelman (Singapore)
Biomedical freezer	Sanyo (Moriguchi, Osaka, Japan)
Caster tray, Gelchamber, various sizes	Biorad (Hercules, CA, USA)
Centrifuge 5415R	Eppendorf (Eppendorf, H, Germany)
CKX41 inverted brightfield microscope	Olympus (Shinjuku, Tokyo, Japan)
Olympus IX81 microscope	
Electronic Precision Balance	Sartorious (Goettingen, Germany)
Enspire Multiplate reader	Perkin Elmer (Waltham, MA, USA)
FACS Canto	Becton Dickinson (Fanklin Lakes, NJ, USA)
Finnpipette Multichannel FI 30-300ul / 5-50ul	Thermo Fisher Scientific (Waltham, MA, USA)
Forma steri-cycle CO2 incubator	Thermo Fisher Scientific (Waltham, MA, USA)
Fridge	ARDO (Italy)
GelDoc-It® Imaging System	UVP (Upland, CA , USA)
Infors RT Multitron Standard, Shaker	Infors (Bottmingen Switzerland)
intello wave (microwave)	LG (Seoul, Korea)
Labquake® Tube Shaker / Rotor	Thermo Fisher Scientific (Waltham, MA, USA)
LSR Fortessa	Becton Dickinson (Fanklin Lakes, NJ, USA)
LSR II laser	Becton Dickinson (Fanklin Lakes, NJ, USA)
Matrix Pipette, 8 channel , various sizes	Thermo Fisher Scientific (Waltham, MA, USA)
Magnetic Cell Seperation System	Miltenyi (Bergisch Gladbach, Germany)
Microvette® CB 300 µl, Clotting Activator/Serum, red US code	Sarstedt AG & Co. (Nümbrecht Germany)
Mini centrifuge 6K	Stratagene (La Jolla, CA, USA)
MP-3500 - 250P	Major Science (Saragota, CA, USA)
Multishaker PSU 20, Table shaker	BIOSAN (Riga, Latvia)
Nanodrop 1000 Spectrophotometer	Thermo Fisher Scientific (Waltham, MA, USA)

Novex Mini cell, gel chamber, vertical	Invitrogen (Carlsbad, CA, USA)
OPTIM2	avacta analytical (Wetherby, UK)
Pipette Aid	Drummond (Birmingham, AL, USA)
Pipetts, various sizes, mono channel	Eppendorf (Eppendorf, H, Germany)
Power Pac Basic Supply	Biorad (Hercules, CA, USA)
Proteon XPR36	Biorad (Hercules, CA, USA)
Rocker 400 pump	Rocker Scientific (New Taipei City 244, Taiwan)
Scanner	Hewlett Packard (Palo Alto, CA, USA)
Sorvall Evolution RC, Ultracentrifuge	Thermo Fisher Scientific (Waltham, MA, USA)
Sorvall Legend RT centrifuge	Thermo Fisher Scientific (Waltham, MA, USA)
Spectrophotometer 1300 Classic	GE Healthcare (Little Chalfont, UK)
Thermal cycler, 96 well 0.2ml	Life Technologies (Carlsbad, CA, USA)
Temperature Controller	Poly Science (Niles, Illinois, USA)
Trans-Blot Turbo system	Biorad (Hercules, CA, USA)
Vortex Genie 2	Scientific Industries (Bohemia, NY, USA)
Liquid Nitrogen Tanks	various

Appendix VI: CD84 plasmid sequencing

CD84-H1

GGTAGATATGAAGGTAGTAGATCTTGGTGATGGTTTCCTCATTCTCTTCATTG
ATGTCTGCTTTGTAAGTTCCTGCATCTTCCATCCTCAGGTCTCTAATGACCAGGTCA
TACTTCTGATCTATGATTTCTATTCGTCCTTTATAAGTGCCCTGGGTTATGGTAACTT
CAGCTTTATTGACTCCTGGTTTTATAAAAGCAACAGATGATTGAGAAGTCCAGGCAA
TGTTGTCAATTTTCTTTGGTTCTTGAATATTTAAGAGGAAAGTAACTGACTCCCCAA
GAATCCCATTCATTACCACCGGGTCTGCATCTTTTCCTGCTGCTTCAGACCAGGTTT
GTAGGCAAAGGAACCAGATCCACAGATGGCGCTGGGCCATGGTGGCGGCTCTAG
ACAGCTTGGGTGTGGTCTCTCCCCTGAGACGGGTGGCGTCTAGCGTAGGCGCCG
GTCACAGCTTGGATCTGTAACGGCGCAGAACAGAAAACGAAACAAAGACGTAGAG
TTGAGCAAGCAGGGTCAGGCAAAGCGTGGAGAGCCGGCTGAGTCTAGGTAGGCT
CCAAGGGAGCGCCGGACAAAGGCCCGGTCACGACCTGAGCTTTAAACTTACCTAG
ACGGCGGACGCAGTTCAGGAGGCACCACAGGCGGGAGGCGGCAGAACGCGACT
CAACCGGCGTGGATGGCGGCCTCAGGTAGGGCGGCGGGCGCGTGAAGGAGAGA
TGCGAGCCCCTCGAAGCTTCAGCTGTGTTCTGGCGGCAAACCC

CCCGGTGGTAATG CATTACCACCGGG (reverse complemented)

CD84- H2

AAGGTAGTAGATCTTGGTGATGGTTTCCTCATTCTCTTCATTGATGTCTGCTT
TGTAAGTTCCTGCATCTTCCATCCTCAGGTCTCTAATGACCAGGTCATACTTCTGAT
CTATGATTTCTATTCGTCCTTTATAAGTGCCCTGGGTTATGGTAACTTCAGCTTTATT
GACTCCTGGTTTTATAAAAGCAACAGATGATTGAGAAGTCCAGGCAATGTTGTCAAT
TTTCTTTGGTTCTTGAATATTTAAGAGGAAAGTAACTGACTCCCCAAGAATCCCATT
CATTACCATCGGGTCTGCATCTTTTCCTGCTGCTTCAGACCAGGTTTGTAGGCAAA
GGAACCAGATCCACAGATGGCGCTGGGCCATGGTGGCGGCTCTAGACAGCTTGG
GTGTGGTCTCTCCCCTGAGACGGGTGGCGTCTAGCGTAGGCGCCGGTCACAGCTT
GGATCTGTAACGGCGCAGAACAGAAAACGAAACAAAGACGTAGAGTTGAGCAAGC
AGGGTCAGGCAAAGCGTGGAGAGCCGGCTGAGTCTAGGTAGGCTCCAAGGGAGC
GCCGGACAAAGGCCCGGTCACGACCTGAGCTTTAAACTTACCTAGACGGCGGACG
CAGTTCAGGAGGCACCACAGGCGGGAGGCGGCAGAACGCGACTCAACCGGCGTG
GATGGCGGCCTCAGGTAGGGCGGCGGGCGCGTGAAGGAGAGATGCGAGCCCCT
CGAAGCTTCAGCTGTGTTCTGGCGGCAAACCCGTTGCGAAAAAGAACGTTCACGG
CGACTACTGCACTTATATACGGTTCTCCCCCACCC

CCCGATGGTAATG CATTACCATCGGG (reverse complemented)